Weathering History of Granitoids of the South Mountain Batholith, N.S., Canada: Mineralogy, Geochemistry and Environmental Implications of Saprolites

by

Anne Marie O'Beirne-Ryan

Submitted in partial fulfilment of the requirements

for the degree of Doctor of Philosophy

at

Dalhousie University

Halifax, Nova Scotia

August 2006

Your file Votre référence
ISBN: 978-0-494-19592-5
Our file Notre référence
ISBN: 978-0-494-19592-5

DALHOUSIE UNIVERSITY

To comply with the Canadian Privacy Act the National Library of Canada has requested that the following pages be removed from this copy of the thesis:

Preliminary Pages

Examiners Signature Page (pii)

Dalhousie Library Copyright Agreement (piii)

Appendices

Copyright Releases (if applicable)

TABLE OF CONTENTS

LIST OF FIGURES

LIST OF TABLES

ABSTRACT

Devonian granitoids comprising the South Mountain Batholith, the bedrock of much of southern Nova Scotia, are locally enriched in heavy metals and radioactive elements. Although post-glacial weathering is minimal, the granitoid bedrock has been subjected to deep decomposition at least three times since the batholith's initial exposure at surface. The remnants of these weathered profiles, or saprolites, record physical, chemical and environmental characteristics different from fresh granitoid bedrock.

The oldest weathering episode occurred prior to deposition of Carboniferous strata and these saprolites have subsequently been relithified. Their geochemistry and mineralogy reflect both the weathering episode and subsequent diagenetic effects. Intense depletion of most elements resulted in a dominantly quartz-kaolinite material, consistent with development under warm humid conditions, in agreement with paleoclimatic reconstructions.

An argillaceous granitic saprolite sequence 30 metres thick beneath Triassic sedimentary strata represents a younger weathering episode. The Pre-Triassic saprolite is geochemically characterized from base to top by increase in oxidation (increase in Fe^{3+} / Fe^{2+}), hydration (increase in LOI), and decrease in CaO, Na_2O, and REEs; it is mineralogically characterized by the persistence of biotite as well as an increase in kaolinite-to-smectite ratio. The persistence of biotite together with some K-feldspar and smectite, is consistent with warm, semi-arid conditions during development. Pre-Pleistocene weathering is characterized by its arenaceous nature, minimal clay development, the onset of increased oxidation and hydration, and incipient migration of mobile elements. These features are consistent with warm temperate conditions, as was typified in Cretaceous or Eocene times.

General textural, geochemical and biotite-breakdown intermediate products confirm that these saprolites represent three different weathering episodes. When re-exposed at surface, these saprolites are open systems with weakened structural strength. Fission track data from fresh and weathered samples indicate that original weathering conditions resulted in the redistribution of uranium to sites where oxidizing acidic conditions may more readily liberate this uranium, and most likely result in release of radon to the surrounding waters and soils. Similarly, when previously weathered mineralized zones are re-exposed to water and oxygen at the surface as a result of road construction, building, or quarrying, loosely-bound elements including potentially toxic elements, can be liberated.

ACKNOWLEDGMENTS

The completion of this degree would not have been possible without the help and encouragement of a number of very special people: family, mentors, friends and students. Thank you first to my family, who lived through the experience with me, and especially thank you for the times this was not easy! So thanks to my daughters, Fiona, Kerrianne, and Erin, who encouraged me when the juggling of teaching and thesis became almost too much, and to Bob, my husband, without whose support and encouragement both on a personal and a "geological" level, I would not be at this stage. Your ongoing belief in me and patience kept me going through good times and bad - thank you so very much. And also *go raibh maith agat* to my father, who introduced me to granites in the mountains of Ireland, and inadvertently pointed me on the geological path from an early age.

To Marcos Zentilli, my supervisor: I owe a big thank you for your patience, and your continued encouragement to keep the environmental aspect to the fore. Thank you especially for your understanding and indeed, the teaching door you cracked open just a little further for me in 1997: while it allowed me to step into an increased teaching mandate, it also continued to give me a reason to complete this degree, although it also meant the process was prolonged.

To Peter Reynolds who not only provided valuable input to earlier drafts of parts of the thesis, but also took a risk in allowing me to pursue my dream in teaching while still working on this thesis; many thanks, Peter. My interest in environmental aspects of geology was first piqued when Jarda Dostal asked me to teach environmental geology, and I have not looked back since. Thank you Jarda for this, and for your valuable contributions and insights into earlier drafts of parts of this work. Barrie Clarke, Patricia Stoffyn, Bob MacKay, Gordon Brown, Debra Wheeler from Dalhousie Earth Sciences Department, as well as Phil Finck, Garth Prime, Paul Smith, Ralph Stea, Terry Goodwin, Mike MacDonald, George O'Reilly, and Brian Fisher from NSDNR, have either contributed conversations, lent me an ear, helped with editing, or pointed me in new directions at various times throughout the process, and for this I thank you all. John Wightman and Larry Riteman earn a special thank you for allowing me access to newly-drilled core, as does Beatrice Levi, who analyzed and processed the XRD data.

Funding for this research came from a NSERC Discovery Grant to M. Zentilli. In addition, some of the analytical work was done through the Metals in the Environment project.

And finally to my students, who are the reason I undertook this venture in the first place, and to my friends, who were there when I needed a break - thank you.

Chapter 1

Introduction

1.1 Preamble

The motivation for this study was to understand the nature and distribution of radon and uranium in the environment, specifically in relation to the region underlain by the South Mountain Batholith, Nova Scotia, the largest granitoid intrusive complex in the eastern seaboard of North America. During the initial stages of research, it became obvious that in order to assess these and other potential environmental problems associated with the rocks of the South Mountain Batholith, it would be necessary to study the nature of the weathering of the granitoids. A literature search revealed only passing reference to weathering of the granitoids, and no detailed study of the nature, timing, and degree of weathering of this large intrusive complex had been undertaken. Therefore this study is the first attempt at categorizing the nature and timing of weathering of the granitoids of the South Mountain Batholith, and examines the implications of this weathering for the occurrence and distribution of uranium, radon and other elements into the wider environment.

In situ weathered horizons provide geologists an opportunity to examine the initial transitions from granitoids to sediments, and the processes and products of these transitions; data from such natural laboratories allow for the development of models that encompass the worlds of the igneous petrologist, the sedimentologist, and the soil scientist. Weathered rocks are chemically and physically different to their unweathered parents or protoliths, and the potential for geochemical dispersion of toxic elements into the environment is increased by weathering, particularly if the parent rock is enriched in toxic elements, and the pH-Eh conditions during weathering are appropriate.

The initial search for appropriate weathered sites proved difficult, because locations were not well documented, or had been overgrown since their first descriptions

in various reports (McNeil 1954; Cumming 1979; Grant 1989, 1997; Finck et al. 1993, 1994). As with many cases in science, a fortuitous trip to the Nova Scotia Department of Natural Resources provided three key data trails, which were to prove invaluable in identifying not only the effects of one episode of extensive weathering on the granitoid, but three such paleosurfaces of different ages. In turn, the recognition of these ancient surfaces led to developing an understanding of the stratigraphy of weathering of the granitoid rocks of the South Mountain Batholith of southwestern Nova Scotia, and the chemical and mineralogical changes produced during these weathering processes.

One of these key data trails was the invitation to examine core drilled through granitoid material underlying several metres of consolidated Triassic sediments. A cursory examination of this granitoid had shown that, although visibly identical to the typical monzogranite, and although biotites are more or less intact, the feldspars are variably altered to clay minerals, and the "rock" is soft and crumbly to the touch. The question posed at that time then became: what process or processes were involved in changing this rock in this way; was it a hydrothermal event, or a weathering event, or some combination of both? (J. Wrightman, pers.comm., 2000).

The second key data trail led to the identification of several surface sites within the South Mountain Batholith where loose, gravelly, weathered granitoid had been extracted for use as aggregate (G. Prime, pers. comm., 2000). In some localities, weathered horizons clearly underlie glacial till (P. Finck, pers. comm., 2000).

A third key data trail led to core drilled in the Windsor, Nova Scotia, in 2002 (L. Rightman, pers. comm., 2002). These drill cores intersected weathered granitoid at depths of over 300 m.

Much of southwestern Nova Scotia is underlain by granitoid rocks of the South Mountain Batholith of Devonian age. Geological events since that time have resulted in the subsequent deposition of Carboniferous strata on this granitoid basement in some localized regions, in other localised areas, the granitoid rocks have been buried beneath Triassic sediments. Glacial till of Pleistocene age, and of varying thickness, blankets the granitoid rocks over much of the region. Each of these reburial events required that

the granitoids first be exposed at surface potentially allowing for processes of weathering and erosion to occur. Each of these subsequent sedimentary sequences records a weathering and erosion event that is recorded in paleoweathered horizons developed and partially preserved on the granitoids.

This thesis investigates the timing of these weathering events, the mineralogical and geochemical changes that each produced, the environmental conditions prevailing at the time of their development, and the potential for modern-day environmental concerns related to the occurrence and distribution of these weathered horizons.

The study provides data on three separate weathering episodes, millions of years apart, that acted upon chemically similar parent monzogranite, allowing the development of an understanding of the response of a granitoid of given chemical composition to different weathering environments at different times. In addition, one of these weathering episodes (the most recent event) is recorded on several chemically different granitoids within the South Mountain Batholith, allowing a greater understanding of the effects of parent rock on the resultant chemical weathering.

1.2 Organization of the thesis

This thesis encompasses a geomorphological, paleoenvironmental, and stratigraphic record and implications of weathered horizons developed on the granitoids of the South Mountain Batholith, Nova Scotia. An additional component of the study addresses the mineralogical and geochemical nature of weathering of these rocks, and the implications of weathering events for environmental considerations.

Chapters 2 through 5 and part of 6 within the thesis represent manuscripts either already published, or prepared for submission for publication. Some repetition is therefore deliberate and unavoidable. These chapters have been reformatted to conform to thesis format, and figures and tables renumbered within the chapters for clarity and consistency. Abstracts and acknowledgements for a given published paper

are listed in the individual chapter, in regular thesis format. References from all chapters are compiled in their entirety at the end of the thesis.

Chapter 2 of the thesis is an overview of the geographic extent of the region included in the study, and the geomorphological, stratigraphic, and paleoenvironmental aspects of the research. This chapter is the manuscript of O'Beirne-Ryan and Zentilli (2003), published in the Canadian Journal of Earth Sciences. Chapter 3 is an application of the understanding of the products of weathering as they relate to subsequent sedimentary strata, that is, the incorporation of corestones into subsequent strata, and is published in Sedimentology (Ryan et al., 2005).

Mineralogical and geochemical studies of the weathered horizons are presented in chapters 4 and 5 respectively, and are manuscripts intended for submission in Fall 2006. Chapters 4 and 5 represent the first attempt at characterizing the weathering of the South Mountain Batholith from mineralogical and geochemical perspectives. A summary of Chapter 5 has been accepted at time of print, for publication in Atlantic Geology, "Weathering of Devonian monzogranites as recorded in the geochemistry of saprolites from the South Mountain Batholith, Nova Scotia Canada", AM O'Beirne-Ryan and M Zentilli, and is included as an Appendix. Chapter 6 is a compilation of work undertaken by the author in collaboration with others in relation to weathering and Hg and U-Rn in the environment, and includes the portion of a document written exclusively by the author, published within a chapter of a text on Hg in Kejimkujick Park (Smith et al., 2005, published in O'Driscoll et al., 2005). In addition, Chapter 6 focusses on U-Rn and the environment, and includes an unpublished report on integration of U-Rn data for the Province into a GIS which the author undertook (1999). Chapter 6 concludes with an overview of fission track work on uranium distribution within the fresh and weathered granitoid, in order to assess the potential for U mobility during the weathering process. Chapter 7 synthesises and summarises key components of the thesis, and outlines recommendations for future work.

Chapter 2

Paleoweathered Surfaces on Granitoids of Southern Nova Scotia: Paleoenvironmental Implications of Saprolite

Preamble

This chapter is a reformatted version of the manuscript of AM O'Beirne-Ryan and Zentilli (2003), "Paleoweathered surfaces on Granitoids of Southern Nova Scotia: Paleoenvironmental Implications of Saprolite", published in Canadian Journal of Earth Sciences, Volume 40, p. 805-817. As the first author, AM O'Beirne-Ryan undertook all the fieldwork and research, prepared and wrote the manuscript. The coauthor suggested corrections to the manuscript prior to submission to the journal.

2.1 Abstract

In addition to minor post-glacial weathering effects, a complex history of three distinct weathering events has been identified within the granitoids of the South Mountain Batholith of southwestern Nova Scotia. Weathering prior to deposition of Carboniferous strata produced a well-developed saprolite, an *in situ* weathering profile.

Feldspars and micas are altered to clay minerals, and only weak preservation of granitic texture is evident. Subsequent burial and relithification have masked the original weathering mineralogy in this horizon. Beneath Triassic clastic sedimentary rocks is a thick horizon (30 metres) of weathered granitoid. This biotite-bearing argillaceous saprolite exhibits an intensifying-upward weathering zonation typical of weathered horizons, with increased proportions of clay minerals at the upper levels. A younger arenaceous saprolite of Pre-Pleistocene age can be found beneath glacial till at a number of locations throughout the batholith. These paleoweathered horizons attest to relatively warmer climates at several times in the geologic past. Their patterns of preservation imply some were much thicker and more widely distributed before partial erosion. The eroded materials may have formed the sediment for quartz sand in the Carboniferous sequence, clay and silica sand deposits of Cretaceous age, and a sandy till of Pleistocene age. The remnants preserved *in situ* today serve as significant conduits for water, and the geochemistry, mineralogy, and textures of these weathered profiles may enhance mobility and migration of U and Rn. These weathered horizons are mechanically weak, and the possibility of their presence should be considered when selecting construction and waste disposal sites.

2.2 Introduction

Saprolites, or the *in situ* weathered profiles that retain the textural integrity of the parent rock, record a period of intense weathering. Saprolite occurrences are unexpected in southern Nova Scotia, which has been conspicuously scoured by ice in the geologically recent past. Despite glacial erosion, these weathered horizons are found at a number of localities throughout the granitoids of southern Nova Scotia. Their preservation and occurrence raises questions regarding the nature of glaciation at these sites, pre-Quaternary paleoclimates, and landscape evolution in the region. Because saprolites are weathered remnants derived from fresh bedrock, their physical and

chemical properties typically differ from those of their unweathered parent, and their presence can contribute to a number of potential geotechnical and environmental problems. Saprolites have considerably higher permeability than their unweathered equivalent and can thus significantly affect groundwater flow rates and flow patterns (Jiao, 2000). Chemical changes within minerals during the weathering process may release useful soil elements such as K, Ca, and P, and also radioactive elements such as U or Rn (Chatterjee, 1983), any of which may enter the soil or hydrologic systems (Tieh et al., 1980). Preliminary fission track data from this study (O'Beirne-Ryan and Zentilli, 1999) suggest that U and Rn may be released during weathering. Known U and Rn anomalies in groundwater (O'Reilly, 1982) close to some of these weathered surfaces suggest that there may be a connection between the occurrence of U or Rn in groundwater, and leaching of U from nearby saprolites. Of further interest is the possibility that recent changes in atmospheric pH, that is, acidic precipitation, may have affected the rate of release of elements from these partially decomposed weathered granites, in particular, where they are exposed. Acidic precipitation may contribute to increased rates of chemical weathering and release of elements, or may change the buffering capacity of the rock. Understanding the nature of these saprolites is key to understanding such potential environmental and geotechnical concerns.

Weathered granitoid material on the South Mountain Batholith of Southern Nova Scotia has been reported previously (McNeil, 1954; Cumming, 1979; Grant, 1989, 1997; Finck et al., 1993, 1994; Prime, 2001), although no detailed study of the age or mineralogical and chemical nature of these weathered profiles has been undertaken. This research documents the relative chronological sequence of three separate saprolite-forming events on the South Mountain Batholith. The study also reports the variability within the saprolites formed at various times and the implications for paleoenvironmental conditions at the times of their formation.

2.3 Previous Work

The development of saprolites in tropical regions has been studied extensively (Velbel, 1985; Nesbitt and Young, 1989; Nesbitt and Markovics, 1997). The occurrence of saprolites in more temperate regions has only recently received more attention, as studies of these paleoweathered surfaces have made increasingly significant contributions to our understanding of paleoclimate and landscape evolution (Thomas, 1994; Lidmar-Bergstrom et al.,1997). Power and Smith (1994) compared saprolites found in very different climates in Ireland, Corsica, and southeast Brazil, and Lidmar-Bergstrom et al. (1997, 1999) documented numerous paleoweathered surfaces of various ages in glaciated terrain in Sweden. Some of these examples testify to the preservation of ancient highly weathered horizons, even under conditions of intense glacial erosion.

Chalmers (1898) described "sedentary rock", which he defined as rock decomposed *in situ* beneath the glaciated surface in many parts of Eastern Canada, and which he interpreted to be of Tertiary age. Other workers in the Atlantic Region of Canada have discussed the difficulties in determining the timing of saprolite development (Gauthier, 1980; Wang et al., 1981, 1982; McKeague et al., 1983; Grant, 1989; Bouchard et al., 1995), although most agree that saprolites preserved at a number of localities throughout Atlantic Canada either formed during warmer interglacial times or prior to the Pleistocene glaciations. These weathered surfaces preserved in glaciated terrain are significant in establishing the locally limited nature of glacial erosion (Grant, 1989). Leybourne et al., (2000) refer to a period of weathering and gossan formation during the Late Tertiary at the Murray Brook massive sulphide deposit, New Brunswick. In Cape Breton Island, Nova Scotia, McKeague et al. (1983), Wang et al. (1982), and Grant (1989), have described saprolite beneath till, and in the Cobequid Highlands of Nova Scotia, Rutherford and Thacker (1988) identified saprolite that they consider to have formed from the underlying rock during interglacial or preglacial times.

In southwestern Nova Scotia, previous work on weathering of the granitoids documented the distribution of some weathered granitoid horizons and provided a generalized field description of the surface outcrops (McNeil, 1954; Cumming, 1979; Grant, 1989, 1997; Finck et al., 1993, 1994). "Saprolite" was not used in these previous studies, and terms such as "residuum" or "weathered granite", applied to these paleosurfaces has led, in part, to an underestimation of their significance.

2.4 General Geology

The saprolites and their parent rocks discussed herein are located in southern Nova Scotia, which lies in the Meguma Zone of the Appalachian Orogen (Fig. 2.1). The Meguma Zone (Williams, 1995) is considered to be an allochthonous fragment accreted onto the eastern margin of the North American continent (Schenk, 1995). Rocks of the Meguma Zone are characterized by the presence of a thick sequence of Cambro-Ordovician slates and quartzites referred to collectively as the Meguma SuperGroup (Schenk, 1995). These Cambro-Ordovician rocks are overlain by Silurian sedimentary and volcanic sequences, and all have been intruded by Late Devonian granitoids of the South Mountain Batholith. This study focuses on the saprolites of the South Mountain Batholith (Fig. 2.2).

The South Mountain Batholith is the largest batholith in the Appalachian Orogen, with approximately one-third of the Meguma Zone underlain by peraluminous granitoid rocks. The lithologies of the batholith range in composition from biotite granodiorite and rarely more mafic rocks, to leucogranite (MacDonald, 2001). Although a complex history of intrusion within the batholith is evident, geochronological evidence suggests that all plutons were intruded and cooled during a short interval at ca. 372 Ma (Clarke et

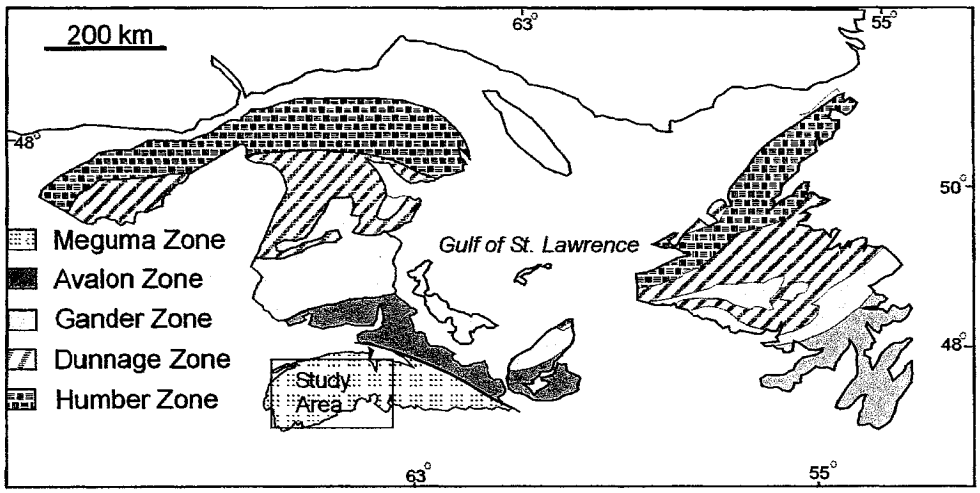

Fig. 2.1. Map of the Atlantic Provinces, showing the study area in relation to the geology of Atlantic Canada (modified after Williams, 1995)

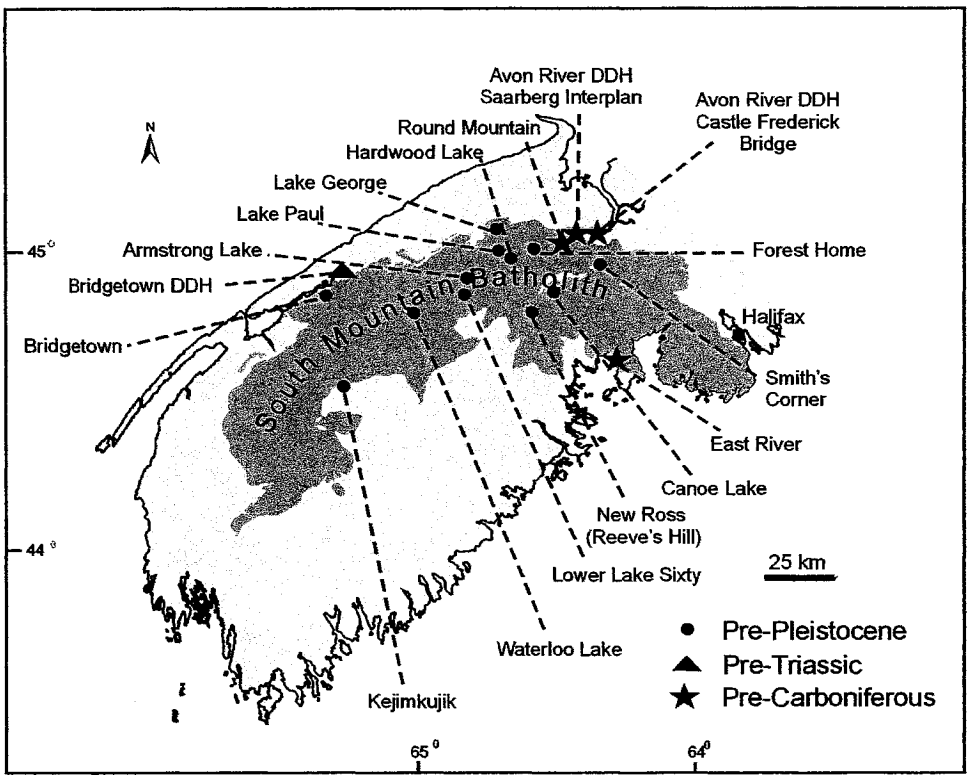

Fig. 2.2. Map of the South Mountain Batholith, showing locations of saprolite occurrences.

al. 1993; MacDonald, 2001). At various localities along the margins of the batholith, the granitoids are unconformably overlain by Carboniferous strata (Horton or Windsor Group) or by Triassic clastic sedimentary strata of the Fundy Group. The present-day surface of the batholith forms an elevated region of low relief in southern Nova Scotia, and much of the region is blanketed by unconsolidated Pleistocene glacial deposits (Finck and Stea 1995). Mineralization of varying types and styles, including U enrichment, can be found throughout the batholith (Chatterjee 1983; MacDonald 2001). Saprolite developed on such mineralized zones may result in significant mobilization or migration of certain elements, such as soluble U or gaseous Rn.

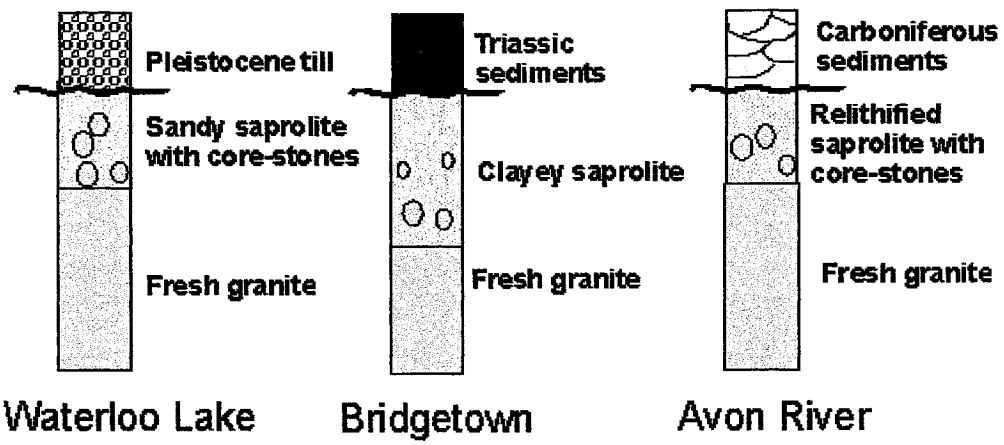

Fig. 2.3. Generalized stratigraphy of the saprolites of various ages in southern Nova Scotia. Not to scale.

Locations where weathered granitoid horizons are found at the surface and in drill core within the batholith are given in Figure 2.2 (McNeil, 1954; Giles, 1981; Finck et al., 1993, 1994). The best exposures of these saprolites are in the north-central and western portions of the batholith, close to the present-day highest elevations of the batholith (Fig. 2.2). Weathered granitoids found in drill core are overlain either by Horton Group sandstones of Carboniferous Age (Quarch et al., 1981), by Windsor Group limestones of Carboniferous age (Giles, 1981), or by Triassic sandstones and

shales (Wightman, 1999). Figure 2.3 summarizes the generalized stratigraphic relations within each paleoweathered sequence.

The degree of weathering is determined using two field classifications, both of which are semi-quantitative in nature: Ollier (1965) based his classification on the friability of the material, and Selby (1985) based his on the mass strength (Table 2.1). The physical properties of the saprolite units are outlined in Table 2.2. Both adopted a 5-point scale in which the highest score is assigned to the most weathered material. In general, the weathered horizons of the South Mountain Batholith show similar values under both classifications (Table 2.2), and are moderately to intensely weathered. Table 2.2 also provides a summary of the parent rock types (MacDonald, 2001) and the clay mineralogy of the fine fractions as determined by x-ray diffraction.

Table 2.1. Degree of weathering as determined in the field, after Ollier (O) (1965) and Selby (S) (1985)

Rank	**Descriptive term**	**Ollier (1965) (based on friability)**	**Selby, (1985) (based on mass strength)**
1 (O) I (S)	Fresh	Hammer tends to bounce off rock	Little or no sign of discolouration, loss of strength or other signs of weathering
2 (O) II (S)	Slightly weathered	Easily broken with hammer	Slightly discoloured, especially along joints; not much weaker than when fresh
3 (O) III (S)	Moderately weathered	Rock can be broken with a kick, but not by hand	Less than half the rock decomposed or disintegrated. Fresh rock fragments are present as blocks or corestones which fit together
4 (O) IV (S)	Highly weathered	Rock can be broken apart in the hands, but does not disintegrate in water	Rock is discoloured throughout; more than half of the rock material is decomposed; discoloured rock is present as blocks or rounded corestones
5 (O) V (S)	Completely weathered	Soft rock that disintegrates when immersed in water	All rock material is decomposed to soil but the original rock texture or fabric is largely preserved

Table 2.2 Characteristics of the weathered samples from the South Mountain Batholith, Nova Scotia

sample locality (Fig. 2.2)	rock type ***	argillic / arenaceous	age ****	max thick/ depth	mineralogy of clay-sized fractions and approximate maximum percentage**	degree of weathering Ollier (1965) Friability	Selby (1985) Mass strength	surface / core
Waterloo L	monzogranite	arenaceous	3A	2-6m	kao + chl + ?verm +/-il(<5%)	2 - 4	II - IV	surface
Hardwood L	monzogranite	arenaceous	3A	2-6m	kao + chl + ?verm +/-il(<5%)	2 - 4	II - III	surface
Smith Corner	leucomonzo	arenaceous	3A	2-6m	kao + chl + ?verm (<5%)	2 - 4	II - IV	surface
Reeve's Hill	leucogranite	arenaceous	3A	2m+/-	not available	1 - 4	I - IV	surface
Forest Home	leucogranite	arenaceous	3A	2m+/-	not available	2 - 4	II - IV	surface
Bridgetown	leucomonzo	arenaceous	3A	0-4m	kao + chl +?verm +/- il (<5%)	1 - 4	I - III	surface
Lr Lake Sixty	leucomonzo	arenaceous	3A	1-5m	not available	2 - 3	II - III	surface
Armstrong L	granodiorite	gravelly	3B	< 1m	not applicable	altered - gravelly surface		surface
Loon Lake	leucomonzo	gravelly	3B	< 1m	not applicable	felsic - gravelly surface		surface
Lake George	leucomonzo	gravelly	3B	< 1m	not applicable	unaltered- gravelly surface locally		surface
Bridgetown*	monzogranite	argillic	2	30 m	kao + dioct smect (20-60%)	4-5	III - V	core
Round Hill	monzogranite	relithified	1A	2-6m	not available	relithified weathered rock		surface
East River	monzogranite	relithified	1B	> 4m	not available	relithified weathered rock		core
Castle Frederick	monzogranite	relithified	1B	5m	not available	relithified weathered rock		core

* Bridgetown drill core

** kao =kaolinite; chl=chlorite; verm=vermiculite; il=illite; dioct smect = dioctahedral smectite

*** rock type as identified in MacDonald, 2001 (leucomonzo =leucomonzogranite)

**** 1A and 1B are pre-Carboniferous; 2 is pre-Triassic; 3A is pre-Pleistocene (pre-glacial); 3B is pre-Pleistocene, some peri-glacial

2.4.1 Pre-Carboniferous Weathering

Drilling through Carboniferous sediments intersected weathered granitoid at the Avon River and at East River (Fig. 2.2), although in only two of the drill cores, is the underlying fresh granitoid intersected (DDH# CFB-7 at Castlefrederick Bridge, Avon River, and DDH# ER-4, East River, Fig. 2.2). In addition, an outcrop of weathered granitoid beneath Horton Group strata has been found near Round Mountain (Fig. 2.2). At all three localities, the weathered granitoid has been relithified, as indicated by the tightly-cemented nature of the rock. This pre-Carboniferous horizon is most easily identified as a paleoweathered horizon where it is observed with the underlying unweathered parent and the overlying Carboniferous material (Fig. 2.4).

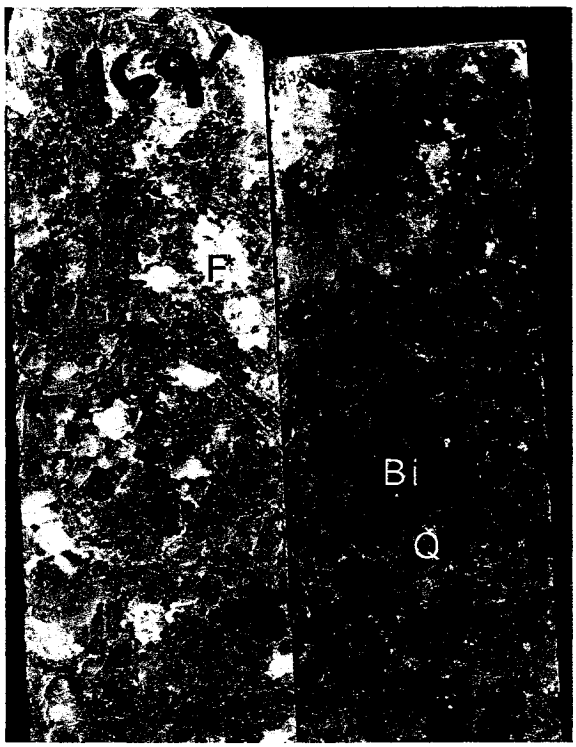

Fig. 2.4. Drill core of sub-Carboniferous paleoweathered granitoid (depth 1169') and fresh underlying granitoid (1186'). Biotite and feldspars have been completely replaced by clay minerals, and the relative proportion of quartz increased. Ghost pseudomorphs of clay after biotite and feldspar are labelled as Bi* and F respectively. Q = quartz; Bi = biotite; F = feldspar.

The preserved paleoweathered granitoid profile ranges in thickness from 3 to over 6 m. Vertical zoning within the paleoweathered profiles confirms the alteration formed as a result of a weathering process rather than hydrothermal alteration. This zoning is defined by the gradual upward destruction of the original "granitic" texture, and

the development of clay minerals at the expense of feldspar and biotite. In these profiles, the saprolite has been relithified to form a compact material in which only quartz from the original granite remains, although ghost pseudomorphs of micas and feldspars form part of the cementing matrix (Fig.2.4). Microprobe analyses indicate that the mineralogy is dominated by quartz and kaolinite, and even in the lowermost levels of the weathering profile, both biotite and feldspars have been intensely altered. The clay mineralogy present may not only represent original weathered mineralogy, but may also reflect diagenesis superimposed on weathering, which resulted in the subsequent relithification of this weathered horizon. Thermochronological data indicate that these rocks were buried to a depth of at least 4 km at temperatures of more than 150°C in the Early Permian, before exhumation at approximately 280 Ma (Ryan and Zentilli, 1993). Burial of a poorly-consolidated saprolite to these depths affected the textural and mineralogical features of this weathered horizon, as observed in petrographic examination.

The existence of a paleoweathered surface on the granitoid beneath Carboniferous strata confirms that not only was there rapid exhumation of the batholith, but also a subsequent period of intense weathering. This weathering was followed by an episode of partial erosion of the granitoid and its weathered surface, and deposition of the Horton Group strata in the Lower Carboniferous (Fig. 2.3). Paleogeographic reconstruction of Early Carboniferous positioning of Nova Scotia suggests that climatic conditions were likely tropical or sub-tropical (Calder, 1998). The complete breakdown of the biotite and the feldspar in the pre-Carboniferous weathered horizon suggests that weathering was intense during the development of these paleosurfaces. However, the absence of gibbsite suggests that leaching was insufficient to remove all silica during feldspar weathering, although it is possible that the relithification process evident in these horizons may have modified the mineralogy that initially developed during weathering.

Basal Horton Group strata are commonly arkosic in nature, as would be expected in rapidly weathered and eroded granitic terrain, and their overall mineralogy is similar to those of the underlying granitoids (Calder et al., 1998). Within the basal Horton Group, there is a high-purity quartz sand unit, the *glass sand* unit of Bell (1929),

which serves as a marker bed. The presence of this unit is enigmatic, as the apparent mineralogical maturity is not consistent with the proposed sedimentary environment of deposition. It is suggested here that the source of this glass sand unit was a highly-developed granite saprolite. Erosion of such a mature quartz-clay saprolite could explain the existence of these younger quartz-rich sand layers.

2.4.2 Pre-Triassic Saprolites

Three closely-spaced drill cores (DDH#s WP-99-2, - 3, -4) through Triassic sandstones and shales in the Bridgetown area of Nova Scotia, intersect intensely weathered granitoid at a depth of approximately 33 m (Fig. 2.2). The weathered profile developed on the granitoid in the drill cores is at least 30 m thick. The unweathered parent granitoid is encountered at the bottom of all three drill cores. Unlike the pre-Carboniferous weathered horizon which has been preserved in a relithified state, the pre-Triassic horizon is preserved as an unmodified saprolite; isovolumetric weathering has permitted the retention of granitic texture throughout the saprolite sequence, and in outward appearance, the saprolite is identical to the fresh granitoid. On closer inspection, the saprolite can be readily distinguished from the fresh granitoid as it crumbles to the touch, easily allows the insertion of a knife (Fig. 2.5), and the feldspars have been extensively weathered to clay minerals. The relatively high proportion of clay minerals developed, suggest that this saprolite should be referred to as an "argillaceous" saprolite (Lidmar-Bergstrom et al., 1997). In two of the drill core sections, the granitoid has been hydrothermally altered prior to weathering, and the mineralogy is of mixed hydrothermal and weathered origin. For the purpose of this study, only the unaltered but weathered drill core has been included.

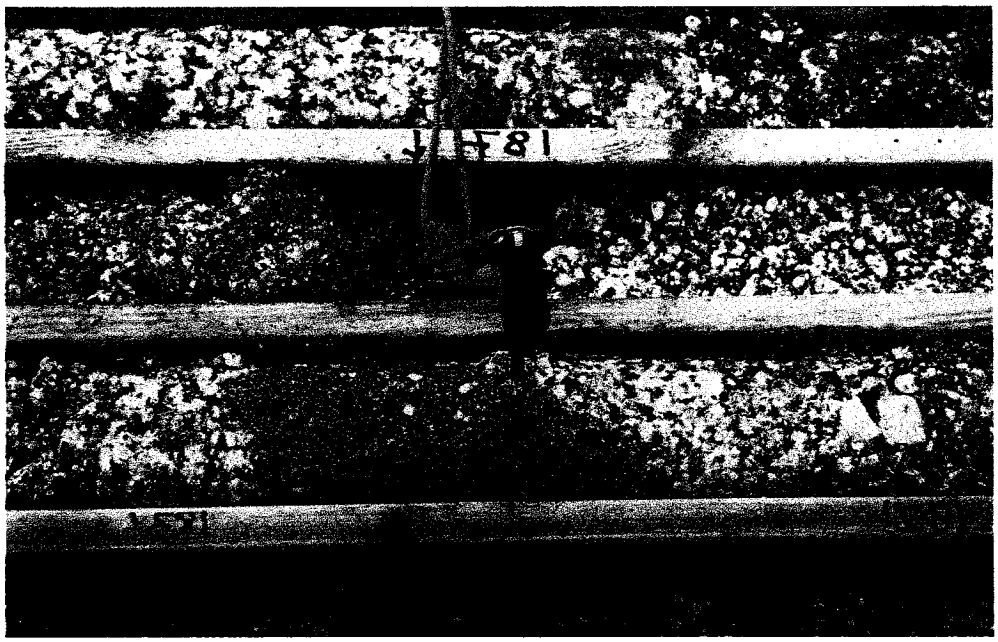

Fig.2.5. Complete disaggregation in granitoid with xenolith, as shown by penknife inserted into core, Bridgetown drill core #2

Field and laboratory evidence indicate a definite zonation from base to top of the generalized saprolite. In a complete mature weathered profile, saprolite is overlain by a soil developed from the weathering process. In the process of soil development, the saprolite in the upper levels loses its integrity and no longer retains the textures of the parent material. No soil has been preserved in the pre-Triassic weathering profile, nor is there evidence of destruction of the granitic texture in any but the uppermost couple of centimeters. The absence of a soil layer, and the persistence of granitic texture, suggest that the uppermost portion of the weathered profile was eroded prior to deposition of Triassic sediments, and that the remaining weathered section is only the lower part of a more extensive weathered profile.

Mineralogical changes within the preserved portion of the saprolite from base to top include a number of features that are compatible with the existence of a weathered profile, rather than a hydrothermal effect. There is an increase in overall proportions of clay minerals from base to top, consistent with weathering progressing from the top downwards. Throughout most of the profile, biotite is present and remains relatively unaltered at a macroscopic scale, even where the plagioclase and ultimately the

potassium feldspar have weathered to clay minerals. Clearly identifiable biotite throughout the profile is not typical of weathering profiles in general (Goldich 1938; Nesbitt and Young 1984). Relatively fresh biotite together with more intensely altered feldspars in the pre-Triassic saprolite is in contrast to the pre-Carboniferous saprolite, where both biotite and feldspars were altered during weathering. The pristine outward appearance of biotite in the pre-Triassic saprolite together with highly weathered feldspars, even at distances of 25 m above the fresh granitoid, suggests that conditions during formation were atypical, although Setterholm et al. (1989) report a similar preservation of fresh biotite in saprolite developed on schists and granitoids in Minnesota. In both the lower and upper levels of the pre-Triassic saprolite, plagioclase is weathered to clay minerals, whereas there is extensive alteration of the K-feldspar to clay minerals only at higher levels within the profile, consistent with typical feldspar weathering in granitoids (Goldich, 1938; Nesbitt and Young, 1984). Weathering of plagioclase typically precedes weathering of K-feldspar, as the Ca and Na are more readily removed from the system during early stages of weathering (Goldich 1938; Nesbitt and Young 1984). The resultant clay mineralogy in the pre-Triassic saprolite is dominated by kaolinite with lesser montmorillonite, and the relative proportions of kaolinite to montmorillonite increase upwards, as does the overall abundance of clay minerals. The diminution of grain size, particularly evident in the quartz grains, is similarly more intense towards the top of the sequence.

These systematic variations throughout the profile are expected in a weathering profile, where the most intense weathering is closest to the surface. At the base, the boundary between the saprolite and the fresh granite or the weathering front, appears to be sharp. At the top, above the unconformity, clasts of the saprolite have been incorporated into the overlying Triassic sandstones. The incorporation of clasts from the weathered zone into the overlying sediments confirms that the underlying saprolite represents a partially-eroded section of an even thicker weathering profile.

In addition to abundant primary (weathering) kaolinite in the pre-Triassic saprolite, the presence of montmorillonite and the persistence of biotite throughout most of the pre-Triassic profile indicate that the weathering event was insufficiently intense to leach the granitoid of all its soluble cations. This suggests that the climate may have

been more temperate than tropical in nature at the time this weathered surface developed. Although Gerrard (1994) cautions against basing interpretations of climatic conditions solely on the clay mineralogy present, he concludes that the presence of some clays and the absence of others does provide an indication of paleoclimatic conditions, with the presence and persistence of montmorillonite suggesting arid to semi-arid conditions during formation. Calvo et al. (1983) and Ismail (1970) also suggest that the development of montmorillonite is more likely to occur under semi-arid to arid conditions, or alternatively under moist, alkali conditions; more intense leaching, as expected under more acidic conditions, would remove the cations from the developing clay. The absence of gibbsite is a further indication that leaching of cations during weathering was less intense, as all clays present (kaolinite and montmorillonite) retain elements other than aluminum and oxygen. Thus it seems reasonable either to propose that semi-arid conditions prevailed during weathering, or that leaching processes involved predominantly alkaline conditions, or indeed, that a combination of semi-arid weathering under alkaline conditions prevailed during the formation of this profile. The persistence of these conditions throughout the development of a thick saprolite mantle, may provide clues as to why biotite is so well preserved throughout most of this saprolite horizon.

In addition to establishing the existence of a prolonged period of weathering in pre-Triassic times, the thickness of these weathered profiles, and the fact that they had been partly eroded prior to deposition of the Triassic sediments, suggest that more extensive regions of weathered horizons may have developed during this time. These weathered horizons probably provided a rich source of sediment, which is long-since eroded, explaining its sparse distribution today. The intensity and depth of the weathering profile developed in pre-Triassic times, and the dominance of kaolinite in this profile, suggest that this intense weathering event may have provided source material for such deposits as the Cretaceous kaolinite clays and quartz sands in Nova Scotia. Stea et al. (1995) have suggested that the source material for the Cretaceous kaolinite and quartz sand deposits may have been distal. The recognition in this study of the presence of a thick saprolite rich in kaolinite, of pre-Triassic or Early Triassic age, offers a potential proximal source for these kaolinite and quartz sand deposits. The sub-Triassic weathering profile attained a minimum thickness of 30 m; if this weathering

event was widespread, then subsequent erosion of the weathered horizon means that great quantities of kaolinite were eroded and potentially deposited elsewhere. A comparative study of weathering-resistant minerals within the weathered profile and in the Cretaceous sediments may provide additional evidence.

2.4.3 Pre-Pleistocene Saprolites

Pre-Pleistocene paleosurfaces on the South Mountain Batholith can be clearly distinguished from outcrops of granitoids undergoing chemical and mechanical weathering at present, in both the intensity and depth of modification as a result of weathering processes. The paucity of clay mineral development in these horizons is one factor that suggests they represent a different, younger, weathering event than either the pre-Carboniferous or the pre-Triassic weathering. The pre-Pleistocene paleosurfaces are overlain locally by glacial till (Fig. 2.6A), confirming their pre-glacial origin. Near Digby, Nova Scotia, an outcrop of North Mountain basalt of Early Jurassic age displays a similar arenaceous weathering profile (Prime, G., Nova Scotia Dept of Natural Resources 2001 pers.comm., and Fig. 2.7), providing evidence of a post-Early Jurassic age for this weathering. These field relations bracket the age of the weathering event as between Early Jurassic and Pleistocene.

These exposed weathered horizons are 0-6 m in thickness (Table 2.2), retain the granitic texture of the underlying parent, and are dominantly sandy or arenaceous in nature, unlike the clay-rich saprolites of pre-Triassic age. The saprolitic profiles have provided a rich source of ready-made gravel, and most good exposures of this material are found in partially excavated pits or quarries (Fig. 2.6B). The outcrop manifestation of these pre-Pleistocene saprolites varies from one location to another. At several locations, the weathered surface is identified by the presence of a thick sandy saprolite profile (0.5 m - 4 m or more) developed over the entire outcrop (Waterloo Lake (Fig. 2. 6B), Hardwood Lake, Smith's Corner, Lower Lake Sixty). The saprolites may have preserved corestones of unweathered or incipiently-weathered granitoid; in such cases, a medium-grained sandy saprolite is well-developed in between the corestones (Fig. 2. 6D). As weathering proceeds along joints, a rounded core of unweathered granitoid is

surrounded by weathered material. The presence of these rounded boulders of granitoid composition in locally-derived till, as found in the overlying till at Waterloo Lake, for example (Fig. 2.6A), is significant in that it attests to local derivation of well-rounded material within a sediment (O'Beirne-Ryan et al., 2001).

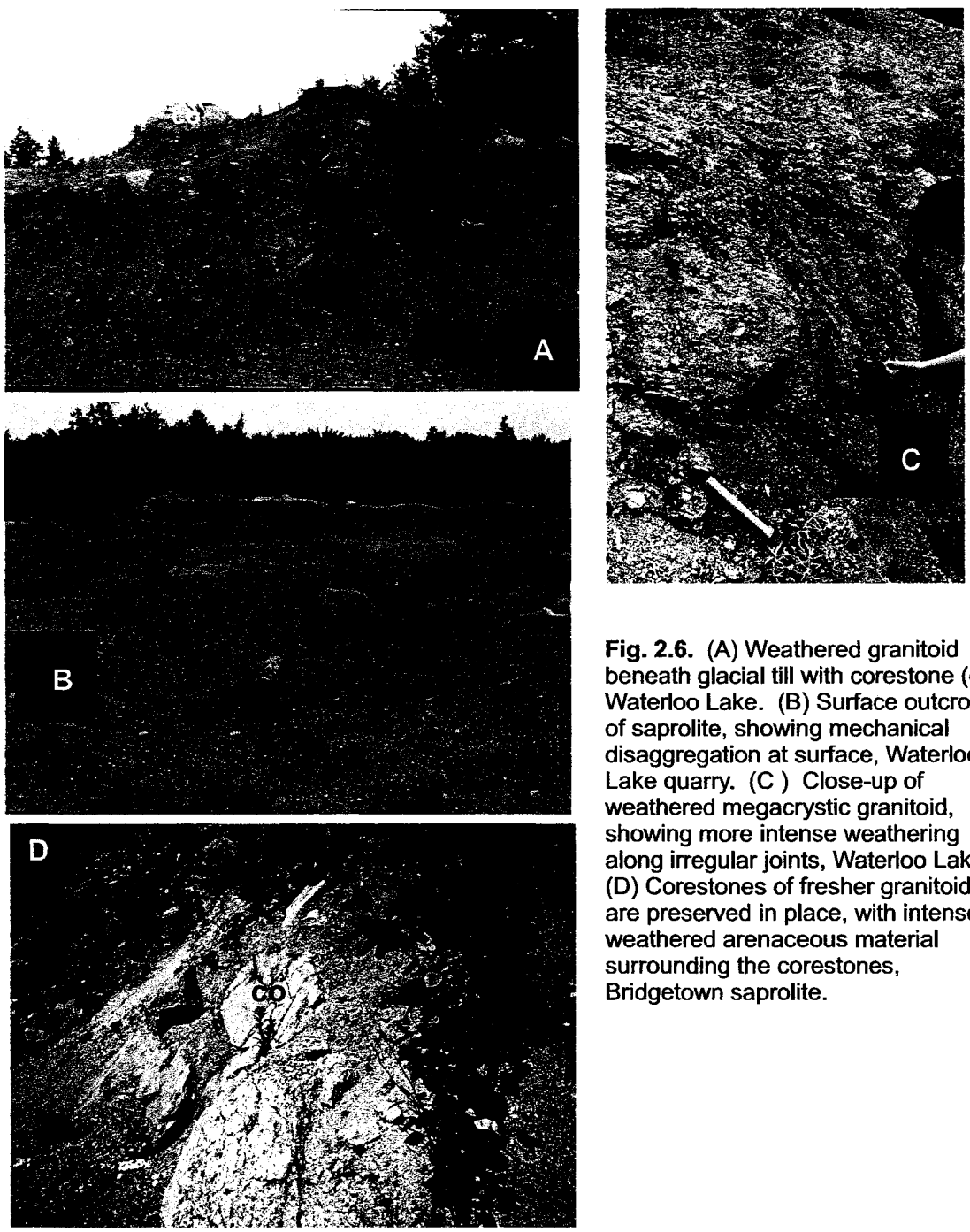

Fig. 2.6. (A) Weathered granitoid beneath glacial till with corestone (co), Waterloo Lake. (B) Surface outcrop of saprolite, showing mechanical disaggregation at surface, Waterloo Lake quarry. (C) Close-up of weathered megacrystic granitoid, showing more intense weathering along irregular joints, Waterloo Lake. (D) Corestones of fresher granitoid are preserved in place, with intensely weathered arenaceous material surrounding the corestones, Bridgetown saprolite.

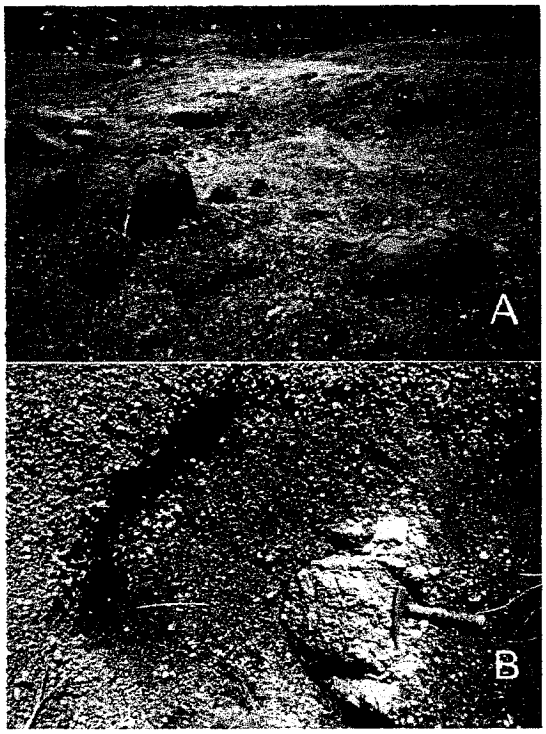

Fig. 2.7. Saprolite developed on North Mountain Basalt of Triassic age. (A) Highlights corestones of basalt. (B) Close-up of the saprolite. (Photo courtesy of G.Prime, Nova Scotia Department of Natural Resources).

At first glance, the saprolite resembles the parent granitoid in texture and overall structure. It differs from the underlying unweathered or incipiently weathered granitoid in its extremely friable nature and the presence of extensive irregular microfractures that typically form centres of more intense weathering (Fig. 2.6C). Locally, along some of these joint patterns, a reddish-brown oxidation develops, and produces a mottled appearance (Fig. 2.6C). Elsewhere, no such colouration change is evident between the fresh rock and the crumbly weathered material in the joints (Fig. 2.6D). These sandy saprolites found today beneath till of Pleistocene age or at surface, are chemically less modified as a result of weathering than the argillaceous saprolites of pre-Triassic Age (O'Beirne-Ryan and Zentilli, 2003). Setterholm et al. (1989) refer to similar less-friable but obviously weathered horizons as "saprock". In the absence of a complete weathered profile on the Nova Scotia granitoids of pre-Pleistocene age, the more general term "saprolite" has been used.

X-ray diffraction studies confirm the paucity of clay minerals in these weathered profiles (typically less than 5%), and indicate that the clay minerals present are different

from the clays of the pre-Triassic saprolite (Table 2.2). The feldspars show varying degrees of mild to moderate chemical weathering. Typically plagioclase is more intensely weathered than K-feldspar, although in outward appearance, all feldspars maintain their euhedral to subhedral shape (Fig. 2.8), with microcracks developed throughout. Biotite commonly exhibits incipient oxidation.

These surface outcrops of saprolite are of low relief, and are best developed on coarse-grained inequigranular or megacrystic parent granitoid, which varies in composition from monzogranite to leucogranite (Table 2.2). The texture and/or mineralogy of parent material may be key to the nature of the weathered profile developed. At sites where both fine- to medium-grained equigranular felsic granitoid and coarse-grained inequigranular more mafic granitoid are found in the same outcrop, such as at Waterloo Lake and at Smith's Corner, the nature of the weathering on the two rock types differs. The coarse-grained, more mafic granitoid, which is also more permeable than the fine-grained granitoid, develops a weathered mantle (Fig. 2.9A) in which weathering clearly intensifies upwards. The fine-grained equigranular granitoid more typically develops a thin veneer of angular fragments with less intense chemical weathering (Fig.2.9B). This suggests that the equigranular more felsic granitoid is more resistant to chemical weathering than other granitoid rocks of differing texture and composition.

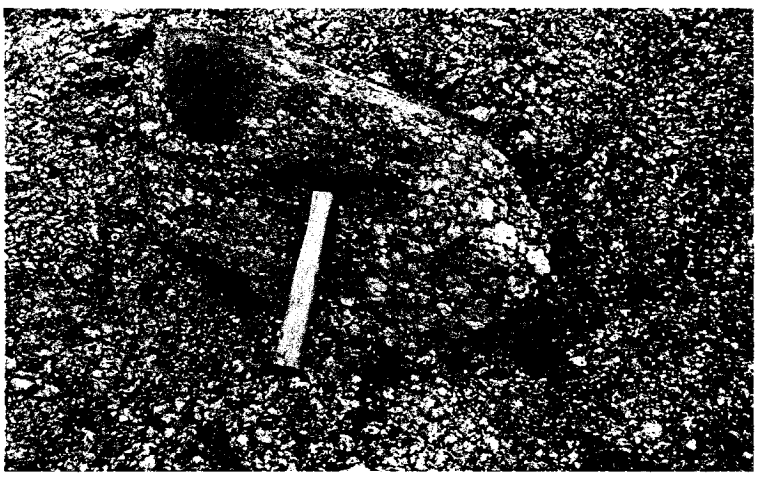

Fig. 2.8. In situ unconsolidated megacrystic granitoid showing numerous microfractures, Waterloo Lake.

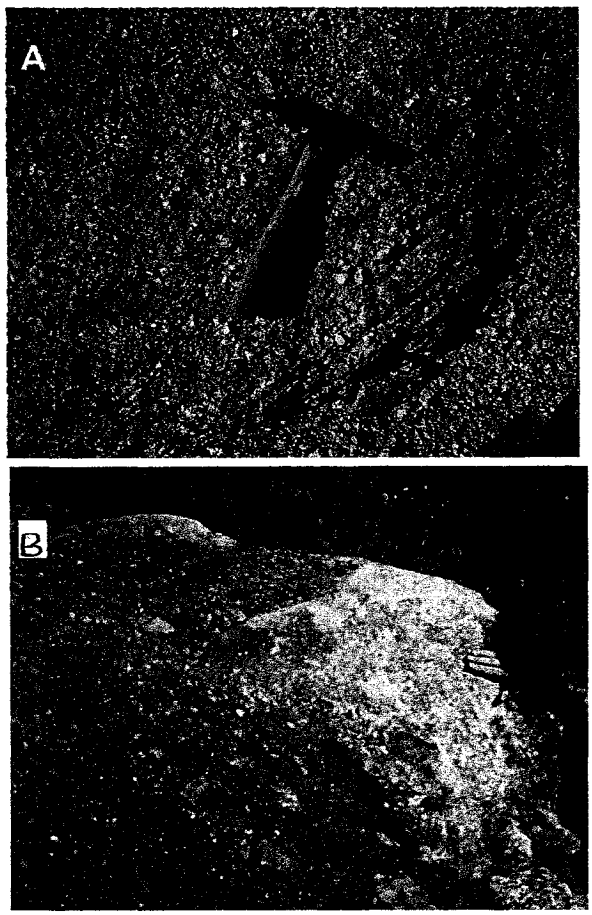

Fig. 2.9. Smith's Corner quarry. (A) Coarse-grained inequigranular monzogranite, showing ready disaggregation at surface; fragments are sub-angular to rounded. (B) Medium-grained equigranular granite, showing only small amounts of weathering on surface. Fragments are angular and show less disintegration than in A.

Differences in hydrologic regimes at different sites can also affect the intensity of weathering observed. Weathering will progress more rapidly in well-drained environments than in water-saturated environments (Thomas 1994). At present, there is no evidence that there were different hydrologic regimes at the different sites. Detailed mapping in relation to ancient land surfaces would be required in order to confirm or refute this possibility, but the glacial cover in Nova Scotia makes such detailed mapping difficult. The nature of the paleotopography may have been significant in determining the intensity of weathering. Weathering profiles are more readily preserved if weathering is not immediately followed by erosion, and preservation of weathered profiles would be more likely in regions of gentle slope, or regions in which soil cover protected the weathering profile, rather than in regions of high relief. The weathering profiles preserved under the glacial till are commonly in relatively flat-lying or gently sloping locations, in regions of higher elevation within the batholith.

At some localities (eg. Waterloo Lake), physical breakdown of the saprolite has resulted in the development of an unconsolidated gravelly material. At Big Bald Mountain, NB, this type of material has been referred to as "non-saprolite residuum" by Bouchard et al. (1995). In southern Nova Scotia, this gravelly material is similar in overall mineralogy to the saprolite, but it no longer retains the textural integrity of the parent rock (Fig. 2.8). Texturally, this *in situ* unconsolidated material ranges from clay-sized particles to fragments up to 10 cm or more in diameter. These fragments are rounded to angular, and may consist of individual mineral grains, or more commonly of mineral aggregates. In other localities, particularly where the granitoid had been hydrothermally altered or where a fine-grained facies is present, no true saprolite exists, and a gravelly layer of angular fragments directly overlies incipiently-weathered granitoid. This gravelly material may be separated from the parent granitoid by a thin horizon of clay, less than 1 cm in thickness. McKeague et al., (1983) described similar broken surfaces in exposed regions surrounding an occurrence of saprolite in Cape Breton, and suggested that, if not for the extensive forest cover, the region might be referred to as a blockfield or "felsenmeer", produced as a result of frost-fracturing of bedrock. Given the extensive evidence of glacial activity in proximity to the southern Nova Scotia saprolite locations, it is possible that physical weathering contributed to the development of some of the more gravelly surfaces, although their development may well have been precipitated by the presence of chemically-weakened fractures.

In discussing saprolites in Nova Scotia and elsewhere in the Atlantic Provinces, McKeague et al., (1983), Grant, (1989), and others have suggested that the preservation of saprolites beneath till is the result of cold-based glaciers overlying these localities, as the material has not been removed by glacial erosion. If a thick sequence of saprolite had developed prior to glaciation, then it is possible that glacial erosion may have been extensive but not complete at these localities. Supporting evidence can be recognized in some of the tills in the region, where abundant gravelly granitoid material is locally derived (Finck and Stea, 1995; Fig. 2.10). Furthermore, the clasts within the till itself are variably weathered, some rotted and some pristine; if weathering had occurred after incorporation of the clasts into the till, then all clasts of the same size and same rock type should be similarly weathered, which they are not. These factors combine to suggest that it is possible glacial erosion occurred over regions within the

South Mountain Batholith which had been deeply weathered prior to glaciation, but that varying degrees of glacial erosion of these surfaces have exposed different levels within the saprolitic profiles at the various sites.

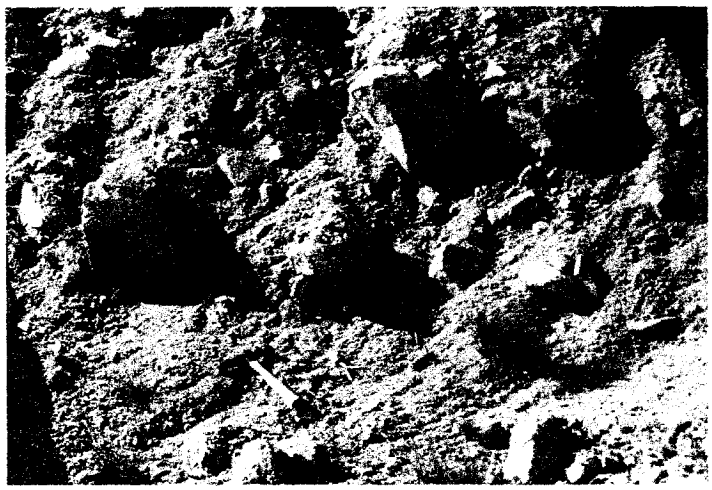

Fig. 2.10. Sandy till of granitic composition in the Halifax area.

2.5 Discussion

2.5.1 Age of saprolites and implications for landscape evolution within the Meguma Zone

Saprolites developed on the granitoids of southern Nova Scotia of pre-Carboniferous, pre-Triassic, and pre-Pleistocene age, each with distinctly different features (Table 2.2), attest to multiple episodes of exhumation, weathering, and reburial in southern Nova Scotia since Devonian times (Fig. 2.11). Distinct differences in the style and mineralogical make-up of the saprolites of different ages, suggest that different environmental conditions prevailed during the formation of each. This, in turn, suggests variations in climate, or at least, variations in hydrologic and atmospheric regimes during each time period. In particular, distinctive features of the pre-Carboniferous paleoweathering include the complete weathering of biotite as well as feldspars, and the relithification of the weathered horizon. Within the pre-Triassic

weathering horizon, the biotites are preserved in an argillaceous saprolite in which feldspar is moderately to strongly weathered, and there is no relithification of the saprolite. Such differences indicate that the pre-Triassic saprolite cannot represent re-exposed pre-Carboniferous weathering surfaces. The preserved pre-Pleistocene weathered surfaces have low proportions of clay minerals. Basalts of Early Jurassic age exhibit weathering features similar to those of the sub-Pleistocene saprolites, and confirm an episode of weathering that post-dates the Early Jurassic. It can be argued that the granitoids in the highlands of the South Mountain Batholith where these pre-Pleistocene saprolites occur, would have been exposed to weathering during the mid-Cretaceous, which led to karstification in the Mississippian carbonates and evaporites of the Windsor Group (Davies et al., 1984) and deposition of Aptian-Albian strata (Stea et al., 1995). Davies et al. (1984) indicate a period of pre-mid-Cretaceous deep weathering and karstification under relatively warm conditions in the Atlantic margin from Labrador (Gross, 1968) to Long Island, New York, where lateritic weathering has affected the bedrock (Blank, 1978). In Labrador, weathering has enhanced the economic viability of Precambrian iron formations (Gross, 1968). Furthermore, current work by Grist and Zentilli (1999) makes a case, on the basis of apatite fission track data, for increased mean annual surface temperatures in Late Cretaceous-Early Eocene time, which could have coincided with relatively deep weathering in the granitic highlands as late as the Eocene. This evidence constrains the timing of the peak of weathering in the pre-Pleistocene to Cretaceous-Early Eocene.

2.5.2 Environmental and geotechnical implications

In addition to providing information on the paleoclimate, the presence of saprolites is of particular concern from an engineering and environmental geochemistry perspective.

In most surface outcrops of saprolitic profiles in the South Mountain Batholith, there is a weakening of the rock strength and an increase in permeability. A till cover over much of the batholith makes it difficult to determine the extent of these weakened rocks in populated areas. Of further significance to development or construction, is the

fact that in many localities, saprolite development is spatially restricted to joint and fracture zones. The potential existence of friable, permeable material up to several metres in thickness, or of greater aerial extent, urges caution in construction, slope modification, and in the selection of sites for waste disposal or septic field development, particularly in regions of till coverage, which may serve only to hide weakened bedrock below.

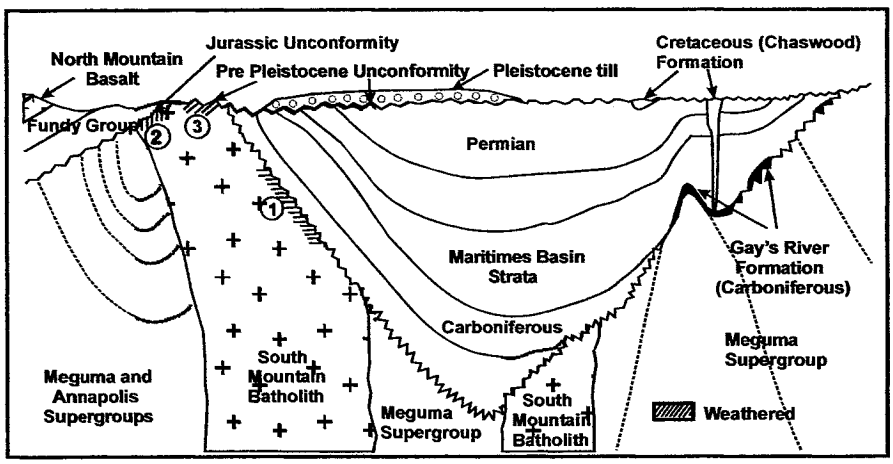

Fig. 2.11. The relative timing of saprolite development as it relates to the geologic history of southern Nova Scotia. Diagram modified after Moore et al., 2000. 1,2, and 3 refer to the Pre-Carboniferous, Pre-Triassic, and Pre-Pleistocene saprolites respectively.

The friable and permeable nature of saprolites provide for rapid infiltration of fluids, as well as creating conduits for groundwater flow, changing dramatically the hydrologic regime typically expected within a terrane of granitic bedrock. Surface saprolites within Nova Scotia are commonly situated on high ground, and drainage is downslope from these regions. Modification of water as a result of interaction between the bedrock and surface or groundwater is likely on three counts: (a) the friable nature of the material means that there are many microchannels developed within the saprolite, exposing a greater surface area of the granitoid to interaction with water; (b) the rocks have already undergone some chemical change, but weathering has not been intense, so there is possibly a considerable amount of soluble material readily available within the saprolite; (c) precipitation in Nova Scotia is acidic, potentially increasing the rate of chemical reaction within the minerals and along grain boundaries, and the potential for release of acid-soluble elements, such as U, into groundwater.

An additional factor in relation to groundwater contamination and increased weathering potential, is the seasonality of the Nova Scotia climate. Cold winters mean little infiltration during the winter months. Commonly, this period of low temperature is followed by rapid flushing during spring thaw, which may reduce the likelihood of intense leaching, but on the other hand, may increase the rate of mechanical breakdown of the saprolite, particularly saprolite exposed at surface. Summer and autumn rains may create conditions more favourable to greater leaching, as temperatures are higher and rates of fluid flow generally slower, thus contact time with mineral surfaces is longer. Furthermore, the potential for contamination of groundwater or surface water as a result of interaction with saprolites is particularly significant where these rocks have been either physically or chemically disturbed. Physical disruption of weathered horizons is evident in the present-day exposures of these weathered materials in excavated pits and quarries. Chemical modification is possible subsequent to this physical disruption, and/or where hydrothermal alteration prior to saprolite development has resulted in concentration of elements such as U within the weathering zone.

Continued chemical breakdown on these disturbed surfaces of loose gravel-like material is evident in the development of a thin cover of soil and vegetation, at previously excavated sites from which material has not been removed in the past 5 to 10 years. Further research into the weathering process from a geochemical and mineralogical perspective form additional components of this research project (O'Beirne-Ryan and Zentilli, 2003).

2.6 Acknowledgments

Without the help of Garth Prime and Phil Finck of Nova Scotia Department of Natural Resources, many of the outcrops of pre-Pleistocene weathering would have gone undiscovered. We would like to thank John Whiteman and Larry Riteman for allowing us access to the drill core. We are grateful to Beatrice Levi for her XRD input. Thanks to Bob Ryan for his continued support of the project. The authors gratefully acknowledge the suggestions of Jeanne Percival and one anonymous reviewer.

Chapter 3

Rounded Cobbles That Have Not Travelled Far: Incorporation of Corestones from Saprolites in the South Mountain Area of Southern Nova Scotia, Canada

Preamble

Chapter 3 is the reformatted manuscript by RJ Ryan, AM O'Beirne-Ryan and M. Zentilli (2005), "Rounded cobbles that have not travelled far: Incorporation of corestones from saprolites in the South Mountain area of southern Nova Scotia, Canada", published in Sedimentology, volume 52, p. 1109-1121. AM O'Beirne-Ryan did 40% of the writing, particularly as related to the nature of weathering, as well as suggestions and corrections prior to final submission to the journal.

3.1 Abstract

Saprolitic palaeosurfaces occur at several localities on the granitoid rocks of the South Mountain Batholith of Nova Scotia. There are three ages of saprolites within the study area, pre-Pleistocene, pre-Triassic and pre-Carboniferous. Within these "in place" weathered horizons there are remnant ellipsoidal blocks of unweathered granitoid referred to as corestones. These corestones are isolated rounded pods of relatively unweathered material surrounded by rotted granitoid saprolitic material. The weathered material which surrounds these corestones is poorly consolidated and easily eroded. The erosion of these horizons produces a lag deposit that contains many rounded corestones which can be incorporated into subsequent sedimentary units. The rounded boulders, cobbles and pebbles of granite within many of the Pleistocene glacial deposits in southern Nova Scotia are probably related to the incorporation of these saprolite

related structures, given the locally derived (within 400 m of the source) nature of the tills. The presence of saprolites at unconformities of various ages on the South Mountain granitoid rocks suggests that incorporation of saprolitic material probably occurred along a number of palaeosurfaces in the past. The recognition of this process has implications for the interpretation of rounded granite-clast conglomerates and quartz-rich sandstones of various ages within the stratigraphic record of eastern Canada. Similar palaeosurfaces elsewhere in the world also have related saprolite-derived sedimentary rocks associated with them. In summary, well rounded spherical pebbles, cobbles and boulders of granitoid material incorporated in sedimentary strata, need not have traveled far from source nor are they necessarily recycled from older conglomerates.

3.2 Introduction

The starting point for all clastic sedimentary rocks is the weathering process of pre-existing rocks. Nonetheless, weathering processes have not received the degree of detailed study by sedimentologists warranted by their intricate role within the rock cycle. This paper concentrates on the information that sedimentologists and stratigraphers can derive from a better understanding of the weathering processes involved in the sediment creation, in particular, the implication of these processes on the incorporation of weathered rock and pre-rounded clasts into sedimentary strata.

The existence of well-rounded cobbles in intraformational conglomerates within sequences that lack the sedimentological characteristics of long transport and aggressive abrasion necessary to produce rounded clasts, has been problematic. Most often, in the absence of any evidence of long transport, these rounded clasts are attributed to recycling of cobbles and boulders from older conglomerates. These clasts have been interpreted as older cobbles recycled into younger sedimentary strata, such as in the basal conglomerates of the Carboniferous Horton Group in Nova Scotia. Similarly it has been difficult to explain why well-rounded cobbles and boulders occur in locally derived glacial tills, such as the Beaver River Till in southern Nova Scotia. As a

consequence of the ongoing study of weathering profiles (saprolites) of varying ages on the granitoid rocks of the South Mountain Batholith (O'Beirne-Ryan and Zentilli, 2003) the identification of remnants of the weathering profile on the granitoids may hold the key to reinterpreting many of the rounded cobbles and boulders observed in sedimentary sequences in Nova Scotia and elsewhere.

3.3 General Geology

The rocks and saprolites referred to in this paper are located in the South Mountain Batholith of southern Nova Scotia. Southern Nova Scotia forms the Meguma Zone of the northern portion of the Appalachian Orogen (Fig. 3.1A). The Appalachian Mountains stretch from Newfoundland to southern United States. The Meguma Zone is thought to be an allochthonous fragment accreted onto the eastern margin of the North American continent and represents the final stage of continent building in eastern North America. The zone or terrane is characterized by the presence of a thick sequence of Cambro-Ordovician meta-sedimentary slates and quartzites referred to as the Meguma Group. These rocks are in turn overlain by younger sedimentary and volcanic sequences. The Meguma Group rocks have been intruded by Late Devonian granitoids of the South Mountain Batholith (Williams, 1995; Fig. 3.1B).

Approximately one third of the Meguma Zone is underlain by peraluminous granitoid rocks ranging from biotite granodiorite to leucogranite (MacDonald et al., 1992). The South Mountain Batholith is the largest intrusive igneous body in the Appalachian Orogen. The granitoids of the South Mountain Batholith comprise numerous map units which can be assigned to 13 plutons (MacDonald et al., 1992). Textures range from megacrystic, coarse-grained to medium-grained equigranular, to very fine-grained units. The plutons can be grouped together into two main stages: 1) older, predominantly granodiorite and monzogranite plutons, and 2) younger plutons, dominated by monzogranite, leucomonzogranite and leucogranite (MacDonald et al., 1992; Fig. 3.1B). Although there is a complex history of intrusion within the batholith, the geochronological evidence indicates that all plutons were intruded and crystallized

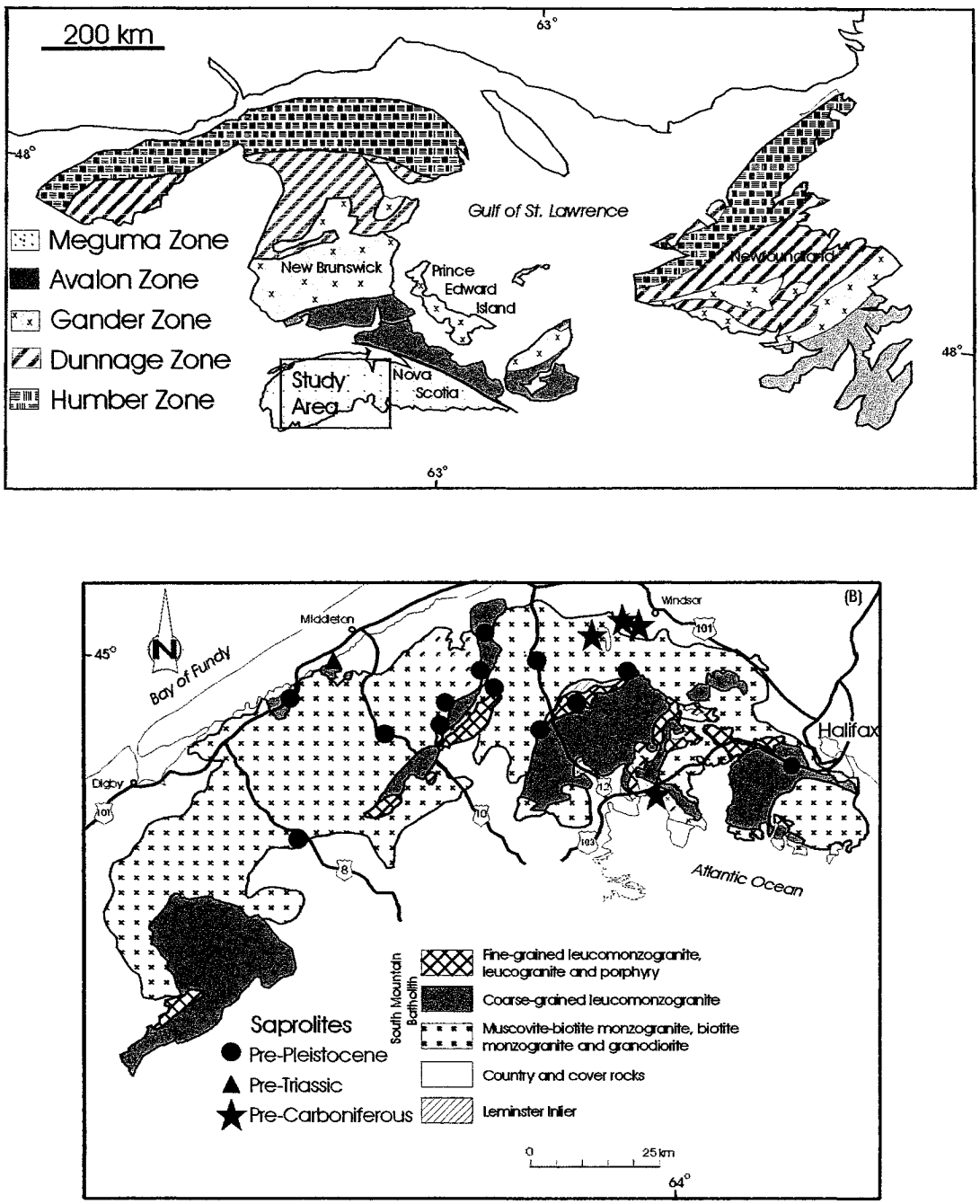

Fig. 3.1. (A) Location of the study area and general geological setting of the northern Appalachians, after Williams (1995). (B) Geology of the South Mountain Batholith and saprolite locations, after MacDonald et al. (1992).

during a short time interval at *ca* 370 Ma (MacDonald *et al.*, 1992). The age of the intrusion and the subsequent uplift and erosion of the cover rocks and the batholith itself, are important in the understanding of the weathering profiles of the South Mountain Batholith. At various localities along the margins of the batholith, exposures of the granitoids are unconformably (nonconformities) overlain by Early Carboniferous sedimentary rocks and by Triassic clastic sedimentary strata. However, the most common strata overlying the South Mountain Batholith are unconsolidated Pleistocene glacial tills (Finck & Stea, 1995).

O'Beirne-Ryan and Zentilli (2003) have reported the presence of deep weathered profiles at the surface of exhumed granitoids in southern Nova Scotia. There are numerous localities of weathered palaeosurfaces preserved on top of the South Mountain Batholith (Fig. 3.2), however the best exposures occur in the north-central and western portions of the batholith. Many of these palaeoweathered horizons, or saprolite localities, have been used for aggregate production. The aggregate producers take advantage of the ease of excavation to produce road fill for the local area. The excavation of the weathered granite creates excellent exposures of the weathering profile (O'Beirne-Ryan and Zentilli, 2003).

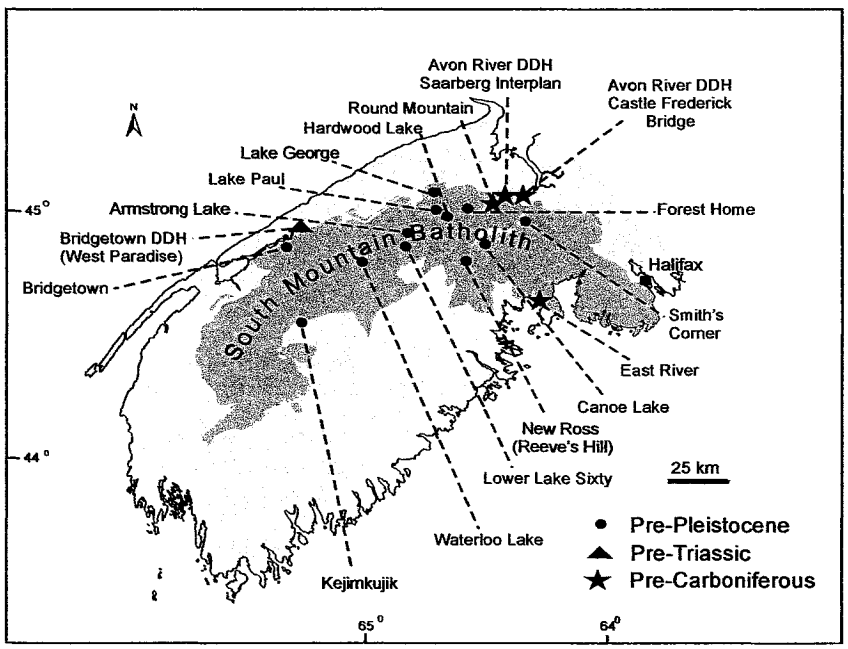

Fig. 3.2. Sample locations and location names of saprolite occurrences on the SMB.

3.4 Weathering, Saprolites, and Corestones

A variety of terms have been applied by various workers to describe weathered rocks, so for the purpose of clarity the nomenclature used for this paper is presented here. Saprolite is soft decomposed and/or disaggregated rock, which has been weathered in place from a sedimentary, metamorphic or igneous rock. Lidmar-Bergstrom et al., (1997) suggest that saprolites can be divided into two classes: arenaceous (sand-rich) and argillaceous (clay-rich). Arenaceous saprolites may contain up to 25% quantities of clay and silt, although most contain less than 5% of fine material. The quartz, K-feldspar and mica give these arenaceous saprolites a gravelly appearance. The upper portion of most mature saprolite profiles includes a zone in which only the more weathering-resistant minerals survive. The upper zones of such mature profiles typcially consist of combinations of varying proportions of quartz, clay minerals, bauxite, and iron oxyhydroxides, with clay and quartz dominating in most weathered granitoid profiles (Nesbitt & Young, 1989). Incipient or immature profiles, those manifesting less intense chemical weathering, do not show such extensive degradation. Saprolites represent a unique geological event and these horizons are often referred to as weathered palaeosurfaces when they occur within stratigraphic successions. The saprolite horizons can be subdivided further based on field observations of the cohesiveness of the weathered material. The term "disaggregated arenaceous saprolite" is used herein to describe the sand- and gravel-like material in which the structural integrity of the rock has been severely diminished, leaving sand to gravel-sized residuum (Fig. 3.3). Similar rotten granitoid material, differing in that it retains the granitic textures and better retains cohesiveness, often occurs deeper within the weathering horizon and is referred to herein as "cohesive arenaceous saprolite" (Fig. 3.4).

Fig. 3.3. Arenaceous saprolite material resultant from weathering of a granite, white areas are composed of weathered plagioclase (Finck photo) .

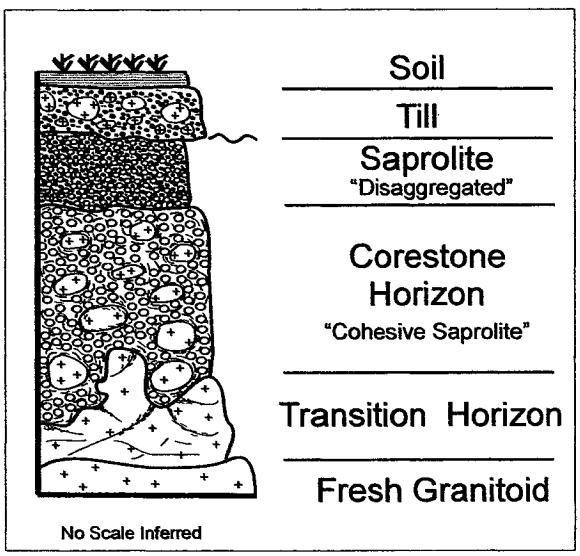

Fig. 3.4. Idealised pre-Pleistocene profile through a soil, till and saprolite on the granitoids of the South Mountain Batholith. Not to scale.

Corestones are ellipsoidal to sub-angular blocks of bedrock formed by progressive weathering of the bedrock along cross-cutting fracture systems. The block is isolated from fresh bedrock by weathered material as spheroidal weathering progresses. Corestones typically occur in granitoid or basaltic rocks which are jointed and preferentially weathered on the fracture surfaces. The presence and patterns of fractures and joints are controlling factors in the development and size of the corestones. The weathering begins along surfaces where ground and surface water

can infiltrate; as the weathering proceeds, the original block may be separated from the bedrock surface by an intervening deeply weathered horizon or an irregular crag connected to the unweathered bedrock (Fig. 3.5). In the Nova Scotia samples studied, either cohesive or disaggregated arenaceous saprolite is the material found most often surrounding corestones. Cohesive saprolites are often made up of aggregates of grains rather than individual mineral grains, bound loosely together so as to be sampled as blocks, however they can easily be crushed with a hammer. A hammer test is the obvious method to distinguish the weathered horizons: instead of the ringing of the hammer on fresh granite, the saprolite response to the hammer is a resounding dull thud.

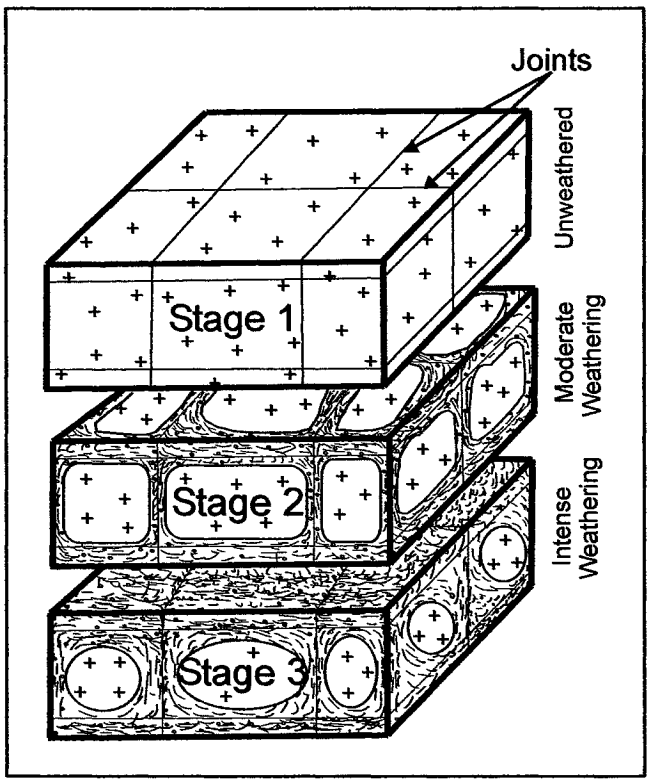

Fig. 3.5. Idealized development of corestones through time: stage 1 is the early initial onset of the weathering along the fractures; stage 2 constitutes the more intense weathering along the fractures due to prolonged weathering; and stage 3 is the very intense weathering that can no longer be directly attributed to weathering along fractures as these have been obliterated by the weathering process, therefore leaving the rounded corestones surrounded by granular and/or arenaceous saprolite. Boxed in the figure do not represent a profile, but rather a process; corestones do not occur beneath the solid parent rock.

3.5 Saprolites of the South Mountain Batholith

Deeply weathered granitoids have been reported in the study area by previous workers including McNeil (1954), Stea (1982), Grant (1989, 1997), Finck & Stea (1995), and Prime (2001), however no detailed study of the nature, age, significance in landscape development, or environmental implications was undertaken before that of O'Beirne-Ryan and Zentilli (2003). Previous workers have discussed the difficulties in determining the timing of saprolite development in the Atlantic region of Canada (Wang et al., 1982; McKeague et al., 1983; Bouchard et al., 1995), although most agree that the saprolites formed either in warm interglacial periods or prior to the Pleistocene glaciation events. Grant (1989) suggested that these horizons represented pre-glacial or Tertiary weathering. O'Beirne-Ryan and Zentilli (2003) documented three episodes of saprolite development on the granitoids of the South Mountain. They described saprolites of three distinct ages preserved on the South Mountain Batholith overlain by Pleistocene glacial till, Triassic-Jurassic sandstone and Carboniferous strata respectively (Fig. 3.6). Saprolites of pre-Pleistocene age dominate in outcrop occurrences within the batholith. In addition, drilling has revealed the presence of a thick sequence of argillaceous saprolite of pre-Triassic age in the Bridgetown area, and relithified pre-Carboniferous saprolite in the Windsor area (O'Beirne-Ryan and Zentilli, 2003). Only one surface outcrop of pre-Carboniferous saprolite has been found, at Round Mountain, near Windsor, Nova Scotia (Fig. 3.2). To date, the pre-Triassic saprolite has only been found in drill core.

Seventeen localities of saprolites were selected for the purpose of this study (Fig. 3.2). The saprolites range in thickness from a few centimetres to approximately 30 m. The horizons range in colour from light pinkish grey to red-brown. The variation in the colour reflects the degree of alteration and/or the composition of the original or parent granitoid. O'Beirne-Ryan and Zentilli (2003) also emphasize that the thicknesses and physical characteristics of saprolite units are inextricably related to the original granitoid rock composition and grain size, citing examples of thick profiles developed on the coarse grained granitoid parent rocks compared to very thin profiles developed on fine-grained granitoids at the same locality.

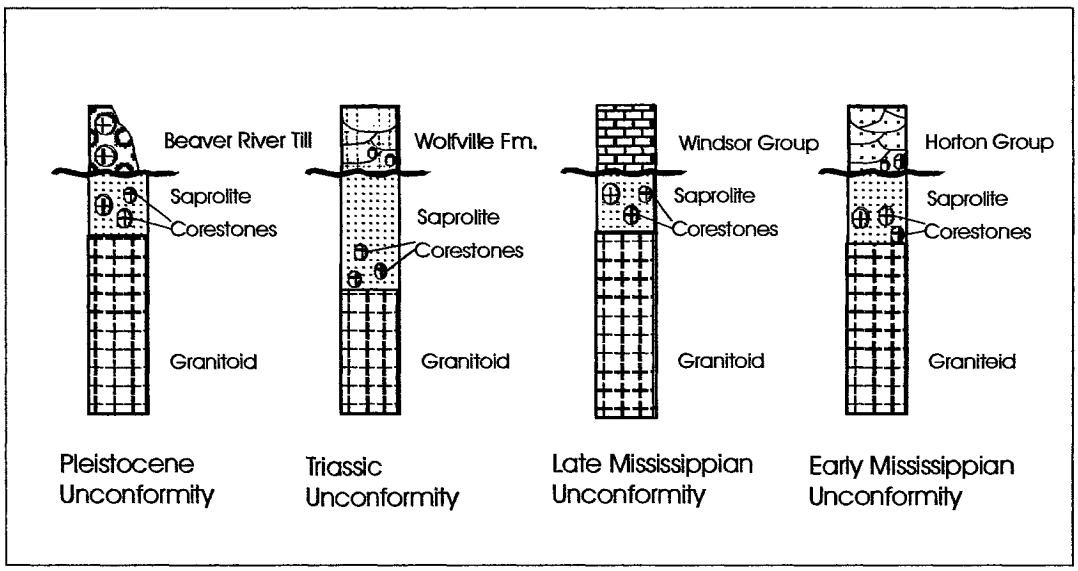

Fig. 3.6. Stratigraphic positions of the unconformities on saprolites, southern Nova Scotia. Not to scale.

3.5.1 Pre-Carboniferous Weathered Profiles

The pre-Carboniferous weathered profiles are found under either the Early Mississippian clastic strata of the Horton Group or underlying the marine limestones and evaporites of the Late Mississippian Windsor Group (Fig. 3.6). The pre-Carboniferous weathered profiles found within the area differ in appearance from the younger saprolites and represent the oldest preserved weathering event of the South Mountain Batholith. The pre-Carboniferous paleoweathered surfaces are argillaceous saprolites that have been relithified as a result of subsequent burial by as much as 5 km of Carboniferous sedimentary strata (Ryan & Zentilli, 1993; O'Beirne-Ryan and Zentilli, 2003). The relithification results in an indurated rock of granitoid-like texture, however on closer examination it is clear that the individual grains are more rounded in nature than the parent monzogranite and biotite is absent. Mineralogy is dominated by quartz and clay minerals. O'Beirne-Ryan and Zentilli (2003) point out that these horizons no longer exhibit isovolumetric weathering and therefore are no longer "saprolites" *sensu stricto*. Lidmar-Bergstrom et al., (1997) have described similar relithified saprolites

from palaeosurfaces in Sweden. There are some interesting implications of the pre-Carboniferous weathering in regards to the exhumation of the South Mountain Batholith. The *circa* 370 Ma batholith must have been exhumed from 8-12 km depth and exposed for a sufficient time for the saprolite to develop, and all of this must have happened prior to the deposition of the overlying strata, which are as old as 355 Ma. Similar pre-Carboniferous saprolites have been observed by the authors in south central Cape Breton, Nova Scotia, suggesting a regional scale pre-Carboniferous weathering event.

3.5.2 Pre-Triassic Saprolites

Three closely spaced drill cores (DDH WP-99-2, WP-99-3, and WP-99-4) through the Triassic sandstones and shales intersect intensely weathered granitoids beneath the erosional Triassic unconformity (Fig. 3.2). The saprolite is up to 30 m thick and fresh monzogranite is found at the bottom of the drill holes (Fig. 3.7).

Unlike the pre-Carboniferous argillaceous weathered horizon that was preserved in a relithified state, the pre-Triassic saprolite is preserved as an unmodified saprolite, retaining the original granitic textures (O'Beirne-Ryan and Zentilli, 2003). In the upper part of the preserved portion of the saprolite, all of the plagioclase and most of the K-feldspar has altered to clay and the biotite has been variably weathered, however throughout most of the saprolitic profile some remnant plagioclase has been observed and the K-feldspar and biotite are megascopically intact. Granitoid texture is preserved throughout the thickness of the saprolite, although there is a definite chemical zonation from the base to the top of the horizon (O'Beirne-Ryan and Zentilli, 2003a). Intervals of less weathered granite are intersected within the saprolite core towards the base of the drill hole section and are interpreted as being corestones (Fig. 3.7).

3.5.3 Pre-Pleistocene Saprolites

The pre-Pleistocene saprolites are the most widespread saprolites in southern

Nova Scotia. These horizons are typically 1-10 metres thick and display a vertical zonation of disaggregated arenaceous saprolite at the surface to cohesive arenaceous saprolites with corestones deeper in the profile, and finally into fresh bedrock (Fig. 3.8). The difference between the pre-Triassic and the pre-Pleistocene saprolites lies in the degree of mineralogical change, and in particular, in the higher proportion of clay minerals developed in the pre-Triassic saprolite (O'Beirne-Ryan and Zentilli, 2003).

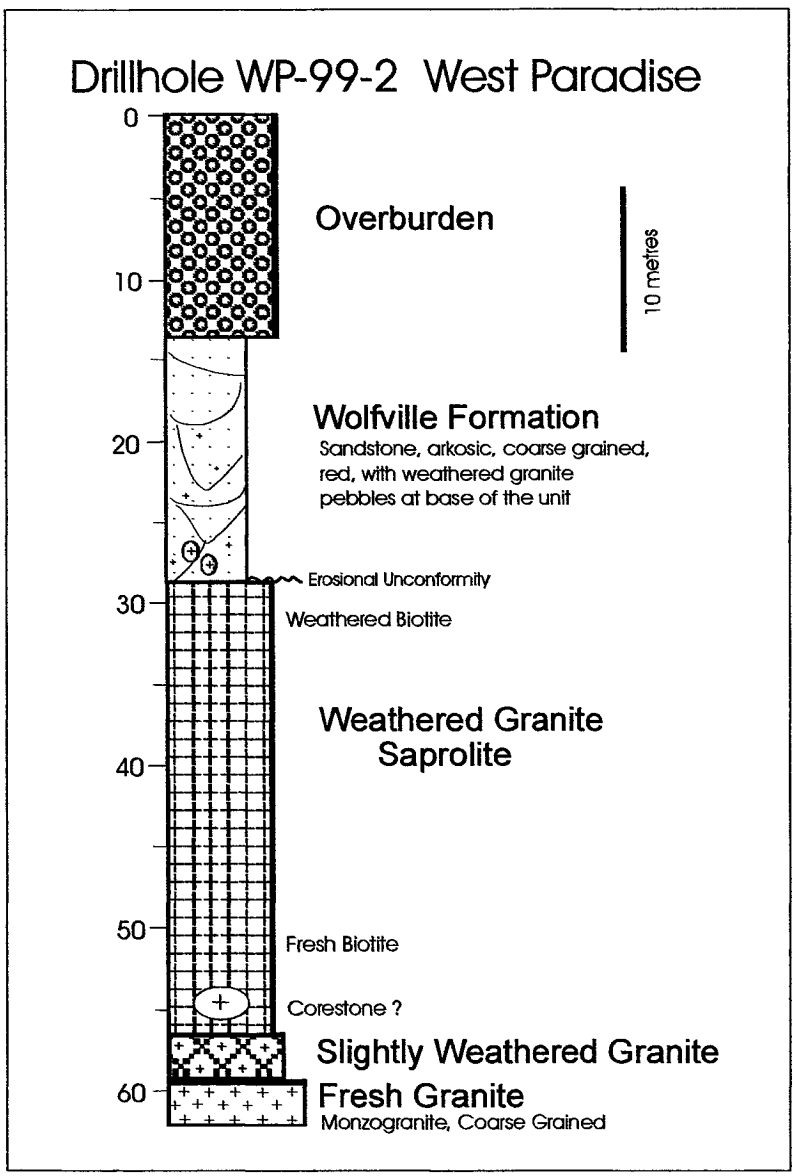

Fig. 3.7. Drillhole WP-99-02, drilled at West Paradise, near Bridgetown, Nova Scotia

The plagioclase in the pre-Pleistocene saprolites is minimally kaolinized, the K-feldspar is intact and clay minerals represent less than 5% of the saprolite. O'Beirne-Ryan and Zentilli (2003) have documented post-Triassic weathering profiles in the Jurassic basalts of the North Mountain confirming the presence of both pre-Triassic and pre-Pleistocene weathering horizons. It is interesting to note that these younger saprolites are arenaceous in nature, and in this respect, correlate with the sandy (grus) saprolites of the pre-Pleistocene of Europe (Mignon & Lidmar-Bergstrom, 2001)

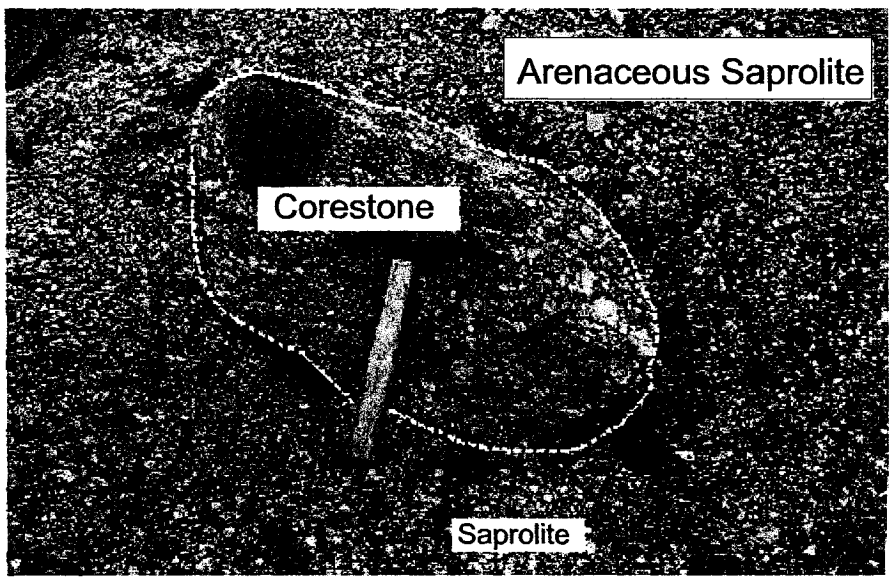

Fig. 3.8. Example of a corestone weathered out of cohesive gravelly saprolite lying at surface at Waterloo Lake. Note the presence of the xenolith within the corestone. Hammer for scale.

3.6 Corestones

Corestones are the remnants of the original rock within a weathered saprolite. In most cases, the interiors of the corestones themselves are relatively unaffected by the weathering process, although their exterior may have a rim of weathered material (Nesbitt, 1979; Fig. 3.5). These rims tend to exfoliate from the surface in an onion skin manner, the common spheroidal weathering features of granitoids; in the extreme, these corestones themselves may be weathered to a cohesive arenaceous saprolite, and

ultimately to a disaggregated arenaceous saprolite, if they continue to be exposed to more intense weathering.

In the saprolitic horizons of the South Mountain Batholith, corestones are variably developed, ranging greatly in size from several metres in diameter to a few centimetres in diameter (Figs 3.8 and 3.9) and are elliptical to spheroidal in shape, although less advanced weathering produces more angular corestones. Waterloo Lake (Figs 3.8 & 3.9) and Bridgetown (Fig. 3.10) are localities where the corestones have been observed *in situ* (Fig. 3.2). They are also present and exposed at surface at Round Mountain, within the relithified saprolite of pre-Carboniferous age (Fig. 3.2 and Fig. 3.11).

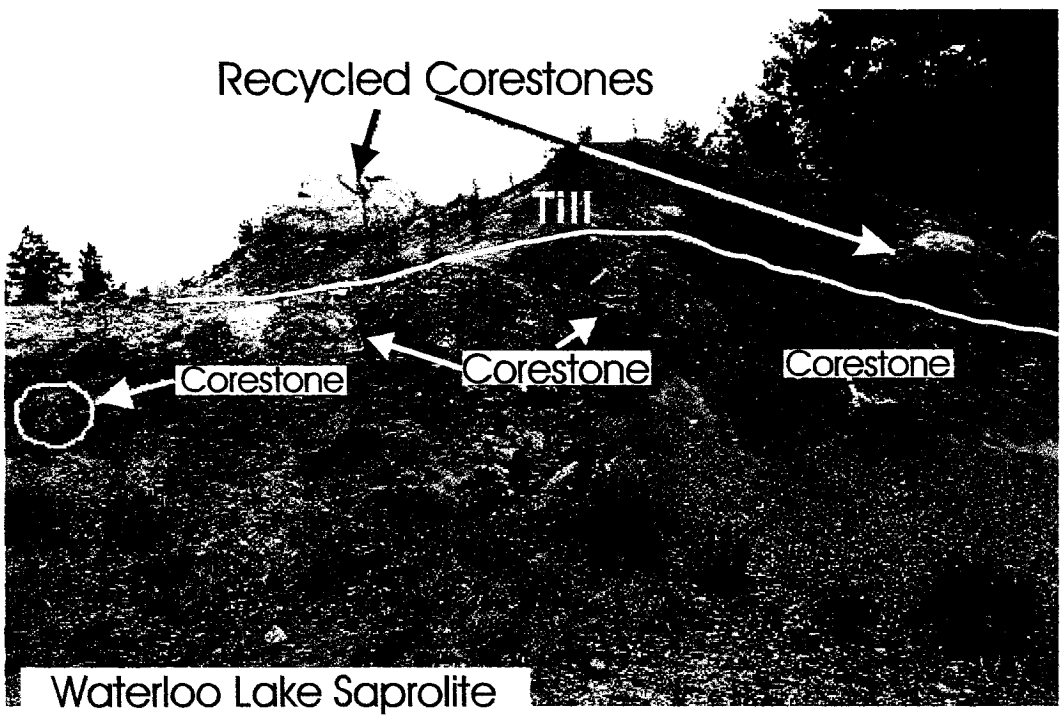

Fig. 3.9. Saprolite and overlying Beaver River Till at Waterloo Lake. Note the presence of corestones in the till unit.

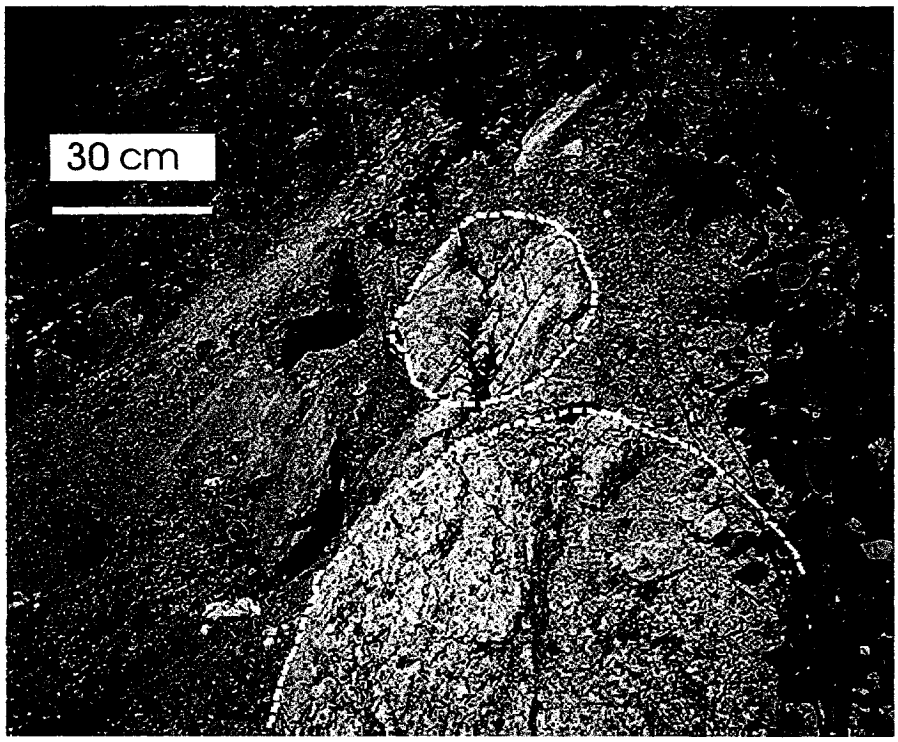

Fig. 3.10. Corestones developed in a granitoid at Bridgetown, Highway 101 locality.

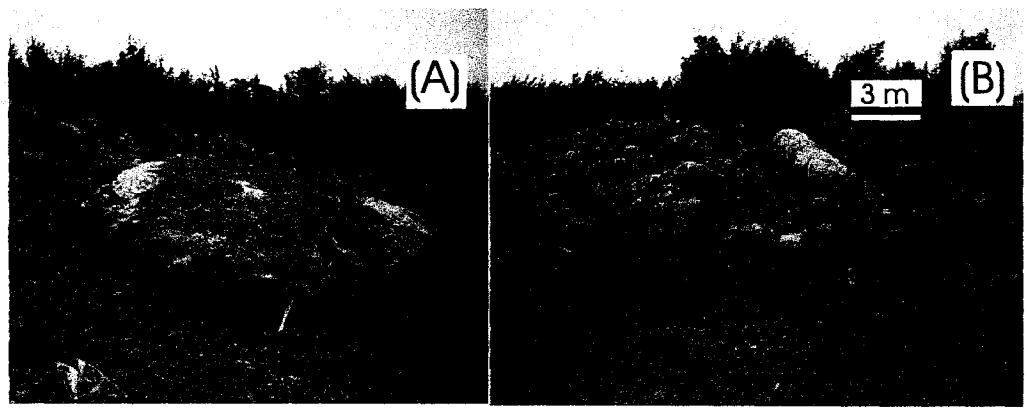

Fig. 3.11. (A) Relithified saprolite horizon with corestone at Round Mountain. (B) Note the occurrence of weathered-out corestones lying on the surface, le behind as undesirable by the aggregate producers.

3.7 Incorporation of Corestones and Saprolitic Material into Succeeding Stratigraphic Units

The concept of weathered crystalline rock being a source of material for tills was first proposed by Chalmers (1898) for tills in eastern Canada. Emerson (1917) also reached a similar conclusion based on observations of tills in the New England States of the United States. Despite the obvious relationship between the weathered material and the tills, reference to this connection has been implied without explanation, or ignored by many subsequent researchers. Feininger (1971) concluded that much of the northern hemisphere was covered by a mantle of weathered material overlying the crystalline rocks prior to the Pleistocene and that this saprolite was the major source of detritus incorporated into Pleistocene tills over granitic terranes. The principal argument put forward by many workers (e.g. Flint, 1957) against the contribution of weathered mantles as sources for tills, is the presence of relatively fresh biotite and feldspar in the tills. However, O'Beirne -Ryan & Zentilli (2003a) have documented thick saprolite development in which significant quantities of these minerals are preserved within the weakened weathered horizons, and Feininger (1971) also points out that these minerals occur in abundance within the weathered rock surrounding corestones at the base of weathered horizons. Migon & Lidmar-Bergstrom (2001) have documented many examples of arenaceous saprolites with minimal mineralogical decomposition in Northern Europe; these authors attribute a Neogene age to these saprolites. Mahaney (1995) documents pre-glacial weathering in the source area of many tills in central Canada as evidenced by weathering surface textures on quartz grains studied by scanning electron microscope. The total contribution of the weathered horizons to the tills is unclear, however the fact that these weathered rocks contribute to till development is undeniable (Fig. 3.12). The other point of interest in the Nova Scotia examples is that there are various ages of saprolite development and therefore the older horizons may have contributed material to older sedimentary strata.

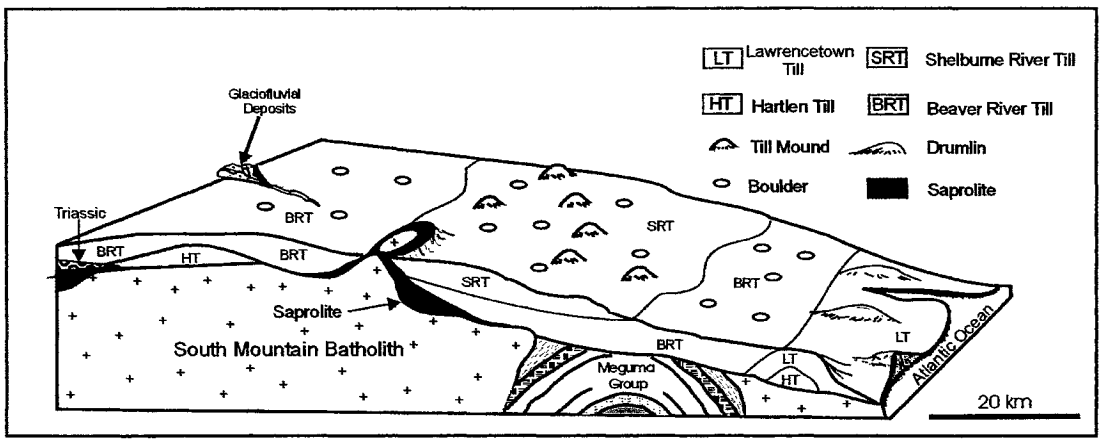

Fig. 3.12. Model for the till stratigraphy and saprolite occurrences, modified after Finck and Stea (1995).

Incorporation of corestones in subsequent stratigraphic units is predictable given that these fresh rounded boulders and cobbles of granite are contained within poorly consolidated rotted granitoid or saprolite within the weathered profile. It is not hard to imagine how the gravelly, more weathered material surrounding the corestones and irregular tors can be eroded away leaving a palaeosurface with numerous corestones exposed on a surface commonly referred to as a blockfield or felsenmeer (Feininger, 1971). Subsequent fluvial erosion and deposition could concentrate the corestones as traction load within channel lag deposits, and arkosic sands derived from the saprolite would probably form the matrix of the conglomerates. Examples elsewhere of the incorporation of corestones into younger conglomerates include the Late Cenozoic deposits in San Benardino County, California (Powell et al., 2000), and pebble to boulder granite clasts in an arkosic matrix of Early Proterozoic Cobalt Group in Ontario, which overlies a palaeosurface (saprolite) formed on the Late Archaean granites (Rainbird et al., 1990). Similar examples of saprolite-derived sedimentary rocks have been documented in the French Massif Central and Aquitaine Basin by Simon-Coinçon et al., (1997), and by Migon & Lidmar-Bergstrom (2001) for the tills of southeast Sweden. The exterior slightly weathered rims on the corestones are quickly abraded leaving well-rounded clasts of fresh granitoid. Conglomeratic gravels are commonly concentrated along the basin margins where the stream gradients are high and

therefore capable of boulder transport. Basinward, where the lower gradient streams lose their carrying capacity for the larger clasts, the conglomerates will grade laterally into arkosic sand bodies. Pettijohn (1975) suggested that well rounded oligomictic granite conglomerates pose difficulties in the interpretation of their depositional environments. There is an over-representation of granite cobble conglomerates in the sedimentary rock record, given the commonly accepted sedimentary processes of long-transport or conglomerate-recycling necessary to produce this lithology. Uplift and erosion of unweathered granitoid uplands should result in the deposition of arkoses with scattered granite pebbles or larger more angular blocks of granite, as opposed to the rounded boulder and cobble clasts found in many granite conglomerates. The incorporation of the corestones from saprolite horizons is probably the most reasonable explanation for the observed abundance and textural relationships within many granite conglomerates.

3.8 Nova Scotia Examples

Emphasis herein is on the stratigraphic and sedimentological significance of saprolite material incorporation into younger stratigraphic units in Nova Scotia.

Stea et al., (1996) have recognized extensive Cretaceous silica sand and clay deposits up to 200 m thick in central and northern Nova Scotia. Stea et al., (1996) also postulated that the source area for the strata must have been a deeply weathered granitic terrane. In modern deep weathering mature profiles, saprolites on granitoids commonly grade upwards to clay-quartz horizons (that is, the mineralogy resulting from intense weathering) and soils developed on these weathered surfaces. In the weathering surfaces of the study area, no record of exclusively quartz-clay or soil horizons has been found. This suggests that the uppermost parts of the mature saprolite profiles have been eroded and the weathered rocks preserved below the unconformity are the erosional remnants of an originally much thicker horizon. Whereas O'Beirne-Ryan and Zentilli (2003) have documented pre-Triassic weathered palaeosurfaces in which 30 m of argillaceous saprolite is preserved, it is reasonable to

assume that the upper parts of these saprolite profiles could have been exposed and subsequently eroded, transported and deposited as Cretaceous silica sands and clays. In the southern Appalachians of Georgia, USA, a similar geological setting exists with deep saprolites developed on granitoids along the uplands adjacent to Cretaceous silica sands and kaolin deposits of the Piedmont (Schroeder et al., 1997). Migon & Lidmar-Bergstrom (2001) document a similar strong correlation of kaolinitic saprolites and sedimentary kaolin deposits in northern Europe.

In the Mississippian Horton Group of Nova Scotia, there is a sequence of clean quartz-rich sandstones referred to as the Glass Sand Unit. Ryan (1998) interpreted the environment of deposition of this unit as one of low sinuosity streams or shallow lacustrine deltas, based on the paleocurrent data, channel morphology, and interdigitation of the sandstone with lacustrine shales. Ryan (1998) attributed the high mineralogical maturity of the glass sand unit to a monomineralic source area. The Horton Group clastic sedimentary rocks unconformably overlie saprolites in the Avon River area (Figs 3.2 & 3.6). The recognition of pre-Carboniferous argillaceous saprolites by O'Beirne-Ryan and Zentilli (2003) in the highland areas adjacent to and underneath the basin margins provides a potential detrital source area for the mineralogically mature Glass Sand unit.

Tilting of such palaeosurfaces related to subsequent basin development (e.g. Carboniferous Maritimes Basin or the Mesozoic Fundy Basin in Eastern Canada) could afford the opportunity of corestone and saprolite incorporation into the overlying units. In places where the younger sedimentary units onlap onto the weathered palaeosurface the sediments may simply infill around the corestones of a blockfield, forming a basal conglomerate after lithification. In areas of significant topography near basin margins, the weathered material from the highland areas may be incorporated into alluvial fans to form the basal arkosic conglomerates of the Horton Group (Fig. 3.5). In drill hole WP-99-2 there are kaolinized granite pebbles within an arkosic sandstone of the Triassic Wolfville Formation that have been eroded from the underlying weathered granite horizon (Figs 3.6 & 3.7).

The best examples of corestone incorporation into the succeeding sequences

within the study area come from the Quaternary strata. Where the saprolites are overlain by the Pleistocene Beaver River Till (Finck & Stea, 1995) there are numerous well-rounded granitoid boulders and cobbles surrounded by an arkosic matrix in the till (Fig. 3.9) . Finck & Stea (1995) studied clast lithologies with bedrock and calculated clast dispersal equations, which estimated the Beaver River Till unit had an average transport renewal distance of 400 metres. Over such a short travel distance it is clear that the rounded nature of the boulders and cobbles is not related to abrasion and rounding during transport (Fig. 3.12). Furthermore, the size of the boulders and pebbles in the tills is comparable to the size variation of corestones in the underlying saprolites. Cumming (1979) suggested that many of the rounded boulders in the tills of southern Nova Scotia may have originated as corestones although he did not observe any saprolites or *in situ* corestones in the area. In southern Nova Scotia along the margins of the South Mountain Batholith, there are glacio-fluvial deposits of stratified sands and gravels. One specific example is evident within a gravel quarry at West Paradise near drill hole WP-99-2 (Fig. 3.2), where approximately 35 m of sand and gravel were deposited at the topographic break along the northwestern contact of the batholith, which has incorporated granitoid boulders probably sourced as corestones from proximal saprolite horizons (Fig. 3.13).

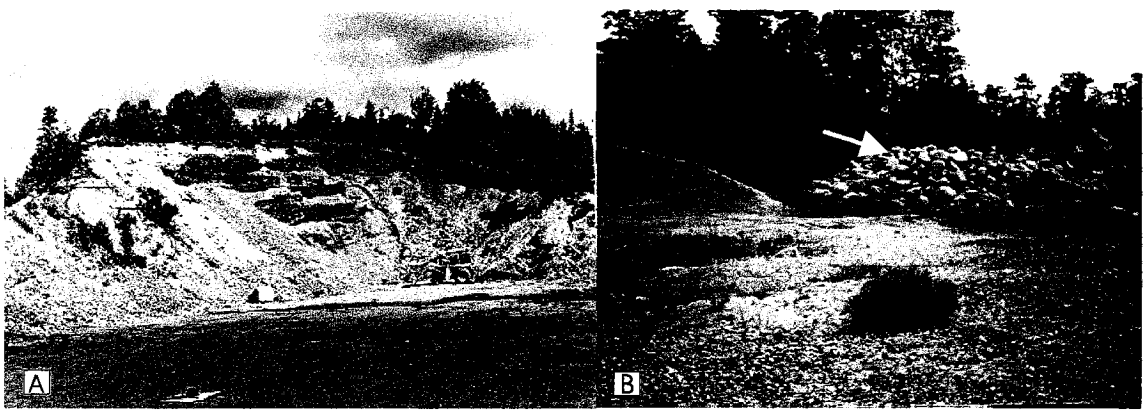

Fig. 3.13. (A) Glaciofluvial deposits at West Paradise composed of abundant rounded pebbles and boulders of granite. (B) Corestones stockpiled from a gravel producer near West Paradise, Nova Scotia.

3.9 Conclusions

There are numerous localities where saprolites are developed on the Devono-Carboniferous granitoids of the South Mountain Batholith of southern Nova Scotia. The saprolites occur beneath three erosional unconformities, the Pleistocene, the Triassic and the Carboniferous. The argillaceous weathered profiles below the Carboniferous strata have been relithified and are consequently texturally different and distinguishable from the younger saprolites. The saprolites beneath the Triassic are argillaceous and have not been re-lithified, whereas the pre-Pleistocene saprolites are arenaceous in nature. In all cases found to date, the profiles remaining have had their upper portions eroded. It is likely that these missing more highly-weathered quartz- and clay-rich horizons may have been a source of quartz-rich sandstones in the Carboniferous and silica sands and clay within the Cretaceous strata in Nova Scotia.

The stratigraphic distribution of the saprolites provides constraints on the timing of exhumation events in southern Nova Scotia. The saprolites developed on the South Mountain Batholith commonly have remnant zones of elliptical unweathered corestones. These corestones develop due to progressive weathering along cross-cutting fractures in the granitoids, producing ellipsoidal corestones. The corestones are surrounded by disaggregated or cohesive arenaceous to argillaceous saprolite.

These corestones may become separated from the more easily eroded saprolite, producing numerous rounded boulders and cobbles of relatively fresh granitoids. The boulders released in this way can be incorporated into subsequent sedimentary sequences, as evidenced by the corestones found within strata in southern Nova Scotia. Whereas in the study area these saprolite-related corestones were produced at different times during the exhumation of the batholith, corestones were incorporated into Carboniferous Horton Group, Triassic Wolfville Formation and the Pleistocene Beaver River Till. Examples of similar corestone development on weathered palaeosurfaces elsewhere in Atlantic Canada (Wang et al., 1982) indicate that corestone incorporation into the stratigraphic record elsewhere in the region is likely.

In summary, well rounded spherical pebbles, cobbles and boulders of granitoids within sedimentary units need not have traveled far from the source area, nor are they necessarily recycled from older conglomerate units. It is therefore important for sedimentary geologists to consider the possibility of corestone incorporation from weathered palaeosurfaces when interpreting depositional environments for granitoid clast conglomerates.

3.10 Acknowledgments

The authors would like to thank Garth Prime, Phil Finck and Ralph Stea for their help in locating many of the localities, and Krista Page for her help in the field. The authors would like to acknowledge the financial support of the Nova Scotia Department of Natural Resources through the Toxic Substances Research Initiative (Health Canada) as part of the investigation into Hg in the Kejimkujik Natioinal Park, and a National Sciences and Engineering Research Council of Canada grant to Marcos Zentilli. The authors would also like to thank P. Migon and E. McBride for their reviews and constructive suggestions.

Chapter 4

Weathering of the South Mountain Batholith, Nova Scotia, Canada as Reflected in the Mineralogy

Preamble

This chapter represents the final draft stages of a manuscript for submission in the fall of 2006, by AM O'Beirne-Ryan and M Zentilli, entitled "Weathering of the South Mountain Batholith, Nova Scotia, Canada, as reflected in the mineralogy". As first author, AM O'Beirne-Ryan undertook all of the research and writing, including the microprobe and petrographic work. Suggestions from M. Zentilli were incorporated into the research and writing, particularly in the final stages of preparation of this draft.

4.1 General Introduction to the Problem

Granitoids of the South Mountain Batholith of southwestern Nova Scotia, Canada, record weathering events from three different times in the geologic past (O'Beirne-Ryan and Zentilli, 2003) (Fig. 4.1). The weathering mineralogy and geochemistry record not only the changes that occurred during these times, but also provide a window into the nature of the various paleoenvironments at the time of weathering. Research over the past two decades confirms that weathering generates an entire spectrum of mineralogical and textural alteration features that can be used to better understand the weathering process itself (e.g. Nahon, 1991; Gerrard, 1994; Velde, 1995; Delvigne, 1998). This paper focusses on the mineralogical aspect of

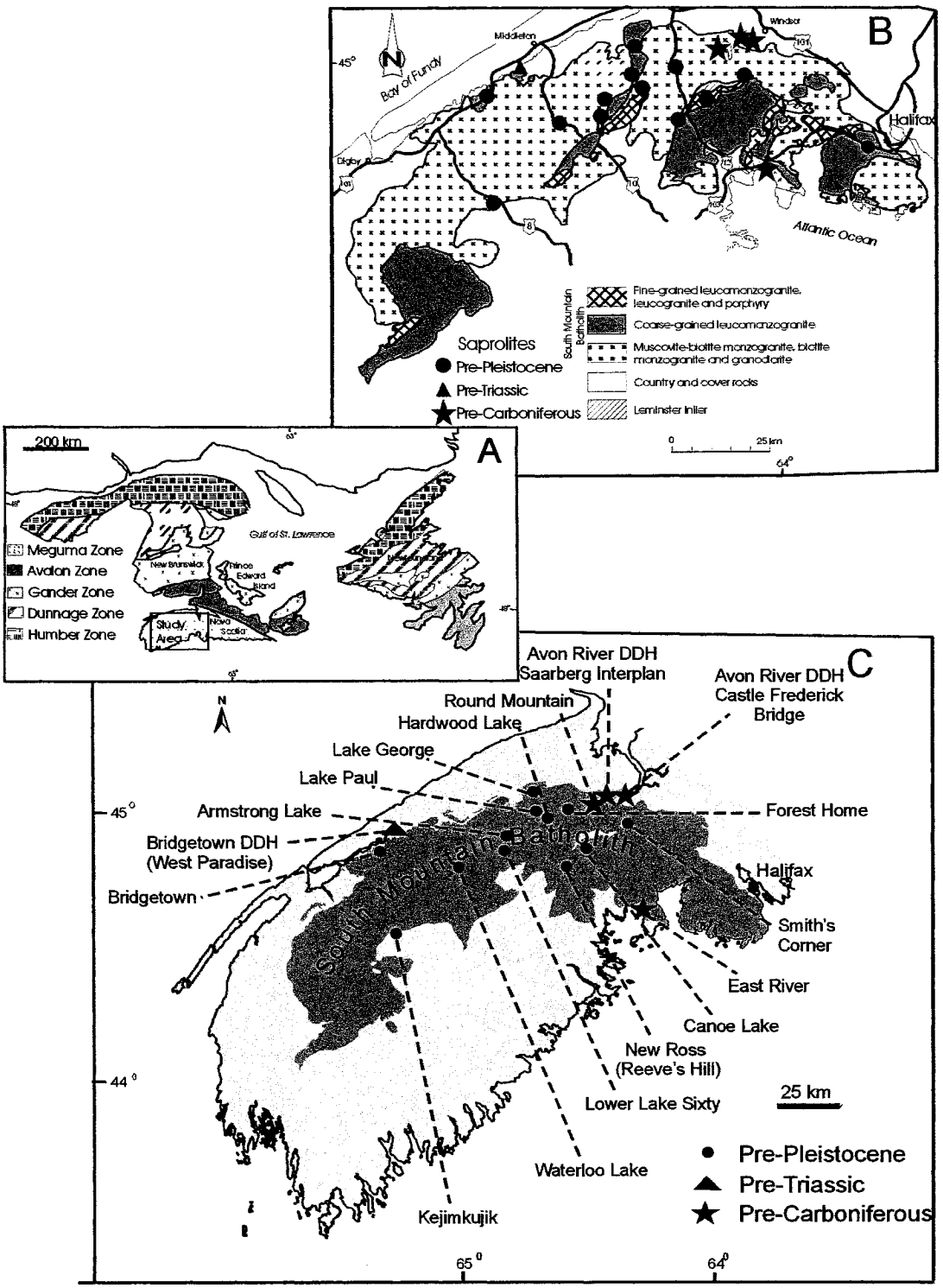

Fig. 4.1. (A) Location of the study area and general geological setting of the Northern Applachians (after Williams, 1995). (B) Geology of the South Mountain Batholith, with saprolite locations (after MacDonald, 1992). (C) Sample locations and location names of saprolite on the South Mountain Batholith (after O'Beirne-Ryan and Zentilli, 2003).

weathering as part of a broader study in which the stratigraphic, geochemical, and mineralogical characteristics of weathered granitoids of the South Mountain Batholith (a) a comparison of the mineralogy and textures of the weathering profiles of three different ages; (b) a comparison of XRD and microprobe data for biotites in particular, and clay mineralogy in general, for the two younger profiles; and (c) implications for paleoenvironmental conditions at the times of weathering.

Weathering profiles of the South Mountain Batholith (SMB) are of three distinctly different ages: (a) Pre-Carboniferous, overlain by Carboniferous sedimentary strata, and found mainly in drill core, with rare surface exposures; (b) Pre-Triassic, overlain by Triassic sandstones and shales, documented only in drill core, and (c) Pre-Pleistocene, overlain locally by Pleistocene till, and found at surface as well as in water well drilling locations (Fig.4.1; O'Beirne-Ryan and Zentilli, 2003). Subsequent erosion has stripped the uppermost parts of the weathered profiles away, and particularly in the youngest sequence, only the lowermost and least altered part of the weathered profile remains (O'Beirne-Ryan and Zentilli, 2003). The older sequences record thicker, more complete profiles (Fig. 4.2), although neither preserves a complete profile.

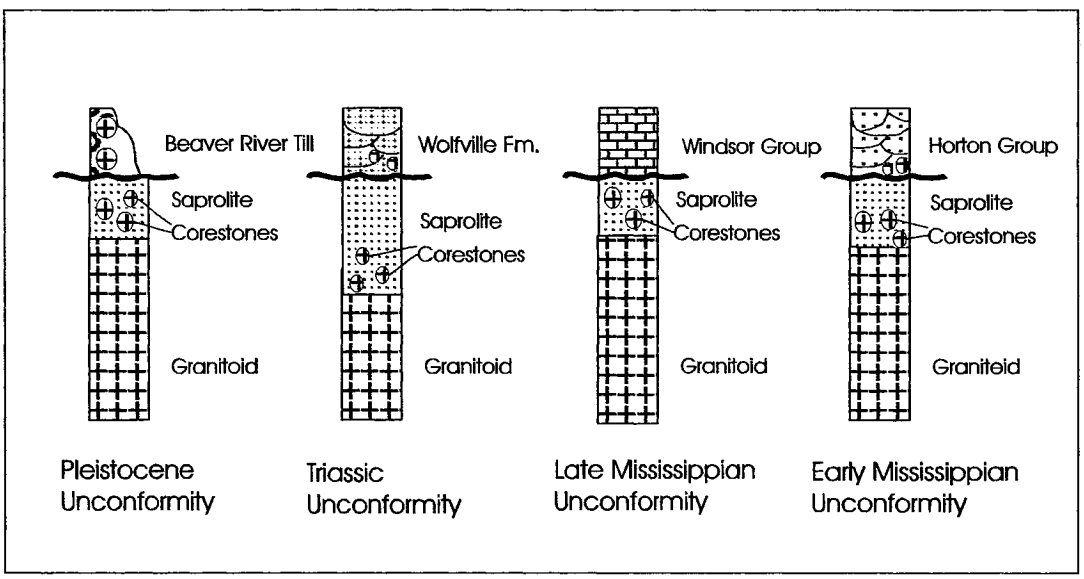

Fig. 4.2. Stratigraphic positions of the unconformities on saprolites, southern Nova Scotia. Not to scale.

The three different weathered paleoenvironments recorded in the monzogranites of the SMB, and the inherent differences between these profiles despite their similar parent material, help us understand not only the possible conditions present during their formation, but also the nature and potential for element liberation and migration within the materials as the intensity of weathering increases. Temperature, the level of the water table, soil moisture content, rainfall, and oxygen concentrations all have a considerable effect on the weathering process. Changes to the present day environment in terms of temperature, redox changes, and rainfall, may well modify the current mineralogical and geochemical state of these incompletely weathered systems, particularly when they are re-exposed at surface. Ongoing changes within these profiles can be acceletated and minerals precipitated when re-exposed at surface as a result of quarrying activities, changes in the level of the water table, and redistribution of loose mantle elsewhere for the purposes of road bed construction, etc.. Examining the nature of change in these paleosurfaces, and the processes that operated as minerals were broken down at or near surface, can help us understand and predict the potential and possible nature of change today, or in the near future.

4.2 Chemical weathering: Background

The nature of weathering of rocks at the earth's surface is dependent on a number of factors including mean annual surface temperature and seasonality, rainfall amount and seasonality, topographic conditions, the nature of the parent rock, the presence and distribution of fractures and joints in the parent rock, biological activity, and the pH and Eh conditions prevailing at a given point in time. In the early stages of weathering, equilibrium is rarely established and water and its dissolved gases (particularly O_2 and CO_2) play a significant role (e.g. Nahon, 1991). Water moves through the cracks, dissolving some elements which subsequently are removed from the site of weathering, and transporting others to sites where reaction can occur. Weathering is a self-perpetuating process: during physical and chemical weathering, cracks and channelways within the rock are created and are physically as well as chemically enlarged as the weathering proceeds, leading to further weathering. The

nature of reactions is governed by the parent mineralogy and texture, as well as by the pH and Eh conditions, and the rates of these reactions are strongly affected by temperature and biological activity (e.g. Nahon, 1991; Wilson, 2004).

In a classic study of igneous rock weathering, Goldich (1938) established a sequence of differential weathering for minerals which, in most simplistic terms, represents the reverse of the order in which minerals crystallize from a magma, Bowen's Reaction Series for the rock-forming minerals: the minerals that weather first are the minerals that formed at highest temperatures. In terms of the peraluminous granitoids of the South Mountain Batholith (SMB), the dominant minerals are plagioclase feldspar, K-feldspar, quartz, and biotite, with accessory apatite, ilmenite, and zircon; as expected, plagioclase and biotite alter first. In some of the granitoid phases, and reflecting the peraluminous nature of the batholith, muscovite, andalusite, cordierite, garnet, and tourmaline are also present (MacDonald et al., 1992). The high proportion of feldspars and biotite mean that these minerals dominate the chemistry of the weathering. This paper focusses on the breakdown of biotite. Early in this study, examination of thin sections from one of the paleoweathered profiles indicated that biotite breakdown was a complex process, with biotite in some form persisting through most of profile, and therefore recording changes throughout a sequence. In contrast, in these monzogranites of the South Mountain Batholith, plagioclase loses its identity early in the weathering process, and K-feldspar retains its original identity until much later in the weathering progression. This sequence resulted in biotite serving as the focus mineral for the study. In addition, Tardy et al. (1973) note that the biotite-to-clay transformation is a better indicator of climate than the plagioclase-to-clay transformation.

Bakker (1967), Tardy et al. (1973), Gerrard (1994), Sequiera Braga et al. (2002), and others, have discussed the paleoweathering environment in terms of the secondary mineralogy developed. These authors all conclude that intensity of weathering is generally reflected in the secondary mineralogy generated: (a) under the least-intense conditions, smectites develop and are typical of weathering under temperate conditions; (b) kaolinite may develop under a wide range of conditions; and (c) gibbsite develops most commonly under conditions of intense (e.g. tropical) weathering.

However, Bouchard and Jolicoeur (2000), Gerrard (1994), and Sequira Braga et al. (2002), point out the need to recognise the potential for the existence of variable microenvironments, both in terms of the nature of the parent mineral, and in terms of the topographic and hydrologic conditions at a given location. For example, in poorly-drained, low-lying regions, smectites are likely to be preserved, whereas in upland, well-drained regions, kaolinite is commonly preserved, even during the same weathering event (Bouchard and Jolicoeur, 2000).

4.3 Biotite - to - clay weathering processes and terminology

4.3.1 Terminology

Clay mineral and biotite terminology is complex, and clay analytical methodologies have evolved over a period of several decades. As a result, the nomenclature in the literature is variable and can be confusing. For example, the term "hydrobiotite" is now considered unacceptable (Reider et al., 1998), but in the literature, hydrobiotite may refer to a variety of different compositions, depending on the author. Velde (1995) notes that hydrobiotite refers to a regular mixed layer mineral of biotite and trioctahedral smectite; Acker and Brinker (1992) use the term hydrobiotite to refer to interstratified biotite-vermiculite; and Coleman et al. (1963) and Wilson (1970) use the term hydrobiotite to mean interstratified biotite-vermiculite, the basal spacing of which is approx. 24Å. Kretzschmar et al. (1997) simply refer to an intermediate weathering product of biotite - kaolinite as interstratified biotite-vermiculite.

Similarly, the term "vermiculite" has variable meanings: Wilson (2004) discusses Barshad's (1948) conclusion that the vermiculitization reaction in the simplest sense is a relatively straightforward reaction in which interlayer K is exchanged for ions from the surrounding environment, and obviously depends upon relatively low K-contents in the surrounding environment. In other words, if the surrounding solutions are K-rich, vermiculitization will not happen, as the process of K-release from the biotite cannot occur if the solutions are already saturated with respect to potassium. Vermiculite

originally referred to the worm-like form of the micaceous mineral which had unique swelling properties upon heating (Harbin, 2003), classified on the basis of XRD analysis. Wilson (2004) discusses the coupled interlayer K-release and the oxidation of Fe^{2+} to Fe^{3+} in the octahedral layer to produce vermiculite. Wilson (2004) further concludes that the oxidation of iron precedes the release of K from the interlayer, and indeed, is not necessarily accompanied by the release of K from the interlayer, in which case, the term "oxybiotite" may be used (Gilkes et al., 1972). Jeong and Kim (2003) conclude that biotite can be intensely oxidised (Fe^{2+} to Fe^{3+}), and still retain most of its K in a 10Å structure, thus retaining its "biotite" nature. Moon et al. (1994) argued that layer charge loss during vermiculitization was accompanied by Fe^{2+} and Mg loss from the octahedral layer, which resulted in Al from the tetrahedral layer "moving' into the octahedral layer, replacing the lost Fe and Mg. Mortimer and Little (1998), working on metamorphic biotites, produced diagrams using a compilation of existing data, in which the fields of vermiculites, illites, biotites, smectites, and kaolinites are delineated in terms of Fe+Mg+Mn oxides vs Al_2O_3, and K_2O versus SiO_2. In their study, Mortimer and Little (1988) outline the continuous nature of the transitions between many of these minerals during weathering, diagenesis, and early metamorphism.

As a result of the complexity of clay mineral terminology, in particular as it relates to the weathering of micas, the following protocol has been adopted in this study: (a) the terms "hydrobiotite" and "oxybiotite" are avoided; (b) the term "illite" is used only in conjunction with muscovite, as in "illite/muscovite", as XRD analysis is not available for the grains in question; (c) the terms "smectite" and "vermiculite" are used specifically to refer to alteration products identified by XRD (Levi, pers. com., 2002); (d) microprobe analysis of alteration products of biotite producing vermiculite-like and smectite-like minerals, are referred to as vermiculite/smectite or weathered biotite. There is an inherent uncertainty in naming clay minerals based on chemical analysis (Wilson 2004), however microprobe analysis can give us insights into the details of the transitions occurring during weathering, and thus provide a valuable tool in developing an understanding of the weathering process. Ferrell and Carpenter (1990) discuss the benefits and limitations of microprobe analysis of clay minerals, and point to the fact that a typical 10 μm beam produces x-rays over approximately 15 μm diameter. Fifteen micrometers represents in the order of 200 unit cells, and an average value over these

200 unit cells is measured in this way (Ferrell and Carpenter, 1990). For mixed layer clays, an average of the combined composition of the different layers may be as close as the microprobe analysis can detect.

4.3.2 Biotite weathering processes and products

The nature of biotite weathering has been studied in detail by a number of authors (Acker and Brinker, 1992; Bisdom et al., 1982 Eswaran and Heng, 1976; Farmer et al., 1971; Gilkes, 1973; Ismail, 1969; Jeong and Kim, 2003; Jolicoeur et al., 2000; Kretzschmar et al., 1997; and Meunier and Velde, 1978). The transformation from biotite to kaolinite with few or no intermediate phases has been reported by Kretzschmar et al. (1997), Jolicoeur et al. (2000), and Bisdom et al. (1982). Commonly, the transformation of biotite to kaolinite involves a number of intermediate weathering products, and typically progresses from biotite through interstratified or mixed-layer biotite - clay to kaolinite (Jeong and Kim, 2003; Meunier and Velde, 1978; Acker and Bricker, 1991; Bisdom et al., 1982). Kretzschmar et al. (1997) summarize the varying intermediate phases produced, and conclude that these different sequences are climate-dependent, as outlined in the following:

(I) biotite –> interstratified biotite-vermiculite –> vermiculite (–> hydroxy-Al-interlayered vermiculite, kaolinite, smectite) (temperate-humid)

(II) biotite –> vermiculite –> smectite (arid and semi-arid)

(III) biotite –> hydrobiotite (vermiculite/biotite herein) –> kaolinite (or biotite –> kaolinite directly) (well-drained, warm, humid) .

However, Jolicoeur et al. (2000) caution against concluding that a given clay mineral automatically implies a given climate type, as position on slope, slope orientation, and changes in water table will all also impact on the clay mineralogy formed; the better the drainage, the more leaching of cations is likely.

Whether purely climate-controlled, topograpically controlled or a combination of

the two, structural transformations accompany these chemical changes, and can take the form of either layer or edge weathering (Bisdom et al. 1982). Layer weathering results in the opening of interlayers in the biotite, which allows for K^+ replacement by exchangeable cations (including possibly H^+). This in turn creates mixed or interstratified layers of biotite-vermiculite, or biotite-smectite, for example (Bisdom et al., 1982). Structural changes resulting from edge weathering cause openings in biotite layers along edges and fractures, in which case wedge-shaped openings are commonly found, forcing the layers apart. In this case, an intergrade biotite-vermiculite is formed (Bisdom et al., 1982). Layer weathering produces distinct layers of uniform thickness, whereas edge weathering produces distinct layers of varying thickness and extent. In order to maintain charge balance, loss of K^+ is accompanied by changes to the octahedral layers, particularly as Fe^{2+} is oxidised to Fe^{3+} (Gilkes et al., 1972). Increased changes to the octahedral layers ultimately results in changes in the tetrahedral layers, at which point structural integrity of the original biotite is compromised. The new mineralogy formed (for example, kaolinite + oxides / hydroxides or gibbsite + oxides/ hydroxides) is no longer similar to biotite in structural arrangement. In this way, chemical changes are accompanied by structural changes, which further contribute to the physical disaggregation of the rock.

4.4 Methodology

Petrographic analysis of thin sections from fresh parent and variably weathered samples allows determination of textural or micromorphological changes resulting from the weathering process, as well as preliminary determination of mineralogical changes; however, because of the fine-grained nature of the changes occurring during weathering, limited information of the chemical changes is available through standard petrographic means. A detailed study of the clay mineralogy was undertaken using XRD (of Pre-Pleistocene and Pre-Triassic samples only) and microprobe analysis. Information on sample preparation, analytical conditions and equipment for XRD and microprobe analysis are given in Appendix A1 and A2 respectively. X-ray scans of selected mineralogical sites provided information on the fine-scale chemical changes

occurring within a mineral, and provide more quantitative data than the SEM.

The data are presented in the following way in order to be consistent between the weathered profiles of differing ages: (a) the oldest weathered profile is described first, followed by the younger profiles; (b) within a given weathered profile, data are presented in the order fresh through to most weathered samples; (c) microprobe chemical data on biotites and their alteration products (except for kaolinite) are recalculated based on 22 oxygens (Banfield and Eggleton, 1986; Smith and Cavell, 1978). For simplicity, all Fe in biotite is calculated as Fe^{2+}, although it is acknowledged that the more weathered the sample the more oxidised, and hence the iron is most likely present in variable Fe^{3+}:Fe^{2+} in the more intensely weathered products.

4.5 Results

A summary diagram of the systematic changes that occur throughout the weathered sequences is given in Appendix A2.

4.5.1 Pre-Carboniferous Weathering Profile

Weathered profiles developed on monzogranite from two drill cores were selected for study (Fig. 4.1) (O'Beirne-Ryan and Zentilli, 2003). Thin sections were cut from samples in the fresh monzogranite, half-way up the weathered section, and from the uppermost part of the preserved sections; the total preserved thickness of each of the weathered profiles is approximately 5 metres (Fig. 4.2 and Appendix A2). Unlike the younger profiles, these two sequences have been relithified as a result of post-weathering diagenesis. In one of the sequences, the complete transformation of the parent minerals to the weathered mineralogy occurs closer to the underlying fresh rock, however both drill cores exhibit the near-complete transformation of minerals to weathered products within the section available.

Ryan and Zentilli (1993) used fission track analysis to determine that the Lower

Carboniferous sediments, and as well as these weathered profiles, were buried to depths of 5 km at approximately 150°C subsequent to their development. The age of maximum burial is bracketed at ca. 300 Ma, an age that appears to be confirmed by homogenization of the Rb-Sr system in clays at the sub-Carboniferous unconformity in central Nova Scotia (Ravenhurst and Zentilli, 1987). As a result of this burial event, the saprolites developed on the monzogranite are relithified, and their mineralogy is dominated by a combination of secondary (weathering) and tertiary (diagenetic) mineralogy (Fig. 4.3, Table 4.1). A consequence of these multiple events is that the present-day mineralogy of the relithified saprolite is dominated by kaolinite, illite/muscovite and calcite (as identified by microprobe analysis, Fig. 4.3, Table 4.1) and quartz, with minor amounts of Ti-oxides, apatite, zircon, and a secondary carbonate mineral, probably ankerite (Fig. 4.3B, Table 4.1). Only the quartz, apatite and zircon remain from the original unweathered parent, although the rounded and embayed edges of the quartz suggest some dissolution has occurred (Fig.4.3B). Weathering has resulted in the complete breakdown of the feldspars (both plagioclase and K-feldspar) and biotite (Fig. 4.3B and 4.3F). Kaolinite is pseudomorphic after the feldspars and biotite, and the original grain boundaries for some grains can still be determined, even though the present-day mineralogy is essentially dominated by kaolinite. In the case of biotite in particular, the cleavage planes are marked by fine-grained Ti-oxides, producing phanto-alteromorphs in the terminology of Delvigne (1998) (Fig. 4.3B,C, F). Interestingly, unlike the younger weathered profiles, only rare Fe-oxides or oxyhydroxides are found along these cleavages or grain boundaries. Although XRD analysis of these Pre-Carboniferous weathered profiles has not been undertaken, microprobe analysis of the biotites in the deeper portions of the weathered profiles indicate that there is a transition sequence developed between the original biotite and the end-product kaolinite (Fig. 4.3C and E, Fig. 4.4, Table 4.1).

Table 4.1.

Pre-Carboniferous - biotites and weathered biotites

Sample	SiO2	TiO2	Al2O3	FeO	MnO	MgO	CaO	Na2O	K2O	**Total**	Si	AlIV	AlVI	Ti	Fe2	Mn	Mg	Ca	Na	K	O
1186-2-1	33.97	3.01	18.45	20.75	0.38	6.84	0.00	0.32	9.57	**93.28**	5.36	2.64	0.79	0.36	2.74	0.05	1.61	0.00	0.10	1.93	22.00
1186-2-2	34.04	3.71	18.56	21.09	0.00	6.28	0.00	0.27	9.48	**93.42**	5.36	2.64	0.80	0.44	2.78	0.00	1.47	0.00	0.08	1.90	22.00
1186-2-3	40.89	2.70	18.97	17.43	0.33	4.90	0.00	0.29	10.59	**96.11**	6.05	1.95	1.36	0.30	2.16	0.04	1.08	0.00	0.08	2.00	22.00
1186-2-4	33.50	3.75	17.14	20.12	0.40	6.25	0.00	0.28	8.98	**90.42**	5.44	2.56	0.72	0.46	2.73	0.06	1.52	0.00	0.09	1.86	22.00
1186-2-5	34.37	1.11	27.15	16.65	0.36	2.96	3.19	0.00	1.60	**87.38**	5.34	2.66	2.32	0.13	2.17	0.05	0.69	0.53	0.00	0.32	22.00
1186-3-1	33.87	3.19	18.13	20.97	0.51	6.57	0.00	0.00	9.43	**92.66**	5.39	2.62	0.78	0.38	2.79	0.07	1.56	0.00	0.00	1.91	22.00
1186-3-2	35.00	4.04	18.29	21.53	0.38	6.56	0.00	0.27	9.80	**95.86**	5.38	2.62	0.70	0.47	2.77	0.05	1.50	0.00	0.08	1.92	22.00
1186-3-3	33.69	4.19	17.63	21.13	0.34	6.58	0.00	0.29	9.32	**93.17**	5.34	2.66	0.63	0.50	2.80	0.05	1.55	0.00	0.09	1.89	22.00
1186-3-4	33.87	4.52	17.36	21.15	0.42	6.35	0.00	0.00	9.11	**92.78**	5.38	2.62	0.62	0.54	2.81	0.06	1.50	0.00	0.00	1.85	22.00
CFC-1183-3.11	31.81	3.89	19.33	25.79	0.41	6.24	0.09	0.19	6.99	**94.73**	5.01	2.99	0.60	0.46	3.40	0.06	1.47	0.02	0.06	1.41	22.00
CFC-1183-3.18	30.61	3.73	19.40	29.37	0.36	6.49	0.15	0.14	4.87	**95.13**	4.84	3.16	0.46	0.44	3.89	0.05	1.53	0.03	0.04	0.98	22.00
CFC-1183-3.22	33.68	4.05	19.21	25.16	0.45	6.49	0.09	0.23	7.83	**97.18**	5.15	2.85	0.61	0.47	3.22	0.06	1.48	0.02	0.07	1.53	22.00
CFC1183-2.01	32.62	3.55	18.27	22.93	0.40	6.40	0.00	0.30	8.42	**92.89**	5.22	2.79	0.66	0.43	3.07	0.05	1.53	0.00	0.09	1.72	22.00
CFC1183-2.04	33.11	3.52	18.06	21.70	0.40	6.23	0.00	0.00	9.15	**92.17**	5.32	2.69	0.73	0.43	2.91	0.05	1.49	0.00	0.00	1.87	22.00
CFC1183-2.09	33.90	3.85	18.34	21.90	0.00	6.47	0.00	0.37	9.39	**94.22**	5.32	2.69	0.70	0.45	2.87	0.00	1.51	0.00	0.11	1.88	22.00
CFC1183-2.11	33.02	3.64	17.79	21.67	0.00	6.30	0.00	0.36	9.04	**91.82**	5.32	2.68	0.69	0.44	2.92	0.00	1.51	0.00	0.11	1.86	22.00
CFC1183-3.02	30.06	3.88	18.17	25.73	0.36	6.11	0.00	0.00	5.68	**89.99**	4.99	3.01	0.54	0.48	3.57	0.05	1.51	0.00	0.00	1.20	22.00
CFC1183-3.05	26.74	2.41	19.67	30.58	0.36	5.48	0.00	0.00	1.51	**86.75**	4.64	3.36	0.65	0.31	4.43	0.05	1.42	0.00	0.00	0.33	22.00
CFC1183-3.07	29.87	4.00	18.18	26.66	0.41	6.14	0.00	0.27	5.10	**90.63**	4.93	3.07	0.47	0.50	3.68	0.06	1.51	0.00	0.09	1.07	22.00
CFC1183-3.08	27.60	3.29	18.48	28.63	0.00	5.92	0.18	0.00	3.23	**87.33**	4.75	3.25	0.49	0.43	4.12	0.00	1.52	0.03	0.00	0.71	22.00
CFC1183-5-1.1	34.04	4.00	17.72	21.61	0.34	6.41	0.00	0.26	9.56	**93.94**	5.36	2.64	0.65	0.47	2.85	0.05	1.51	0.00	0.08	1.92	22.00
CFC1183-x.01	33.74	4.18	17.99	21.92	0.50	6.33	0.00	0.00	9.46	**94.12**	5.31	2.69	0.64	0.50	2.89	0.07	1.49	0.00	0.00	1.90	22.00

Pre-Carboniferous Feldspars

Sample	SiO2	Al2O3	CaO	Na2O	K2O	**Total**	Si	Al	Ca	Na	K	X	Z	**Ab**	**An**	**Or**
CFC-1183-3.10	68.20	20.65	0.08	11.47	0.05	**100.44**	11.85	4.23	0.02	3.86	0.01	16.08	3.89	**99.4**	**0.4**	**0.3**
CFC-1183-3.2	59.34	23.83	4.43	8.90	0.54	**97.04**	10.88	5.15	0.87	3.16	0.13	16.02	4.16	**76.1**	**20.9**	**3.0**
CFC-1183-3.6	60.93	24.72	5.42	8.49	0.52	**100.08**	10.83	5.18	1.03	2.93	0.12	16.01	4.09	**71.8**	**25.3**	**2.9**
CFC-1183-3.8	67.83	20.45	0.21	12.09	0.02	**100.60**	11.81	4.19	0.04	4.08	0.01	16.00	4.14	**98.9**	**0.9**	**0.1**
CFC-1183-3.9	60.57	25.08	5.64	8.36	0.39	**100.03**	10.77	5.25	1.07	2.88	0.09	16.02	4.06	**71.3**	**26.6**	**2.2**

Table 4.1. Continued (C) CFC - ILLITE / MUSCOVITE

Sample	Analysis	Locatid	Mineral	SiO2	TiO2	Al2O3	FeO	MgO	CaO	Na2O	K2O	Total	Si	AlIV	AlVI	Ti	Fe2	Mg	Ca	Na	K	O	Fe_FeM
CFC-1119A-Bi12	Nov6-03	biot12	mus	49.87	0.15	32.34	1.65	1.46	0.16	0.12	8.83	**94.58**	6.58	1.42	3.61	0.02	0.18	0.29	0.02	0.03	1.49	22	0.39
CFC-1119B-B-7	nov6-03	biot 07	mus	50.24	0.14	33.09	1.53	1.39	0.22	0.04	8.68	**95.32**	6.56	1.44	3.66	0.01	0.17	0.27	0.03	0.01	1.45	22	0.38
CFC-1183-3.20	aug1-01	biot 20	mus	50.77	0.14	28.98	2.10	2.11	0.27	0.14	8.03	**92.54**	6.83	1.17	3.43	0.01	0.24	0.42	0.04	0.04	1.38	22	0.36
CFC1168-2.02	aug1-01		mus	47.18	0.00	31.89	1.38	1.56	1.13	0.00	5.67	**88.81**	6.53	1.47	3.72	0.00	0.16	0.32	0.17	0.00	1.00	22	0.33
CFC1168-2.06	aug1-01		mus	46.85	0.00	32.58	1.00	0.90	0.00	0.00	6.15	**87.48**	6.55	1.45	3.91	0.00	0.12	0.19	0.00	0.00	1.10	22	0.38
CFC1170-2.01	aug1-01		mus	46.40	0.00	35.99	1.25	0.80	0.00	0.53	9.78	**94.75**	6.17	1.83	3.81	0.00	0.14	0.16	0.00	0.14	1.66	22	0.47
CFC1170-2.02	aug1-01		mus	45.91	0.29	35.70	0.96	0.66	0.00	0.48	8.12	**92.12**	6.20	1.80	3.88	0.03	0.11	0.13	0.00	0.13	1.40	22	0.45
CFC1170-2.03	aug1-01		mus	44.92	0.00	36.09	0.62	0.33	0.00	0.25	4.73	**86.94**	6.26	1.74	4.18	0.00	0.07	0.07	0.00	0.07	0.84	22	0.51

CFC Ti-oxides - note low FeO compared to younger Ti-oxides, Pre-Triassic and Pre-Pleistocene

Sample	Mineral	SiO2	TiO2	Al2O3	FeO	MnO	MgO	CaO	Na2O	K2O	Total
CFC-1119A-Bi10	Ti ox	0.28	91.65	0.76	0.83	0.11	0.06	0.34	0.03	0.18	**94.23**
CFC-1119A-Bi25	Ti ox	0.00	94.08	0.14	0.65	0.09	0.00	0.41	0.00	0.08	**95.45**
CFC-1119A-Bi27	Ti ox	0.00	94.34	0.05	0.28	0.09	0.00	0.07	0.00	0.08	**94.92**
CFC-1119A-Bi5	Ti ox	0.00	94.92	0.04	0.27	0.09	0.00	0.11	0.00	0.05	**95.48**
CFC-1119B-B-5	Ti ox	0.93	89.92	1.54	0.91	0.12	0.00	0.62	0.00	0.07	**94.12**
CFC-1183-3.15	Ti ox	0.17	94.38	0.02	0.38	0.84	0.00	0.20	0.03	0.09	**96.11**
CFC-1183-3.21	Ti ox	0.76	93.62	0.44	0.61	0.08	0.05	0.18	0.03	0.18	**95.93**
CFC-1183-3.26	Ti ox	0.19	94.06	0.08	0.51	0.07	0.00	0.22	0.04	0.11	**95.28**
CFC1168-2.07	Ti ox	0.72	92.07	1.20	0.76	0.00	0.00	0.00	0.00	0.00	**94.75**
CFC1170-1.05	Ti ox	3.06	86.48	2.34	2.57	0.00	0.00	0.16	0.00	0.00	**94.61**

Fe-Mn-Mg-Ca Carbonate - ankerite? - CFC

Sample	Analysis	Minera	SiO2	TiO2	Al2O3	FeO	MnO	MgO	CaO	Total
CFC-1119A-Bi13	Biot 13A	FeC	0.00	0.04	0.00	13.93	3.52	12.62	28.79	**58.91**
CFC-1119A-Bi13	Biot 13B	FeC	0.00	0.01	0.00	16.00	3.94	14.27	29.12	**63.33**
CFC-1119A-Bi14	Biot 14	FeC	0.00	0.03	0.00	15.01	4.77	10.00	26.89	**56.70**
CFC-1119A-Bi15	Biot 15	FeC	0.00	0.00	0.00	15.38	4.41	10.32	27.28	**57.40**
CFC-1119A-Bi16	Biot 16	FeC	0.00	0.01	0.00	13.55	3.46	12.89	28.77	**58.67**
CFC-1119A-Bi17	Biot 17	FeC	0.00	0.01	0.00	15.31	4.90	8.49	26.50	**55.20**
CFC-1119A-Bi26	Biot 26	FeC	0.00	0.33	0.06	15.27	4.70	10.12	27.81	**58.30**
CFC-1119A-Bi9	Biot 9	FeC	0.00	0.18	0.01	17.69	5.50	8.98	28.07	**60.42**
CFC-1119B-B-4	Biot 4	FeC	0.00	0.11	0.00	15.34	4.25	10.69	27.72	**58.11**
CFC-1119B-B-6	Biot 6	FeC	0.00	0.09	0.00	15.40	4.54	10.58	28.21	**58.83**
CFC1168-2.05		FeC	0.20	0.00	0.00	14.48	4.57	8.81	27.20	**55.26**
CFC1168-2.09		FeC	3.09	0.00	1.89	13.44	4.09	9.42	26.56	**58.49**
CFC1170-1.03		FeC	0.00	0.00	0.00	13.63	4.24	9.92	27.60	**55.39**
CFC1170-2-1d	clays2	FeC	0.00	0.03	0.01	14.13	0.00	9.02	28.73	**51.92**

Table 4.1 continued. Pre-Carboniferous Kaolinites.

Sample	SiO2	TiO2	Al2O3	FeO	MgO	CaO	Na2O	K2O	**Total**	Si	AlIV	AlVI	Ti	Fe2	Mg	Ca	Na	K	O
1186-3-6	43.48	0.60	34.09	4.58	1.25	0.00	0.00	1.44	**85.44**	3.65	0.00	3.37	0.04	0.32	0.16	0.00	0.00	0.15	14
CFC-1119A-Bi18	46.68	0.00	38.74	0.11	0.02	0.02	0.04	0.05	**85.66**	3.74	0.00	3.66	0.00	0.01	0.00	0.00	0.01	0.01	14
CFC-1119A-Bi19	45.51	0.00	36.64	0.06	0.03	0.06	0.02	0.05	**82.36**	3.79	0.00	3.60	0.00	0.00	0.00	0.01	0.00	0.01	14
CFC-1119A-Bi2	46.14	0.07	38.54	0.02	0.01	0.01	0.03	0.00	**84.82**	3.74	0.00	3.67	0.00	0.00	0.00	0.00	0.01	0.00	14
CFC-1119A-Bi22	46.44	0.00	38.78	0.07	0.04	0.04	0.04	0.02	**85.43**	3.73	0.00	3.67	0.00	0.01	0.00	0.00	0.01	0.00	14
CFC-1119A-Bi23	46.54	0.00	39.30	0.18	0.03	0.06	0.02	0.03	**86.16**	3.71	0.00	3.69	0.00	0.01	0.00	0.01	0.00	0.00	14
CFC-1119A-Bi24	46.47	0.00	39.36	0.08	0.02	0.05	0.06	0.03	**86.08**	3.71	0.00	3.70	0.00	0.01	0.00	0.00	0.01	0.00	14
CFC-1119A-Bi25	46.11	0.00	38.56	0.05	0.03	0.03	0.05	0.05	**84.88**	3.73	0.00	3.68	0.00	0.00	0.00	0.00	0.01	0.01	14
CFC-1119A-Bi3	46.12	0.01	38.70	0.01	0.00	0.00	0.04	0.00	**84.87**	3.73	0.00	3.69	0.00	0.00	0.00	0.00	0.01	0.00	14
CFC-1119A-Bi4	46.24	0.14	39.27	0.03	0.00	0.01	0.03	0.04	**85.75**	3.71	0.00	3.71	0.01	0.00	0.00	0.00	0.00	0.00	14
CFC-1119A-Bi7	46.44	0.03	38.57	0.02	0.00	0.00	0.03	0.00	**85.09**	3.75	0.00	3.66	0.00	0.00	0.00	0.00	0.00	0.00	14
CFC-1119B-B-1	46.52	0.01	38.92	0.01	0.01	0.01	0.04	0.00	**85.51**	3.74	0.00	3.68	0.00	0.00	0.00	0.00	0.01	0.00	14
CFC-1119B-B-8	46.02	0.00	38.87	0.09	0.02	0.07	0.03	0.02	**85.11**	3.72	0.00	3.70	0.00	0.01	0.00	0.01	0.00	0.00	14
CFC-1119B-Bi10	46.92	0.00	39.71	0.13	0.05	0.10	0.04	0.04	**86.98**	3.71	0.00	3.70	0.00	0.01	0.01	0.01	0.01	0.00	14
CFC-1119B-Bi11	47.14	0.00	38.73	0.09	0.04	0.02	0.05	0.32	**86.40**	3.76	0.00	3.63	0.00	0.01	0.00	0.00	0.01	0.03	14
CFC-1119B-Bi12	46.65	0.00	38.13	0.11	0.06	0.05	0.05	0.44	**85.48**	3.76	0.00	3.62	0.00	0.01	0.01	0.00	0.01	0.05	14
CFC-1119B-Bi13	45.80	0.00	38.37	0.05	0.00	0.04	0.01	0.07	**84.32**	3.73	0.00	3.68	0.00	0.00	0.00	0.00	0.00	0.01	14
CFC-1119B-Bi9	46.55	0.00	38.37	0.03	0.01	0.04	0.05	0.01	**85.07**	3.76	0.00	3.65	0.00	0.00	0.00	0.00	0.01	0.00	14
CFC-1183-3.14	46.51	0.04	38.77	0.14	0.03	0.04	0.04	0.02	**85.59**	3.74	0.00	3.67	0.00	0.01	0.00	0.00	0.01	0.00	14
CFC-1183-3.19	46.38	0.05	38.85	0.28	0.09	0.05	0.06	0.04	**85.78**	3.72	0.00	3.67	0.00	0.02	0.01	0.00	0.01	0.00	14
CFC-1183-3.24	43.84	0.04	38.34	3.92	0.44	0.09	0.07	0.04	**86.78**	3.57	0.00	3.68	0.00	0.27	0.05	0.01	0.01	0.00	14
CFC-1183-3.28	46.74	0.01	38.57	0.21	0.08	0.04	0.05	0.04	**85.74**	3.75	0.00	3.64	0.00	0.01	0.01	0.00	0.01	0.01	14
CFC-1183-3.3	46.20	0.01	37.19	0.37	0.26	0.21	0.09	0.08	**84.42**	3.77	0.00	3.58	0.00	0.03	0.03	0.02	0.01	0.01	14
CFC1168-2.01	44.84	0.00	36.91	0.00	0.00	0.00	0.00	0.00	**81.75**	3.76	0.00	3.65	0.00	0.00	0.00	0.00	0.00	0.00	14
CFC1168-2.03	46.71	0.00	38.27	0.00	0.00	0.00	0.00	0.34	**85.32**	3.76	0.00	3.63	0.00	0.00	0.00	0.00	0.00	0.04	14
CFC1170-1.01	44.42	0.00	36.75	0.00	0.00	0.00	0.00	0.00	**81.17**	3.75	0.00	3.66	0.00	0.00	0.00	0.00	0.00	0.00	14
CFC1170-1.02	46.14	0.48	37.18	0.00	0.00	0.00	0.00	0.00	**83.80**	3.78	0.00	3.59	0.03	0.00	0.00	0.00	0.00	0.00	14
CFC1170-1.04	46.15	0.00	37.76	0.00	0.00	0.00	0.00	0.00	**83.91**	3.77	0.00	3.63	0.00	0.00	0.00	0.00	0.00	0.00	14
CFC1170-1.06	45.27	0.00	37.31	0.00	0.00	0.00	0.00	0.00	**82.58**	3.76	0.00	3.65	0.00	0.00	0.00	0.00	0.00	0.00	14
CFC1170-2-1a	45.04	0.01	35.93	0.12	0.05	0.00	0.13	0.03	**81.31**	3.80	0.00	3.57	0.00	0.01	0.01	0.00	0.02	0.00	14
CFC1170-2-1f	45.91	0.00	36.27	0.00	0.06	0.00	0.03	0.02	**82.29**	3.82	0.00	3.56	0.00	0.00	0.01	0.00	0.01	0.00	14
CFC1170-2.04	46.00	0.00	37.94	0.00	0.00	0.00	0.00	0.00	**83.94**	3.76	0.00	3.65	0.00	0.00	0.00	0.00	0.00	0.00	14
CFC1170-2.05	46.39	0.00	38.44	0.00	0.00	0.00	0.00	0.00	**84.83**	3.75	0.00	3.66	0.00	0.00	0.00	0.00	0.00	0.00	14
CFC1183-2.02	45.73	0.00	37.54	0.33	0.00	0.00	0.00	0.00	**83.60**	3.76	0.00	3.64	0.00	0.02	0.00	0.00	0.00	0.00	14
CFC1183-2.03	42.30	0.00	35.16	4.64	0.58	0.00	0.00	0.00	**82.68**	3.63	0.00	3.55	0.00	0.33	0.07	0.00	0.00	0.00	14
CFC1183-2.05	46.14	0.00	37.58	0.42	0.00	0.00	0.00	0.00	**84.14**	3.77	0.00	3.62	0.00	0.03	0.00	0.00	0.00	0.00	14
CFC1183-2.12	46.65	0.00	38.14	0.26	0.00	0.00	0.00	0.00	**85.05**	3.77	0.00	3.63	0.00	0.02	0.00	0.00	0.00	0.00	14
CFC1183-3.04	46.82	0.00	37.99	0.00	0.00	0.00	0.00	0.00	**84.81**	3.79	0.00	3.62	0.00	0.00	0.00	0.00	0.00	0.00	14
CFC1183-3.06	46.81	0.00	37.89	0.00	0.00	0.00	0.00	0.00	**84.70**	3.79	0.00	3.61	0.00	0.00	0.00	0.00	0.00	0.00	14
CFC1183-5-1.2	46.35	0.00	37.70	0.90	0.24	0.00	0.00	0.00	**85.19**	3.76	0.00	3.60	0.00	0.06	0.03	0.00	0.00	0.00	14
CFC1183-5-1.3	45.75	0.00	37.40	0.93	0.21	0.00	0.00	0.00	**84.29**	3.75	0.00	3.61	0.00	0.06	0.03	0.00	0.00	0.00	14
CFC1183-x.02	42.32	0.00	34.72	5.95	0.71	0.00	0.00	0.00	**83.70**	3.62	0.00	3.50	0.00	0.43	0.09	0.00	0.00	0.00	14

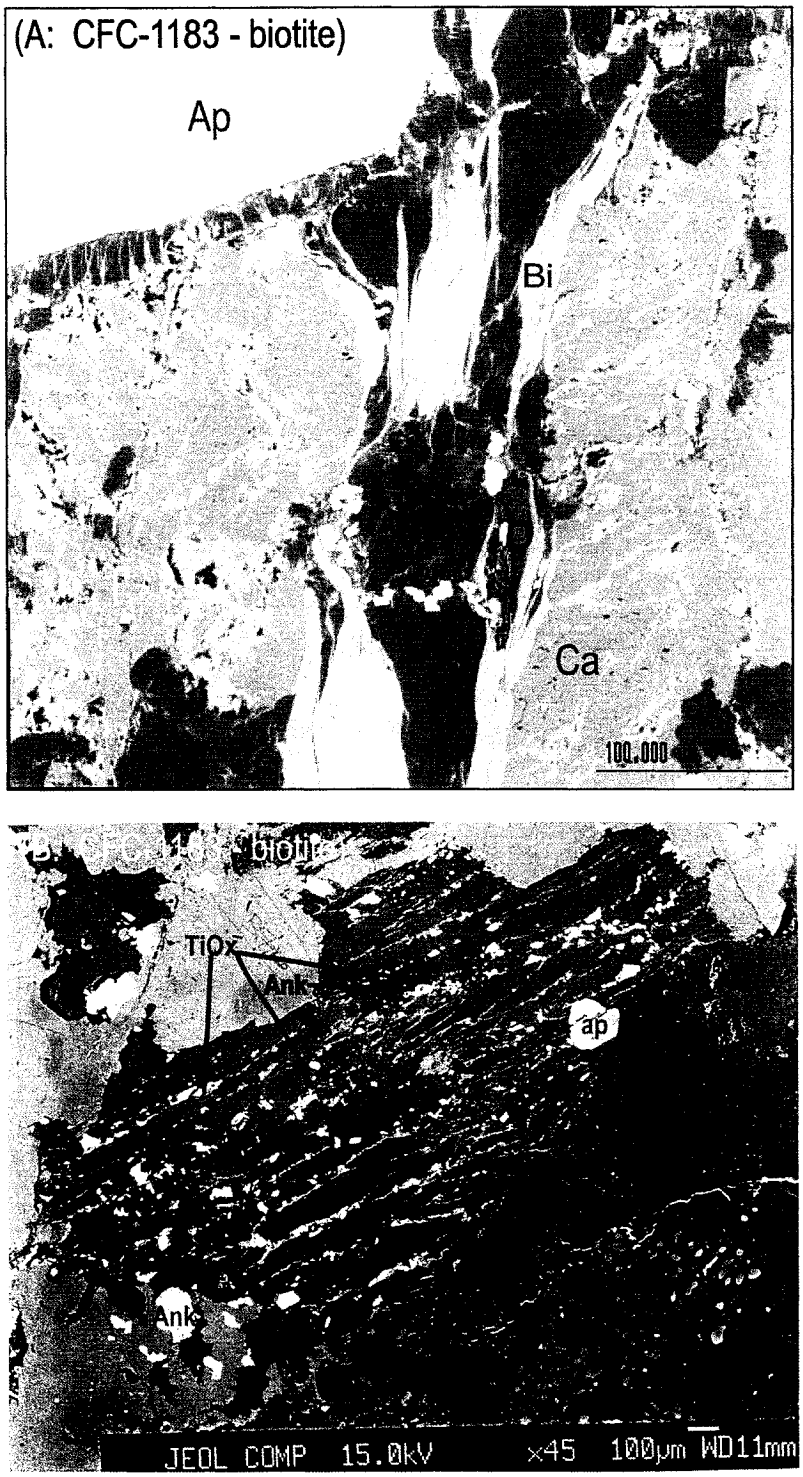

Fig. 4.3 (A) and (B). (A) Biotite(Bi) -> Kaolinite(Kao) with diagenetic calcite (Ca) and primary apatite (Ap) . (B) Biotite pseudomorphed by kaolinite (Kao), with primary apatite (Ap) and secondary titanium oxides (TiOx) developed during weathering, and diagenetic illite/muscovite and ankerite (Ank). Lower right corner is kaolinite (Kao) and quartz (qtz) pseudomorph after feldspar.

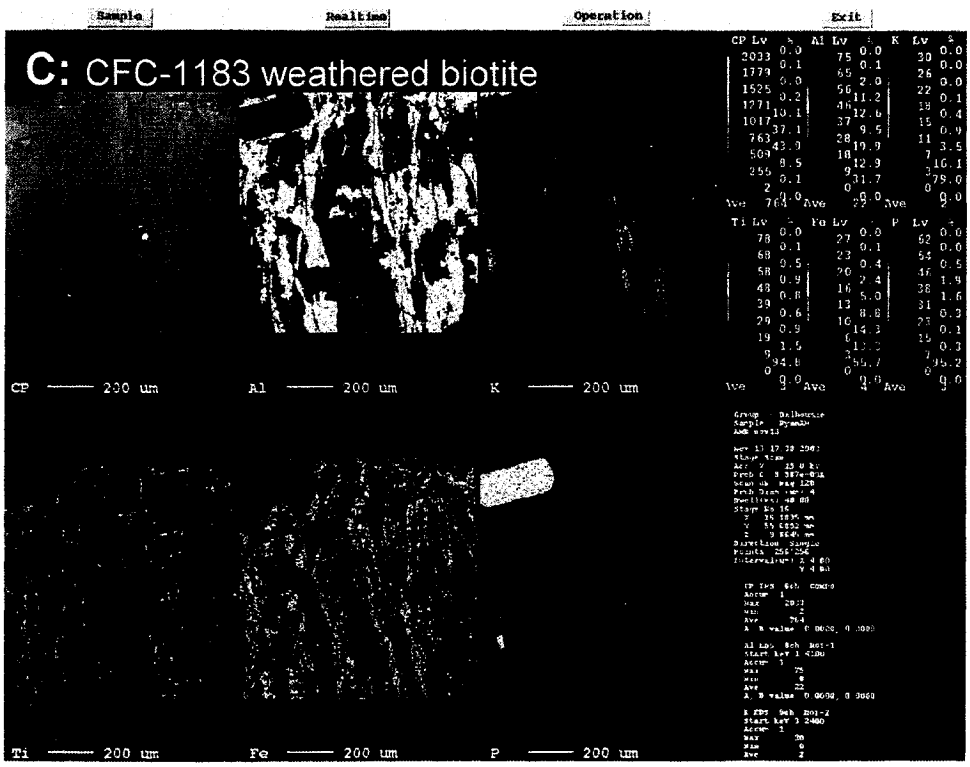

Fig. 4.3C: Partially wearthered biotite with Ti oxides along cleavages and unweathered apatite (upper left corner).

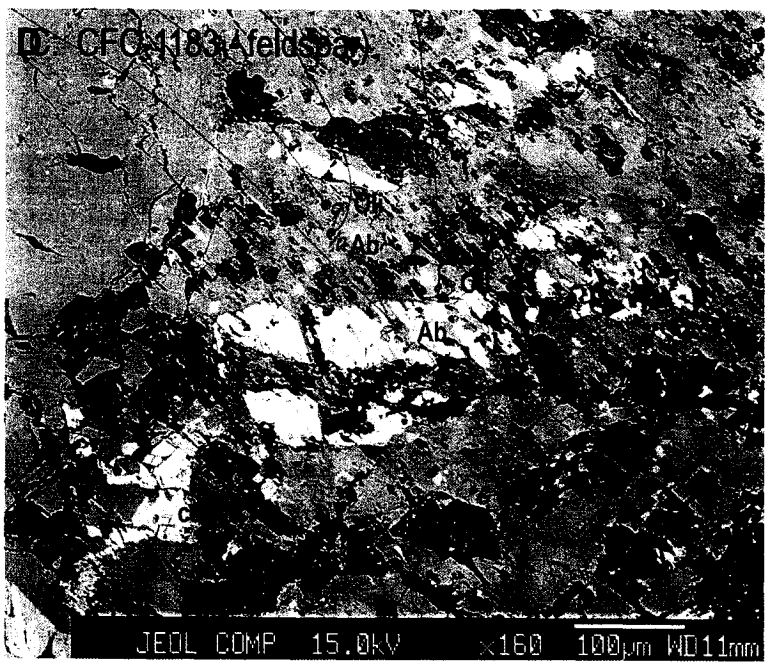

Fig. 4.3 D. Feldspar (plagioclase (Ol) and albite (Ab) weathering near base of Pre-Carboniferous saprolite. Note the patches of kaolinite (Kao) produced during weathering and the diagenetic calcite (cal).

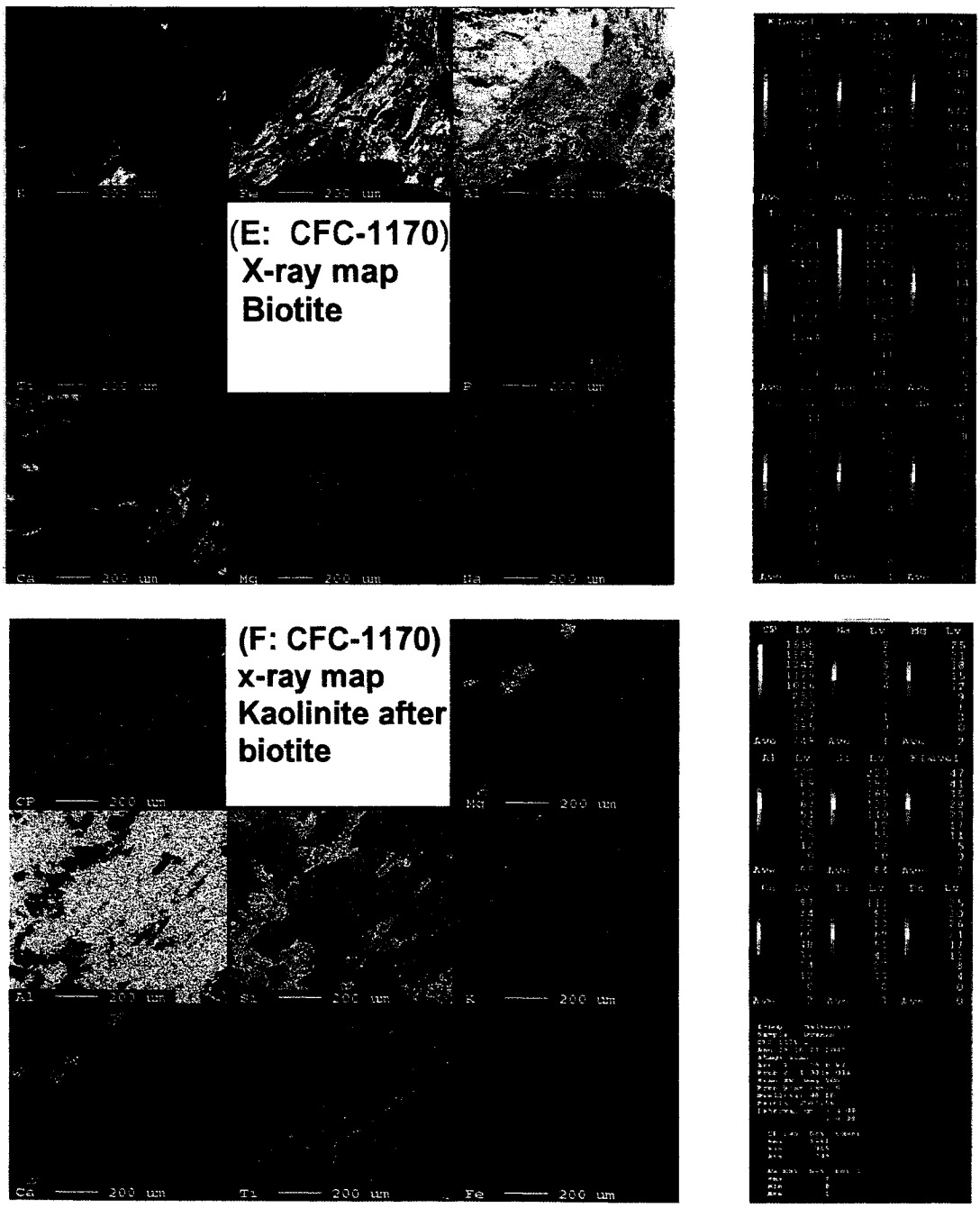

Fig. 3.4 E and F. (E) X-ray map of weathered biotite, from near top of preserved part of Pre-Carboniferous saprolite. (F) X-ray map of biotite which has been completely pseudomorphed by kaolinite and titanium oxides. Note the patches of diagenetic ankerite.

The transition involves a systematic change from fresh to weathered biotite, which is reflected in a loss of K from the interlayer sites, and a concomitant increase in tetrahedral Al (reflecting a decrease in Si) and total iron (as Fe^{2+}) (Fig. 4.3C and 4.3E). Further alteration of the biotite resulted in total replacement of the biotite by kaolinite, with the cleavage traces marked by Ti-oxides (Fig. 4.3B and 4.3F); the Ti from the biotite ultimately remaining within the system. The kaolinite developed from biotite has trace amounts of Ti present, distinguishing it from the kaolinite formed from feldspar, which has no Ti present (Fig. 4.3D, Table 4.1). During diagenesis, muscovite/illite and calcite partially replaced some of the original weathered material, and these minerals are commonly found in some of the former feldspar grains rather than in other minerals, although they do occur in the altered biotites deeper in the sequence as well (Fig. 4.3A). Much of the Fe has been removed from the system, although rare veinlets of Fe oxides/oxyhydroxides are present (Fig 4.3D), and small quantities of iron remains in Ti oxides. Ankerite has incorporated some of the remaining Fe from any secondary oxides that may have developed along the cleavages or grain boundaries (Fig.4. 3B, F). Graphic representation of changes in biotite composition is represented in Figure 4.4.

4.5.2 Pre-Triassic Monzogranite

The preserved portion of the Pre-Triassic profile is considerably thicker than the preserved portion of the Pre-Carboniferous profile, at approximately 30 metres thick. The weathered profile is immediately overlain by Triassic sedimentary strata, and the boundary between the weathered profile, and the Triassic sediments is at present-day depths of approximately 30 metres. Mineralogical and chemical changes occur from the weathering front in contact with the granite to the top of the weathered profile, and clearly define systematic changes indicative of increased degree of weathering from base to top. This weathered profile is classified as an argillaceous saprolite, and has not been subject to significant post-formation diagenesis (O'Beirne-Ryan and Zentilli, 2003). Back scatter images and petrographic photomicrographs of the Pre-Triassic weathering profile are given in Figure 4.5, and microprobe data are presented in Table 4.2.

Fig. 4.4. Chemistry of weathering biotite from Pre-Carboniferous saprolite, as reflected in (A) K_2O versus SiO_2,
(B) FeO+MgO+MnO versus Al_2O_3, and
(C) Si - (Al^{IV} +Al^{VI}) - (Ca+Na+K)

Black diamonds are from fresh parent;
Purple diamonds are biotites from saprolite 1 metre above fresh parent.

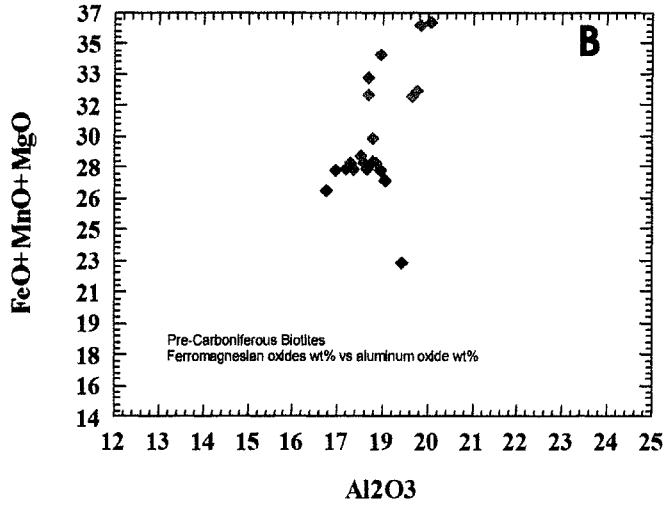

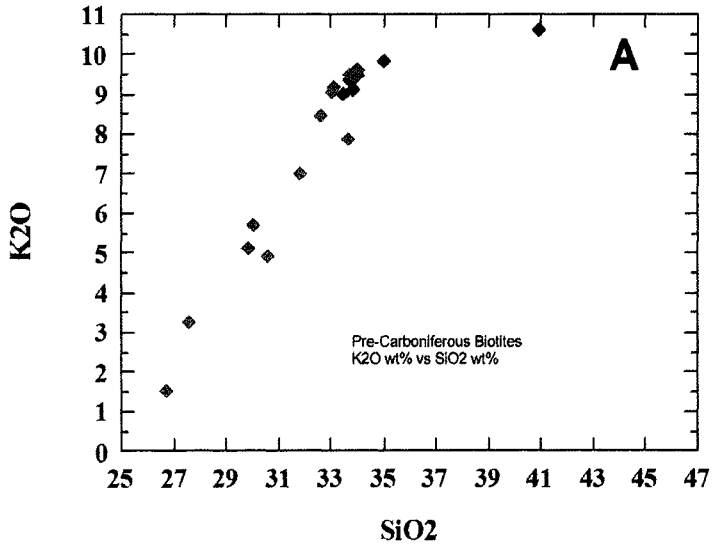

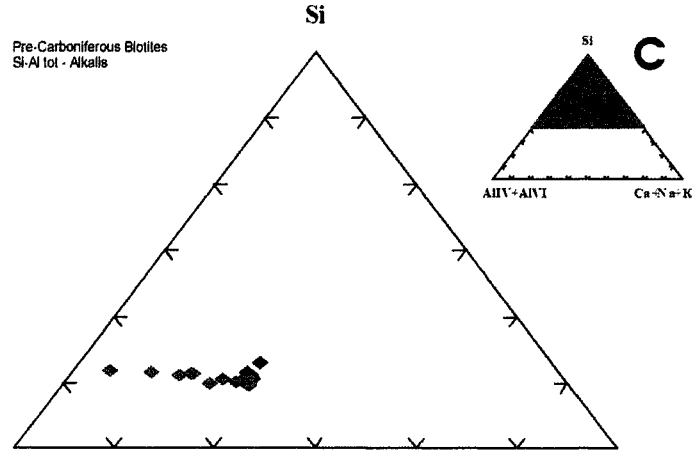

(Diagram modified after Jolicoeur et al., 2000)

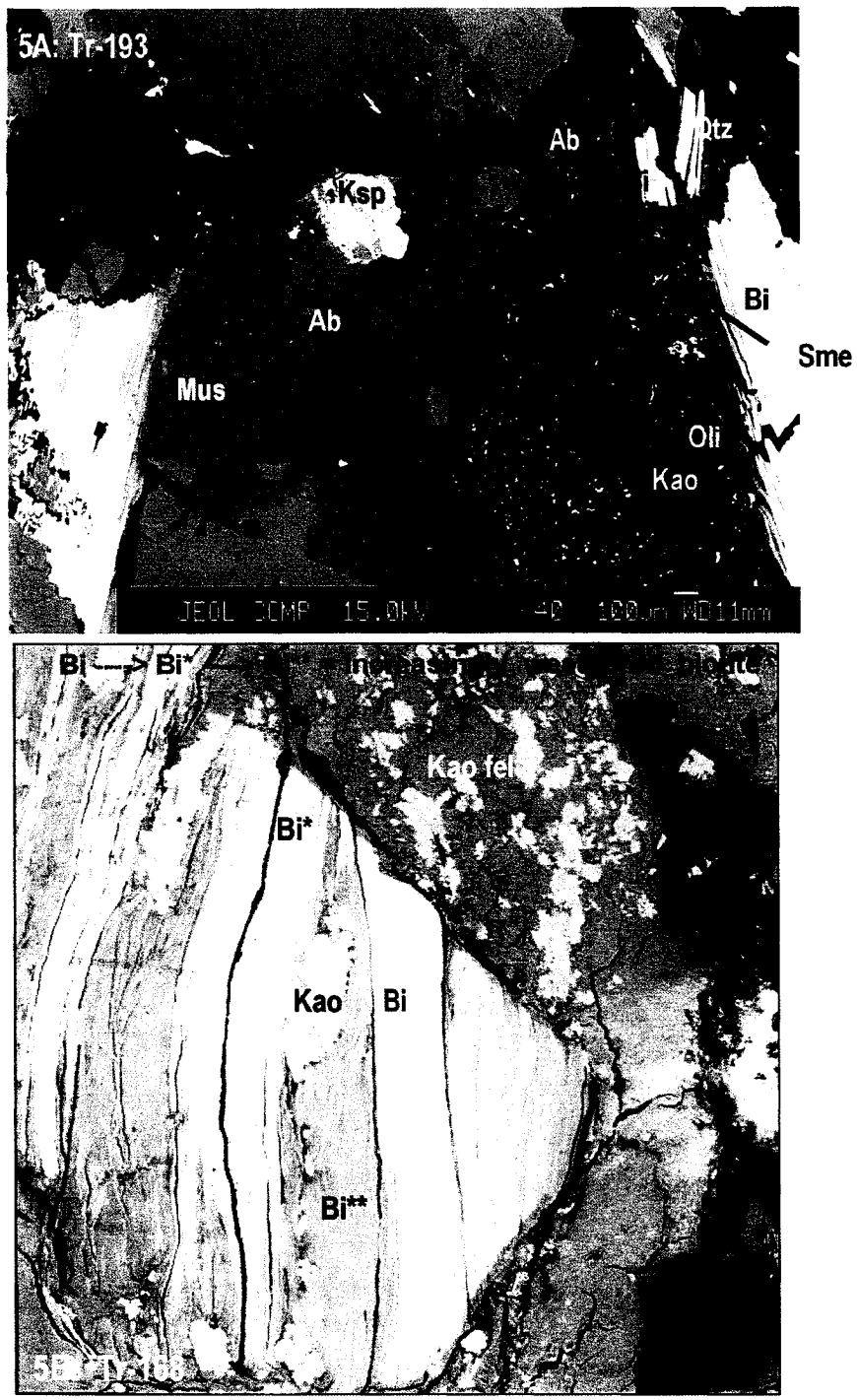

Fig. 4.5 (A and B). (A) Back scatter image of weathering-induced fracturing of Pre-Triassic saprolite, near base of saprolite, with kaolinite (Kao)and smectite (Sme) developed in plagioclase (Oli -Ab) and biotite (Bi) respectively. Primary k-feldspar (Ksp), muscovite (Mus) and quartz (Qtz) are also present. (B) Back scatter image of at 10 m up from fresh granitoid. Biotite (Bi) and Plagioclase (Kao fel) in varying degrees of breakdown to intemediate biotite products (Bi* and Bi**) and Kao (from biotite and plagioclase).

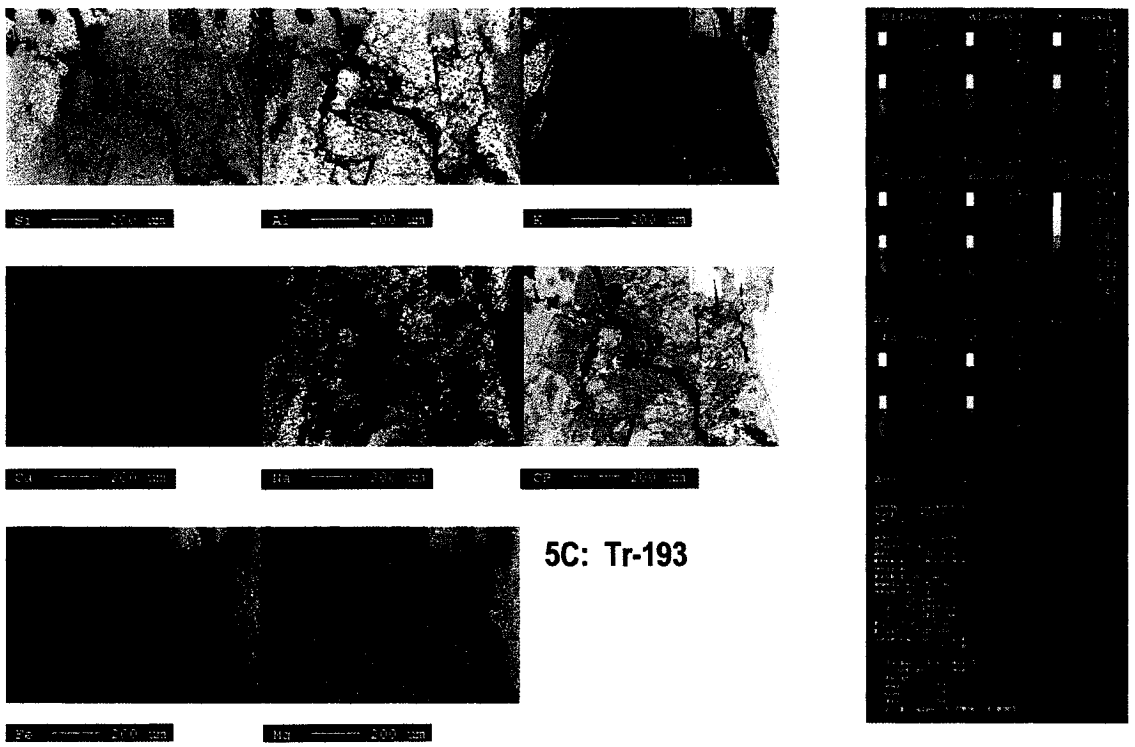

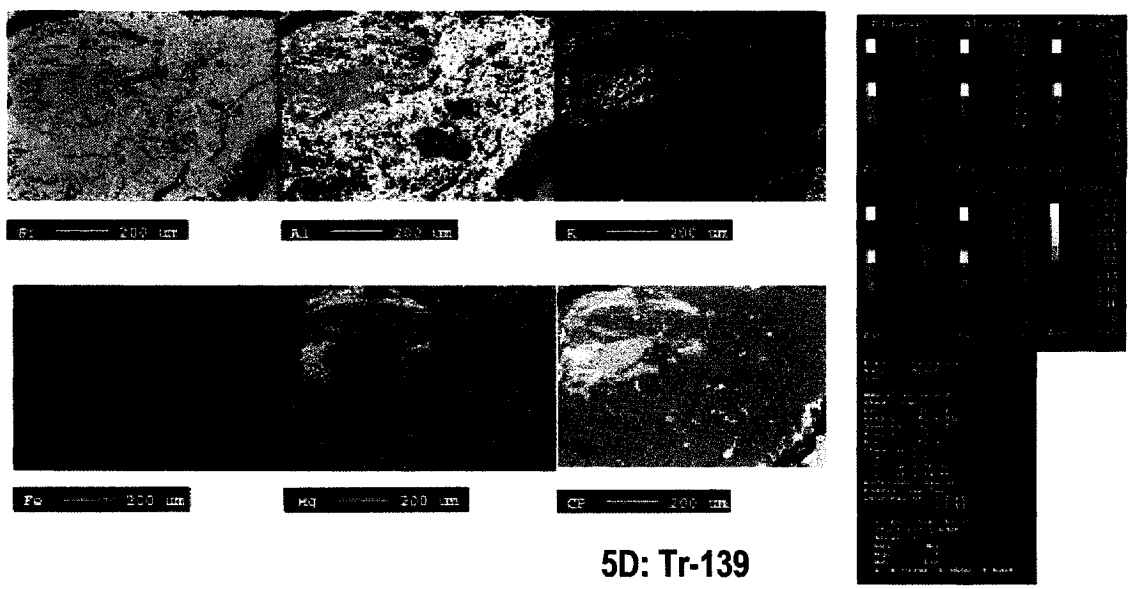

Fig. 4.5 (C and D). Pre-Triassic weathering. (C) X-ray map of weathering-induced fracture feldspar (from 4.5A). (D) Kaolinized feldspar (Na-rich) with variably weathered biotite grain, approx. 20 m up from fresh granitoid.

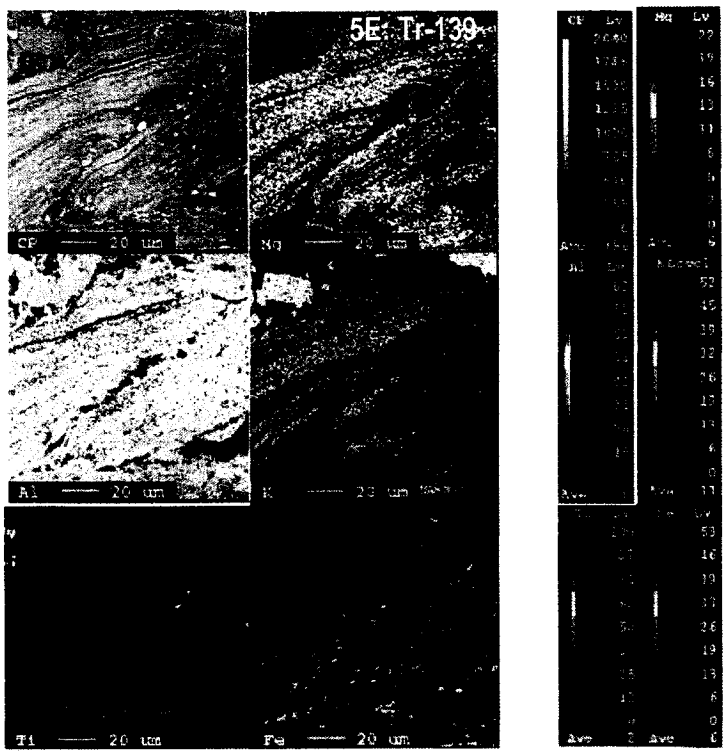

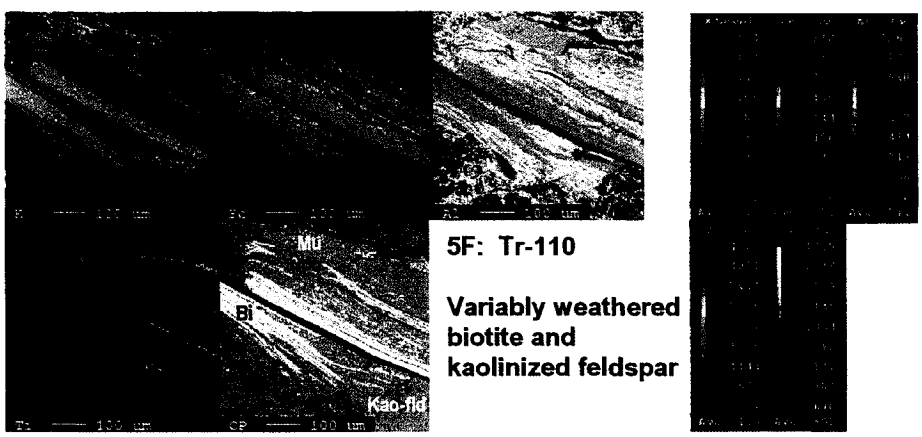

Fig. 4.5 (E and F) (E) X-ray map of weathered and bent biotite, 20 m up from fresh biotite, Pre-Triassic saprolite. (F) X-ray map of variably weathered biotite from top of preserved portion of Pre-Triassic saprolite. Note that some of original biotite remains, even at 30 m up from fresh granitoid.

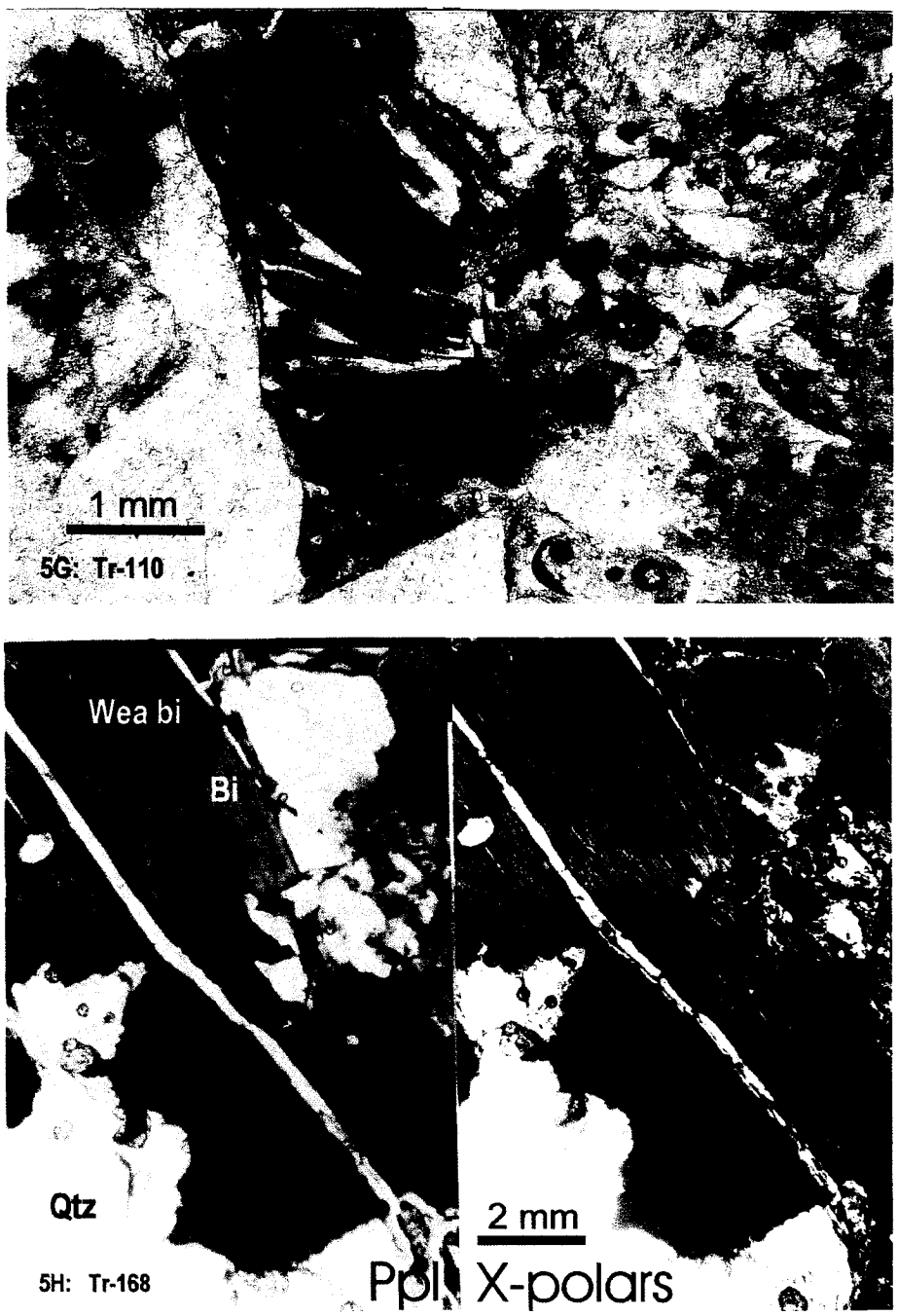

Fig. 4.5 (G and H). (G)Plasma-like texture of saprolite at top of preserved saprolite beneath Triassic sediments. Not the disaggregated nature of biotite, which typically retains its brown colour, even 30 m up from fresh granitoid; cloudy sections are highly weathered feldspar. (H) Weathering biotite with cleavage-parallel fracture, 10 m up from fresh biotite. (Wea bi = weathered biotite; Qtz = quartz; Ppl = plain-polarised light, and X-polars = cross-polarised light).

Table 4.2. Pre-Triassic mineral analyses from microprobe

Biotites and weathered biotites

Sample	SiO2	TiO2	Al2O3	FeO**	MnO	MgO	CaO	Na2O	K2O	**Total**	Si	AlIV	AlVI	Ti	Fe2	Mn	Mg	Ca	Na	K
Tr-110-02-01	38.87	3.86	18.35	17.62	0.3	5.11	0.23	0.14	9.16	**93.64**	5.638	2.362	0.7725	0.421	2.138	0.037	1.105	0.036	0.04	1.695
Tr-110-1a.01	35.86	4	18.25	19.33	0.41	6.26	0	0	9.07	**93.18**	5.57	2.43	0.9085	0.468	2.511	0.054	1.45	0	0	1.7975
Tr-110-2.01	34.16	3.53	16.12	17.65	0.36	5.56	0	0	8.22	**85.6**	5.7485	2.2515	0.943	0.447	2.484	0.052	1.395	0	0	1.7645
Tr-110-2.02	36.09	3.78	17.41	19.78	0.36	6.13	0	0	8.74	**92.29**	5.6625	2.3375	0.8795	0.446	2.596	0.048	1.434	0	0	1.7495
Tr-110-2.04	29.99	3.15	14	21.83	0.36	4.44	0.23	0	6.17	**80.17**	5.552	2.448	0.604	0.439	3.38	0.057	1.226	0.046	0	1.457
Tr-110-a.01	35.56	3.03	18.26	17.71	0.38	6.25	0.3	0	7.57	**89.06**	5.687	2.313	1.126	0.365	2.369	0.052	1.49	0.052	0	1.5445
Tr-110-a.02	43.95	0	30.44	5.53	0	1.73	0.18	0	1.43	**83.26**	6.4445	1.5555	3.701	0	0.678	0	0.378	0.029	0	0.2675
Tr-110-x-01	42.72	0	30.45	6.07	0	1.56	0.26	0	1.37	**82.43**	6.357	1.643	3.6935	0	0.756	0	0.346	0.042	0	0.26
Tr-110-x-02	34.27	3.15	17.31	19.96	0.32	6.02	0.25	0	7.48	**88.76**	5.5905	2.4095	0.916	0.387	2.723	0.044	1.464	0.044	0	1.5565
Tr-110-x-03	35.86	2.67	18.33	20.18	0.4	5.78	0.27	0	7.99	**91.48**	5.6605	2.3395	1.068	0.317	2.664	0.054	1.36	0.046	0	1.609
Tr-139-1.01	37.51	2.17	17.81	15.64	0	4.72	1.26	1.68	7.43	**88.22**	5.9965	2.0035	1.3495	0.261	2.091	0	1.125	0.216	0.521	1.5155
Tr-139-1.02	36.84	3.74	17.16	18.59	0	5.24	0.18	0.4	9.03	**91.18**	5.816	2.184	1.0065	0.444	2.455	0	1.234	0.031	0.123	1.8185
Tr-139-1.03	37.33	3.45	17.3	19.44	0	5.72	0.18	0.31	9.02	**92.75**	5.805	2.195	0.973	0.404	2.528	0	1.326	0.03	0.094	1.7895
Tr-139-1.09	40.75	1.87	19.49	13.62	0	4.96	0.52	0.58	7.56	**89.35**	6.2475	1.7525	1.7665	0.216	1.746	0	1.134	0.086	0.173	1.4785
Tr-139-2.03	38.9	0.44	13.14	13.95	0	0.89	0.23	0	8.09	**75.64**	7.126	0.874	1.9605	0.061	2.137	0	0.243	0.045	0	1.8905
Tr-139-2.04	35.34	4.53	16.2	18.27	0.28	4.87	0.57	0.89	8.66	**89.61**	5.7205	2.2795	0.8085	0.552	2.473	0.039	1.175	0.099	0.28	1.7885
Tr-139-2.05	37.34	3.71	16.95	18.19	0.37	5.46	0.32	0.52	8.87	**91.73**	5.851	2.149	0.979	0.438	2.384	0.049	1.276	0.054	0.158	1.773
Tr-139-2.06	40.28	1.75	19.09	15.34	0	4.12	0.49	0	6.92	**87.99**	6.291	1.709	1.8025	0.206	2.004	0	0.96	0.082	0	1.379
Tr-168-2.01	38.67	3.16	17.45	17.78	0.49	4.96	0.43	0.28	7.63	**90.85**	6.024	1.976	1.225	0.371	2.317	0.065	1.152	0.072	0.085	1.5165
Tr-168-x.02	37.43	3.44	17.51	19.33	0.4	5.48	0.18	0.32	8.65	**92.74**	5.8115	2.1885	1.013	0.402	2.51	0.053	1.269	0.03	0.097	1.7135
Tr-168-x.03	35.3	3.21	20.3	17.5	0.41	5.4	0	0.26	7.64	**90.02**	5.5675	2.4325	1.338	0.381	2.309	0.055	1.27	0	0.08	1.5375
Tr-168-x.04	42.7	1.89	23.52	11.74	0.32	4	0.31	0	5.69	**90.17**	6.269	1.731	2.3355	0.209	1.442	0.04	0.876	0.049	0	1.0655
Tr-168-x.05	45.48	0.28	24.22	10.83	0	4	0.18	0	3.87	**88.86**	6.5875	1.4125	2.719	0.031	1.312	0	0.864	0.028	0	0.715
Tr-193-5.05	34.46	2.96	17.85	22.8	0.44	6.82	0.06	0.12	8.99	**94.5**	5.3975	2.6025	0.69	0.349	2.987	0.059	1.593	0.01	0.037	1.7965
Tr-193.01	33.63	2.65	19.09	21.96	0	6.69	0	0.28	9.78	**94.08**	5.2905	2.7095	0.827	0.314	2.889	0	1.569	0	0.086	1.9625
Tr-193.05	34.07	3.26	19.15	22.35	0	6.62	0	0	9.95	**95.4**	5.2855	2.7145	0.784	0.381	2.9	0	1.531	0	0	1.969
Tr-201-1.01	33.41	4.16	17.92	21.87	0.52	6.37	0	0.33	9.76	**94.34**	5.2675	2.7325	0.595	0.494	2.884	0.07	1.497	0	0.101	1.963
Tr-201-1.02	33.71	3.92	18.25	21.93	0.34	6.26	0	0.26	9.58	**94.25**	5.3005	2.6995	0.68	0.464	2.884	0.046	1.468	0	0.08	1.922
Tr-201-1.03	33.86	2.67	19.07	22.47	0.34	6.74	0	0	9.71	**94.86**	5.2915	2.7085	0.801	0.314	2.937	0.045	1.57	0	0	1.936
Tr-201-3.04	34.1	3.81	18.06	22.22	0.44	6.54	0	0	9.88	**95.05**	5.3255	2.6745	0.647	0.448	2.902	0.058	1.523	0	0	1.9685
Tr-205-2-01	34.2	4.16	18.06	22.25	0	6.42	0	0.31	9.64	**95.04**	5.328	2.672	0.6415	0.488	2.899	0	1.491	0	0.094	1.916
Tr-205-2-02	34.49	4.27	17.92	22.15	0.47	6.49	0	0	9.96	**95.75**	5.342	2.658	0.6105	0.498	2.869	0.062	1.499	0	0	1.968

Table 4.2 continued.

Pre-Triassic feldspars

Sample	SiO2	TiO2	Al2O3	FeO	MnO	MgO	CaO	Na2O	K2O	**Total**
Tr-139-3.01	64.19	0	18.62	0	0	0	0	0	17.33	**100.14**
Tr-139-3.02	64	0	18.93	0	0	0	0	1.59	14.96	**99.48**
Tr-139-3.03	63.38	0	18.61	0	0	0	0	1.31	15.15	**98.45**
Tr-139-3.04	63.59	0	18.11	0	0	0	0	0	16.75	**98.45**
Tr-139-3.05	64.66	0	18.93	0	0	0	0	1.42	15.36	**100.37**
Tr-139-3.06	64.46	0	18.45	0	0	0	0	0	16.9	**99.81**
Tr-139-3.07	61.87	0	17.55	0	0	0	0	0.31	16.11	**95.84**
Tr-168-2.03	64.03	0	18.37	0	0	0	0	0.45	16.36	**99.21**
Tr-193-5.01	69.8	0	19.26	0.03	0.009	0	0.26	9.96	0.16	**99.48**
Tr-193-5.08	65.14	0	20.37	0.02	0.02	0	1.59	10.09	0.18	**97.41**
Tr-193-5.11	66.58	0	19.5	0.008	0.02	0	0.51	10.79	0.15	**97.56**
Tr-193.02	63.9	0	18.45	0	0	0	0	0.72	15.35	**98.42**
Tr-193-5.06	63.41	0	18.22	0.04	0.02	0	0.06	1.2	14.12	**97.07**
Tr-193-5.12	63.56	0	18.28	0.05	0.03	0.005	0.08	1	14.29	**97.30**
Tr-193.03	64.67	0	21.37	0	0	0	2.09	9.88	0.27	**98.28**
Tr-193-5.10	59.55	0	23.31	0.04	0.03	0	5.3	7.84	0.26	**96.33**
Tr-201-4.10	62.34	0.01	22.13	0.005	0.01	0.004	3.82	8.83	0.24	**97.39**
Tr-201-4.4	62.32	0.04	17.53	0.03	0.012	0.014	0.085	0.45	15.13	**95.61**
Tr-201-4.1	65.14	0.03	22.26	0.03	0.03	0	3.54	7.24	0.32	**98.59**
Tr-201-4.10	66.79	0.009	19.24	0.005	0	0	0.368	10.62	0.08	**97.11**
Tr-201-4.11	65.74	0	20.45	0.009	0.008	0	1.29	10.18	0.27	**97.95**
Tr-201-4.2	59.33	0.01	24.14	0.02	0.005	0	6.27	7.5	0.22	**97.50**
Tr-201-4.3	63.2	0.02	21.91	0.01	0	0	4.17	9.11	0.24	**98.66**
Tr-201-4.5	61.04	0.02	22.74	0.03	0.006	0	4.63	8.38	0.18	**97.03**
Tr-201-4.7	59.23	0.02	23.91	0.05	0.01	0	6.19	7.56	0.32	**97.29**
Tr-201-4.8	60.51	0.03	23.38	0.01	0.004	0	5.42	7.97	0.18	**97.50**
Tr-201-4.9	62.34	0.01	22.13	0.005	0.01	0.004	3.82	8.83	0.24	**97.39**

Pre-Triassic kaolinite

Sample	SiO2	TiO2	Al2O3	FeO	MnO	MgO	CaO	Na2O	K2O	**Total**
Tr-110-1a.02	43.98	0	28.65	7.74	0	1.99	0.28	0	2.19	**84.83**
Tr-110-a.02	43.95	0	30.44	5.53	0	1.73	0.18	0	1.43	**83.26**
Tr-110-x-01	42.72	0	30.45	6.07	0	1.56	0.26	0	1.37	**82.43**
Tr-139-1.05	41.83	0	27.36	0.33	0	1.18	1.17	0	1.36	**73.23**
Tr-193-5.09	53.2	0	22.62	0.42	0.01	2.68	2.26	0.07	0.51	**81.77**
Tr-201-4.13	50.93	0.01	31.21	0.91	0.02	1.73	0.86	0.13	2.21	**88.01**
Tr-201-4.6	55.93	0.02	23.3	0.81	0.004	3.42	1.87	0.62	2.62	**88.59**

Pre-Triassic Muscovite / illite

Sample	SiO2	TiO2	Al2O3	FeO	MnO	MgO	CaO	Na2O	K2O	**Total**
Tr-139-1.04	45.56	0	36.76	0.6	0	0.32	0	0.27	5.42	**88.93**
Tr-168-2.04	46.21	0	37.14	0.46	0	0	0	0	10.14	**93.95**
Tr-193-5.07	46.55	0.31	34.83	1.45	0.04	0.69	0.002	0.53	9.6	**94.00**
Tr-193-5.13	47.23	0.05	34.52	1.65	0.06	0.88	0.01	0.39	9.67	**94.46**
Tr-193-5.14	46.42	0.29	34.4	1.42	0.02	0.7	0.007	0.54	9.4	**93.20**
Tr-201-4.12	47.14	0.05	36.43	0.12	0.02	0.06	0.12	0.11	9.35	**93.40**

At the base of the weathered profile, the original mineralogy remains relatively unchanged from the parent monzogranite; the development of fractures along grain boundaries and through individual grains marks the onset of the weathering process. Moving upwards in the section (2 metres from weathering front), the plagioclase loses its identity as clay minerals replace the original feldspar, resulting in a dark, dusty appearance to the thin section, and in the plagioclase grains in particular. Alkali feldspar is essentially unaffected at this stage of development. Fracture quantity and intensity increases, resulting in the formation of "sub-grains" of altered plagioclase, and minor alteration along the fractures in biotites (Fig. 4.5A, C). Weathering at this level is still dominated by fracturing, as well as by the alteration of plagioclase. Ten metres up from the weathering front, fracturing is ubiquitous, the secondary mineralogy is extensively developed, and although both K-feldspar and minor plagioclase are found in the clay-sized fraction, only the K-feldspar is recognisable in thin section (Fig. 4.5H); XRD data indicate that the feldspar (plagioclase) at this level is extensively altered to kaolinite and smectite (Fig. 4.6A, sample 168).

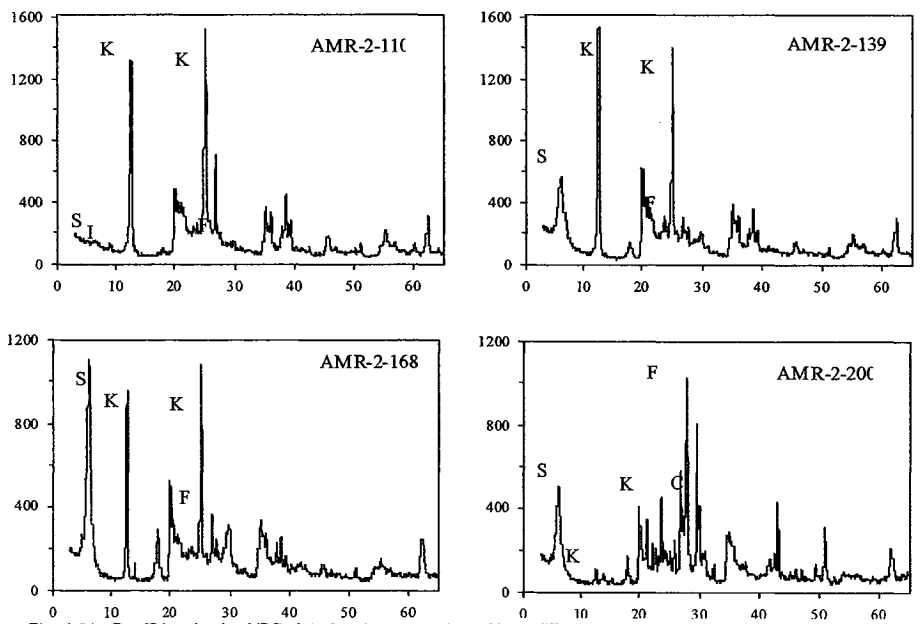

Fig. 4.6A. Pre-Triassic clay XRD data for clay seperates. X-ray diffractograms of the clay mineral separates (see Table 4.3 for changes after saturation with ethylene glycol, and heating). Observe the difference in scale. Abbreviations: C = calcite, F = feldspar, I = illite, K = kaolinite, and S = smectite.

At this level in the weathering profile, XRD patterns of biotite separates indicate that biotite dominates, with trace development of kaolinite, and the dominant impact of weathering on the biotite appears to be to break it into smaller grains (Fig. 4.5H and 4.6B)

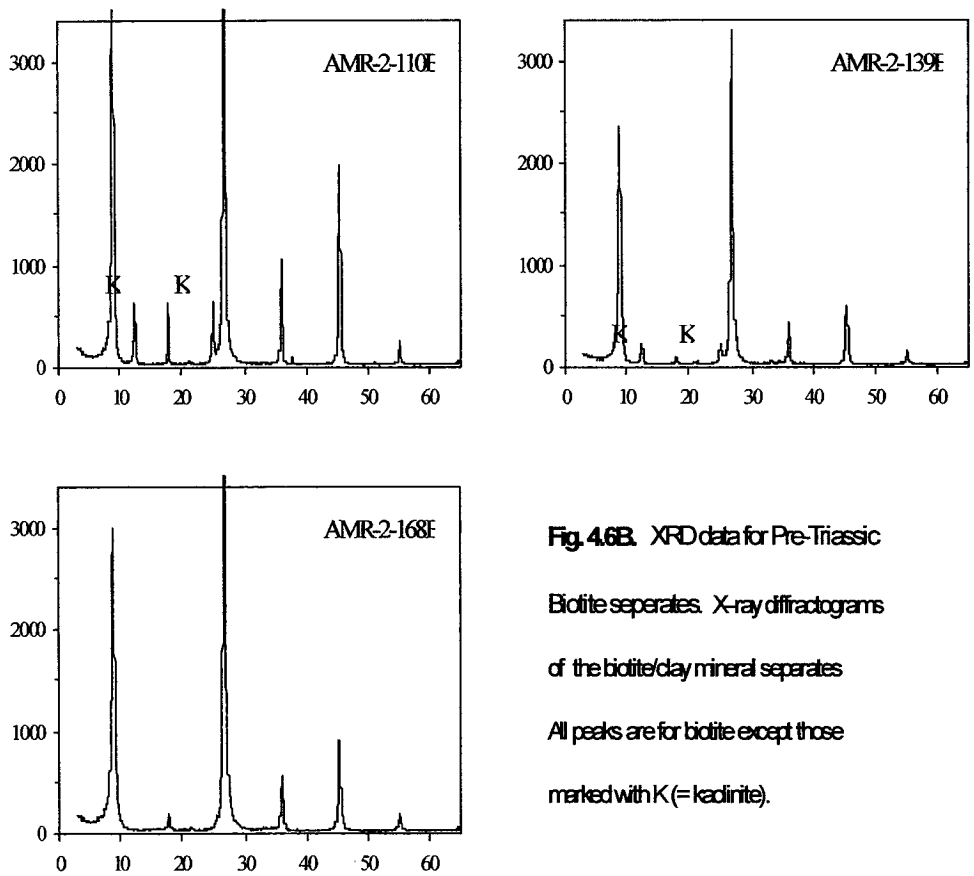

Fig. 4.6B. XRD data for Pre-Triassic Biotite seperates. X-ray diffractograms of the biotite/clay mineral separates All peaks are for biotite except those marked with K (= kaolinite).

However, microprobe analysis of biotites, even in these deeper levels of the weathered profile, suggest that the breakdown of biotite is more complex than simply biotite with minor kaolinite, as suggested by XRD analysis; chemical analysis of these weakly weathered biotites indicates that weathering resulted in the development of

interlayers of a K-poor hydrated phase (vermiculite / smectite) (Fig. 4.5B, H) and "fresh" biotite. De la Calle and Suquet (1988) discuss the compositional continuum of biotite through vermiculite through smectite, and note that high-charge smectites are essentially similar to vermiculites, as also noted by Velde (1995). The chemical (and hence mineralogical) changes that occur as a result of this incipient weathering of the biotite, result in a loss of K, Fe, Ti and tetrahedral Al, with a concomitant increase in Si (Fi 4.7 A-C). These interlayers of weathered "biotite" form parallel to the cleavage traces. This transformation is accompanied by fanning of the edges of the biotite (Fig. 4.5B, H), and minor volume increase. Lobes of kaolinite within the biotite (Fig. 4.5B) suggest that although some of the material to form the kaolinite may have come from the breakdown of biotite, it is not an atom-for-atom replacement of biotite by kaolinite, and is more typical of edge weathering effects, where wedging of the biotite along cleavages has allowed for the in-migration of allochthonous material (Bisdom et a., 1982). Associated with this interlayer weathering is the release of some of the Ti and Fe from the biotites, resulting in the development of Fe-oxides/oxyhydroxides, and Ti-oxides, typically aligned along the cleavages or grain boundaries, similar to those seen in Fig. 4.5F.

Approximately 20 m up from the weathering front (sample # 139) fractures are wider, although a number are also infilled with broken primary grains and secondary minerals such as kaolinite and Fe-oxyhydroxides. No plagioclase remains even in the fine fraction, although pseudomorphs of plagioclase, now replaced by clay minerals, are evident. At this level XRD data indicated that the proportion of kaolinite in the fine, felsic fraction (feldspar-clay fraction, biotite removed) is greater than the proportion of smectite (Fig. 4.6A). Alkali feldspar and biotite are still present, although grain size has diminished, particularly in the biotite, and fanning in altered biotite is commonly developed (Fig. 4.5D and E). The biotites *sensu stricto* have a 10-20% reduction in absolute K_2O content relative to the "fresh" parent biotites, reflected also in their lower totals, presumably as a result of increased amounts of H_2O present (Table 4.2, Fig.4 7B and C). Clouding in the K-feldspar is noticeable, and kaolinite can be found along fractures within the K-feldspar. XRD analysis of biotites from this level identifies the phases present as biotite, minor kaolinite, and minor hematite (Fig. 4.6B).

Fig. 4.7. Chemistry of weathering biotite from Pre-Triassic saprolite, as reflected in:
(A) K_2O versus SiO_2,
(B) FeO+MgO+MnO versus Al_2O_3, and
(C) Si - (Al^{IV} +Al^{VI}) - (Ca+Na+K)

Dark brown is unweathered biotite from less weathered samples (#s 205, 201, 193);
Pink is weathered biotite from sample 168;
Dark orange is weathered biotite from sample 139;
Pale orange is weathered biotite from sample 110.

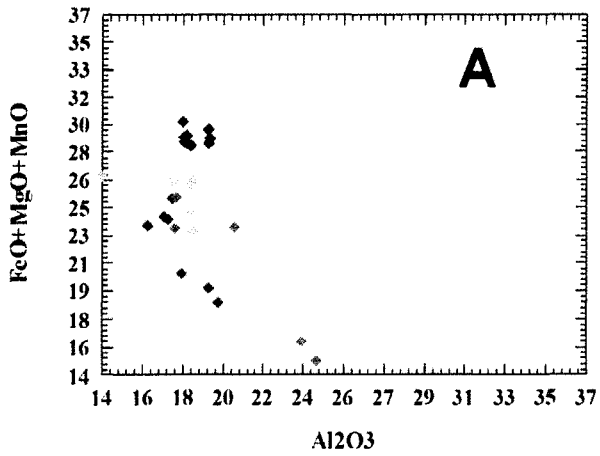

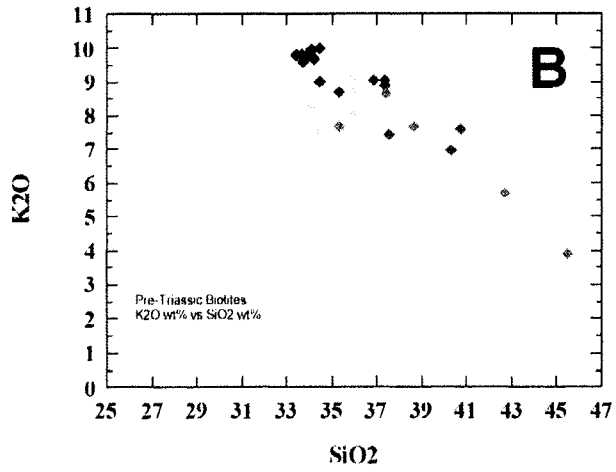

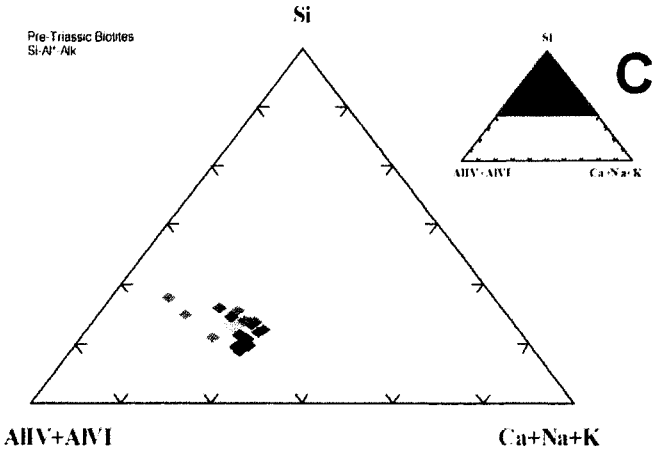

(Diagram modified after Jolicoeur et al., 2000)

As in the samples from deeper in the profile, X-ray mapping and backscatter images from the microprobe indicate a complex biotite weathering pattern (Fig. 4.5D and E and Fig 4.7; Table 4.2). From these images, it is estimated that typically more than 50% of the original biotite remains in any one original grain (Fig. 4.5E); the remaining component is a mix of vermiculite/smectite-like composition and kaolinite. Fe and Ti oxides/hydroxides commonly occupy many of the cleavage traces, fractures, and grain boundaries of these developing mesomorphs (Fig. 4.5E).

In the uppermost part of the preserved weathering profile, fracturing and mineralogical changes are most intense. XRD analysis indicates that the fine felsic fraction is dominated by kaolinite with minor illite (?) and only trace quantities of smectite (Fig. 4.6A). K-feldspar, quartz and biotite persist, although grains are commonly broken and fractured, and the proportion of unaltered K-feldspar and biotite is reduced (Fig. 4.5G). Textures at this level assume a plasma-like appearance (Fig. 4.5G) (Delvigne, 1998). X-ray diffraction analysis of biotite separates from this level indicate the presence of biotite with minor kaolinite, although as with the sample from 20 m above the weathering front, microprobe backscatter images and x-ray maps portray a complex picture of weathering (Fig. 4.5F; Table 4.2). Systematic changes in the biotites from the fresh part of the grain to the more altered portion of the biotite include: the loss of interlayer K, octahedral Fe^{2+}, and tetrahedral Al; increase in Si, increase in octahedral Al, and an assumed increase in hydration (Fig. 4.7A-C, Table 4.2).

In summary, the key systematic mineralogical and textural changes observed from fresh to most weathered sample within the Pre-Triassic section are as follows: (a) An increase in number and width of fractures, initially concentrated along boundaries, but moving up through the section, the number and width of fractures within grains also increases; (b) Intense weathering of plagioclase to a mixture of smectite and kaolinite, resulting in the absence of plagioclase in the top half of the preserved section; (c) Incipient chemical weathering of K-feldspar to kaolinite, increasing in intensity and amount towards the top of the profile, and physical break-up of crystals towards the top of section (although some K-feldspar remains, even in the uppermost level); (d) incipient complex weathering of biotite, although some little-altered biotite remains even in most weathered levels. This complex weathering is accompanied by the development of Ti

oxides as well as Fe oxides and oxyhydroxides along cleavages and grain boundaries, the fanning of biotite grain boundaries, the bending of grains, and the break up of larger crystals into smaller grains which may or may not have the same orientation; and (e) Clay composition as identified by XRD changes from smectite-dominant to kaolinite-dominant. A summary diagram of these changes is given in Appendix A2.

4.5.3 Pre-Pleistocene Weathering Profile

Pre-Pleistocene weathering produced an arenaceous loose material, with minimal clay mineral development. Mineralogical and micromorphological changes in profiles of this age are much less intense than in either the Pre-Carboniferous or the Pre-Triassic profiles, although only the fresh and mildly weathered samples were observed petrographically; the weathered loose material was not mounted for petrographic study, because of its disaggregated nature. Observed changes reflect the incipient nature of the chemical weathering, and provide us with a window on the onset of chemical weathering processes in these rocks sometime between the Early Jurassic and the Pleistocene glaciation (O'Beirne-Ryan and Zentilli, 2003). The profiles from which fine material was most readily available for XRD analysis included two profiles from two different monzogranites of similar chemical composition, and two profiles from monzonites of different composition. X-ray diffraction of the fine materials from the profiles examined are dominated by feldspars and quartz, with minor biotite and illite, and trace amounts of chlorite, kaolinite, and possibly vermiculite. One of the monzonites (Forest Home) also had trace amounts of phrenite present, and no apparent vermiculite (Levi, pers.com. 2001), but otherwise, the mineralogy of the fine material as recorded by XRD analysis, was similar for all four profiles. Smectites were not detected in any of the profiles. Petrographic examination of the thin sections would suggest that it is likely that the chlorite and illite/muscovite in these samples represent a pre-weathering late-stage alteration, and thus are not necessarily indicative of a weathering mineralogy. Kaolinite and vermiculite (where present) represent the secondary mineralogy formed at the early stages of weathering of these rocks. Microprobe analysis confirms the minimal alteration of the feldspars and biotite, with only small patches of kaolinite developed, or incipient

widening of cleavages within the biotite and minor breakdown to vermiculite - smectite (Fig. 4.8 Table 4.3). Figure 4.8A is an SEM image of biotite weathering, clearly showing the development of K-poor layers ("sme") and lenses of kaolinite. Weathering of the biotite in this sample is dominated by edge weathering, with variable thicknesses of kaolinite-rich lenses developed. However, the "smectite"-rich layer is of reasonably uniform thickness throughout, as is typical of layer weathering.

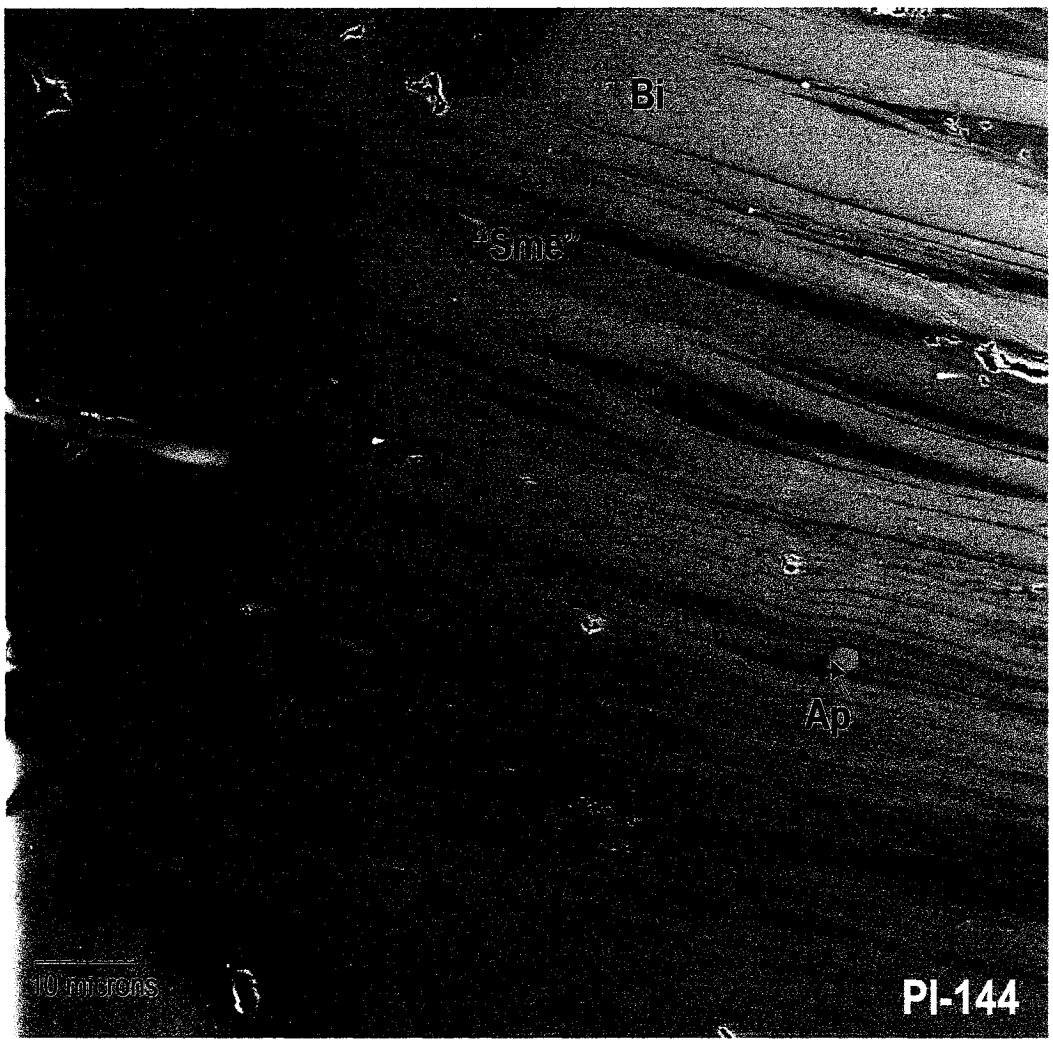

Figure4.8A: Biotite (SEM) weathering to "smectite" and kaolinite. Note how the fracture goes around the inclusion of apatite (Ap) in the centre of the grain. Note also the slight fanning along the biotite grain edge, where kaolinite is more prevalent.

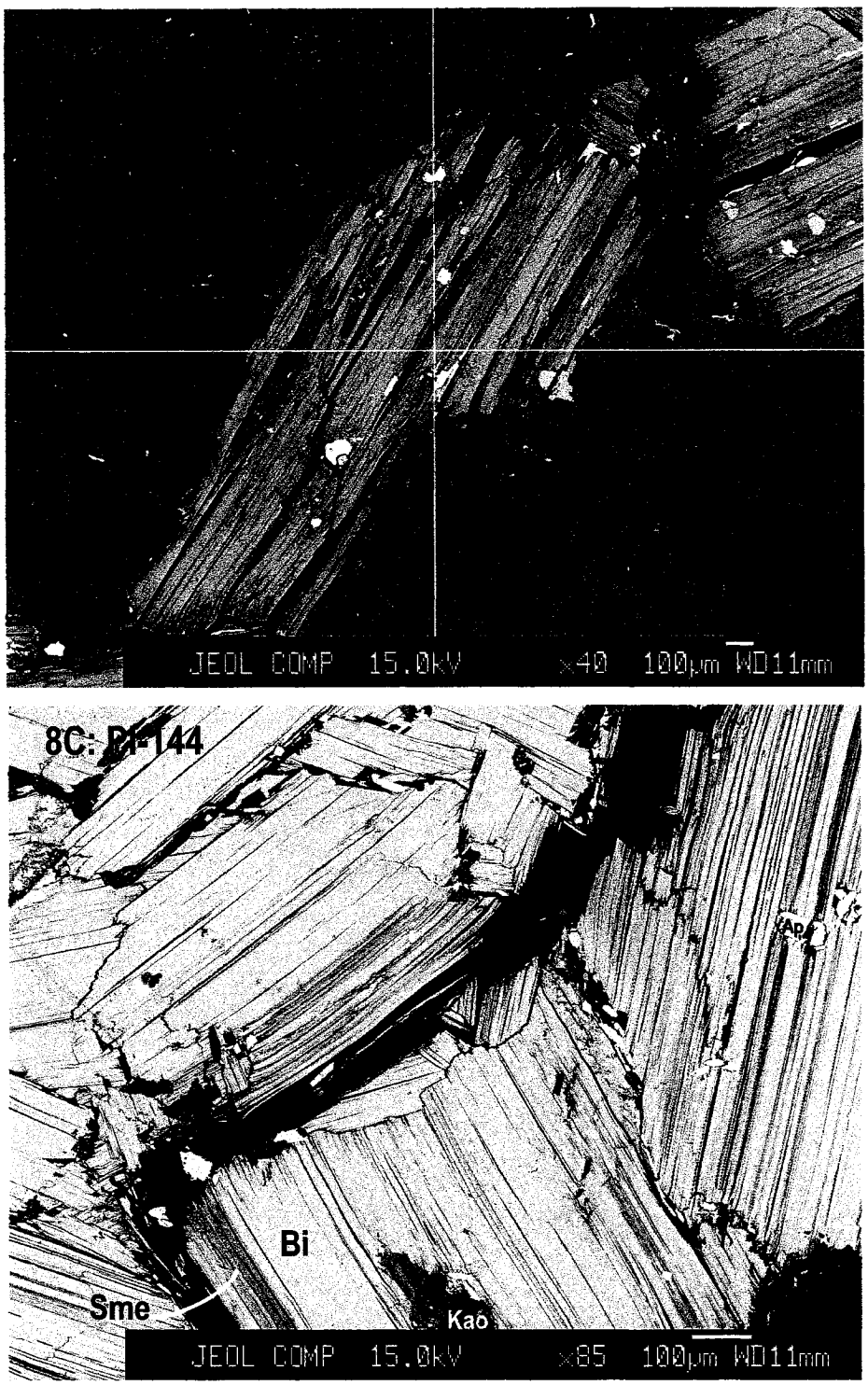

Fig. 4.8 (B and C). (B) Backscatter image of biotite surrounded by felspars in Pre-Pleistocene weathered monzonite. Dominant weathering features include "strings" of kaolinite in the biotite (darker grey, along cleavages), and weathering-induced microfractures. (C) Biotite with incipient weathering to "smectite" and weathering-induced fractures in weathered biotite monogranite.

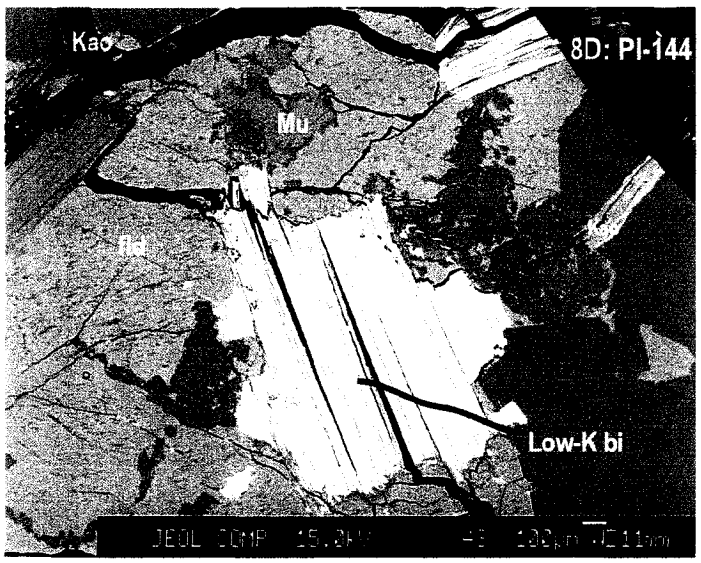

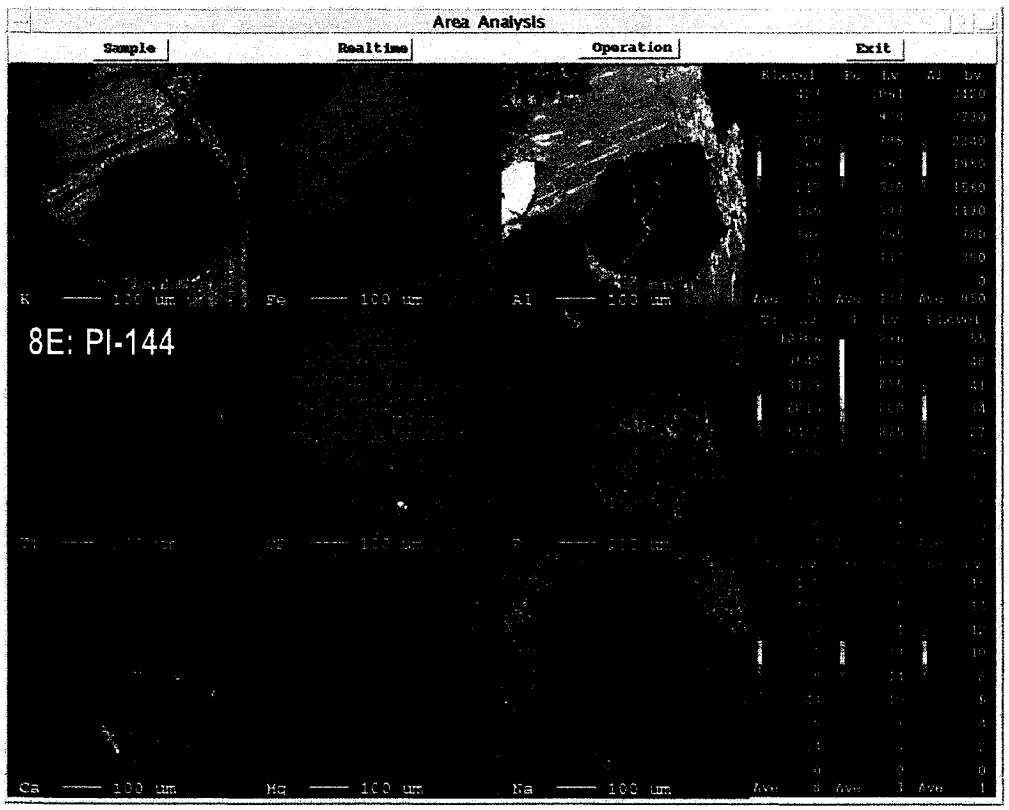

Fig. 4.8 (D and E). (D) Incipient weathering of biotite from weathered biotite monzogranite beneath Pleistocene till. Biotite is weathered to a Low K-biotite (Low-K bi), with some kaolinite (Kao) developed along fractures through the grains. Primary feldspar (fld), quartz (Qtz) and muscovite (Mus) are also present. (E) X-ray map of incipiently-weathered biotite from weathered monzogranite, with apatite grain. Weathering in the biotite is most noticeable along the grain margins.

Table 4.3. PRE-PLEISTOCENE mineral analyses from microprobe

Biotites and weathered biotites

Sample	SiO2	TiO2	Al2O3	FeO	MnO	MgO	CaO	Na2O	K2O	**Total**	Si	AlIV	AlVI	Ti	Fe2	Mn	Mg	Ca	Na	K	O
amr-132-01	35.87	2.62	20.77	23.60	0.51	4.49	0.00	0.10	9.83	**97.79**	5.42	2.58	1.11	0.30	2.98	0.07	1.01	0.00	0.03	1.89	22
amr-132-03	35.77	2.73	20.74	22.47	0.46	4.60	0.01	0.14	9.60	**96.52**	5.44	2.56	1.16	0.31	2.86	0.06	1.04	0.00	0.04	1.86	22
amr-132-04	37.04	1.13	24.68	19.12	0.18	2.54	0.39	0.07	4.12	**89.27**	5.72	2.28	2.21	0.13	2.47	0.02	0.59	0.07	0.02	0.81	22
amr-132-05	26.19	13.61	17.55	18.19	0.17	2.42	0.41	0.13	2.64	**81.31**	4.61	3.39	0.24	1.80	2.68	0.03	0.63	0.08	0.04	0.59	22
amr-132-bi-13	34.61	2.78	19.58	21.17	0.47	4.30	0.01	0.13	9.64	**92.688**	5.49	2.52	1.14	0.33	2.81	0.06	1.02	0.00	0.04	1.95	22
amr-132-bi-15	33.40	2.58	18.93	21.99	0.47	4.29	0.00	0.09	9.49	**91.24**	5.42	2.58	1.04	0.32	2.99	0.07	1.04	0.00	0.03	1.97	22
amr-132-bi-20	35.26	3.02	18.49	21.28	0.34	4.98	0.02	0.10	9.63	**93.12**	5.56	2.44	0.99	0.36	2.81	0.05	1.17	0.00	0.03	1.94	22
amr-132-bi-25	36.48	3.23	17.93	20.29	0.35	5.24	0.02	0.07	9.68	**93.29**	5.70	2.30	1.00	0.38	2.65	0.05	1.22	0.00	0.02	1.93	22
amr-132-Bi102	35.26	3.01	18.49	21.28	0.34	4.98	0.02	0.10	9.63	**93.11**	5.56	2.44	0.99	0.36	2.81	0.05	1.17	0.00	0.03	1.94	22
amr-132-Bi107	36.48	3.22	17.93	20.29	0.35	5.24	0.02	0.07	9.68	**93.28**	5.70	2.30	1.00	0.38	2.65	0.05	1.22	0.00	0.02	1.93	22
amr-132-Bi82	34.47	3.54	17.93	21.09	0.33	6.35	0.00	0.13	9.52	**93.362**	5.43	2.57	0.76	0.42	2.78	0.04	1.49	0.00	0.04	1.92	22
amr-132-Bi83	34.95	2.91	19.41	21.91	0.43	4.20	0.00	0.09	9.63	**93.53**	5.50	2.50	1.10	0.35	2.88	0.06	0.99	0.00	0.03	1.93	22
amr-132-Bi95	34.61	2.78	19.58	21.17	0.47	4.30	0.01	0.13	9.64	**92.688**	5.49	2.52	1.14	0.33	2.81	0.06	1.02	0.00	0.04	1.95	22
amr-144-5.01	35.06	3.43	18.08	21.02	0.27	6.58	0.00	0.13	9.51	**94.08**	5.47	2.53	0.79	0.40	2.74	0.04	1.53	0.00	0.04	1.89	22
amr-144-5.02	34.65	3.34	19.12	17.12	0.18	6.19	0.11	0.02	5.95	**86.68**	5.62	2.39	1.26	0.41	2.32	0.03	1.50	0.02	0.01	1.23	22
amr-144-5.03	34.68	3.40	19.88	16.57	0.22	6.14	0.14	0.03	5.23	**86.29**	5.60	2.40	1.37	0.41	2.24	0.03	1.48	0.02	0.01	1.08	22
amr-144-5.04	34.83	3.40	17.94	20.21	0.28	6.53	0.00	0.13	9.43	**92.75**	5.49	2.51	0.82	0.40	2.67	0.04	1.54	0.00	0.04	1.90	22
amr-144-5.06	34.16	3.36	19.92	16.38	0.18	6.18	0.25	0.00	4.35	**84.784**	5.58	2.42	1.41	0.41	2.24	0.03	1.51	0.04	0.00	0.91	22
amr-144-5.07	34.47	3.54	17.93	21.09	0.33	6.35	0.00	0.13	9.52	**93.362**	5.43	2.57	0.76	0.42	2.78	0.04	1.49	0.00	0.04	1.92	22
amr-144-Bi01	34.21	3.59	18.07	22.65	0.33	6.68	0.02	0.16	9.41	**95.12**	5.33	2.67	0.65	0.42	2.95	0.04	1.55	0.00	0.05	1.87	22
amr-144-Bi02	35.05	3.98	18.28	22.29	0.33	6.47	0.02	0.18	9.74	**96.34**	5.38	2.62	0.68	0.46	2.86	0.04	1.48	0.00	0.05	1.91	22
amr-144-Bi03	34.79	3.87	18.01	22.55	0.34	6.51	0.00	0.18	9.55	**95.803**	5.38	2.62	0.65	0.45	2.91	0.05	1.50	0.00	0.05	1.88	22
amr-144-Bi04	34.53	3.80	18.20	20.48	0.28	6.02	0.06	0.05	8.37	**91.79**	5.48	2.53	0.87	0.45	2.72	0.04	1.42	0.01	0.02	1.69	22
amr-144-Bi05	35.31	3.80	18.40	19.03	0.29	6.26	0.05	0.05	8.84	**92.03**	5.55	2.46	0.95	0.45	2.50	0.04	1.47	0.01	0.02	1.77	22
amr-144-Bi06	34.60	4.22	17.92	23.02	0.36	6.28	0.00	0.15	9.59	**96.14**	5.35	2.66	0.61	0.49	2.97	0.05	1.45	0.00	0.05	1.89	22
amr-144-Bi07	34.78	3.75	18.00	23.09	0.34	6.56	0.00	0.17	9.50	**96.19**	5.37	2.64	0.64	0.44	2.98	0.04	1.51	0.00	0.05	1.87	22
amr-144-Bi12	34.96	3.67	18.19	22.95	0.32	6.61	0.00	0.13	9.51	**96.34**	5.37	2.63	0.67	0.42	2.95	0.04	1.52	0.00	0.04	1.87	22
amr-144-Bi13	34.68	3.38	18.35	22.27	0.28	6.72	0.00	0.14	9.51	**95.33**	5.37	2.63	0.72	0.39	2.89	0.04	1.55	0.00	0.04	1.88	22
amr-144-Bi14	33.56	3.09	19.08	19.76	0.18	6.31	0.04	0.01	5.97	**87.995**	5.45	2.55	1.10	0.38	2.68	0.03	1.53	0.01	0.00	1.24	22
amr-144-Bi15	34.27	2.80	20.18	18.23	0.17	6.44	0.11	0.00	5.08	**87.282**	5.51	2.49	1.33	0.34	2.45	0.02	1.54	0.02	0.00	1.04	22
amr-144-Bi30	33.55	2.96	18.31	21.11	0.06	6.29	0.00	0.00	7.43	**89.71**	5.44	2.56	0.93	0.36	2.86	0.01	1.52	0.00	0.00	1.54	22
amr-144-Bi31	32.12	2.83	19.14	19.86	0.00	5.90	0.06	0.00	4.56	**84.47**	5.41	2.59	1.20	0.36	2.80	0.00	1.48	0.01	0.00	0.98	22
amr-144-Bi32	34.53	3.32	18.47	18.82	0.05	6.28	0.00	0.00	8.18	**89.65**	5.54	2.46	1.03	0.40	2.53	0.01	1.50	0.00	0.00	1.68	22
amr-144-Bi33	34.11	3.15	19.65	17.48	0.00	6.17	0.08	0.00	5.59	**86.23**	5.55	2.45	1.32	0.39	2.38	0.00	1.50	0.01	0.00	1.16	22
amr-144-Bi34	34.03	2.97	20.13	17.09	0.02	6.29	0.06	0.00	5.20	**85.79**	5.54	2.46	1.40	0.36	2.33	0.00	1.53	0.01	0.00	1.08	22
amr-144-Bi45	34.23	3.66	18.31	21.16	0.37	6.28	0.03	0.15	9.57	**93.76**	5.38	2.62	0.77	0.43	2.78	0.05	1.47	0.01	0.05	1.92	22
amr-144-Bi49	34.41	4.06	18.26	20.63	0.36	6.37	0.04	0.14	9.68	**93.95**	5.38	2.62	0.75	0.48	2.70	0.05	1.49	0.01	0.04	1.93	22
amr-144-Bi50	34.37	3.62	18.31	20.76	0.30	6.52	0.03	0.13	9.53	**93.57**	5.40	2.60	0.78	0.43	2.73	0.04	1.53	0.01	0.04	1.91	22
amr-144-Bi54	34.05	3.33	18.42	20.80	0.33	6.49	0.06	0.11	9.72	**93.31**	5.37	2.63	0.80	0.40	2.75	0.04	1.53	0.01	0.03	1.96	22
amr-144-Bi56	31.68	3.11	18.52	17.75	0.26	7.32	0.06	0.28	8.70	**87.68**	5.25	2.75	0.87	0.39	2.46	0.04	1.81	0.01	0.09	1.84	22
amr-144-Bi57	32.61	3.20	18.87	18.40	0.26	7.38	0.04	0.24	7.55	**88.55**	5.31	2.69	0.93	0.39	2.51	0.04	1.79	0.01	0.08	1.57	22
amr-144-Bi58	33.50	3.65	17.79	21.18	0.30	6.47	0.00	0.15	9.48	**92.52**	5.35	2.65	0.70	0.44	2.83	0.04	1.54	0.00	0.05	1.93	22
amr-144-Bi59	34.92	3.42	18.23	21.21	0.31	6.59	0.00	0.15	9.80	**94.63**	5.43	2.57	0.77	0.40	2.76	0.04	1.53	0.00	0.05	1.95	22
amr-144-Bi60	33.40	3.48	21.79	15.57	0.26	6.25	0.36	0.02	1.36	**82.49**	5.47	2.53	1.67	0.43	2.13	0.04	1.53	0.06	0.01	0.28	22
amr-144-Bi61	33.09	3.38	21.54	15.27	0.13	6.00	0.38	0.01	1.48	**81.28**	5.49	2.51	1.70	0.42	2.12	0.02	1.49	0.07	0.00	0.31	22
amr-144-Bi76	35.06	3.43	18.08	21.02	0.27	6.58	0.00	0.13	9.51	**94.08**	5.47	2.53	0.79	0.40	2.74	0.04	1.53	0.00	0.04	1.89	22
amr-144-Bi77	34.65	3.34	19.12	17.12	0.18	6.19	0.11	0.02	5.95	**86.68**	5.62	2.39	1.26	0.41	2.32	0.03	1.50	0.02	0.01	1.23	22
amr-144-Bi78	34.68	3.40	19.88	16.57	0.22	6.14	0.14	0.02	5.23	**86.28**	5.60	2.40	1.37	0.41	2.24	0.03	1.48	0.02	0.01	1.08	22
amr-144-Bi79	34.83	3.40	17.94	20.21	0.28	6.53	0.00	0.13	9.43	**92.75**	5.49	2.51	0.82	0.40	2.67	0.04	1.54	0.00	0.04	1.90	22
amr-144-Bi80	33.02	3.00	22.08	14.96	0.17	6.25	0.81	0.00	0.06	**80.352**	5.48	2.52	1.80	0.38	2.08	0.02	1.55	0.14	0.00	0.01	22
amr-144-Bi81	34.16	3.36	19.92	16.38	0.18	6.18	0.25	0.00	4.35	**84.784**	5.58	2.42	1.41	0.41	2.24	0.03	1.51	0.04	0.00	0.91	22

Table 4.3 continued.

Kaolinite - Pre-Pleistocene

Sample	SiO2	Al2O3	FeO**	MgO	CaO	Na2O	K2O	**Total**	Si	AlIV	AlVI	Fe2	Mg	Ca	Na	K	O
amr-132-bi-10	46.04	32.85	4.15	0.28	0.02	0.11	0.79	**84.24**									
amr-132-bi-11	46.56	32.10	3.94	0.42	0.06	0.11	0.90	**84.09**	8.13	0.00	6.60	0.58	0.11	0.01	0.04	0.20	28
amr-132-Bi92	46.04	32.85	4.15	0.28	0.02	0.11	0.79	**84.24**	8.04	0.00	6.75	0.61	0.07	0.00	0.04	0.18	28
amr-132-Bi93	46.56	32.10	3.94	0.42	0.06	0.11	0.90	**84.09**	8.13	0.00	6.60	0.58	0.11	0.01	0.04	0.20	28
amr-144-Bi26	46.85	31.27	3.95	0.91	0.10	0.03	0.69	**83.80**	8.20	0.00	6.45	0.58	0.24	0.02	0.01	0.15	28
amr-144-Bi35	45.87	33.70	2.56	0.37	0.00	0.00	0.24	**82.74**	8.03	0.00	6.95	0.38	0.10	0.00	0.00	0.05	28
amr-144-Bi36	45.16	31.71	4.17	0.49	0.00	0.00	0.40	**81.93**	8.08	0.00	6.68	0.62	0.13	0.00	0.00	0.09	28
amr-144-Bi70	45.30	35.95	0.10	0.09	0.00	0.02	0.47	**81.93**	7.91	0.09	7.30	0.02	0.02	0.00	0.01	0.11	28
amr-144-Bi71	45.96	36.17	0.00	0.04	0.00	0.00	0.00	**82.17**	7.96	0.04	7.33	0.00	0.01	0.00	0.00	0.00	28
amr-144-Bi72	46.33	36.14	0.04	0.07	0.00	0.03	0.23	**82.84**	7.97	0.03	7.30	0.01	0.02	0.00	0.01	0.05	28

Muscovite - Pre-Pleistocene data

Sample	SiO2	TiO2	Al2O3	FeO	MgO	CaO	Na2O	K2O	**Total**	Si	AlIV	AlVI	Ti	Fe2	Mg	Ca	Na	K	Cations	O
amr-132-bi-03	45.75	0.20	35.12	1.18	0.52	0.00	0.25	10.44	**93.46**	6.19	1.81	3.79	0.02	0.13	0.11	0.00	0.07	1.80	13.92	22
amr-132-bi-04	46.49	0.52	23.96	6.22	4.07	0.03	0.09	10.06	**91.44**	6.64	1.36	2.67	0.06	0.74	0.87	0.01	0.03	1.83	14.21	22
amr-132-bi-09	46.01	0.66	31.53	2.10	1.23	0.00	0.23	9.84	**91.6**	6.37	1.63	3.51	0.07	0.24	0.25	0.00	0.06	1.74	13.88	22
amr-132-bi-12	45.39	0.51	32.81	1.40	0.79	0.04	0.23	9.72	**90.89**	6.31	1.70	3.67	0.05	0.16	0.16	0.01	0.06	1.72	13.84	22
amr-132-bi-14	45.93	0.48	33.74	1.26	0.76	0.00	0.47	9.75	**92.39**	6.27	1.73	3.70	0.05	0.14	0.16	0.00	0.12	1.70	13.87	22
amr-132-bi-24	46.81	1.69	31.34	2.17	1.33	0.00	0.19	9.66	**93.19**	6.37	1.63	3.39	0.17	0.25	0.27	0.00	0.05	1.68	13.81	22
amr-132-bi-26	45.83	0.96	34.01	1.27	0.66	0.00	0.47	9.93	**93.13**	6.22	1.78	3.66	0.10	0.14	0.13	0.00	0.12	1.72	13.88	22
amr-132-bi-27	48.22	0.95	35.05	1.24	0.71	0.00	0.29	6.33	**92.79**	6.38	1.62	3.84	0.10	0.14	0.14	0.00	0.07	1.07	13.36	22
amr-132-Bi106	46.81	1.09	31.34	2.17	1.33	0.00	0.19	9.66	**92.59**	6.40	1.60	3.45	0.11	0.25	0.27	0.00	0.05	1.69	13.82	22
amr-132-Bi108	45.83	0.95	34.01	1.27	0.66	0.00	0.47	9.93	**93.12**	6.22	1.78	3.66	0.10	0.14	0.13	0.00	0.12	1.72	13.88	22
amr-132-Bi109	48.22	0.95	35.05	1.24	0.71	0.00	0.29	6.33	**92.79**	6.38	1.62	3.84	0.10	0.14	0.14	0.00	0.07	1.07	13.36	22
amr-132-Bi85	45.75	0.20	35.12	1.18	0.52	0.00	0.25	10.44	**93.46**	6.19	1.81	3.79	0.02	0.13	0.11	0.00	0.07	1.80	13.92	22
amr-132-Bi86	46.49	0.52	23.96	6.22	4.07	0.03	0.09	10.06	**91.44**	6.64	1.36	2.67	0.06	0.74	0.87	0.01	0.03	1.83	14.21	22
amr-132-Bi91	46.01	0.66	31.53	2.10	1.23	0.00	0.23	9.84	**91.6**	6.37	1.63	3.51	0.07	0.24	0.25	0.00	0.06	1.74	13.88	22
amr-132-Bi94	45.39	0.51	32.82	1.40	0.79	0.04	0.23	9.72	**90.9**	6.30	1.70	3.67	0.05	0.16	0.16	0.01	0.06	1.72	13.84	22
amr-132-Bi96	45.93	0.48	33.74	1.26	0.76	0.00	0.47	9.75	**92.39**	6.27	1.73	3.70	0.05	0.14	0.16	0.00	0.12	1.70	13.87	22
amr-144-Bi16	45.74	1.38	33.15	2.76	1.13	0.00	0.26	10.34	**94.76**	6.17	1.83	3.44	0.14	0.31	0.23	0.00	0.07	1.78	13.97	22
amr-144-Bi23	46.22	0.82	34.41	1.43	0.62	0.00	0.31	9.81	**93.62**	6.23	1.77	3.69	0.08	0.16	0.13	0.00	0.08	1.69	13.83	22
amr-144-Bi24	45.88	0.40	33.66	1.98	0.77	0.00	0.35	9.37	**92.41**	6.27	1.73	3.69	0.04	0.23	0.16	0.00	0.09	1.63	13.84	22
amr-144-Bi39	45.98	0.76	35.44	0.96	0.63	0.01	0.37	10.56	**94.705**	6.15	1.86	3.72	0.08	0.11	0.13	0.00	0.10	1.80	13.93	22
amr-144-Bi42	44.78	2.06	33.01	1.13	0.58	0.02	0.28	10.06	**91.92**	6.18	1.83	3.54	0.21	0.13	0.12	0.00	0.08	1.77	13.85	22
amr-144-Bi43	45.22	1.08	33.96	1.40	0.52	0.02	0.35	9.90	**92.45**	6.19	1.81	3.66	0.11	0.16	0.11	0.00	0.09	1.73	13.87	22
amr-144-Bi46	45.17	0.94	34.21	1.21	0.49	0.02	0.34	9.77	**92.15**	6.19	1.81	3.71	0.10	0.14	0.10	0.00	0.09	1.71	13.85	22
amr-144-Bi47	44.35	1.49	33.69	0.97	0.44	0.00	0.40	10.16	**91.503**	6.14	1.86	3.64	0.16	0.11	0.09	0.00	0.11	1.80	13.90	22
amr-144-Bi55	47.31	0.42	30.90	0.92	0.42	0.02	0.30	9.00	**89.29**	6.61	1.39	3.70	0.04	0.11	0.09	0.00	0.08	1.61	13.63	22
amr-144-Bi62	45.34	0.81	34.17	1.08	0.55	0.00	0.37	9.89	**92.21**	6.21	1.79	3.72	0.08	0.12	0.11	0.00	0.10	1.73	13.86	22
amr-144-Bi63	45.74	0.56	34.74	0.85	0.47	0.00	0.40	9.96	**92.72**	6.22	1.79	3.77	0.06	0.10	0.10	0.00	0.11	1.73	13.86	22
amr-144-Bi73	45.82	0.21	34.53	1.14	0.57	0.00	0.33	9.76	**92.36**	6.25	1.75	3.79	0.02	0.13	0.12	0.00	0.09	1.70	13.84	22
amr-144-Bi74	45.44	0.19	34.91	1.07	0.47	0.00	0.35	10.28	**92.71**	6.19	1.81	3.80	0.02	0.12	0.10	0.00	0.09	1.79	13.92	22
amr-144-Bi75	48.44	0.21	36.11	0.98	0.47	0.00	0.21	6.26	**92.68**	6.39	1.61	4.00	0.02	0.11	0.09	0.00	0.05	1.05	13.33	22

Table 4.3 continued

Feldspars - Pre-Pleistocene

Sample	SiO2	Al2O3	FeO**	MgO	CaO	Na2O	K2O	**Total**	**Ab**	**An**	**Or**
amr-132-bi-05	63.08	17.65	0.59	0.08	0.00	0.13	16.44	**97.97**	**1.2**	**0.0**	**98.8**
amr-132-bi-18	63.75	17.60	0.40	0.04	0.00	0.13	16.68	**98.60**	**1.2**	**0.0**	**98.8**
amr-132-Bi100	63.77	17.60	0.40	0.04	0.00	0.13	16.68	**98.62**	**1.2**	**0.0**	**98.8**
amr-132-Bi87	63.08	17.65	0.59	0.08	0.00	0.13	16.45	**97.98**	**1.2**	**0.0**	**98.8**
amr-144-Bi65	62.68	17.53	1.13	0.00	0.28	0.13	15.42	**97.17**	**1.2**	**1.5**	**97.3**

Oxides - Pre-Pleistocene

Sample	SiO2	TiO2	Al2O3	FeO	MnO	MgO	**Total**
amr-132-06	0.17	52.53	0.22	25.58	7.32	0.09	**85.91**
amr-132-bi-19	3.72	10.39	1.59	70.02	0.17	0.10	**85.99**
amr-132-bi-21	3.79	1.54	1.59	75.00	0.20	0.10	**82.22**
amr-132-bi-22	4.13	4.64	1.66	70.91	0.25	0.03	**81.62**
amr-132-bi-23	2.53	72.09	1.12	15.11	0.09	0.17	**91.11**
amr-132-Bi101	3.72	10.09	1.59	70.02	0.17	0.10	**85.69**
amr-132-Bi103	3.79	1.54	1.59	75.00	0.20	0.10	**82.22**
amr-132-Bi104	4.13	4.84	1.66	70.91	0.25	0.03	**81.82**
amr-132-Bi105	2.53	72.10	1.12	15.11	0.09	0.17	**91.12**
amr-144-Bi19	0.37	57.67	0.30	31.84	0.61	0.01	**90.8**
amr-144-Bi20	0.28	94.69	0.17	2.91	0.04	0.04	**98.13**
amr-144-Bi21	0.23	96.38	0.15	1.09	0.04	0.00	**97.89**
amr-144-Bi22	0.83	55.88	0.99	28.86	0.90	0.00	**87.46**
amr-144-Bi28	0.00	57.74	0.00	30.23	2.21	0.00	**90.18**
amr-144-Bi29	0.25	77.58	0.07	15.24	0.18	0.00	**93.32**
amr-144-Bi40	0.58	63.33	0.29	23.29	0.65	0.00	**88.14**
amr-144-Bi44	0.27	58.27	0.26	28.38	0.45	0.00	**87.63**
amr-144-Bi66	0.66	63.71	0.32	22.14	0.54	0.01	**87.38**
amr-144-Bi67	0.26	63.09	0.20	23.71	0.48	0.01	**87.75**

In part, the differences between these two weathering products reflects the retention of the biotite structure by the "smectite", and the different structure of the kaolinite; in contrast to the kaolinite lobe developed in the biotite in Figure 4.8C, the kaolinite within the biotite in Figure 4.8A more likely represents development directly from the biotite itself, and not from material migrating in from outside the biotite grain. However, most of the biotite weathering in this sample is dominated by the development of smectite-vermiculite rather than by kaolinite (Fig. 4.8A, C, D). The propagation of a fracture through the section, demonstrates the interplay of physical and chemical weathering, even on the scale of 10 - 100 μm. Propagation of a fracture through the biotite along cleavage and around an apatite grain (Fig. 4.8A), continues through the adjacent feldspar. Fanning along the biotite grain boundary allowed for widening of the fracture and its continuation into the feldspar, suggesting the critical contribution of biotite breakup to the disaggregation of the rock as a whole.

Data from biotites and their alteration products are plotted in Fig. 4.9A-C. Although not as dramatic as the changes in the more intensely weathered Pre-Carboniferous and Pre-Pleistocene profiles, these data indicate that a trend towards a decrease in K is accompanied by a decrease in Fe2+, tetrahedral Al, and Ti, and an increase in octahedral Al, as well as an assumed increase in hydration (based on low totals). The liberated Ti and Fe remain locally within the system as oxides and oxyhydroxides, similar to that observed in the Pre-Triassic profile.

4.6 Discussion

4.6.1 Weathering intensity, environment, and age

Both the Pre-Carboniferous and the Pre-Triassic profiles are preserved beneath unweathered strata of Carboniferous and Triassic age respectively, and thus preserve an original record of weathering during these times. The existence in the region of weathered basalts of post-Early Jurassic age (O'Beirne-Ryan and Zentilli, 2003) is testimony to a post-Early Jurassic period of weathering.

Fig. 4.9. Chemistry of weathering biotite from Pre-Pleistocene saprolite, as reflected in:
(A) K_2O versus SiO_2,
(B) FeO+MgO+MnO versus Al_2O_3, and
(C) Si - (Al^{IV} +Al^{VI}) - (Ca+Na+K)

Dark blue is unweathered biotite from monzogranite (#144); pale blue is weathered biotite from monzogranite (#144); turquoise is unweathered biotite from monzonite (#132).

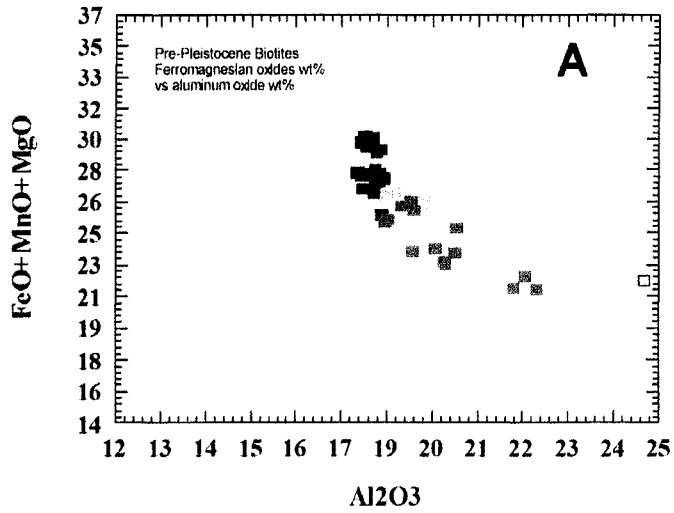

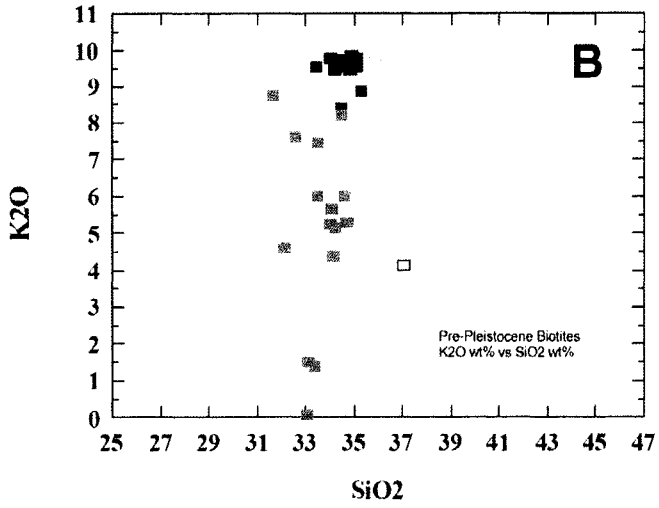

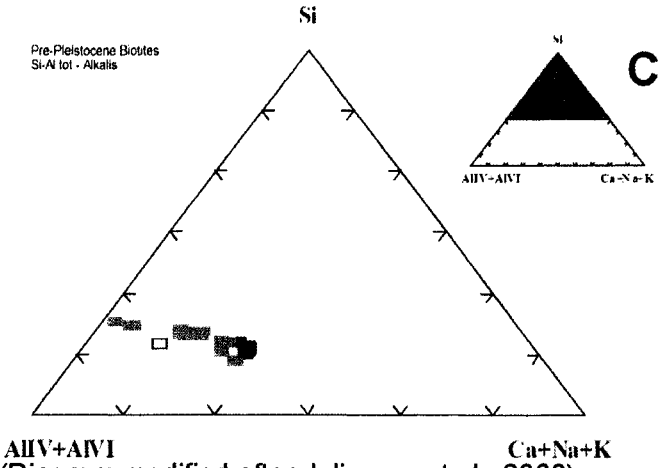

(Diagram modified after Jolicoeur et al., 2000)

The presence of Pleistocene tills overlying the youngest weathered profile, puts an upper age limit on the youngest weathering event, although it is possible that surface exposures of these younger profiles continue to weather today. The weathering trends within the biotites for the different ages of profiles suggest that different conditions prevailed during each weathering event.

4.6.1.1 Pre-Carboniferous conditions

Even allowing for compaction during diagenesis, the complete transformation of feldspars and biotite to kaolinite and secondary oxides in the Pre-Carboniferous within 2-3 metres of fresh rock, suggests a relatively intense period of weathering (Wilson, 2004; Kretzschmar et al., 1997; Bakker, 1967; Tardy et al., 1973; Gerrard, 1994; and Sequiera Braga et al., 2002) which allowed for the leaching of all the alkalis from the feldspars and the biotite, leaving only kaolinite and secondary oxides remaining. This intense weathering process did not however, result in gibbsite development nor did it destroy the apatite (did not mobilize P), suggesting that the weathering process did not go to the point of complete laterite development. That is, the conditions may have been warm and humid, but they were not so intense as to completely remove all but Al and Fe from the weathered profile.

In all of the saprolite profiles of the SMB, the breakdown of biotites ultimately results in the development of kaolinite. However, the intermediate products formed during the initial and early stages of biotite breakdown, record a different sequence for each of the three profiles. The breakdown of biotite during the Pre-Carboniferous weathering event resulted in the retention of Ti in oxides in the immediate area, defining the cleavage and borders of the original biotite in some cases (Fig. 4.3). However, x-ray mapping of biotites and their immediate surroundings, indicate that little Fe oxides/oxyhydroxides are preserved (Fig. 4.3). The removal of much of the Fe from the upper reaches of this profile is unique among the three ages of profiles, however the retention of Ti in secondary phases, and the persistence of at least some of the apatite is common to all three ages of profiles, as is the development of kaolinite from biotite as the

end product of the weathering processes. The initial breakdown products of biotite in the Pre-Carboniferous profile shows an increase in Fe-Mg-Mn and Al, and a concomitant decrease in Si with increased weathering (Fig. 4.4B and C).

Migration of Fe out of the weathered profile, as is found in the Pre-Carboniferous profile, is atypical during weathering, as any iron released is likely to be oxidised in a weathering environment, and therefore insoluble under most conditions. Acker and Bricker (1992) discuss the possibility of out-migration of Fe, either prior to the formation of Fe^{3+} species, or subsequently, as Fe^{3+} is re-reduced to Fe^{2+}, and consequently liberated. If the conditions during weathering are highly acidic, Fe^{3+} oxides can dissolve, and may be removed in solution (Acker and Bricker, 1992). However, highly acidic conditions should also result in the dissolution of apatite, and this has not happened. Another possibility is that the Fe^{3+} oxides were reduced during burial and diagenesis, and reduction of Fe^{3+} oxides could have resulted in the formation of the more soluble Fe^{2+}. The presence of Fe-bearing carbonates formed during diagenesis in this profile, adds support to the idea that diagenetic processes impacted on the Fe in this weathered profile. Further support for the possible impact of diagenesis on the behaviour of Fe in the saprolite, is the presence of overlying dark shales of the Lower Horton Bluff Formation, which would suggest that indeed, reducing conditions existed during burial, at least in localized regions where these shales directly overlie the South Mountain Batholith. The network of fractures formed in the saprolitic profile during weathering, later allowed for easy infiltration of carbonate-bearing solutions during diagenesis. Carbonate-bearing fluids offer an alkaline environment, thus contributing to providing a suitable environment for the preservation of the original apatite (Fig. 4.3B) and the precipitation of some of the iron into carbonate phases, despite the otherwise near-complete modification of this rock by the weathering and diagenetic processes. Interestingly, throughout these processes, phanteromorphs of the original biotites remain, most clearly recorded in the Ti-oxide traces developed along former cleavages in the original biotite (Fig. 4.3A and F).

4.6.1.2 Pre-Triassic conditions

In contrast to the complete destruction of the biotites and feldspars under weathering conditions during the Pre-Carboniferous, the preservation of partially altered biotites and K-feldspars, even in the uppermost preserved part of the 30 metre thick profile, suggests that conditions during weathering were somewhat different to those of the Pre-Carboniferous weathering event. XRD analysis of the Pre-Triassic profile indicates that smectite formation dominated the clay mineralogy of the lower reaches of the profile. The development of smectites has been associated with arid conditions (Kretzschmar et al., 1982; Gerrard, 1994), or at least seasonal variation in climate, where there existed a defined dry period, and a "flushing" of cations occurs under intermittent wetting (Acker and Bricker, 1992). The perseverance of biotite during weathering has been attributed to the initial development of an oxidised biotite, which then served to "buffer" further biotite breakdown (Jeong, 2002). Acker and Bricker (1992) argue that development of Fe_2O_3 coatings on biotite may form during weathering if pH conditions are moderate (>pH = 3 - 4), and this can in turn inhibit further weathering. Pereira et al. (1993) attribute the persistence of biotite to the presence of high proportions of K-feldspar which is also subject to weathering, essentially buffering K-loss from biotite. Similarly, Gilkes et al. (1972) suggest that an initial release of K from the interlayer on weathering, results in an adaptation within the structure, which results in less ease of outward migration of K, and therefore reduced rate of weathering. Given that the K-feldspar also persists through the Pre-Triassic profile, this coupled mineralogy may be a contributing factor, however the thickness over which these minerals persist, the presence of smectites, and the complete destruction of biotite in monzogranites during pre-Carboniferous times, in a parent granitoid equally enriched in K-feldspar, suggests that environmental conditions also contributed to the persistence of biotite throughout this profile. Experimental work by Acker and Bricker (1992) on weathering conditions of biotite, indicate that at pH<3, weathering rates of biotite increased 4-fold. It is possible that seasonal monsoon-like conditions, as suggested for the Permian-Triassic of Pangea (Parrish, 1993), coupled with conditions that were less acidic than those experienced in the Pre-Carboniferous, can account for the retention of biotite throughout the Pre-Triassic sequence, despite the overall argillaceous nature and otherwise extensive

weathering of this profile.

4.6.1.3 Pre-Pleistocene conditions

Processes dominating during the Pre-Pleistocene event differed again. Whereas the overall nature of the weathering involved an arenaceous product rather than an argillaceous product as in the Pre-Carboniferous and Pre-Triassic profiles, mineralogical changes indicate the development of kaolinite as an end product of both feldspar and biotite weathering, albeit in relatively low quantities in the profiles sampled. Intermediate products of biotite weathering of the monzogranite differ from both the Pre-Triassic and Pre-Carboniferous saprolites (Fig. 4.10).

In the fine fraction of the Pre-Pleistocene samples, vermiculite is identified by XRD, although smectites are not recorded in XRD analysis. Weathering of the Pre-Pleistocene resulted in the loss of potassium and slight loss of Fe^{2+}(tot), similar to that of the Pre-Triassic, however the proportion of Fe^{2+}(tot) lost relative to K is considerably less in the Pre-Pleistocene (Fig. 4.10), and the increase in total SiO_2 relative to K_2O is minimal in the Pre-Pleistocene, unlike the relative SiO_2 enrichment in the Pre-Triassic samples (Fig. 4.10). This suggests less disruption to the octahedral and tetrahedral layers in the Pre-Pleistocene biotite weathering than in either the Pre-Carboniferous or Pre-Triassic weathering, and may reflect a temperate climate during development. This youngest weathering event resulted in a less intense leaching process, although it is important to note that the alteration products of these biotites from the youngest weathering event do not follow the same trend as those of the older events, and therefore are not simply likely to represent a less complete version of either of the older events.

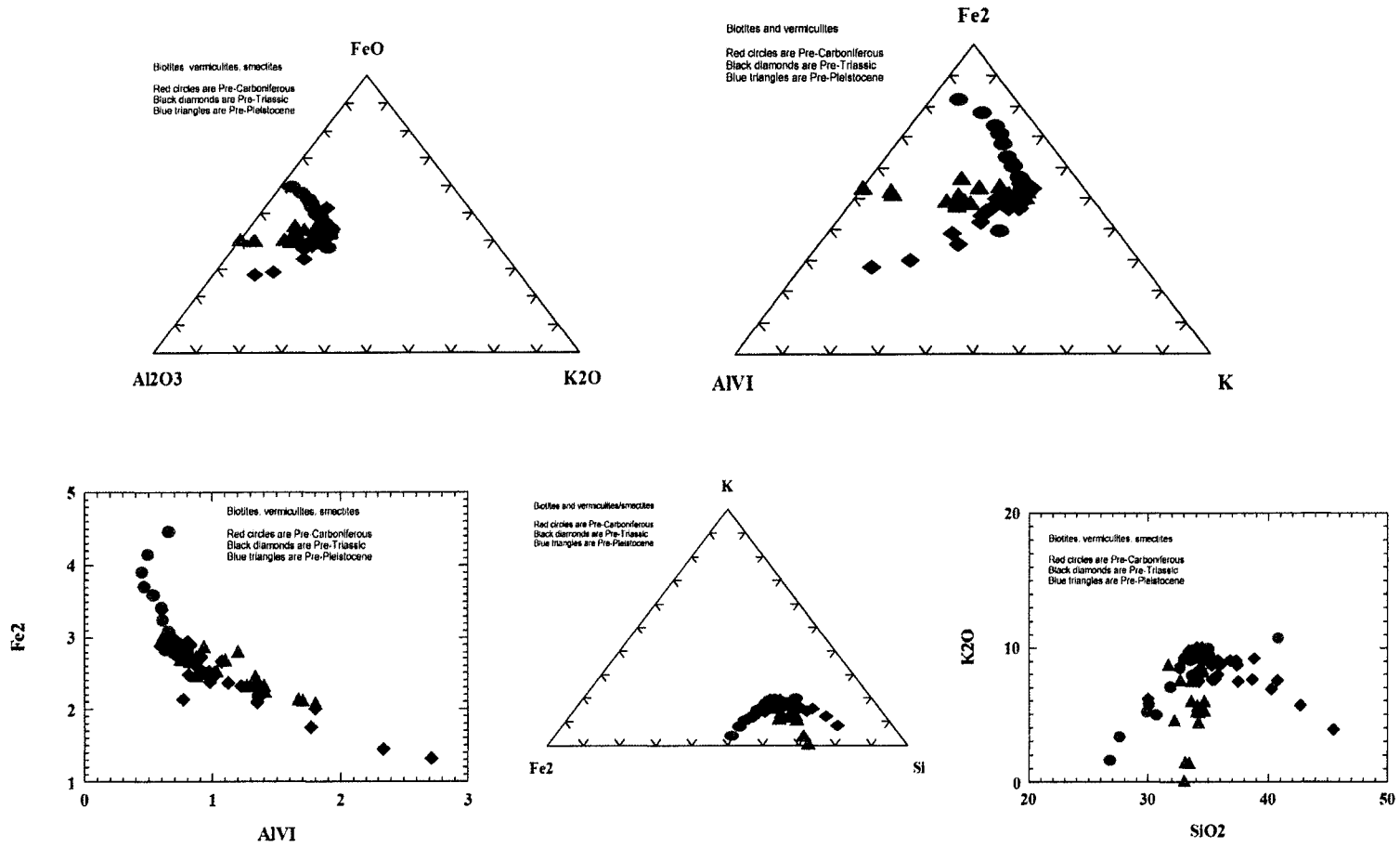

Fig. 4.10. Plots of biotite weathering data from all three weathering suites: red is Pre-Carboniferous; black is Pre-Triassic; blue is Pre-Pleistocene. Unmodified (unweathered) biotite from each suite overlaps around a central range, however as biotite weathers more intensely, the direction of change differs for each of the three suites.

4.7 Conclusions

The weathering mineralogy differentiates the three weathered profiles.

Weathering during three different times in the geologic past has resulted in the development of mineralogical and textural changes that reflect the conditions during the specific weathering event and not simply differences in parent material, as the parent material in each case was similar. Pre-Carboniferous weathering occurred under relatively intense conditions; Pre-Triassic weathering occurred under conditions that were relatively intense, but probably with seasonal arid periods; and Pre-Pleistocene weathering reflects a moderate weathering event in which the climate was likely temperate but warmer than today, as glacially striated surfaces elsewhere on the batholith indicate minimal weathering effects since the retreat of the ice *circa* 10,000 years ago.

Superposition of later processes can modify the weathering record, as in the case of the Pre-Carboniferous diagenetic event, however the weathering record itself has not been obliterated.

The record of weathering in all cases is particularly well preserved in the breakdown products of biotite. The biotites had the same original chemistry in all three profiles, however the series of breakdown products is distinctive to each weathering episode. Alteration sequences within each of the three profiles indicate that although all have kaolinite as a common end product, the intermediate products reflect environments prevailing during the weathering process itself, and are recorded by changes in the relative proportions of cations.

Microprobe spot analysis, combined with XRD and X-ray mapping provide a more complete analysis of the breakdown process in biotite, than does XRD alone.

Chapter 5

Chemical Weathering of Granitoids in the South Mountain Batholith of Nova Scotia: Useful Gravel Deposits or Potential Environmental Contaminators?

Preamble

Chapter 5 is the manuscript by AM O'Beirne-Ryan and M Zentilli, "Chemical weathering of granitoids in the South Mountain Batholith of Nova Scotia: useful gravel deposits or potential environmental contaminators?", intended for submission to Applied Geochemistry in the fall of 2006. A component of this geochemical study has been accepted for publication in Atlantic Geology, entitled: "Weathering of Devonian monzogranites as recorded in the geochemistry of saprolites from the South Mountain Batholith, Nova Scotia Canada", by AM O'Beirne-Ryan and M Zentilli. This paper is included in the Appendices, and is a condensed version of some of the material presented in this chapter. As first author on both of these papers, AM O'Beirne-Ryan has undertaken all of the research and the writing of these papers, and has incorporated suggestions and recommendations from M. Zentilli during both the research and the writing.

5.1 Introduction

The geochemistry of saprolite, the weathered material preserved *in situ* on unweathered parent rock, provides insight into the nature and intensity of chemical weathering processes. Geochemical data from such weathered horizons contribute to our understanding of the geochemical changes occurring at the earth's surface, and the redistribution of elements in supergene ore-forming processes. In addition, the nature

of the geochemical changes provides a basis for recognition of the liberation or concentration of environmentally sensitive elements such as U, Rn, Hg, As, and others, into the surface and near-surface environment. For the weathered horizons of the South Mountain Batholith, Nova Scotia, this study marks the first attempt at characterizing geochemical changes during the early stages of the weathering processes at three different times in the geologic past. The South Mountain Batholith is a specialized multi-phase peraluminous granitoid complex with numerous polymetallic mineral occurrences (Chatterjee and Muecke, 1982). Major, trace, and REE analyses from fresh parent, as well as variably weathered saprolites, provide a basis for understanding the nature of chemical change during the stages of early weathering of a variety of granitoid types and weathering ages within the South Mountain Batholith (SMB). Furthermore, these geochemical data can be used to assess the potential for migration or concentration of environmentally sensitive elements as a result of weathering.

Geochemical signatures of weathering have been the subject of discussion by numerous authors including Condie et al., 1995; Fritz, 1988; Gardner et al., 1978; Goldich, 1938; Horbe e da Costa, 1999; Melfi et al., 1983; Middleburg et al., 1988; Mongelli, 1993, Mongelli et al., 1998; Nedachi et al., 2005; Nesbitt and Young, 1982, 1984, 1989; Price and Velbel, 2000; Sutton and Maynard, 1992; van der Weijden and van der Weijden, 1995, and others, and their conclusions generally hold that weathering results in the liberation of more mobile elements, and the redistribution or retention of elements which are immobile in the near-surface environment. These studies have not addressed specifically the potential for impact on the environment of such chemical changes, nor have they examined the possible impact of different weathering events at different times, on granitoids of similar composition.

A number of locations of granitoid saprolites in varying degrees of preservation can be found in Southwestern Nova Scotia, particularly along the western margin of the batholith (Fig. 5.1). Details of the nature of these weathered horizons can be found elsewhere (O'Beirne-Ryan and Zentilli, 2003), and only a brief overview is presented here.

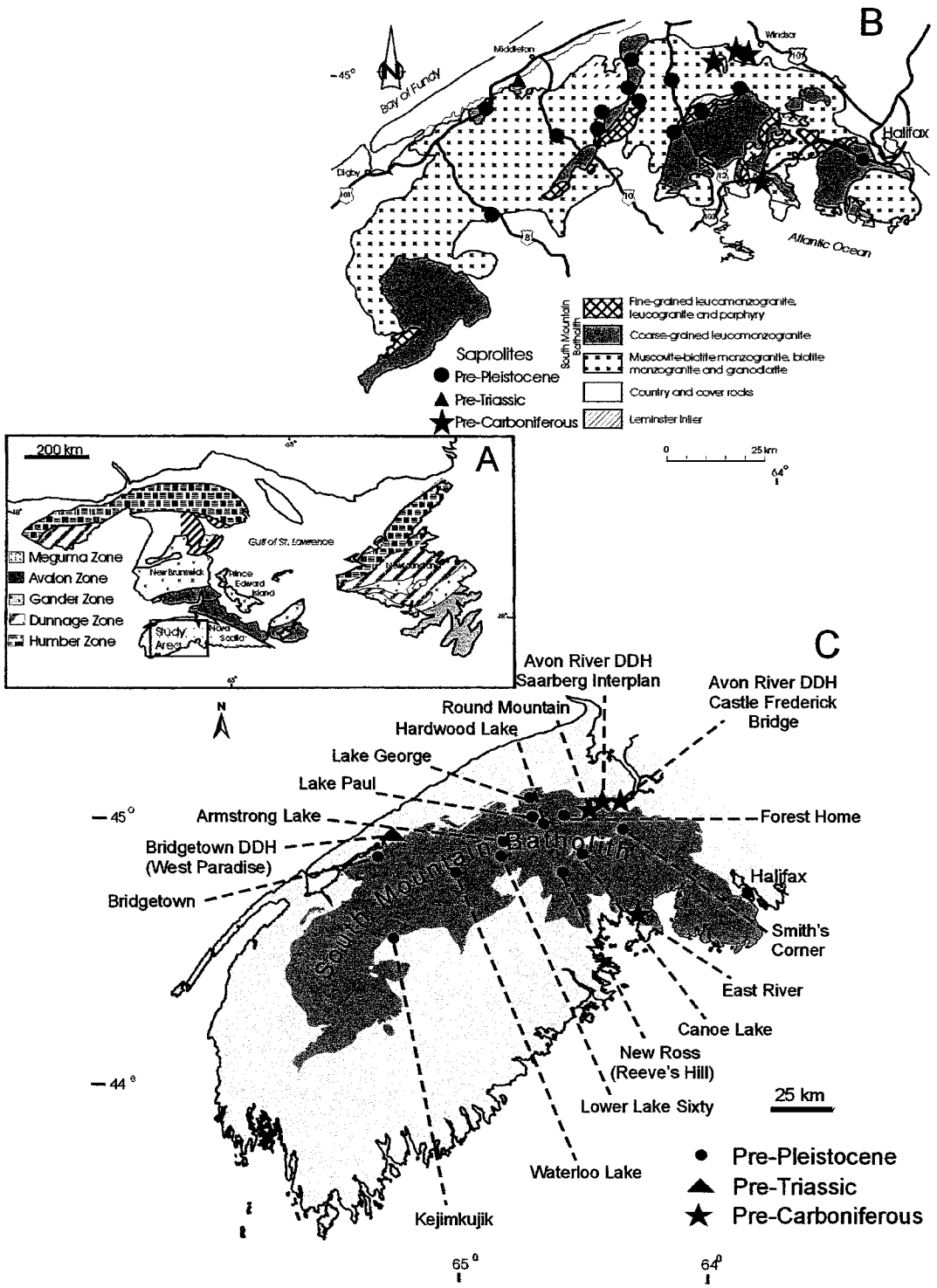

Fig. 5.1. (A) Location of the study area and general geological setting of the Northern Appalachians (after Williams, 1995). (B) Geology of the South Mountain Batholith, with saprolite locations (after MacDonald, 1992). (C) Sample locations and location names of saprolite on the South Mountain Batholith (after O'Beirne-Ryan and Zentilli, 2003).

Weathered horizons of pre-Carboniferous, pre-Triassic, and pre-Pleistocene age, each with distinctly different characteristics, have been recognized at numerous localities throughout southwestern Nova Scotia (Fig. 5.1). The pre-Carboniferous and pre-Triassic horizons have been sampled in drill core, and are overlain by Carboniferous and Triassic strata respectively. The pre-Pleistocene horizons were sampled at surface, where they are locally overlain by Pleistocene till. The preserved portions of the weathered horizons of the SMB, and in particular the sections of pre-Pleistocene age, represent either (a) the lowest levels of a thicker, more complete weathering profile, the bulk of which has now been removed by erosion, and only the lowermost and least weathered 2-6 meters remain, or (b) an arrested stage in the development of a weathering profile, in which case the entire section visible is a complete record of an early, incipient weathering event (O'Beirne-Ryan and Zentilli, 2003). In either case, the weathering process as recorded in the sequences preserved is incomplete, and represents the incipient, or early stage of weathering. As a result, there is a considerable amount of readily available soluble material remaining within many of the saprolites, and the saprolites are "primed" for further chemical alteration. In combination with the intensity of microfractures developed within the saprolites, the acidic precipitation prevailing throughout Nova Scotia today, and the exploitation of these horizons for construction, these horizons are potentially elemental sieves.

5.2 Sampling procedures and methods

Twenty-three samples representing the different degrees of weathering intensity within the weathered horizons were selected and analyzed for major, trace element, and REE geochemical analysis: three samples from each of four surface outcrops of Pre-Pleistocene weathering, five samples from one of the Pre-Triassic drill cores, and three from each of two of the Pre-Carboniferous drill core weathered horizons (Fig. 5.1 and Table 5.1). The samples selected for geochemistry were samples with minimal or no obvious evidence of hydrothermal, significant metasomatic alteration, or post-weathering chemical modification except in the case of the Pre-Carboniferous samples. That is, the aim was to select samples where any changes in chemistry could be

	Pre-Pleistocene											
	Waterloo Lake						Smith's Corner			Forest Home		
SAMPLE	**111f**	**106w**	**107ww**	**112f**	**113Aw**	**144ww**	**145F**	**126W**	**127WW**	**128F**	**129W**	**140WW**
SiO2	67.19	67.31	67.5	67.04	67.83	67.48	73.74	74.47	75.05	72.1	72.95	72.48
TiO2	0.667	0.616	0.497	0.756	0.663	0.68	0.089	0.073	0.062	0.282	0.24	0.251
Al2O3	15.03	15.22	15.58	15.26	15.23	15.06	13.81	13.69	13.78	14.55	13.76	14.26
Fe2O3t	4.78	4.54	4.5	5.38	4.65	4.86	1.43	1.35	1.11	2.33	2.26	2.44
Fe2O3*	0.85	2.00	2.10	1.03	1.77	1.83	0.63	1.03	0.78	1.03	0.97	1.17
FeO*	3.53	2.28	2.16	3.91	2.59	2.72	0.72	0.29	0.3	1.17	1.16	1.14
MnO	0.076	0.076	0.142	0.091	0.08	0.092	0.019	0.015	0.011	0.024	0.026	0.033
MgO	1.17	0.99	0.86	1.3	1.09	1.11	0.11	0.07	0.07	0.37	0.33	0.36
CaO	1.9	1.58	0.86	1.96	1.37	1.13	0.44	0.38	0.32	0.72	0.47	0.46
Na2O	3.19	3.06	2.83	3.11	2.81	2.76	3.29	3.06	2.99	2.87	2.48	2.37
K2O	3.74	4.03	5.66	4.01	4.47	4.33	4.74	5	5.22	5.56	5.57	4.98
P2O5	0.216	0.224	0.104	0.304	0.272	0.262	0.283	0.321	0.294	0.213	0.166	0.141
LOI**	0.8	1.47	1.32	0.8	1.38	1.88	0.8	1.11	0.9	0.99	1.03	1.84
H2Op	0.96	1.11	1.04	0.89	1	1.42	0.51	0.66	0.6	0.74	0.67	1.28
V	85	77	66	94	85	86	19	16	16	38	34	37
Cr	25	22	18	26	23	26	6	6	1	12	8	11
Co	11	11	11	13	10	13	1	1	1	1	1	5
Zr * **	227.7	208	173	225	186.6	201	40.4	38.1	24.8	113	97.3	117.2
Ba	674	695	995	704	806	785	211	164	191	688	446	369
Ni	10	11	4	10	8	9	3	1	1	3	1	3
Cu	11	7	6	14	8	11	7	4	5	6	5	4
Zn	74	77	64	84	86	111	40	28	28	73	74	80
Ga	21	22	20	23	21	22	23	22	23	19	19	21
Rb	146	157	177	192	206	220	466	512	512	232	248	248
Sr	145	134	140	149	143	139	11	7	1	73	43	33
Y***	39.91	41.87	48.42	28.87	25.28	28.16	10.96	12.85	5.25	20.44	26.51	34.22
Nb***	14.5	14.7	11.4	14.3	12.8	13.1	13.8	12.2	9.8	11.2	10.7	12.2
Pb	21	23	25	17	23	36	13	7	13	17	18	22
Th***	12.73	12.68	14.22	12.41	9.99	11.3	4.79	3.68	2.13	8.88	9.41	10.44
U***	3.589	2.971	3.446	3.465	4.872	5.554	2.884	1.336	1.475	3.426	2.666	3.287
Hg ppb ***	1.4	1.3	1.2	1.9	1.2	1.6	3.7	1.9	1.6	1.8	0.9	1.1
Cd ****	0.2	0.4	0.4	-0.2	-0.2	7	-0.2	-0.2	-0.2	0.3	-0.2	-0.2
As******	9	10	8	6	6	14	5	-5	-5	-5	-5	-5
Li******	68	60	58	125	109	115	55	21	25	68	62	64
Sc******	9	8	8	10	9	8	-5	-5	-5	-5	-5	-5
Au******	1	2	3	-1	1	2	2	1	-1	1	-1	-1
Mo******	-1	2	-1	-1	-1	8	-1	-1	-1	-1	-1	-1
Cs	8.562	6.334	9.269	11.931	12.071	15.359	16.546	16.651	16.983	8.172	10.322	13.229
Hf	6.2	5.5	5.0	6.2	5.1	5.5	1.7	1.7	1.2	3.2	2.9	3.5
Ta	1.23	1.23	1.00	1.64	1.40	1.46	2.07	2.60	2.13	0.91	1.04	1.20
La	38.38	35.85	33.90	38.35	22.79	34.97	6.21	4.95	2.79	18.51	15.03	20.21
Ce	79.17	74.63	72.96	80.85	62.90	70.77	14.12	11.48	6.26	41.52	33.66	44.06
Pr	10.385	10.126	9.436	10.636	6.956	9.694	1.864	1.545	0.790	5.105	4.497	5.862
Nd	40.31	39.51	36.53	41.52	27.92	37.71	7.03	5.82	2.91	19.49	17.12	22.75
Sm	8.97	8.94	7.68	9.11	6.52	8.35	2.24	1.90	0.91	4.82	4.19	5.78
Eu	1.402	1.231	1.324	1.486	1.473	1.407	0.160	0.118	0.077	0.787	0.544	0.680
Gd	8.745	8.869	7.490	8.065	6.079	7.579	2.324	2.270	1.009	4.377	4.269	5.757
Tb	1.390	1.456	1.260	1.173	0.977	1.109	0.496	0.51	0.218	0.753	0.783	1.012
Dy	7.644	7.694	8.049	5.883	5.288	5.737	2.421	2.658	1.108	4.054	4.517	5.799
Ho	1.437	1.455	1.853	1.143	0.990	1.054	0.343	0.404	0.156	0.714	0.924	1.211
Er	3.664	3.640	5.535	2.992	2.630	2.749	0.636	0.798	0.304	1.845	2.488	3.170
Tm	0.504	0.479	0.872	0.426	0.392	0.403	0.068	0.088	0.034	0.272	0.362	0.474
Yb	2.83	2.66	5.75	2.72	2.38	2.53	0.40	0.47	0.20	1.52	2.18	2.88
Lu	0.427	0.372	0.882	0.427	0.383	0.39	0.045	0.059	0.023	0.222	0.316	0.397

Table 5.1. Major, trace, and rare earth elements for saprolite suites of the SMB.

	Pre-Triassic				Pre-Carboniferous				Castlefrederick 2		
SAMPLE	**2-201**	**2-193**	**2-168**	**2-139**	**2-110**	**1134**	**1126**	**1119**	**1184**	**1176**	**1168**
SiO2	68.03	67.88	67.73	69.46	66.87	67.45	70.95	65.15	68.71	67.34	66.6
TiO2	0.653	0.609	0.587	0.586	0.68	0.551	0.396	0.449	0.52	0.425	0.528
Al2O3	15.1	14.41	14.99	14.41	16.44	15.35	14.09	15.31	15.28	17.21	16.11
Fe2O3t	4.58	4.27	4.15	4.1	4.77	4.38	3.37	3.82	3.87	1.97	2.1
Fe2O3*	1.00	1.28	3.85	3.92	4.55	n.a.	n.a.	n.a.	n.a.	n.a.	n.a.
FeO*	3.22	2.69	0.27	0.16	0.2	n.a.	n.a.	n.a.	n.a.	n.a.	n.a.
MnO	0.072	0.065	0.09	0.063	0.074	0.1	0.08	0.66	0.1	0.31	0.37
MgO	1.13	1.28	1.25	1.02	1.11	1.1	0.72	1.06	0.89	0.7	0.84
CaO	2.09	1.6	0.8	0.71	0.32	2.13	1.69	3.07	2.29	2.04	2.75
Na2O	3.06	2.52	1.07	0.25	0.2	2.99	2.72	0.01	2.89	0.03	0.01
K2O	4.19	4.25	5.25	5.78	4.82	4.36	4.47	0.2	4.2	0.33	0.38
P2O5	0.224	0.206	0.201	0.197	0.132	0.228	0.175	0.209	0.227	0.07	0.192
LOI**	0.98	2.06	4.94	4.29	5.13	1.05	0.85	10.22	1.38	8.91	9
H2Op	0.83	1.08	2.17	2.51	3.8	n.m.	n.m.	n.m.	n.m.	n.m.	n.m.
V	83	78	68	70	83	76	59	68	74	71	76
Cr	25	18	12	22	31	22	34	27	28	25	29
Co	11	11	11	11	17	10	8	7	11	5	<5
Zr ***	230.4	206.4	174	200.6	247.6	201.7	151	65	183.7	166.6	184.9
Ba	773	847	956	921	664	643	489	37	479	26	36
Ni	9	9	1	7	8	11	4	3	10	<3	12
Cu	7	7	14	11	19	<4	5	<4	7	4	4
Zn	71	70	107	85	75	121	51	6	63	16	7
Ga	21	19	20	19	23	22	18	21	22	24	22
Rb	149	157	218	200	202	173	156	15	158	24	24
Sr	141	130	99	64	43	129	97	34	115	178	48
Y***	41.59	28.44	25.36	27.15	19.84	31.5	27.92	14.62	33.54	24.43	44.34
Nb***	13.9	13.5	12.8	12.2	14.7	13.2	10	4.6	12.8	11	12.5
Pb	20	20	38	46	98	53	23	<3	21	6	<3
Th***	13.23	11.34	12.3	12.5	10.38	11.62	8.22	3.1	11.1	8.71	11.04
U***	4.304	2.642	3.581	3.797	5.017	3.165	3.637	1.382	3.978	3.028	3.887
Hg ppb ****	1.2	3.1	2.2	-0.1	4.7	n.m.	n.m.	n.m.	n.m.	n.m.	n.m.
Cd ******	0.2	0.2	0.2	-0.2	0.3	n.m.	n.m.	n.m.	n.m.	n.m.	n.m.
As******	8	9	12	14	35	n.m.	n.m.	n.m.	n.m.	n.m.	n.m.
Li******	65	61	48	39	36	n.m.	n.m.	n.m.	n.m.	n.m.	n.m.
Sc******	9	8	8	7	9	n.m.	n.m.	n.m.	n.m.	n.m.	n.m.
Au******	1	1	-1	-1	-1	n.m.	n.m.	n.m.	n.m.	n.m.	n.m.
Mo******	-1	1	-1	-1	1	n.m.	n.m.	n.m.	n.m.	n.m.	n.m.
Cs	8.882	13.992	28.577	23.694	22.280	9.940	7.131	0.286	6.556	1.140	1.107
Hf	6.3	5.6	4.8	5.4	6.6	5.6	4.2	1.9	5.0	4.6	5.2
Ta	1.06	1.03	1.04	0.97	1.16	1.14	0.91	0.40	1.10	0.95	1.14
La	36.74	30.33	32.27	33.46	23.79	32.57	22.76	8.60	31.24	32.70	28.72
Ce	79.70	60.05	84.40	94.30	50.18	69.38	49.82	19.12	68.66	68.54	63.47
Pr	10.305	8.529	9.331	9.554	7.185	8.943	6.271	2.478	8.786	8.705	8.455
Nd	40.02	33.77	35.94	38.16	28.09	34.86	24.46	10.34	33.99	33.94	34.23
Sm	9.45	7.49	7.83	8.43	6.28	8.00	5.74	2.62	7.85	7.44	8.28
Eu	1.511	1.425	1.203	1.300	0.626	1.282	1.032	0.337	1.255	1.490	0.966
Gd	8.611	6.975	7.039	7.423	5.520	7.423	5.587	2.973	7.165	6.193	9.106
Tb	1.394	1.068	1.038	1.094	0.794	1.111	0.899	0.518	1.170	0.859	1.526
Dy	7.695	5.684	5.243	5.753	3.947	5.931	5.075	2.729	6.401	4.533	8.278
Ho	1.591	1.058	0.969	1.032	0.738	1.162	1.007	0.533	1.221	0.845	1.581
Er	4.198	2.643	2.457	2.584	1.913	2.916	2.684	1.368	3.207	2.138	4.010
Tm	0.604	0.384	0.333	0.355	0.284	0.419	0.374	0.188	0.457	0.314	0.552
Yb	3.58	2.33	2.11	2.17	1.75	2.55	2.21	1.16	2.60	1.84	3.20
Lu	0.549	0.336	0.302	0.341	0.265	0.362	0.337	0.159	0.396	0.281	0.465

Table 5.1 continued.

considered representative of the weathering process alone as much as possible.

Careful selection of sample sites based on the criteria listed below resulted in the selection of representative samples with variable degrees of weathering from four surface locations and in three drill cores. Criteria considered important in the selection of samples for geochemical analyses included: (a) the presence of minimally weathered parent as well as variably weathered material at the site; (b) "vertical" section from fresh to most weathered; (c) absence of, or minimal hydrothermal alteration; (d) availability of a minimum of three samples of differing degrees of weathering from the same location. Whereas the number of data points for each individual site is not large, it is the comparison of the data between sites which offers interesting insights to the weathering processes involved through time in the South Mountain Batholith.

5.2.1 Pre-Carboniferous Geochemical Samples

The Pre-Carboniferous weathered horizon represents the earliest of the three weathering events, and this horizon is the only one of the three which has undergone re-lithification subsequent to the weathering event. In order to best define the nature of the weathering horizon in the Pre-Carboniferous saprolite, several drill core were examined from a number of drill sites (Fig. 5.1). Of the cores examined, only two showed a complete and relatively undisturbed sequence from fresh biotite monzogranite to overlying Carboniferous sediments. Both of these drill cores intersected fresh coarse-grained biotite monzogranite at their base, at depths of approx. 320 - 350 m. The total thickness of the preserved part of these weathered horizons is 5 - 6 m. For both, samples analyzed included one sample from the fresh parent granitoid, one from half-way up the profile, and one from the top of the profile.

Subsequent to its weathering, the pre-Carboniferous sequence has undergone diagenetic changes, as evidenced by the re-lithified texture observed, the vertically condensed thickness of the weathered profile (O'Beirne-Ryan and Zentilli, 2003), and the post-weathering burial depths of 5 km, as recorded by fission track studies (Ryan

and Zentilli, 1993). Given the intensity of the vertical zonation observed texturally and mineralogically, the geochemical changes present are a combination of weathering effects, with possible superposition of diagenetic changes. The saprolitic horizon developed prior to the deposition of Carboniferous sediments, was most likely an argillaceous saprolite originally (Lidmar-Bergstrom et al., 1997), which has been modified during diagenesis. While it is not possible to precisely quantify the relative contributions of these weathering and diagenetic processes to the elemental signature, constraints based on mineralogical and textural, as well as field relations, allow for an approximation of the weathering signature. Similarly re-lithified horizons are described in Sutton and Maynard (1992) and Fedo et al. (1995), in reference to a post-weathering K-metasomatism event, in which illite and K-feldspar are developed on a sub-Huronian regolith in Ontario.

5.2.2 Pre-Triassic Geochemical Samples

The saprolites of pre-Triassic age are all found in the sub-surface, and are argillaceous in nature. These pre-Triassic saprolites clearly represent a different weathering event than those formed prior to Carboniferous times: there is no evidence of subsequent re-lithification, and the presence of little-altered biotite, even in the uppermost part of the weathered horizon, is distinctly different from the mineralogical and textural nature of the pre-Carboniferous horizon (O'Beirne-Ryan and Zentilli, 2002). One of three drill cores examined yielded samples deemed representative of a weathering sequence. From this drill core, samples from depths of 60.3 m (fresh biotite monzogranite), 60 m (incipiently weathered biotite monzogranite), 57.9 m, 50.4 m, 41.7 m, and 30 m (top of the preserved weathered horizon, just beneath the Triassic sandstones and shales) were selected for geochemical analysis. Even in the highly weathered samples from the top of the preserved horizon, the texture of the original biotite monzogranite is evident. The sample from 60 m was later omitted, as on closer inspection it displayed more intense reddening and alteration of the biotites, and geochemical evidence of hydrothermal effects (the geochemistry was not consistent with vertical-upward changes in all elements). The geochemical data are considered to

represent the changes resulting from the weathering process alone.

5.2.3 Pre-Pleistocene Geochemical Samples

Pre-Pleistocene arenaceous saprolites, with clay minerals forming less than 5% of even the most weathered material, occur at a number of surface localities throughout the South Mountain Batholith (Fig. 5.1). Similar arenaceous saprolites have been reported from Portugal (Gouveia et al., 1993), Sweden (Lidmar-Bergstrom et al., 1997), and Finland (Islam et al., 2002). In some of the Nova Scotia localities, these saprolites are overlain by till of Pleistocene age (Fig. 5.1 - Waterloo Lake, and Fig. 5.2), which establishes a pre-glacial age for this weathering episode (O'Beirne-Ryan and Zentilli, 2003).

Fig. 5.2. Pleistocene till overlying weathered granitoid, Waterloo Lake. Note the large corestone at top centre-left.

The variability in rock types of these arenaceous saprolites, and the variety in intensity and nature of weathering of the surface outcrops, resulted in establishing criteria for sample collection and nomenclature based on degree of weathering rather than on a vertical sequence. This ensured that at locations in which corestones with weathered rims occurred (Ryan et al., 2006), the intensity of weathering, rather than the depth of weathering was the significant criterion in sample selection. Three samples from each site were collected: (a) fresh parent (f), in which the weathering effects were minimal, as judged by the strength of the rock (when hit with a hammer, the sound was not deadened) and the paucity of microfractures; (b) moderately weathered (w), in which the rock responded with a deadened "thud" when hit with a hammer, and the sample, although cohesive, could be broken easily, could be collected by hand, and had extensive microfractures developed; and (c) highly weathered (ww), in which the rock structure had collapsed, and the grains formed an unconsolidated blanket. Given the overall arenaceous nature of the Pre-Pleistocene weathering horizons, and the variety of textural and mineralogical types of these weathered horizons, sampling on the basis of three samples per site was deemed most useful for this study.

Geochemical sample locations include Waterloo Lake (megacrystic biotite monzogranite), Hardwood Lake (porphyritic biotite monzogranite), Forest Home (pinkish, coarse-grained, equigranular leucogranite), and Smith's Corner (porphyritic biotite leucomonzogranite) (Fig.5.1). The biotite monzogranite weathered horizons, although texturally very different from each other, are of similar chemical composition to the biotite monzogranite of the fresh samples from both the sub-Carboniferous and the sub-Triassic drill core (Table 5.1). The geochemical similarity between the original rock in the weathering profiles of the three different ages is fortuitous, as it allows comparison of the response to weathering under differing environmental conditions, at different times in the geologic past. Samples from outcrops at Forest Home and Smith's Corner represent more felsic units of the South Mountain Batholith, and provide a basis for comparison of the response to weathering of differing types of granitoid rocks, under similar environmental conditions, in pre-Pleistocene times.

5.3 Sample preparation, analysis, and precision

All samples were crushed and pulverized (-200 mesh) at Daltech, Halifax, Nova Scotia, and four sample splits were collected from each sample. Analysis of one sample set for majors and trace elements was done by XRF at Saint Mary's University, Halifax, Nova Scotia. Duplicate samples for two samples, and duplicate samples of the internal standard were analyzed to ensure quality control (Appendices A3-A6). Analyses of the duplicate samples indicate variance was within acceptable parameters (David Slaunwhite, pers.com., 2001). These samples were analyzed using a Philips 2400 analytical dispersive spectrometer, fitted with a Rh anode X-ray tube and Philips 2510 102 position sample auto-changer. The major elements and V, Cr, Ba, Ni, Ga, and Sr were measured on fused glass beads. These were prepared by mixing 5 g lithium tetraborate, 300 mg lithium fluoride, and 35 mg lithium bromide with 1 g of sample, and fusing the mixture in a platinum crucible using Claisse Fluxy 3-position rock device, at approximately 1050°C. The melts were then molded into 30 mm disks and analyzed. Co, Nd, Ni, Cu, Zn, Rb, and Pb were determined on pressed pellets, prepared by mixing 10 g of sample with 1.5 g powdered Bakelite and pressing the mixture into a disk approximately 5 mm thick and 40 mm diameter using a Herzog HTP hydraulic press at 20 tonnes for 10 seconds. The pellets were then heated to 180°C for 15 minutes, and cooled prior to analysis. Calibrations used a series of 30-40 geologic standards, and all data were corrected either using theoretically determined alpha coefficients (e.g., major elements) or Compton scatter (e.g., trace elements). Accuracy for this method for silica is within 0.5%; the error is less than 1% for the other major elements. For trace elements, the accuracy is within 5%. Instrument precision, as defined by repeated analysis of a single sample is within 0.6% relative. Sample precision, as defined by measurement of different samples taken from the same aliquot is within 1% on elements done on fused beads, and 0.7% for those done on pressed pellets. For the major elements, the analytical limit is 0.01% for all elements except Ti, P and Mn, which are 0.001%. Limits for elements found in trace amounts are (in ppm): Cr = 4, Co = 5, Cu = 4, Ga = 5, Rb = 2, Ni = 3, Sr = 5, V = 4, Pb = 3, Zn = 5 and Ba = 25.

A duplicate set of samples was analyzed for selected trace and rare earth

elements (REEs) at Geo Labs in Ontario, using ICP-MS. Table 1 includes the data for the REEs and for Zr, Nb, Y, Th, and U; complete data are given in Appendix A4. Samples were prepared using a closed beaker digestion with a combination of four acids (hydrofluoric, hydrochloric, perchloric, and nitric) for 14 days, to ensure complete digestion of all solid phases.

A second duplicate set of samples was sent to Bondar Clegg Laboratories, Vancouver, British Columbia, for Hg analysis and for selected trace element analysis. Mercury concentration was measured on a 1-2 g aliquot using a Cetac Cold Bapour Atomic Absorption unit (Cetac CV-AA), with a lower detection limit of 1 ppb. The trace element suite was prepared using aqua regia digestion, followed by analysis using ICP-AES. Data for Hg, Au, Mo, Cd, Li, As, and S are included in Table 5.1, and trace element data are given in Appendix A5; data for elements analyzed using both aqua regia digestion and either XRF or ICP=MS are given in Appendix A5. Fe_2O_3, determined by titration, and H_2O^+, were analyzed at Daltech, in Halifax. Appendix A6 provides data on duplicate sample analysis, indicating close agreement between samples (within 5% for most elements).

5.4 Results

Chemical weathering of granitoids ultimately involves the conversion of the feldspars and micas to clay minerals. Gardner et al., (1978) argue that because saprolites retain the textures of the parent granitoid, chemical weathering processes are isovolumetric. Middleburg et al., (1988) conclude that isovolumetric weathering is not always readily confirmed, and therefore cannot be assumed. As an alternative, or indeed used in conjunction with isovolumetric weathering, numerous authors have suggested that weathering effects be considered in relation to chemical differences between elements that are mobilized during weathering, and those which do not migrate during surface processes (Duzgoren-Aydin et al., 2002; Goldich, 1938; Harnois, 1988; Middleburg et al., 1988; Mongelli, 1993; Nesbitt, 1979; Nesbitt and Markovics, 1997; Nesbitt and Young, 1982 and 1996; Parker, 1970; Price and Velbel, 2003; Rainbird et

al., 1990; Ruxton,1968; Sueoka et al., 1985; Van der Weijden and Van der Weijden, 1995 Vogel, 1975; and Vogt, 1927). A number of these indices are summarized in Table 5.2, and have been applied to the data from the SMB (Table 5.3). The weathering suites in this study show consistent trends or relatively unchanged values for the Vogt ratio indicator (Vogt, 1927), Vogel's weathering indicator (1973), Nesbitt and Young's Chemical Index of Alteration (1982, 1984, 1989), Harnois' chemical index of weathering (1988), and the weathering index of Middleburg et al., (1988).

A key factor in all of these weathering indices lies in the fact that they rely on the major elements for weathering stage determination, and in particular, for changes in the proportion of alkali and alkali earth elements to aluminum. Price and Velbel (2003) and Duzgoren-Aydin et al., (2002) argue that an important consideration in any weathering index is that it is widely applicable and easy to measure, which is arguably the case in using variations on major element oxides. The CIA, or chemical index of alteration (Nesbitt and Young, 1982; Rainbird et al., 1990) reflects the depletion of total Na, K, and Ca relative to Al, a typical alteration trend in rocks in which feldspars dominate. Typically, unweathered granitoid rocks have CIA values close to 50%, whereas kaolinite, a plausible end product for weathered feldspars, has a CIA value approaching 100% (Nesbitt and Young, 1982). In theory, all stages of weathering will fall between these two values. CIA values clearly increase for the Pre-Triassic and Pre-Carboniferous samples with increased intensity of weathering. The change in CIA values for the Pre-Pleistocene samples is not significant despite significant depletion in Ca and Na (Tables 5.1 and 5.3). The unchanged CIA reflects the slight increase in K relative to Ca and Na, particularly in the Waterloo Lake and Smith's Corner samples, and the less intense weathering of these saprolites. The slight increase in K relative to Ca and Na may be the result of the more megacrystic nature of the parent granitoid at both Waterloo Lake and Smith's Corner. Nesbitt and Young (1984, 1989) also used a ternary plot of Al2O3 - (Na2O+CaO) - K2O to graphically represent this weathering trend, with an initial increase in proportions of Al2O3 and K2O, followed by increases in Al2O3 and decreases in K2O, and data from the Pre-Triassic horizon is plotted together with the average granite weathering trend (Fig. 5.3). Harnois (1988) argued in favour of relating depletion of just Na and Ca in relation to Al, as K was influenced by other factors, such as diagenesis, and was therefore not always a good indicator. Figure 5.4 shows the

increased values of CIW with degree of weathering, for all suites studied, and Figure 5.5 plots CIW against CIA, showing correlation based on Pre-Triassic and Pre-Pleistocene suites. Pre-Carboniferous samples were not included.

Author	Weathering Index
Chemical index of alteration Rainbird et al., 1990 Nesbitt and Young, 1982; 1984	**$(Al_2O_3 / Al_2O_3 + Na_2O + K_2O + CaO) \times 100 = CIA$**
Chemical index of weathering Harnois, 1988	**$(Al_2O_3 / Al_2O_3 + Na_2O + CaO) \times 100 = CIW$**
Van der Weijgen et al., 1995	**% Change in rock = 100 { $(F_{(Ti+Zr)} \times X_s/X_p) - 1$}** where $F_{(Ti+Zr)} = \frac{0.1 \times (Ti_{ppm} + Zr_{ppm})_p}{0.1 \times (Ti_{ppm} + Zr_{ppm})_s}$
Nesbitt and Markovics, 1997	$100 \times \{[(X/Ti)_{parent} - (X/Ti)_{sample})] / (X/Ti)_{parent}\}$
Nesbitt, 1979 (and Mongelli, 1992)	**% Change = $[(X/Al)_{sample}/(X/Al)_{parent} - 1] .100$**
Middleburg et al., 1988	**Plot: % change vs DEGREE of weathering** **DEGREE = $(1-R_{sample}/R_{parent})$** **R = $(CaO+Na_2O+K_2O) / (Al_2O_3+H_2O)$** % change refers to Nesbitt, 1979
Modified weathering potential index. Vogel, 1973	**MPWI = $\frac{(Na_2O+K_2O+CaO+MgO) \times 100}{(Na_2O+K_2O+CaO+MgO+SiO_2+Al_2O_3+Fe_2O_3)}$**
Weathering potential index Ruxton, 1968	**$\frac{100(K_2O+Na_2O+CaO+MgO-H_2O^+)}{(SiO_2+Al_2O_3+Fe_2O_3+TiO_2+FeO+CaO+MgO+Na_2O+K_2O)}$**
Sueoka et al., 1985	Loss on Ignition (LOI)
Parker Index Parker, 1970	**$\frac{(Na)_a + (Mg)_a + (K)_a + (Ca)_a}{0.35 \quad 0.9 \quad 0.25 \quad 0.7} \times 100$** $(X)_a$ = atomic proportion of element X 0.35, etc. refer to ionic bond strength of X-O
Vogt Ratio Vogt, 1927; Roaldset, 1972	**VR = $Al_2O_3+K_2O / MgO+CaO+Na_2O$**
Weathering direction / product index. Reiche, 1943	$100\ SiO_2 / SiO_2+TiO_2+Fe_2O_3+FeO+Al_2O_3 = PI$

Table 5.2. Selected weathering indices.

		Ruxton Ratio	Parker Index	Vogt ratio	Vogel	Nesbitt and Young		Harnois	Middleburg et al		
	SAMPLE	RR	PI	VR	MPWI	CIA mol %	WPI	CIW mol%	R	Degree	Al2O3+Fe2O3t+TiO2
Waterloo Lake	111F	4.47	52.16	3.00	10.31	55.06	13.33	63.33	0.56	0.00	72.64
	106W	4.42	53.08	3.42	9.99	56.44	13.16	65.81	0.52	0.07	72.47
	107WW	4.33	63.64	4.67	10.44	56.25	13.64	71.47	0.55	0.01	72.50
Hardwood Lake	112F	4.39	54.10	3.03	10.59	55.35	13.56	63.74	0.57	0.00	73.18
	113AW	4.45	54.99	3.74	9.99	57.53	13.00	68.16	0.52	0.08	73.14
	144WW	4.48	53.26	3.88	9.65	58.50	13.10	69.55	0.49	0.14	73.02
Forest Home	145F	5.34	57.47	4.83	8.79	56.49	10.85	68.97	0.58	0.00	75.26
	126W	5.44	58.11	5.32	8.68	56.78	10.87	70.51	0.57	0.02	75.89
	127WW	5.45	59.38	5.62	8.73	56.72	10.85	71.47	0.58	0.00	76.22
Smith's Corner	128F	4.96	62.32	5.08	9.66	55.86	12.20	70.70	0.59	0.00	74.71
	129W	5.30	59.77	5.89	9.05	56.72	11.31	73.61	0.58	0.02	75.45
	140WW	5.08	54.44	6.03	8.39	59.32	11.36	75.07	0.49	0.18	75.17
Pre-Triassic	2-201	4.51	55.25	3.07	10.66	54.21	13.55	63.09	0.58	0.00	73.26
	2-193	4.71	52.11	3.46	10.03	56.18	13.07	67.13	0.51	0.13	72.76
	2-168	4.52	50.65	6.49	8.79	63.91	13.04	82.34	0.36	0.38	72.47
	2-139	4.82	49.82	10.20	8.11	65.89	12.54	89.44	0.36	0.38	74.15
	2-110	4.07	41.39	13.04	6.82	73.79	13.02	94.75	0.25	0.57	72.32
Pre-Carboniferous	1134	4.39	56.23	3.17	10.82				0.58	0.00	72.38
	1125	5.04	54.52	3.62	9.79				0.59	-0.03	74.72
	1119	4.26	7.22	3.75	4.90				0.13	0.78	69.42
Pre-Carboniferous	1184	4.50	54.37	3.21	10.47				0.56	0.00	73.10
	1176	3.91	6.50	6.33	3.46				0.09	0.84	69.74
	1168	4.13	7.96	4.58	4.48				0.13	0.78	69.23

Table 5.3. Selected weathering indices applied to saprolite suites of the South Mountain Batholith. Note that CIA, WPI and CIW were not calculated for the Pre-Carboniferous samples, as it was not possible to determine the proportions of cations attributable to weathering rather than to diagenesis.

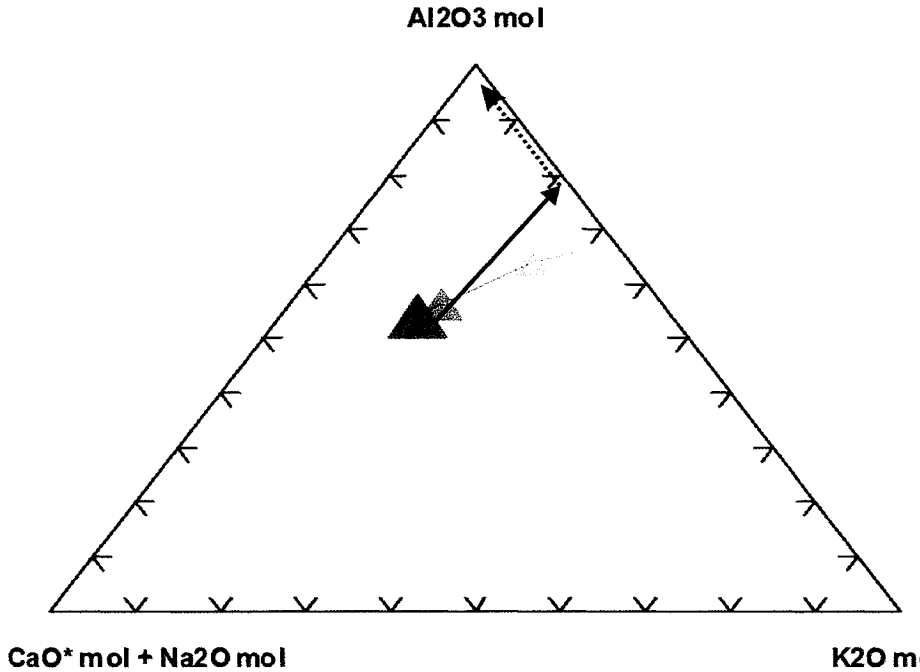

Fig. 5.3. A-CN - K (mol %) diagram for Pre-Triassic saprolite suite. Darkest and largest triangle is fresh; smallest and lightest triangle is from top of preserved section. Black arrows are projected weathering trend of Nesbitt and Young (1989).

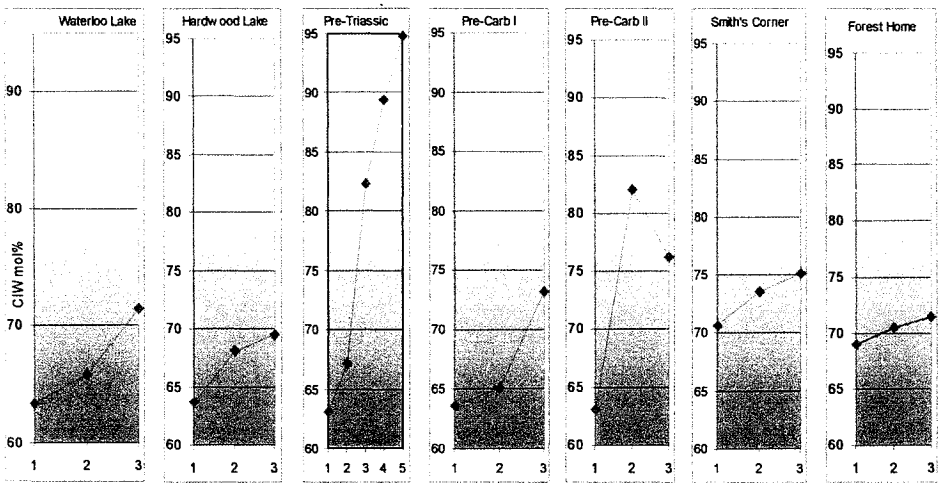

Fig. 5.4. CIW (chemical index of weathering) in mol % versus degree of weathering. 1 trough 5 is from fresh (1) to most weathered (3 or 5). Waterloo Lake and Hardwood Lake are Pre-Pleustocene biotite monzogranite; Pre-Triassic is biotite monzogranite; Pre-Carboniferous is biotite monzogranite; and Smith's Corner and Forest Home are Pre-Pleistocene moznogranite.

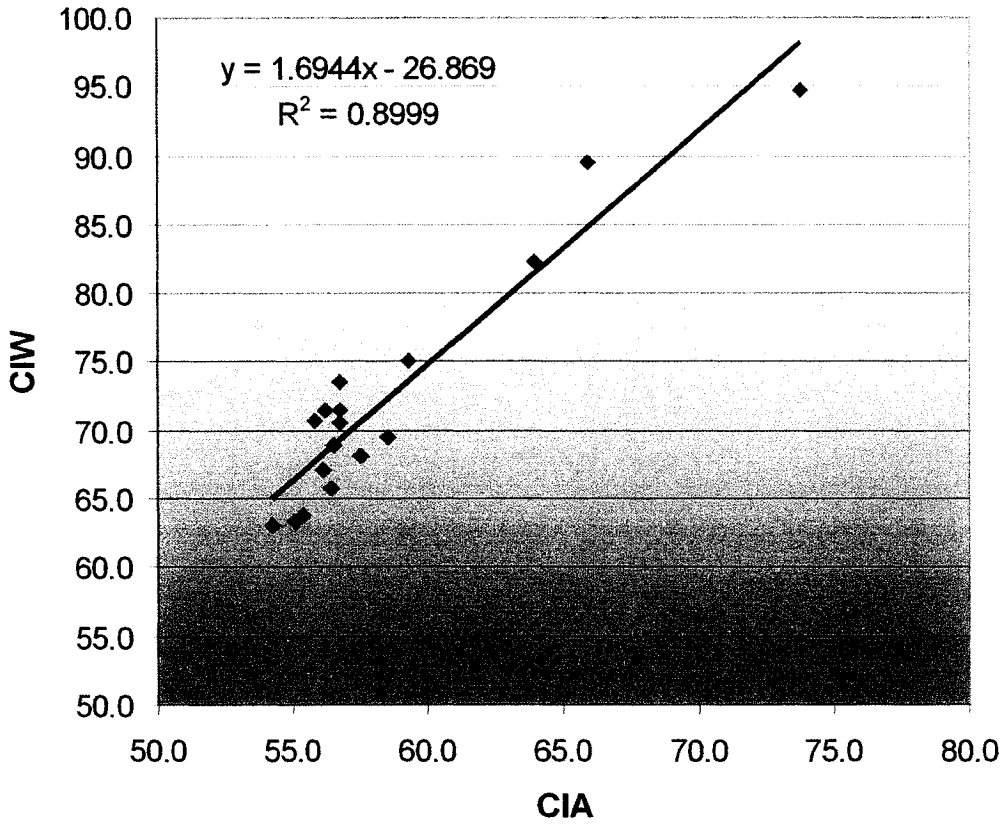

Fig. 5.5. Chemical Index of weathering (Harnois, 1988) vs Chemical Index of Alteration (Nesbitt and Young, 1984) for Pre-Triassic and Pre-Pleistocene suites.

In addition to the weathering indices outlined in the previous paragraph, these authors, and others (Middleburg et al., 1988; Nesbitt and Markovics, 1997; Van der Weijgen and Van der Weijden 1995), use immobile minor or trace elements as normalizing factors. Titanium is used as a normalizing factor with Zr by Van der Weijgen and Van der Weijden (1995), who argue for the combination Ti and Zr, as these occur in different minerals, and the combination provides a more complete picture than either Ti or Zr alone. Gouveia et al., (1993), Middleburg et al., (1988), Nesbitt and Markovics (1997), and conclude that Ti is not mobile during weathering, and hence Ti can be considered a reasonable normalizing element. However, Gardner et al. (1978) discusses the mobility of Ti under weathering conditions, and Nesbitt (1979) concludes that Ti may be mobilized from within a mineral, but is immediately re-precipitated into a new phase. Use of Ti with or without Zr relies on the presence of Ti-bearing minerals in

the rocks. In more highly differentiated granitoids, significant Ti-bearing minerals may be few, and hence the choice of Ti as a normalizing element is such cases is not justified, as argued by Nesbitt and Young (1982), who chose Al rather than Ti as the normalizing element in rocks of very low Ti content. Mongelli (1993) also considered Al immobile during weathering. A comparison of the effects of normalizing the South Mountain Batholith data against Al as opposed to Ti, indicate that both elements result in similar elemental trends for most suites (Fig. 5.6). In the Smith's Corner data set, where Ti is in the 100 ppm range in contrast to the 1000 ppm range for the other granitoids analyzed, the elemental increases suggested by normalizing against Ti are not the same as those indicated by normalizing against Al, particularly in the case of the elements Si, Na, K, and P (Fig. 5.6). However, in all other suites of samples from the SMB where the Ti content is above 1000 ppm, the results of Al-normalization and Ti-normalization are similar. Titanium in the fresh rock of the weathering profiles of the South Mountain Batholith resides in biotite and titanium oxide minerals. Gardner et al. (1978) propose that during isovolumetric weathering, Ti decrease in the early stages of weathering, as measured by decreases in bulk density changes in the rock, is the result of breakdown of biotite. Textural and mineralogical evidence from the weathering profiles of the Pre-Triassic and Pre-Pleistocene saprolites, indicate that even when the biotite weathers significantly and the Ti is mobilized, the Ti remains locally in the system in the form of Ti or Fe-Ti oxides and oxyhydroxides. This localized re-precipitation of Ti, and the fact that in the case of the trace elements, the proportions of these elements are more akin to the proportions of Ti rather than Al, resulted in the choice of Ti as the normalizing element for the weathering profiles of the study area, with the caveat that at lower levels of Ti (<1000 ppm), caution should be exercised in interpreting absolute values of % increases or decreases.

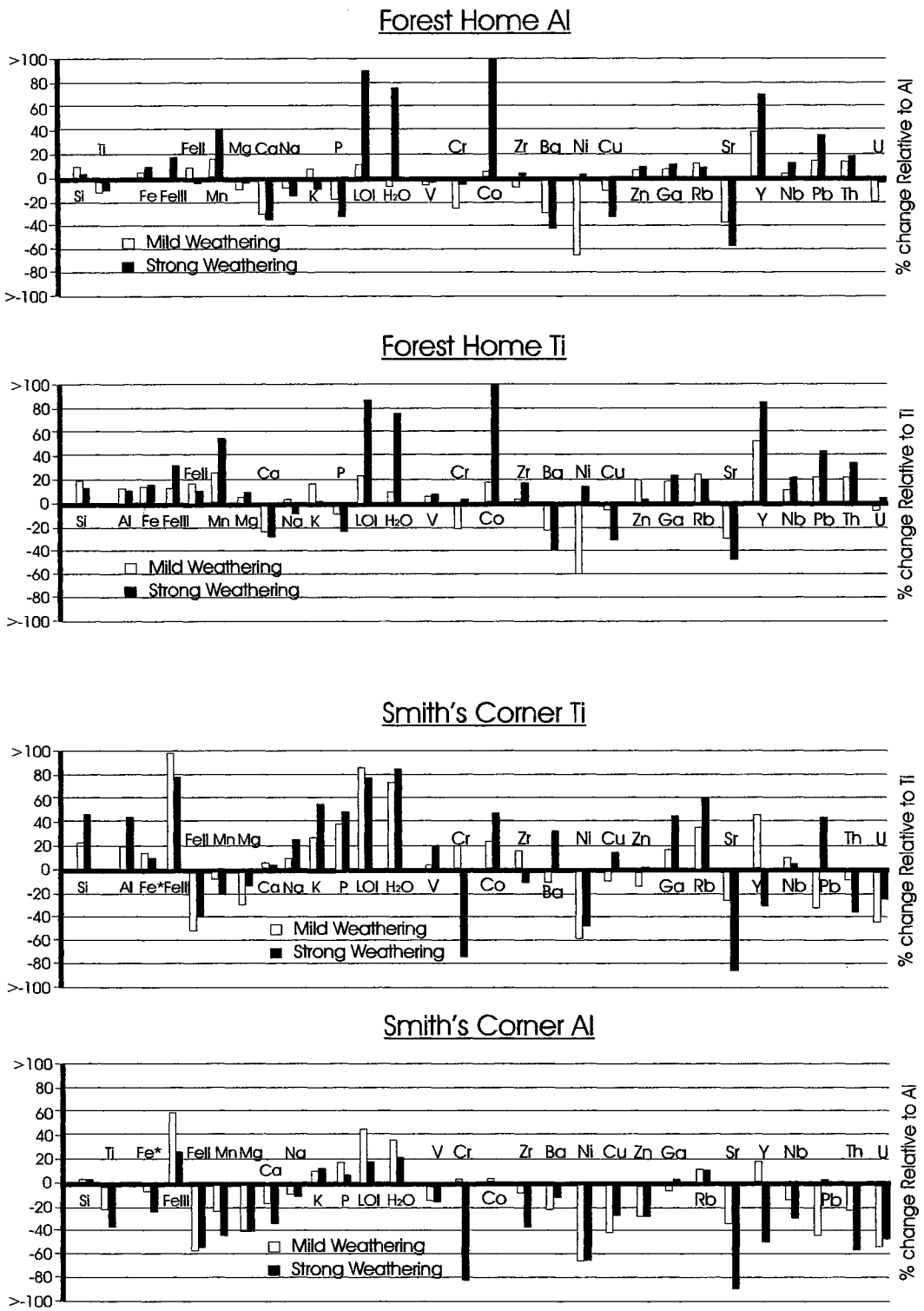

Fig. 5.6. Major and trace element % changes comparing normalization to Ti and Al for Forest Home and Smith's Corner, showing close agreement between losses and gains for Forest Home. Samples are normalized to "fresh" parent, represented by the zero line. For the low-Ti Smith's Corner granitoid, greater differences exist between normalization against Ti and Al, and therefore caution is required when interpreting data from horizons where the parent rock has low Ti content.

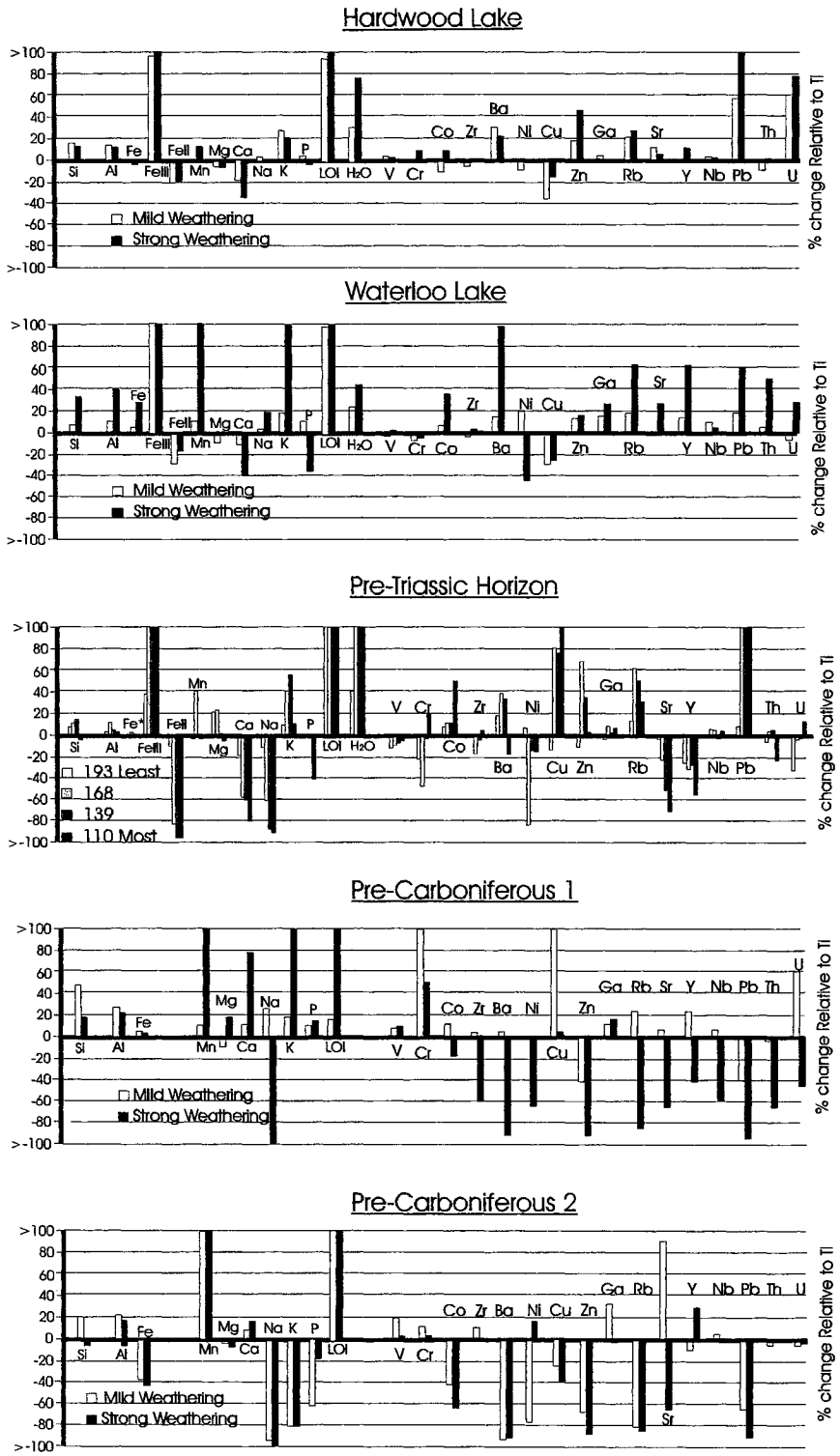

Fig. 5.7. Major and trace element data for biotite monzogranites of Pre-Pleistocene (Waterloo and Hardwood Lake), Pre-Triassic, and Pre-Carboniferous (I and II) saprolite suites. Data normalized to Ti: % change of element X = $[(X/Ti)_{sample} / (X/Ti)_{parent} - 1].100$ (after Nesbitt, 1979); "fresh" parent is normalizing factor, and is represented by the zero line above.

5.4.1 Major Element behaviour during weathering

Changes in weight % of major and trace elements normalized against Ti for each of the weathering suites is graphically represented in Figure 5.7. Fe^{2+}/Fe^{3+}, H_2O^+ and Hg were not determined for the Pre-Carboniferous samples. Differences of less than 20% are not considered significant, as they may reflect sample inhomogeneity or analytical error, in agreement with the interpretations of Cramer and Nesbitt (1983) and van der Weijden and van der Weijden (1995). Increased degree of weathering as determined by field relationships is generally confirmed in the geochemical changes observed. For all suites, notable increases are demonstrated for Fe^{3+} (where measured), LOI, and H_2O^+ (where measured), and decreases are typically observed for Fe^{2+} (where measured) and Ca, with the exception of the Pre-Carboniferous samples, where Ca content increases, in which case, the increase is attributable to post-weathering addition of Ca. The total Fe does not change significantly throughout the weathering process; the increase of Fe^{3+} at the expense of Fe^{2+} reflects the importance of the oxidation process during weathering, and the subsequent re-precipitation of the iron in the immediate environment. Other elemental changes are not consistent between samples, although in most suites, there is a tendency toward decreased P with increased degree of weathering (Fig. 5.7), and for the Pre-Triassic and Pre-Carboniferous suites where weathering has progressed to a greater degree than in the Pre-Pleistocene suites, a decrease in Na is also evident (Fig. 5.7). The behaviour of elements such as Mn, K, and Si is variable between the suites, and is discussed in more detail under Section 5.5 below.

5.4.2 Trace element behaviour during weathering

The data for trace element changes in the weathering suites of the South Mountain Batholith exhibit more variability than the major elements, and most trends that do appear in the younger weathering profiles (Pre-Triassic and Pre-Pleistocene), are not recorded in the Pre-Carboniferous profiles. In the case of the Pre-Carboniferous suite, essentially all trace elements decrease with increased degree of weathering (Fig. 5.7).

Within the Pre-Triassic and the Pre-Pleistocene profiles, there are some broadly similar trends: Rb, Pb, Ba, and Co tend to increase on weathering relative to Ti contents (Fig. 5.7), although in the Forest Home suite, Ba decreases on weathering (Fig. 5.6). Ma and Liu (2002) discussed how Th and Co were immobile in the weathering environment, and Th was also regarded as immobile by Nesbitt (1979). In the suites of this study, Th behaviour is not consistent from fresh to weathered samples (Figs. 5.6 and 5.7). Mongelli (1993) suggested that Cr is mobilized during weathering as a result of oxidation to form a soluble chromate ion, as indicated in Van der Weijgen and Reith, (1982). Chromium data for the saprolites of the South Mountain Batholith do not show a consistent trend within the different suites (Figs. 5.6 and 5.7). Decreases in Cu and Ni levels are recorded in most, but not all of the suites (Figs. 5.6 and 5.7), Ni decrease being consistent with the findings of Turekian (1978). Deviation from these results for individual suites is discussed further below, in Section 5.5.

5.4.3 Rare earth element (REE) behaviour during weathering

Rare earth element data normalized to chondrite, are presented in Table 5.1 and Fig. 5.8. All suites have a negative Eu anomaly, which typically becomes more pronounced with increased degree of weathering (Fig. 5.8). For all suites, with the exception of the behaviour of the HREEs (heavy rare earth elements) in the Waterloo Lake most-weathered sample, and the behaviour of La in the Hardwood Lake samples, there is a general decrease, or little change, in REEs from fresh to weathered samples, in all but the Forest Home suite (Fig. 5.8). Some fractionation of REEs is also observed, as the HREEs are typically more depleted than the LREEs (light rare earth elements) in the weathered samples.

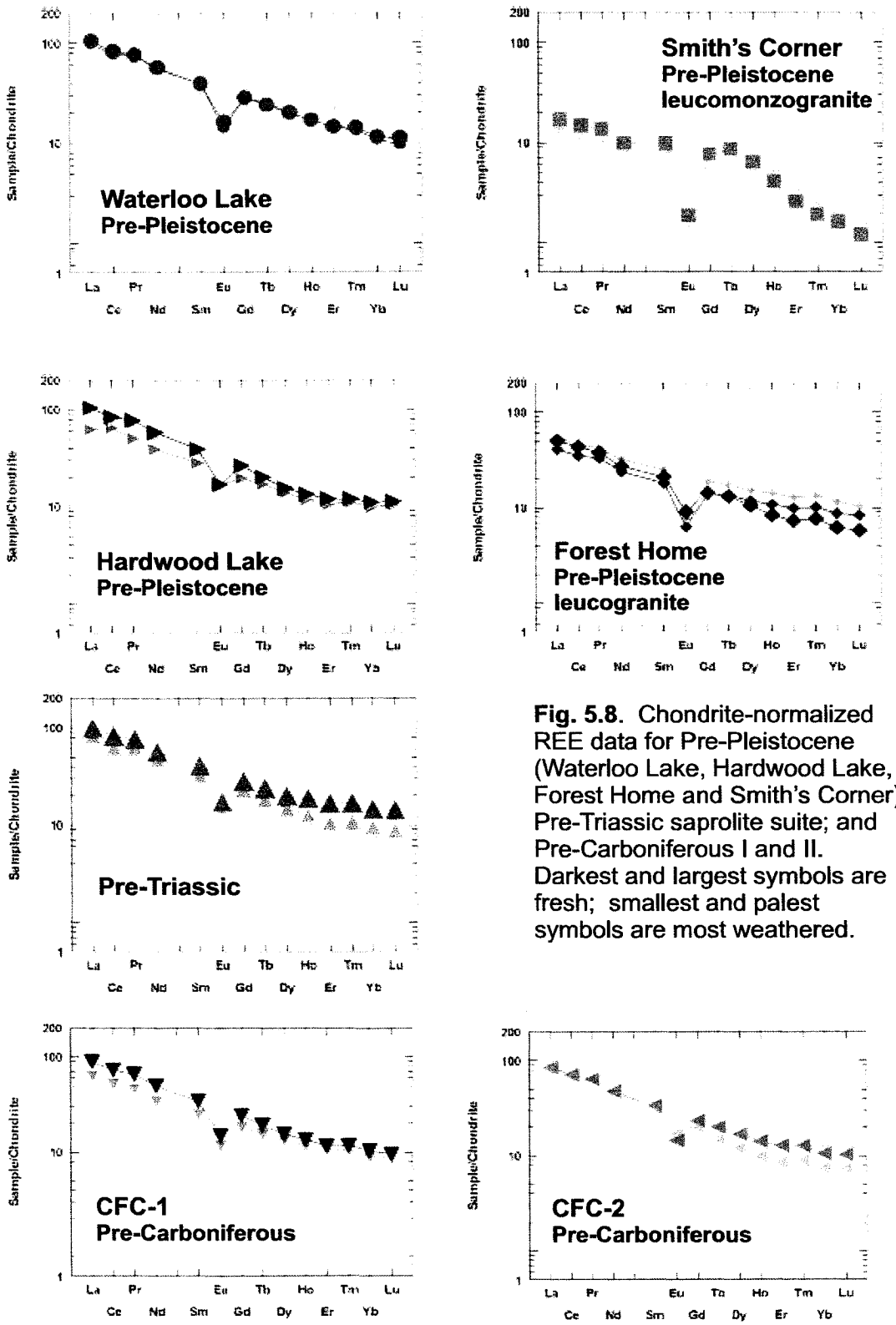

Fig. 5.8. Chondrite-normalized REE data for Pre-Pleistocene (Waterloo Lake, Hardwood Lake, Forest Home and Smith's Corner); Pre-Triassic saprolite suite; and Pre-Carboniferous I and II. Darkest and largest symbols are fresh; smallest and palest symbols are most weathered.

5.5 Discussion

The South Mountain Batholith is a multi-phase peraluminous granitoid complex, with a variety of known mineral occurrences, in particular Sn with related elements, and U with related elements (Chatterjee and Muecke, 1982). In selecting samples for determination of chemical effects of weathering, mineralized regions were avoided in order to establish chemical signatures that could be attributed to weathering. However, it is recognized that weathering of sites with known mineralization would most likely lead to the release of elements such as U or other potentially toxic elements.

Chemical weathering results in changes in the bulk rock geochemistry that reflect both the conditions of weathering and the mineralogy and texture of the parent rock. The sequences documented in this study provide information about the early, or incipient, stages of weathering of the granitoids of the South Mountain Batholith, although the Pre-Carboniferous suites have more dramatic depletion of cations and concomitant increase in aluminum, more typical of regions of greater intensity of weathering of granitoid rocks.

5.5.1 Major element behaviour during weathering

Weathering as reflected in the geochemistry of the pre-Triassic sequence, provides the most complete undisturbed sequence of weathering for the sequences observed within the South Mountain Batholith. This discussion focuses first on the chemical changes in the pre-Triassic sequence, and is followed by discussion of any deviations from this in the older and younger sequences.

Changes in major element chemistry from parent to most weathered are broadly similar to those documented by Nesbitt (1979), Nesbitt et al. (1980), Middleburg et al., (1988), and Fritz (1988) with significant depletion of Na, Ca, and increases in hydration (LOI and H_2O^+ increases) and oxidation effects (Fe^{3+} / Fe^{2+} increases) (Table 5.1, Figs.5. 3 and 5.7). However, deviations from the predicted general trend for granitoids as represented by Nesbitt et al. (1980), are present in the weathered sequence of the pre-Triassic samples of SMB (Fig. 5.3), and reflect the retention of K in the more weathered

samples of this suite. The retention of K, and indeed also of Mg (Table 5.1, Fig. 5.7), is attributed to the persistence of at least some of the biotite as well as much of the alkali feldspar throughout almost all of the preserved weathered horizon. Continuous depletion of Ca and Na with increased degree of weathering is evident (Fig. 5.7), and reflects the early breakdown of plagioclase feldspar. In the most advanced weathered sample, the relative decrease in K (Fig. 5.7) reflects the more intense onset of weathering of potassium feldspar; the persistence of Mg in the most weathered sample (Fig. 5.7), reflects the persistence of some of the biotite, even at this more advanced stage of weathering.

Major element behaviour for the Pre-Pleistocene suite is similar to that of the Pre-Triassic suite, particularly to that of the less weathered samples of the Pre-Triassic suite (Figs. 5.4, 5.6, and 5.7). In the Pre-Carboniferous suite, the behaviour of Ca and Mn deviate significantly from the expected behaviour when compared to the younger suites of this study (Fig. 5.7), and from the sequences documented for example, by Middleburg et al. (1988) and Van der Weijden and Van der Weijden (1995). This increase in Ca and Mn in the Pre-Carboniferous horizons can be attributed to the addition, post-weathering, of Ca and Mn to these horizons. Field observations of Mn-rich coatings on surface exposures of remnant corestones from the pre-Carboniferous weathering event, as well as thin section textural and mineralogical evidence, further supports the later addition of Ca and Mn to the system. The elevated Mn levels are also consistent with the economic Mn mineralization found in granitoids in the surrounding region (Chatterjee, 1983). The re-lithification and subsequent Mn mineralizing event may mask the chemical signature of the weathering event, and the significant decreases in trace elements for these Pre-Carboniferous horizons cannot categorically be assigned to weathering alone, although it is not possible to determine the relative degree of impact of the weathering and later thermal processes. Textural, mineralogical and chemical evidence suggests that the Mn mineralization in the granitic rocks of the region post dates a major weathering event, and it is possible that the highly permeable granite saprolite served as a conduit for the later Mn-rich fluids which formed the economic deposits in the region.

The most significant and consistent changes evident in the weathering of both

the pre-Triassic and the pre-Pleistocene sequences are the notable change in Fe-oxidation and the increase in hydration (Figs. 5.6 and 5.7), (Fe^{2+} / Fe^{3+} data not available for the Pre-Carboniferous suites). The data from this study are in agreement with Fritz (1988), who suggested that an increase in the Fe^{3+} / Fe^{2+} ratio is a good indicator of the onset of weathering, and with Sueoka et al. (1985), who suggest LOI as a possible index of weathering. Oxidation and hydration work together to begin the weathering of biotite, and the feldspars respond primarily to the effects of hydration. However, the total Fe remains relatively unchanged particularly throughout the younger sequence, which means that although it is mobilized, Fe is retained locally as insoluble Fe^{3+} oxides and oxyhydroxides, in agreement with Nesbitt (1979), Middleburg et al. (1988), and van der Weijden and van der Weijden (1995). The increase in H_2O^+ in each of the weathered samples attests to the increase in the structural H_2O present in the lattices of the weathered minerals, that is, this increase reflects the development of clay minerals. The significance of these increases in the weathered samples of oxidized and hydrated minerals lies in their ability to serve as sorbants for metals released as weathering progresses (Smith and Huyck, 1999, Van der Weijden and Van der Weijden, 1995), which may in turn result in temporary or long-term retention of liberated elements within the system.

Perel'man (1986) discusses the concept of geochemical barriers in the formation of ore deposits. The term "geochemical barrier" refers to the existence of sharp chemical gradients, which may result in the precipitation of elements. The development of these barriers is related to changes in temperature, pressure, Eh, and / or pH (Perel'man, 1986). In the surface environment, changes in oxidation-reduction, pH, and to a lesser extent temperature, will produce such barriers during weathering. Given that the geochemical evidence indicates that the environment in which these weathered horizons formed was oxidizing (certainly in the case of the pre-Triassic and pre-Pleistocene horizons), whether a given element is mobilized depends in large part on the pH conditions, the parent mineralogy, and possibly the texture of the parent rock. The formation of Fe and Mn oxides and oxyhydroxides, and clays, introduces oxide and perhaps acidic barriers, which can then result in the adsorption of other elements following their release during weathering. Jenne (1968, 1977) similarly concluded that hydrous oxides of Mn, Fe, as well as clays, are major controls on metal sorption.

Furthermore, the increase in surface area during the physical breakdown of rock provides more potential sites for adsorption to occur.

Perel'man (1986) summarized the behaviour of these secondary phases, and concluded that the clay minerals and Mn hydroxides which have negative surface charge are more likely to adsorb metals, whereas Fe hydroxides with their positive charge are more likely to adsorb P, As, V, and other anions. However, Perel'man (1986) also concluded that Fe-hydroxides typically also have negatively-charged organics or silica associated with them, and therefore, may also adsorb cations. The adsorption of cationic or anionic species (and complexes) onto these secondary phases results in retention of elements locally within the system, as long as conditions remain similar. However, changes in pH, Eh, and / or temperature may result in the subsequent release of these relatively loosely-held elements from their adsorbing hosts. This complex interplay of adsorption-desorption depending dominantly on pH and Eh in the near-surface environment, can explain the variability in proportions of elements in different weathering horizons. In addition, the possibility of changing conditions through time makes it is very difficult to make generalizations as to element behaviour from one weathering horizon to another, or from one depth within the same weathering horizon to a shallower or deeper level, or indeed, for the same weathering horizons at different times.

5.5.2 Trace Element Behaviour during Weathering

Increases in Rb and Ba in particular have been attributed to adsorption or incorporation into the newly-formed clay minerals (Mongelli, 1993), and to retention in K-feldspar during the earlier stages of weathering (Fritz et al., 1988). Garrels and Christ (1965) suggested that Rb is concentrated and retained during the weathering process, as the heavier alkali metal elements are preferentially incorporated into, or adsorbed onto, the newly-developed clays. Wronkiewicz and Condie (1987) similarly concluded that the larger cations Rb and Ba are fixed during weathering and remain in the system, unlike Sr, Ca, and Na, which are more readily leached from the system. The increase in Rb, Pb and Ba in the Pre-Triassic and Pre-Pleistocene suites relative to Ti (Figs. 5.6

and 5.7) is consistent with these interpretations, and is attributed to retention of these elements in K-feldspar, and perhaps in addition to adsorption on, or incorporation into newly-formed clays, as it is only in the uppermost levels of the Pre-Triassic suite that K, Ba, and Rb relatively decrease (Fig. 5.7), and that the K-feldspar is increasingly weathered to clay minerals. Comparison of data from aqua regia digestion and XRF analysis for Pb in particular, indicates that Pb is minimally dissolved during aqua regia digestion, and thus most likely held in silicate phases (Table 5.3). Barium in the Forest Home suite also follows the behaviour of K in this suite, and suggests that the K-feldspar is more susceptible to weathering in this rock (Fig. 5.6).

5.5.3 Redox-sensitive elements

Given the measured changes in increased proportions of Fe^{3+} / Fe^{2+} during weathering of the pre-Triassic and pre-Pleistocene suites (this ratio is not known for the pre-Carboniferous suites), the importance of oxygen in the weathering environment is significant, and may be reflected in the variable behaviour of U, V, Cr, Ce, Eu and other redox-sensitive elements (Figs. 5.6 and 5.7). The lack of consistent weathering trends for these elements may be explained by a combination of retention of these elements in insoluble or weakly-soluble phases such as zircon, and partial adsorption of these elements on the newly-formed Fe-Ti oxides and oxyhydroxides, and clays, and the removal of some ions of these elements in solution. The behaviour of U is discussed further in Chapter 6.

McKinney and Rogers (1992) established that the elements of most interest / concern to the Environmental Protection Agency (US), include the following: Al, As, Ba, Cd, Cr, Co, Cu, Pb, Mn, Hg, Mo, Ni, Se, Ag, Na, Tl, V, and Zn. Of these elements, those regarded as "characteristically hazardous" include As, Ba, Cd, Cr, Pb, Hg, Se, and Ag; Cr and Se, and maybe As, Ba, and Pb, are also considered possible nutrients in low quantities. On the other hand, nutrients that are toxic at higher levels, include Co, Cu, I, Fe, Mn, Mo, Ni, V, and Zn, as well as possibly Be and Li. The elements Al, Be, and Tl are not considered nutrients at any level (Goyer, 1991). Uranium and Th can also be included in a list of elements-of-concern, as they are radioactive. Of the hazardous

elements, Ba, Cr and Pb may reside in major minerals (Levinson, 1980). Ba can reside in K-feldspar, biotite, plagioclase, and muscovite; Chromium can be found in the micas; and Pb in K-feldspar and biotite (Levinson, 1980). Geoavailability of an element or compound as defined by Plumlee (1999), refers to the portion released to the surficial or near-surficial environment through mechanical, chemical or biological processes, which in large part is related to the minerals present in the earth material in question, and the weathering processes and products. In the SMB, Ba is concentrated in the weathering process, but is generally regarded as somewhat mobile under all environmental conditions (Smith and Huyck, 1999). Perel'man (1986) suggested that Ba can be precipitated when the pH of the solution is increased, so initial release of Ba in acidic conditions may be followed by concentration of Ba on clay minerals as the solutions increase in alkalinity with increased dissolution of feldspars. Lead consistently increases during weathering of the SMB, in part as a result of adsorption on secondary minerals, and in part due to retention in K-minerals. However, under near neutral reducing conditions, Pb may be released, as these conditions may also result in the formation of soluble Fe^{2+} on reduction of Fe^{3+} oxides and oxyhydroxides (Smith and Huyck, 1999; Perel'man, 1986). Similarly, any other element adsorbed onto Fe^{3+} secondary minerals, may be released under reducing conditions if Fe^{3+} is reduced to soluble Fe^{2+} (Smith and Huyck, 1999).

The Pre-Triassic and Pre-Pleistocene weathering horizons maintain relatively high levels of many of the trace elements relative to the host rock. Given the highly fractured and permeable nature of these materials, the development of secondary Fe oxides and hydroxides and clay minerals, and the probable adsorption of some elements onto these secondary minerals, there is potential for release of hazardous elements as surface conditions change. Future studies of waters associated with these horizons are necessary to determine which, if any, of these potentially hazardous elements are subject to mobility under present-day conditions. In particular, U levels in water have been documented to vary depending on rainfall (Rose and Keith, 1976; Wodicki, 1959), and also to be elevated, even when not found in elevated quantities in the underlying rocks (unpublished report, O'Beirne-Ryan, 1999; and Dall' Aglio,1971).

The depletion of all trace elements in the weathering horizon of the Pre-

Carboniferous suites where Mn and Ca are increased, suggests that the depletion of the trace elements occurred prior to the increase of Mn and Ca; Mn oxides and oxyhydroxides would typically serve as adsorbants for elements such as Cu, Co, Zn, Ni, Ba, and Sr (Rose et al., 1979), none of which are elevated in the upper weathering levels of the Pre-Carboniferous suites. The strong depletion of these elements during this weathering event suggests an intense weathering environment, in which most elements were leached. Such intense leaching more typically reflects a hot, humid environment during Early Carboniferous times, and is consistent with the sub-equatorial location of Nova Scotia during the Devono-Carboniferous.

5.5.4 REE behaviour during weathering

The REEs in most suites are increasingly depleted, or relatively unchanged on weathering, except for an increase in HREEs in the Waterloo Lake suite, where garnets associated with xenoliths are locally significant in the monzogranite. A general trend towards greater depletion of HREEs relative to LREEs is evident for some of the suites (Fig. 5.8), consistent with that noted by Nesbitt (1979). The variability in the REE patterns of the Forest Home suite where total REEs are lower than in other suites, may be the result of the inhomogeneous distribution, and greater variety of accessory minerals hosting the REEs within this granitoid.

The tendency in the SMB suites for decreasing amounts of REEs during weathering is counter that observed by Nesbitt (1979) and Middleburg et al. (1988), but similar to that documented by Koons (1978). However, Nesbitt concluded that the behaviour of the REEs is dependent on pH conditions, and on which minerals host the REEs. Duddy (1980) and van der Weijden and van der Weijden (1995) suggest that the REEs are concentrated differently in different levels of the weathering horizon, and van der Weijden and van der Weijden (1995) conclude that if there are no available ligands in solution, then the REEs will be mobilized, but immediately adsorbed; if there are available ligands, then the REEs may be removed from the system. Furthermore, if the REEs are concentrated in apatite or some other mineral which weathers more readily than zircon, then ther REEs may be mobilized more readily (Nesbitt, 1979). Aqua regia

dissolution of these samples results in the release of some of the La and Y, but none of the Zr (Table 5.4), indicating that at least some of the REEs (and Y) reside in phases more soluble than zircon. The REE patterns of the weathering horizons of different ages result in a similar chondrite-normalized pattern on weathering (Fig. 5.8). Given that the weathering conditions for the horizons are likely different (O'Beirne-Ryan and Zentilli, 2003), yet the behaviour of the REEs is similar for all ages of weathering, the dominant control on the behaviour of the REEs during weathering is most likely the parent mineral composition.

5.6 Conclusions and recommendations

The geochemistry of the weathered horizons of the South Mountain Batholith reflect the nature of the parent mineralogy as well as the nature of the weathering environment at a given time in the geologic past.

Increases in Fe^{3+} / Fe^{2+} ratio and degree of hydration are excellent indicators of weathering intensity for these rocks. Decreases in Ca as well as P and Na are also typical of weathering processes on the South Mountain Batholith.

Increases in K, Ba, Rb, Pb, and Co are generally observed, particularly in the earlier stages of weathering.

Other elements do not exhibit consistent trends between different suites, reflecting the effects of parent mineralogy and environmental conditions on element liberation.

The incomplete removal of elements from the younger suites, and the more complete removal of elements from the Pre-Carboniferous suites, indicate that further element mobility from these horizons is possible under changing surface or near-surface conditions, for example, acidic precipitation.

Further studies should include analyses of saprolites from sites of known hydrothermal alteration, in order to assess the impact of weathering on such

hydrothermal alteration. Additionally, analyses of waters flushing through hydrothermally altered as well as unaltered saprolites, under different seasonal conditions and differing degrees of acidity of precipitation, will contribute to understanding the potential for U and other elements to be remobilized under hydrological and climatic conditions operating today over regions of saprolite within the South Mountain Batholith.

Chapter 6

Investigation of the Potential for Weathering of Granitoids to Liberate or Concentrate Environmentally Sensitive Elements, Hg, Rn, and U

Introduction

The geologic environment can contribute to elevated levels of naturally occurring toxic elements to the environment (Siegel, 2002). The possibility for Hg and / or Rn-U liberation into the environment as a result of weathering of granitoid rocks is the focus of this chapter.

Section 6.1 is an excerpt from a published document, and represents the author's contribution to a larger transdisciplinary study on Hg in the environment at Kejimkujik National Park in southern Nova Scotia (Smith et al., 2005). The section included herein represents the component contributed by A.M. O'Beirne-Ryan, with suggestions from coauthors.

Section 6.2 is an unpublished report on work related to radon and uranium in well waters and radon in indoor air undertaken by the author, for the Nova Scotia Department of the Environment (1999, unpublished report). The collation of pre existing data, GIS compilation, and interpretation as included herein, were undertaken by the author.

The remainder of the chapter addresses uranium distribution within the weathered horizons, and implications for potentially elevated U and Rn in waters and soils. Portions of this section have been presented in posters and abstracts, and represent work undertaken by the first author, with editorial contributions from other

authors (O' Beirne-Ryan and Zentilli, 2002; 2004; 2005; 2006).

6.1 Mercury release potential on weathering of granitoid rocks

Introduction

As part of a transdisciplinary study on Hg in the environment surrounding Kejimkujik National Park, southern Nova Scotia (Smith et al., 2005), a study of the potential for the release of Hg into the environment from weathering granitoids was undertaken by the author (Smith et al., 2005). The transdisciplinary study was initiated when high levels of Hg were found in loons in Kejimkujik National Park, although there was no known definitive source of this Hg contamination (Burgess et al., 1998; O'Driscoll et al., 2005). As part of the transdisciplinary study, the geologic environment was targeted for sample collection and analysis in order to assess the potential for rock, sediment and soil as the possible source of the mercury. An additional question arose as to whether the granitoids underlying parts of Kejimkujik Park could be contributing to the elevated Hg in the loons as a result of weathering of the granitoid. In order to establish the potential effects of weathering on Hg release from granitoid rocks, samples for this aspect of the transdisciplinary study included whole rock samples of variably weathered granitoid as described in chapter 5, and biotite separates from selected samples of monzogranite. The portion of the manuscript by Smith et al. (2005) undertaken by the author is included in 6.1.1; the only modifications are to format, to comply with the overall format of the thesis, and the inclusion of Table 6.3, the raw data on saprolite suites for the study.

6.1.1 Weathering effects on Hg content in Granitoids

A concurrent study of weathering within the granitoids of the South Mountain Batholith, indicates that these rocks have undergone three separate episodes of subaerial weathering since their intrusion *circa* 372 million years ago (O'Beirne-Ryan

and Zentilli, 2003, 2002). In some cases, the weathered horizon, or saprolite, is preserved *in situ* (Fig. 6.1). Although granitoid outcrops within the Park itself are few, numerous outcrops of granitoids in the surrounding regions indicate that these rocks have been weathered to depths of 5 metres at surface, or beneath a cover of glacial till of Pleistocene age, indicating that the most recent significant weathering event occurred in pre-Pleistocene times (O'Beirne-Ryan and Zentilli, 2003). In drill core beneath unconformities with Carboniferous (the oldest weathering event) and Triassic rocks, these weathered horizons are up to 30 metres in thickness (O'Beirne-Ryan and Zentilli, 2003). The existence of these weathered horizons together with their underlying unweathered parent, provide an opportunity to study the effects of this chemical and physical weathering on the Hg and other element contents of the rock; chemical weathering of rock being one possible significant process involved in the release of Hg into the environment. Relatively low levels of inorganic Hg released through weathering, may become concentrated or more readily bio-available through this process. Of further concern, is that these outcrops of weathered granitoid provide gravel for use in roadbeds, and a number of these outcrops have been extensively quarried for this purpose. One such previously excavated burrow pit is located near the eastern margin of the Park, and local residents report that this had been the source for some of road gravel within the Park itself. Unfortunately, this particular burrow pit has been abandoned and is now overgrown, so no sample was available from this site. However, samples from similar excavations in the region are included in the data for weathering effects and mercury content. Fresh granitoid parent and weathered granitoid samples from the same location are compared (Tables 6.1 - 6.3) in order to document and interpret the effects of weathering on the mercury content of the saprolites.

In order to evaluate the possibility of Hg-release or concentration during weathering of the granitoids, 20 samples, also selected for major and trace element geochemistry, were analyzed for total Hg at ACME Laboratories, Vancouver, B.C.. These 20 samples were taken from 5 surface sites of weathered horizons of pre-Pleistocene age, and one site of drill core, where the weathered horizon is overlain by clastic sediments of Triassic age. These sites were selected as representative of weathered horizons that may also exist beneath the glacial cover in other regions, for

example, in or around Kejimkujik Park.

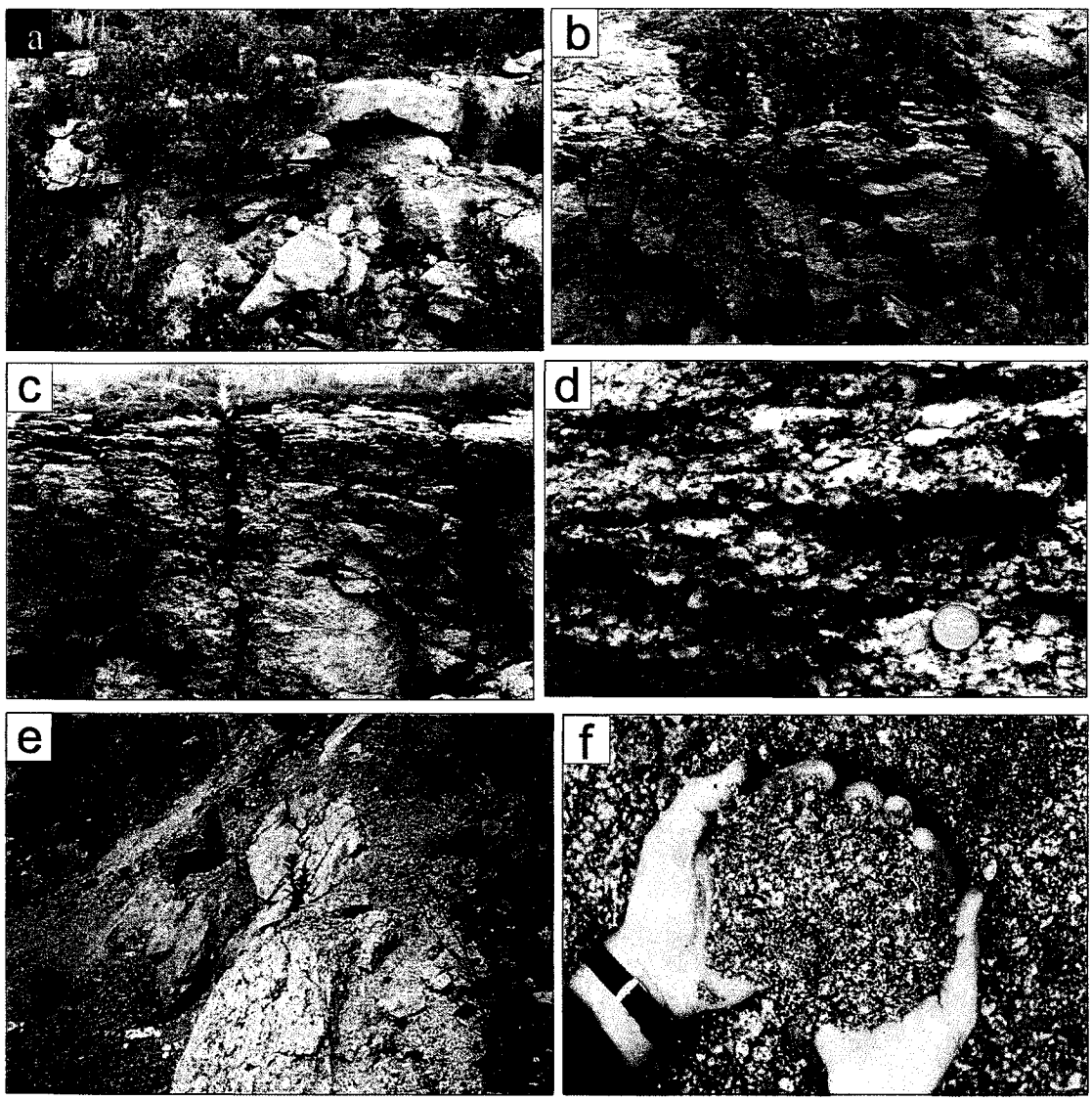

Fig. 6.1. Variably weathered granitoid from South Mountain Batholith: **(a)** fresh granitoid, Highway #101 near Bridgetown; **(b)** incipiently weathered granite, proximal to (a); **(c)** moderately weathered granitoid, with weathering more intense along jointing; **(d)** close-up of (c); **(e)** corestone of fresh granitoid surrounded by strongly weathered saprolite, Highway #101, near location (a); **(f)** intensely weathered arenaceous saprolite, showing crumbly nature of this material.

Lithology	Average Aplite	Average Granite	Average Granite Float	Average Granite Pebbles	Granite Pegmatite	Average Grano-diorite	Average Mafic Porphyry	Average Greisen	Average Weathered Granitoid†	Average Parent† Granitoid†
Element	**n=4**	**n=96**	**n=13**	**n=6**	**n=1**	**n=8**	**n=22**	**n=3**	**n=14**	**n=6**
Al (%)	0.21**	2.01	7.30	1.04	0.17	2.43	2.30	0.39	**1.48**	**1.67**
Ti (%)	0.002**	0.12	0.27	0.09	0.001	0.41	0.19	0.01	**0.16**	**0.18**
Fe (%)	0.65	1.61	2.20	1.81	0.20	3.55	3.94	1.58	**2.21**	**2.30**
Mn (ppm)	234	414	625	354	116	703	549	306	**364**	**380**
Mg (%)	0.01**	0.28	0.48	0.34	0.01	1.08	1.43	0.03	**0.34**	**0.37**
Ca (%)	0.08**	0.57	0.76	0.16	0.20	0.23	1.33	0.20	**0.20**	**0.15**
Na (%)	0.04**	0.41	2.27	0.04	0.03	0.05	0.13	0.03	**0.02**	**0.03**
K (%)	0.17**	0.98	3.09	0.40	0.09	1.47	0.52	0.21	**0.77**	**0.83**
P (%)	0.032**	0.08	0.11	ND	0.06	0.12	ND	0.10	**ND**	**ND**
C (%)	0.20	0.13	ND	ND	ND	0.12	0.15	0.10	**ND**	**ND**
CO2 (%)	0.40**	0.40	ND	ND	ND	ND	ND	ND	**ND**	**ND**
S (%)	0.01	0.02	0.01	0.01	0.01	0.03	0.06	0.89	**BD**	**BD**
Ag (ppm)	8.3	12.0	0.1	0.1	24.0	3.0	0.1	181	**BD**	**BD**
As (ppm)	3.1	7.5	3.3	7.0	1.2	3.2	8.7	6.7	**8.3**	**10.8**
Au (ppb)	17.8**	1.5	2.0	0.5	0.5	1.5	1.4	109	**0.6**	**0.3**
B (ppm)	2.0**	4.1	ND	ND	1.0	1.0	ND	3.0	**ND**	**ND**
Ba (ppm)	16.1**	155	526	36.7	17.9	335	105	92.9	**99**	**87**
Be (ppm)	ND	2.4	2.4	ND	ND	ND	ND	ND	**ND**	**ND**
Bi (ppm)	1.15**	1.4	0.5	2.5	0.7	1.6	2.5	76.6	**BD**	**BD**
Cd (ppm)	0.01**	0.1	0.1	0.2	0.03	0.2	0.5	0.2	**5.7**	**0.0**
Ce (ppm)	ND	57.5	47.4	ND	ND	ND	ND	ND	**ND**	**ND**
Co (ppm)	1.9	4.1	5.2	5.0	0.7	8.5	19.0	2.6	**5.7**	**6.0**
Cr (ppm)	16.9**	18.7	15.6	34.0	15.8	51.8	39.5	12.8	**20.2**	**20.0**
Cu (ppm)	4.7	8.8	4.6	4.8	4.9	9.4	31.0	137	**5.5**	**6.2**
Ga (ppm)	1.0**	5.5	ND	3.7	1.2	10.6	8.4	3.0	**7.6**	**8.2**
Hf (ppm)	ND	1.5	1.1	ND	ND	ND	ND	ND	**ND**	**ND**
La (ppm)	1.1**	14.2	24.5	12.2	0.3	14.7	14.4	6.8	**15.2**	**16.2**
Li (ppm)	ND	77.5	106	81.3	ND	75.0	56.0	ND	**62.1**	**78.7**
Mo (ppm)	1.0	0.9	0.7	0.8	1.6	0.7	1.8	2.7	**0.9**	**0.2**
Nb (ppm)	ND	5.4	9.1	2.2	ND	5.0	4.5	ND	**1.4**	**2.2**
Ni (ppm)	0.6	6.5	10.8	9.5	3.8	11.5	35.8	2.2	**7.0**	**6.8**
Pb (ppm)	14.2	7.5	21.8	4.0	1.3	7.1	6.1	41.2	**4.2**	**2.0**
Pd (ppb)	ND	0.5	ND	0.6	ND	ND	ND	ND	**ND**	**ND**
Pt (ppb)	ND	<2.5	ND	<2.5	ND	ND	ND	ND	**ND**	**ND**
Rb (ppm)	ND	194	181	ND	ND	ND	ND	ND	**ND**	**ND**
Sb (ppm)	0.5**	0.6	0.8	2.5	0.1	1.3	2.5	0.6	**0.4**	**BD**
Sc (ppm)	ND	4.2	6.5	2.5	ND	10.0	6.2	ND	**5.0**	**4.7**
Se (ppm)	0.1**	0.1	ND	ND	0.1	0.5	ND	0.6	**ND**	**ND**
Sn (ppm)	ND	7.8	6.0	<10	ND	<10	<10	ND	**BD**	**BD**
Sr (ppm)	1.7**	23.1	100	2.5	6.1	5.9	53.7	2.1	**11.2**	**4.3**
Ta (ppm)	ND	2.9	1.0	<5	ND	<5	<5	ND	**BD**	**BD**
Te (ppm)	0.02**	0.3	ND	<5	ND	ND	ND	1.8	**BD**	**BD**
Th (ppm)	0.2**	7.7	10.4	ND	0.2	8.3	ND	3.6	**ND**	**ND**
Tl (ppm)	0.1**	0.4	ND	ND	0.1	0.6	ND	0.4	**ND**	**ND**
U (ppm)	0.9**	2.6	1.6	ND	0.9	2.2	ND	2.9	**ND**	**ND**
V (ppm)	1.0	22.0	34.2	21.8	1.0	73.5	70.8	10.5	**25.0**	**27.0**
W (ppm)	5.7**	3.5	1.2	<10	11.3	6.5	<10	5.6	**BD**	**BD**
Y (ppm)	ND	8.2	10.0	7.8	ND	5.0	9.9	ND	**10.8**	**11.3**
Zn (ppm)	20.8	50.2	45.1	43.8	3.7	80.1	69.8	88.3	**66.7**	**71.0**
Zr (ppm)	ND	18.7	27.7	0.8	ND	0.5	3.5	ND	**2.4**	**4.8**

* - value influenced by one or more anomalous samples.
** - value is a single analyses.
*** - assays ranged from below detection to >42 ppm.
ND - Not Determined ; **BD = Below Detection.**
† - average weathered granitoid from † average granitoid parent.
f - one or more samples not analyzed.

Table 6.1. Major and trace element data (averages) for various rock types of Nova Scotia. Columns 9 and 10 are data from saprolite suites of the South Mountain Batholith.

Average Hg (ppb) in Nova Scotia Bedrock					
Lithology	**n**	**Average**	**Median**	**Minimum**	**Maximum**
Aplite	5	9.5	1.9	0.4	42.0
Basalt	3	1.0	0.9	0.2	1.8
Biotite	28	6.0	3.8	0.8	38.9
Black Slate	58	4.5	1.6	0.2	58.6
Breccia	14	6.4	2.8	0.4	47.4
Oliver Mt.Cu Mine	8	36.9	20.7	2.5	173
Mafic Sills & Dykes	8	34.4	20.1	0.6	105
Granite	150	2.0	0.9	BD	24.0
Weathered granitoid*	**14****	**1.5**	**1.3**	**BD**	**3.1**
Granitoid parent*	**6**	**2.3**	**1.9**	**1.1**	**4.7**
Greisen	7	2.5	2.5	1.2	3.8
Meta-greywacke	86	2.7	1.4	0.04	31.8
Hornfels	29	1.2	0.9	BD	5.8
Lichen	2	130	-	125	136
Black limestone	8	202	207	64.0	333
Peat	4	81.6	69.4	38.4	149
Shear Zone	51	8.2	0.8	BD	221
Meta-Siltstone	52	2.1	0.8	0.1	19.3
Slate	85	7.4	2.5	0.1	107
Slate/Wacke	19	0.9	0.8	0.1	1.8
Vein Quartz	25	5.6	4.1	0.2	32.1
Zeolite	2	4.5	-	0.7	8.3

BD = Below Detection

*** Granitoid parent of * weathered granitoid samples**

** one sample showing alteration and weathering was omitted (Hg = 19ppb)

Table 6.2. Average Hg in Nova Scotia Bedrock; Saprolite suite in bold (weathered granitoid and granitoid parent)

			Hg ppb	Hg ppb
Waterloo Lake (F)	Pre-Pleistocene	111F	1.4	3.8
Waterloo Lake (W)	monzogranite	106W	1.3	2.1
Waterloo Lake (WW)		107WW	1.2	1
Hardwood Lake (F)	Pre-Pleistocene	112F	1.9	2.1
Hardwood Lake (W)	monzogranite	113AW	1.2	4.1
Hardwood Lake (WW)		144WW	1.6	ND
Forest Home (F)	Pre-Pleistocene	145F	3.7	ND
Forest Home (W)	leucogranite	126W	1.9	ND
Forest Home (WW)		127WW	1.6	ND
Smith's Corner (F)	Pre-Pleistocene	128F	1.8	ND
Smith's Corner (W)	leucomonzonite	129W	0.9	ND
Smith's Corner (WW)		140WW	1.1	ND
Bridgetown (F)	Pre-Pleistocene	131F	2.6	ND
Bridgetown (W)	leucomonzonite	132W	1.9	ND
Sub-Triassic core (W6)	Pre-Triassic	2201	4.7	ND
Sub-Triassic core (W5)	monzonite	2200	19.5	ND
Sub-Triassic core (W4)		2193	-0.1	ND
Sub-Triassic core (W3)		2168	2.2	5.5
Sub-Triassic core (W2)		2139	3.1	9.6
Sub-Triassic core (F)		2110	1.2	4.4

Table 6.3. Hg values for whole rock and mineral separates for saprolite suites of the South Mountain Batholith. Negative values are below detection; ND = not determined. (F) fresh parent; (W -WW - W6) variably weathered saprolite.

The arenaceous nature of the pre-Pleistocene weathering sites suggests an incomplete weathering process, which in turn suggests that further weathering today may result in ready release of elements such as Hg, from loosely-held sites within the weakened rock.

For consistency in sampling and to facilitate a comparison between weathered samples from different localities, a field and hand sample classification was developed, and samples for geochemistry from the surface outcrops were grouped into 3 possible categories. The first category includes fresh samples (F) selected from sites with minimal obvious physical or chemical weathering effects, that is, they lack obvious weathering effects such as the development of microfractures, clouding of feldspars, or oxidation of biotites. These samples are the parent granitoids in Tables 6.1 and 6.2. The second category includes weathered samples (W), in which physical weathering has resulted in the development of microfractures, chemical weathering has resulted in the clouding of feldspars, and in some cases, oxidation of biotites. However, despite this weathering, the rock is texturally cohesive, although it is difficult to sample this material by hand, as the outcrop crumbles readily to the touch. The third category consist of very weathered samples (WW), in which physical weathering has resulted in the loss of textural cohesion, and the material forms loose gravelly horizons or discontinuous lens along multiple joint planes. In these more highly weathered samples, fragmented feldspars and biotites remain relatively unchanged chemically, except for minor clay (kaolinite, smectite) development and minor oxidation. In addition to the surface outcrops sampled, the 6th parent granitoid in Table 6.1, is from the sub- Triassic weathered horizon. This granitoid was sampled from drill core at depths of 40 metres (top of weathered horizon, directly beneath the unconformity with the Triassic sediments), at 50, 61, 70, 73 (just above the base of the weathering front, in a sample in contact with a hydrothermally altered fault zone), and at 73.2 metres (the latter is in fresh, unweathered, unaltered granitoid). This weathering horizon is argillaceous in nature, and more intensely weathered than the pre-Pleistocene horizons, although its outward granite-like appearance and mineralogy, even in the upper levels just below the Triassic sediments, indicate that the weathering process has not gone to completion. The weathered granitoid samples are averaged values of all of these variably weathered samples from the 6 sites of the fresh parent granitoid. No distinction is made between

the differing granitoid types in this table, however the parent granitoid varies from biotite monzogranite to leucomonzogranite.

In addition to whole rock Hg content, several samples of biotite and clay separates from the weathered horizons were analyzed for Hg at ACME Laboratories in Vancouver, B.C.. These samples were hand-picked from gravel-sized pieces of the weathering material. The purpose for analyzing the mineral separates was to aid in determining the distribution of the Hg within the rock, and to examine the degree to which weathering may have effected this distribution within a given mineral.

6.1.1.1 Whole Rock Hg Geochemistry

Mercury data from whole rock analysis indicate that total Hg within the granitoids is relatively low in comparison to granitoids elsewhere (Sidle, 1993), and these data are summarized in Tables 6.1 - 6.3. No distinction between granitoid types has been made, although the average of 150 samples is low (2 ppb). The data suggest that even with low average levels of Hg in the granitoids, in all cases of the Pre-Pleistocene arenaceous weathering, fresh granite has higher absolute levels of Hg than weathered granite. If weathering was extensive, then even low levels of Hg can result in the release of significant quantities of Hg during the weathering process. Further information on the extent of this weathering event is needed, in order to quantify the possible contribution from such a process.

6.1.1.2 Mineral Hg Chemistry

In all, 3 samples of clay separates and 3 of biotite separates from the weathered horizon in the sub-Triassic drill core were analyzed for Hg; the clay and biotite samples were taken from the same depth within the core, and represent mildly weathered, moderately weathered, and highly weathered samples (Table 6.3). Five additional samples of biotite from 2 surface outcrops were analyzed for Hg (Table 6.3). The total

Hg in clay samples ranged from 1.5-2.9 ppb, and the values from the biotite ranged from 1.0-9.6 ppb. Neither clays nor biotites show consistent trends from fresh to weathered samples.

6.1.1.3 Weathering and Hg distribution

Both fresh and weathered samples of granitoids of varying composition have low levels of Hg. Despite the relatively low levels of Hg in these granitoids and their weathered equivalents, the data indicate that weathering does appear to reduce the amount of Hg in the rock. Regions where large surface areas of weathering granite exist, elevated levels of Hg could result in a concentration of Hg elsewhere. Further work on the relative distribution of Hg in the various types of granitoids, and the extent of the Pre-Pleistocene weathering are required, in order to fully assess the potential for elevated weathering-generated levels of Hg into the environment.

6.1.1.4 Addendum

More recent work by the author on the biotites from the fresh and more weathered samples in the Pre-Triassic horizon and in the Pre-Pleistocene horizon, indicates that at all depths within the horizon, the biotite is variably weathered and individual grains have both fresh and unweathered fractions (Chapter 4). Sample separates from each level within the horizon would therefore potentially contain biotite at all stages of weathering. This may then account for the lack of an observable trend within the biotite separates.

6.2 Integration of pre-existing Rn and U data into a GIS database

Introduction to the Rn - U study

In 1981, the Uranium Task Force (Nova Scotia) undertook an extensive sampling of domestic wells in the Harrietsfield area, located about 8 km south southwest of Halifax. The Harrietsfield area is a region underlain by granitoid rocks of the South Mountain Batholith, and had been identified as an area with anomalous levels of uranium in well waters. Uranium exploration in the late 1970s in the New Ross and Millet Brook areas, also underlain by the South Mountain Batholith, and in the Windsor and Tatamagouche areas, underlain by sandstones and shales, revealed localized elevated levels of uranium and radon in the environment (Fig. 6.2). Figure 6.3 indicates the regions of Nova Scotia for which U and Rn data were available for this study. An additional dataset processed from uranium exploration activity in the 1970s was integrated into a GIS by Page (1999), with contributions from this author.

As a result of these various studies, a large body of data had been collected on Rn and U in well waters and Rn in indoor air for regions where elevated levels of these elements had been detected, either through airborne radiometric studies or through exploration activities. These data had been variably synthesised during the early 1980s and 1990s (Nova Scotia Department of the Environment Report, 1981; MacFarlane, 1983; Grantham, 1986; Jackson, 1991), however these data were not accessible in digital format, and had not been collated into a georeferenced format. As part of the initial drive for undertaking a study of the release of Rn-U during weathering, the author collated these data from a variety of sources, and compiled the complete database from the available data for the Province of Nova Scotia, Department of the Environment. This data set was then integrated into a GIS database by the author, using ArcView©. The resulting database and spatially referenced data were documented in an internal report to the Nova Scotia Department of Environment in 1999. A re-formatted and slightly modified version of this report (editorial modifications only, no modifications to content),

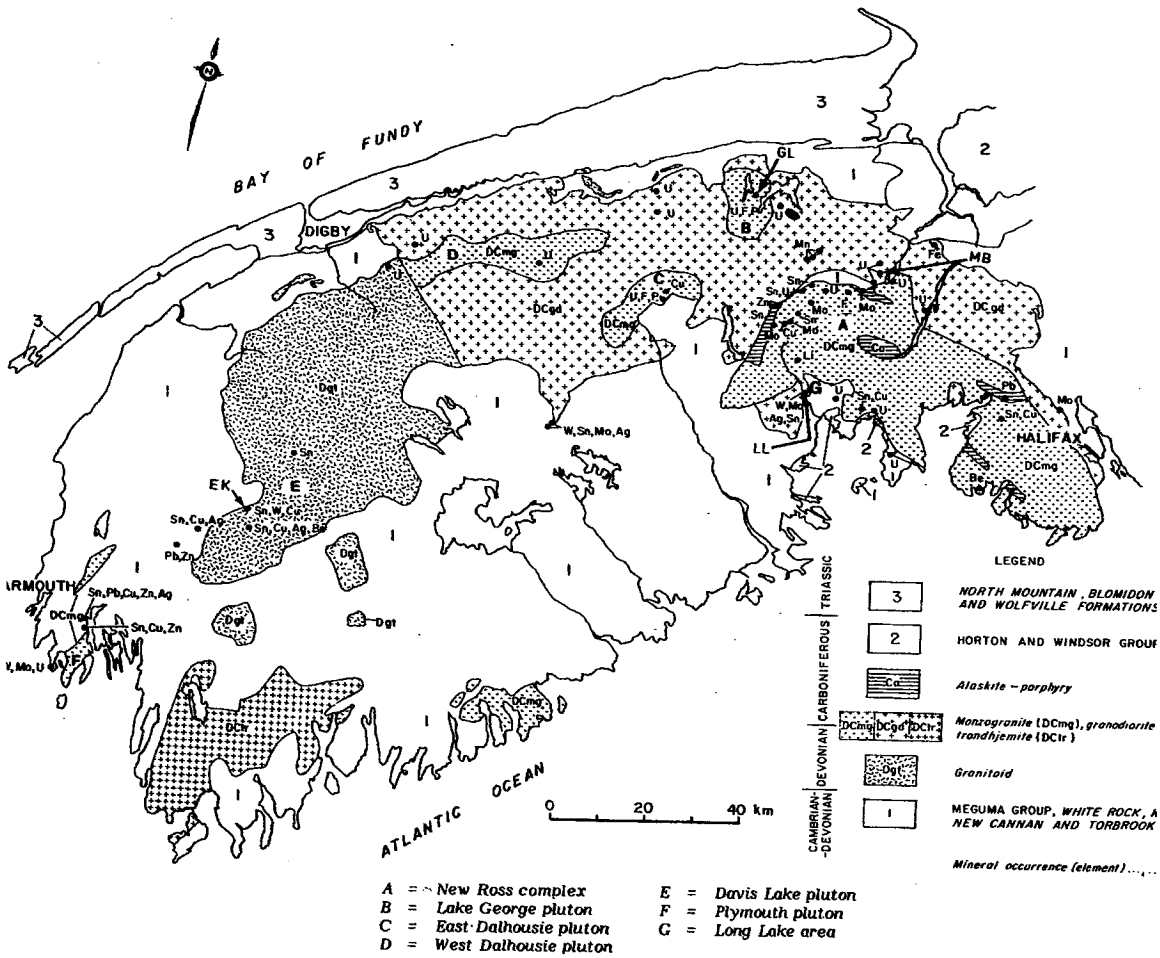

Figure 6.2. Geological map of southern Nova Scotia, showing U mineralization within the South Mountain Batholith (after Chatterjee and Muecke, 1982).

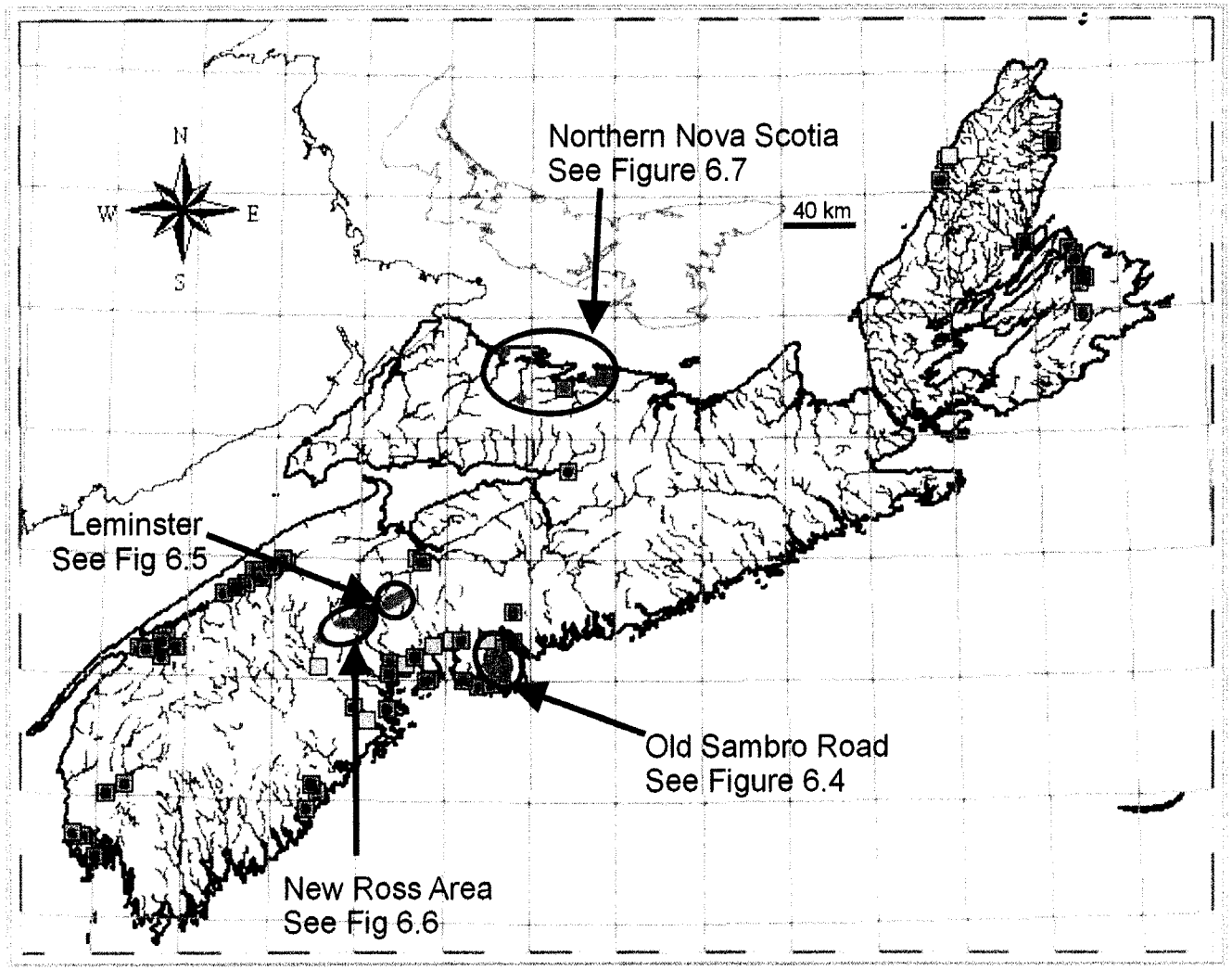

Figure 6.3. Location of uranium and radon in well water surveys.

with the approach and limitations of these data and the geospatially generated information, is presented in Sections 6.2.1 to 6.2.4.

6.2.1 GIS analysis of U, Rn, and Ra well water data and Rn in indoor air for the Province of Nova Scotia

Project Objective

To undertake GIS input of all available uranium, radium, and radon data for the Province of Nova Scotia, as a precursor to detailed study of uranium distribution in rocks, in order to provide a more realistic Rn potential map for the Province.

6.2.2 Introduction

Studies indicate that elevated Radon (Rn) values are not always directly related to elevated Uranium (U) or Radium (Ra), although all three elements are part of a continuous decay series in which Rn follows U and Ra (Stanton et al., 1996). The differing distribution of Rn, Ra, and U in the environment is a result of their behaviour under different chemical conditions, and predicting the distribution of any of these elements depends upon understanding the nature of the element's chemistry and the nature of the surrounding environment. In particular, understanding the nature of the rocks that host and serve as sources of these elements is key to developing a model for their distribution in the environment.

Development of a digital database, which may include tabular and spatial data, is critical to the evaluation of any environmental management issue. This project was undertaken as a component of a PhD thesis by the author, and involved investigation of the spatial distribution of available Rn (and U and Ra) in Nova Scotia, as a preliminary step to developing a more realistic Rn potential map for the Province.

The scope and resultant output of the project as proposed was subject to the nature of the preexisting data available. The usefulness of the data in digital format is dependant upon being able to access the data using a GIS system, and the project was undertaken with the understanding that the Nova Scotia Department of the Environment (DOE) would have in place a GIS stystem.

Originally it was proposed that 800-1200 well water data, 500+ Rn-in-soil gas data, and 800 indoor air data would be assessed and compared to existing datasets available through Nova Scotia Department of Natural Resources. In excess of: (a) 1200 well water data; (b) 500 Rn in soil gas data (all available data); and (c) 700-800 Rn in indoor air data (all data that was made available), have been entered into a database (.dbf) format. The data have been georeferenced as specifically as possible, and preliminary maps produced. Details are outlined in the following sections.

In the following sections, the data are categorized based on the data source (e.g. Uranium Task Force), geographic distribution (e.g. Leminster-Vaughan) and nature of data (e.g. Rn in indoor air). Each section includes a summary of the work done, problems encountered and the resulting limitations, and recommendations for further analyses. The data are included in digital format (.dbf format for the tabular data) and in shapefiles (.shp format for the spatial data). Using a GIS system, there are an infinite number of ways to analyze the data, and not all possibilities are included in this report. Arcview (or other GIS program) is required to make full use of the potential of these data; without Arcview, only a limited "view" of the data can be obtained, as presented in Figure 6.3, an outline map of Nova Scotia, with the various datasets indicated, and Figures 6.4 - 6.8, Tables 6.4 - 6.8.

6.2.2.1 Data management

Missing data (not available, not assessed, etc) is blank in the .wb3 (and usually in the .dbf) files. However, it should be noted that occasionally Arcview would not accept blanks when new data were entered, so "0" also means no data. The original data were

entered into .wb3 format, and these files were then transferred to .dbf format for use in Arcview. Once processed in Arcview, these modified files were once more saved as .dbf files. These latter files are the files included in this report. As a result of these transfers, the .dbf files may show "0" in some entries; these "0" entries correspond to blank entries in the .wb3 files.

1. Uranium values listed in the original data as <0.005 mg/L were assumed to represent "below detection limit" and were assigned a value of 0.003 mg/L for the purposes of data management. O.003 is NOT a true, measured value.

2. Radon values listed in the original data as < 4 pCi/L were assumed to represent "below detection limit" and were assigned a value of 4 pCi/L.

3. All original data for Rn in well water were listed in pCi/L; these were converted to Bq/L using a conversion factor of 37 Bq/L = 1000 pCi/L

4. All original data for Rn in indoor air were listed in pCi/L; these were converted to Bq/m3 using a conversion factor of 22 pCi/L = 800 Bq/m3.

5. Data for the Harrietfield-Brookside area were entered at a scale of 1:50 000; all other data were entered at 1:500 000. This effects the accuracy of the data when represented spatially.

6. Data from the Windsor area are included as 2 separate disks; the work was undertaken by Krista Page, Honours student at Dalhousie Univeristy.

While every attempt has been made to eliminate human error in data management, it is possible that some errors may occur in the final datasets. The author appreciates notification of any errors found, but does not assume liability for such errors.

6.2.3 Uranium Task Force Data

The Uranium Task Force was established in 1979, in response to the discovery of elevated uranium levels in some well waters in the Harrietsfield area. The Nova Scotia Department of the Environment, as one of the contributors to the Task Force, set out to determine the spatial distribution of naturally occurring uranium in groundwater and to determine the possible influence of geology, hydrogeology, and groundwater geochemistry on the levels of uranium in well waters in Nova Scotia. The final report on to the Task Force was produced in April 1983 (MacFarlane, 1983).

Data from the report by MacFarlane (1983) have been integrated into digital databases and corresponding digital maps by the author.

6.2.3.1 Harrietsfield Area

Number of Data output in .dbf format	375 values
File names and tables	OSR.dbf (table) OSR.shp (map) (Table 6.4; Fig. 6.4)
Nature or spatial data output	316 could be georeferenced as follows: - 219 as individual points - 97 data were "grouped"into 9 distinct polygons

6.2.3.1.1 Original Data from the Harrietsfield Area

The original data were made available through Nova Scotia Department of Environment. The data were in hand-written tabular format. Only a portion of the data (Brookside Road, and a short stretch on Old Sambro Road) was available in map form (72 points).

MAP ID	ID	REF	EASTINGS	NORTHINGS	DUG/ DRILLED	WELL DEPTH	WELL DIAMETER	BEDROCK DEPTH	WATER DEPTH	COND	pH	U mg/L	Rn Bq/L	REGION
1	198	OSR97	449334	4937032	dug					81	5.8	0.003	39	Old Sambro Road
2	193	OSR92	449247	4936987	drilled					240	7.8	0.07	294	Old Sambro Road
3	192	OSR91	449236	4936982	dug					340	5.6	0.003	116	Old Sambro Road
4	189	OSR88	449074	4936957	dug					1000	4.9	0.003	118	Old Sambro Road
5	187	OSR86	449065	4936931	dug					94	4.9	0.003	194	Old Sambro Road
6	183	OSR82	449041	4936884	drilled	45	0.5			520	4.6	0.006	188	Old Sambro Road
8	180	OSR77	449073	4936817	drilled	38	0.5					0.003	605	Old Sambro Road
9	177	OSR74	449076	4936732	dug					1700	5.8	0.003	36	Old Sambro Road
10	175	OSR72	449082	4936686	dug					550	5.4	0.003	17.5	Old Sambro Road
11	174	OSR69	449104	4936630	dug					1000	5.5	0.003	41.5	Old Sambro Road
12	173	OSR68	449120	4936595	drilled					3000	4.3	0.005	331	Old Sambro Road
13	168	OSR63	449148	4936539	drilled	80	0.2			1510	5.9	0.005	720	Old Sambro Road
14	166	OSR61	449228	4936413	drilled	85	0.5	2	15	118	6.5	0.003	1055	Old Sambro Road
15	165	OSR60	449225	4936381	drilled	85	0.5			440	5.8	0.003	675	Old Sambro Road
16	161	OSR56	449281	4936330	drilled					830	5.9	0.003	1293	Old Sambro Road
17	164	OSR59	449203	4936346	drilled	65	0.5	2	5	111	6.5	0.003	1457	Old Sambro Road
18	163	OSR58	449225	4936318	drilled	50				150	6	0.003	741	Old Sambro Road
19	162	OSR57	449242	4936295	drilled	58	0.4	45		84	6	0.003	760.5	Old Sambro Road
20	156	OSR51	449351	4936215	drilled	67	0.5			38	5.6	0.003	467	Old Sambro Road
21	158	OSR53	449332	4936142	dug					47	5.8	0.003	10	Old Sambro Road
22	155	OSR49	449632	4935854	drilled	125	0.5	15	12	410	5.5	0.007	1196	Old Sambro Road
23	150	OSR45	449707	4935676	drilled	135	0.5	45		460	6.4	0.02	2529	Old Sambro Road
24	149	OSR44	449725	4935622	dug					153	7	0.003	13	Old Sambro Road
25	148	OSR43	449742	4935607	drilled	64	0.5	18	21	111	6.5	0.03	3230	Old Sambro Road
26	145	OSR40	449794	4935494	drilled					370	6.4	0.02	1646	Old Sambro Road
27	133	OSR27	449694	4935249	drilled	140	0.5	46		380	7	0.11	2250	Old Sambro Road
28	123	OSR17	449543	4934876	drilled					210	6.5	0.02	981	Old Sambro Road
29	147	OSR42	449727	4935524	dug					1630	6.3	0.003	35	Old Sambro Road
30	144	OSR39	449738	4935494	drilled					220	5.8	0.01	318	Old Sambro Road
31	137	OSR32	449702	4935367	drilled					300	5.9	0.009	1247	Old Sambro Road
32	134	OSR28	449673	4935318	drilled	120	0.5	44		390	6.3	0.03	0	Old Sambro Road
33	132	OSR26	449620	4935225	drilled					450	5.9	0.01	1127	Old Sambro Road
34	130	OSR24	449598	4935156	dug					430	5.2	0.003	94	Old Sambro Road
35	126	OSR20	449555	4935044	dug					70	6.4	0.003	23	Old Sambro Road
36	125	OSR19	449530	4934999	drilled	100	0.5			170	6.9	0.06	1285	Old Sambro Road
37	124	OSR18	449519	4934970	drilled	220	0.5	24	28	185	7.3	0.04	2015	Old Sambro Road
38	116	OSR4	449280	4934426	dug					155	5.7	0.003	74	Old Sambro Road
39	204	OSR104	449019	4931312	drilled	120	0.5	15	9	151	7	0.02	777.5	Old Sambro Road
40	222	OSR121	449027	4930757	drilled	100	0.5	55	9	270	6.7	0.04	993.5	Old Sambro Road
41	223	OSR122	449032	4930732	drilled	200				770	5.1	0.003	154.5	Old Sambro Road
42	226	OSR125	449030	4930711	drilled	120	0.5	15		240	6.5	0.02	905.5	Old Sambro Road
43	227	OSR126	449022	4930689	drilled	215	0.5	10		310	6.1	0.03	937	Old Sambro Road
44	228	OSR127	449026	4930660	drilled	100	0.5	14	12	210	6.2	0.02	1002.5	Old Sambro Road
45	234	OSR135	449028	4930520	drilled	147	0.5			113	6.6	0.009	1548	Old Sambro Road
46	235	OSR136	449028	4930495	drilled	145	0.6	20	15	174	5.7	0.003	156	Old Sambro Road
47	239	OSR142	448977	4930240	drilled	120	0.5	15	9	149	6.7	0.009	1314.5	Old Sambro Road
48	240	OSR143	448953	4930186	drilled	145	0.5	28	28	178	6.9	0.01	894	Old Sambro Road

Table 6.4a. Well water U (mg/L) and Rn (Bq/L) as well as additional parameters (if recorded) for wells in the Harrietsfield Area, near Halifax, N.S. . Blank spaces means no data. COND is conductivity.

MAP ID	ID	REF	EASTINGS	NORTHINGS	DRILLED	DEPTH	DIAMETER	DEPTH	DEPTH		pH	mg/L	Bq/L	REGION
49	241	OSR144	448953	4930157	drilled	125	0.5	36	26	159	7	0.009	916	Old Sambro Road
50	242	OSR145	448953	4930132	drilled	150	0.5	40	29	270	7.5	0.01	864	Old Sambro Road
51	244	OSR147	448972	4930086	drilled	155				210	7.1	0.01	764	Old Sambro Road
52	246	OSR150	449014	4929995	drilled	164	0.5	57		220	6.7	0.008	1452.7	Old Sambro Road
53	247	OSR151	449018	4929974	drilled	140	0.5	60		230	7.1	0.008	1078.5	Old Sambro Road
54	249	OSR153	449023	4929920	drilled	150	0.5	57	27	250	7.6	0.04	973	Old Sambro Road
55	251	OSR156	449025	4929833	drilled	174	0.5	60	28	260	7.3	0.03	1266	Old Sambro Road
56	252	OSR157	449030	4929815	drilled	176	0.5	60	28	250	7.6	0.06	1661	Old Sambro Road
57	254	OSR159	449027	4929772	drilled	175	0.5	60	42	290	7.9	0.04	607	Old Sambro Road
58	284	OSR190	449101	4928729	drilled	198	0.5	70	39	260	7.8	0.05	750	Old Sambro Road
59	293	OSR199	449207	4928379	drilled					430	6.6	0.003	836	Old Sambro Road
60	202	OSR102	448967	4931426	dug					500	6.5	0.003	15.5	Old Sambro Road
61	216	OSR114	448863	4931005	drilled	175	0.5	48	23	270	5.7	0.09	0	Old Sambro Road
62	217	OSR116	448920	4930916	drilled	300	0.5	25		167	6.9	0.02	307.5	Old Sambro Road
63	218	OSR117	448960	4930863	drilled	70	0.5	40	65	300	6	0.008	1214.5	Old Sambro Road
64	219	OSR118	448968	4930819	drilled	100	0.5	21	21	270	5.7	0.003	99.5	Old Sambro Road
65	232	OSR132	448969	4930638	drilled	180	0.5	8		360	6	0.02	1242	Old Sambro Road
66	255	OSR160	448974	4929729	drilled	110				240	7.8	0.08	1463.5	Old Sambro Road
67	262	OSR167	448955	4929214	drilled	150	0.5			220	7.2	0.02	1398.5	Old Sambro Road
68	263	OSR168	448961	4929186	drilled	130	0.5	67		220	7.2	0.02	1390	Old Sambro Road
69	267	OSR172	448966	4929141	drilled	300				250	7.5	0.01	978	Old Sambro Road
70	268	OSR173	448966	4929109	drilled					220	7.3	0.03	657.5	Old Sambro Road
71	271	OSR175	448949	4929090	drilled	120	0.5			250	7.6	0.09	723.5	Old Sambro Road
72	272	OSR176	448971	4929033	drilled	210	0.5	80		260	7.7	0.04	472.5	Old Sambro Road
73	281	OSR187	449055	4928654	drilled					250	7.8	0.06	179	Old Sambro Road
74	289	OSR195	449139	4928413	dug					2500	7.5	0.003	35	Old Sambro Road
75	290	OSR196	449142	4928372	n.a.					1360	6.3	0.003	159.5	Old Sambro Road
76	297	OSR203	449287	4927892	dug					80	6.1	0.003	59.5	Old Sambro Road
77	320	BR3	441974	4934117	dug					650	5.5	0.003	33	Brookside
78	321	BR10	442000	4933977	drilled	67	0.5	40	18	620	6.2	0.04	841	Brookside
79	360	BR26	442034	4933688	drilled							0.05		Brookside
80	359	BR27	442037	4933669	drilled							0.05		Brookside
81	322	BR20	442079	4933880	drilled	80	0.5			490	6	0.006	971	Brookside
82	323	BR30	442047	4933571	drilled	225	0.5	89	57	330	7.8	0.08	536	Brookside
83	325	BR53	442205	4933268	drilled	80				141	6.3	0.003	400	Brookside
84	363	BR40	442146	4933462										
85	324	BR41	442170	4933427	drilled					330	6.2	0.003	254	Brookside
86	326	BR62	442364	4933112	drilled	200				210	6.5	0.01	505	Brookside
87	327	BR70	442463	4932985	n.a.							0.008		Brookside
88	328	BR81	442656	4932687	drilled	150	0.5	70	78	161	6.5	0.007	806	Brookside
89	330	BR88	442686	4932455	drilled	150	0.5	48	28	240	7.3	0.005	1345	Brookside
90	329	BR85	442714	4932597	dug	22	3		2	153	6.1	0.003	13	Brookside
91	370	BR89	442728	4932512	drilled	65	0.5	7	10			0.003		Brookside
92	331	BR90	442736	4932483	drilled	160	0.5		30	194	7.1	0.11	2143	Brookside
93	374	BR91	442747	4932458	drilled	164	0.5	79				0.02		Brookside
94	332	BR92	442756	4932430	drilled	150	0.5	68	1	230	7.8	0.02	1466	Brookside
95	333	BR111	443072	4932005	drilled	165	0.5	75		260	7.8	0.07	1095	Brookside
96	335	BR129	443284	4931665	drilled					375	7.5	0.09	2420	Brookside
97	334	BR122	443308	4931771	drilled	100	0.5	32	21	300	6.8	0.01	1714	Brookside
98	336	BR141	443404	4931389	dug					640	6	0.003	34	Brookside

Table 6.4a continued (ii). U and Rn in well waters, Harrietsfield area.

MAP ID	ID	REF	EASTINGS	NORTHINGS	DUG/ DRILLED	WELL DEPTH	WELL DIAMETER	BEDROCK DEPTH	WATER DEPTH	COND	pH	U mg/L	Rn Bq/L	REGION
100	351	ED2	443203	4931748	drilled	190	0.4			240	7.8	**0.09**	**608**	Brookside
101	352	ED8	443085	4931850	drilled	300	0.5	88		300	8.1	**0.06**	**1155**	Brookside
102	373	ED11	443027	4931822	drilled	400	0.5	87				**0.01**		Brookside
103	354	ED9	443042	4931904	drilled	400	0.5	87				**0.02**	**134**	Brookside
104	365	BR140	443232	4931345	n.a.							**0.07**		Brookside
105	350	MP62	443440	4931607	dug	13	3		8	425	6.8	**0.003**	**36**	Brookside
106	349	MP60	443484	4931632	drilled	180	0.5	28		157	7	**0.02**	**624**	Brookside
107	348	MP43	443472	4931936	drilled	160	0.5	59		255	8	**0.04**	**700**	Brookside
108	347	MP42	443464	4931961	dug					300	6.5	**0.003**	**8**	Brookside
109	358	MP33	443496	4932065	drilled	225	0.5	16		220	7.6	**0.06**	**276.5**	Moody Park Subdivision
110	346	MP30	443477	4932121	drilled	235	0.5	86	30	275	8	**0.09**	**599**	Brookside
111	343	MP1	443312	4932003	drilled					230	7.7	**0.06**	**668**	Brookside
112	344	MP15	443321	4932255	drilled	130	0.5	57	25	220	7.8	**0.06**	**921**	Moody Park Subdivision
113	345	MP22	443445	4932280	drilled	360	0.5	56	30	220	7.8	**0.02**	**64**	Brookside
114	362	MP25	443514	4932318	drilled	130	0.5	68	23	210	7.8	**0.03**	**1186.5**	Moody Park Subdivision
115	338	BM2	442827	4932853	drilled	43	0.5	21		240	5.8	**0.003**	**191**	Brookside
116	366	BM3	442848	4932867	drilled	68	0.5	30	18			**0.01**		Brookside
117	339	BM15	443022	4932896	drilled	160	0.5	47		142	6.9	**0.009**	**890**	Brookside
118	340	BM19	443018	4932775	drilled	100	0.5	46		210	7.8	**0.05**	**795**	Brookside
119	345	BM22	443092	4932858	drilled	160	0.5	39				**0.01**		Brookside
120	368	BM24	443088	4932983	n.a.							**0.003**		Brookside
121	341	BM34	442967	4933334	drilled	100	0.5	40		114	6.6	**0.003**	**1304**	Brookside
122	369	BM38	442995	4933373	n.a.	123	0.5	27		1977		**0.06**		Brookside
123	347	BM42	442913	4933490	drilled						7.7	**0.08**		Brookside
124	182	OSR80	449083	4936868	drilled					450	4.6	**0.005**	**251**	Old Sambro Road
125	185	OSR84	449095	4936888	drilled	150	0.5			250	7.1	**0.08**	**501**	Old Sambro Road
126	179	OSR76	449062	4936782	drilled					123	6.3	**0.007**	**1057.5**	Old Sambro Road
127	178	OSR75	449059	4936758	drilled					1050	5.7	**0.003**	**403.5**	Old Sambro Road
128	170	OSR65	449139	4936566	dug					300	5.4	**0.003**	**8.4**	Old Sambro Road
129	167	OSR62	449177	4936508	drilled	85	0.5	2	15	121	6.5	**0.003**	**1060**	Old Sambro Road
130	160	OSR55	449298	4936299	drilled	55	0.5	0	12	800	5.9	**0.003**	**742**	Old Sambro Road
131	157	OSR52	449367	4936189	drilled					550	5.5	**0.003**	**427**	Old Sambro Road
132	152	OSR47A	449684	4935734	drilled	27				66	5.2	**0.006**	**301**	Old Sambro Road
133	153	OSR47B	449689	4935738	dug					181	5.6	**0.003**	**226**	Old Sambro Road
134	143	OSR38	449789	4935440	drilled					330	6.9	**0.02**	**2**	Old Sambro Road
135	136	OSR31	449757	4935375	drilled					300	6.4	**0.02**	**1375**	Old Sambro Road
136	135	OSR29	449716	4935314	drilled					121	6.6	**0.009**	**368**	Old Sambro Road
137	131	OSR25	449677	4935212	dug					93	6.1	**0.003**	**21**	Old Sambro Road
138	120	OSR10	449498	4934712	drilled	50	0.2			610	5.7	**0.003**	**719**	Old Sambro Road
139	118	OSR6	449356	4934477	drilled	100	0.5	15		760	5.6	**0.005**	**842**	Old Sambro Road
140	117	OSR5	449338	4934416										
141	197	OSR96	449292	4937066	dug					550	5.1	**0.003**	**118**	Old Sambro Road
142	195	OSR94	449230	4937046	dug							**0.003**	**90**	Old Sambro Road
143	196	OSR95	449199	4937026	dug							**0.005**	**183**	Old Sambro Road
144	190	OSR89	449105	4936978	dug					290	5.8	**0.003**	**35**	Old Sambro Road
145	184	OSR83	449046	4936897	drilled					460	5.1	**0.005**	**258**	Old Sambro Road
146	151	OSR46	449648	4935693	drilled	120	0.5	29	26	340	5.7	**0.01**	**1233**	Old Sambro Road
147	141	OSR36	449746	4935452	dug					800	6.5	**0.008**	**19**	Old Sambro Road
148	140	OSR35	449737	4935424	drilled					420	6.2	**0.02**	**524**	Old Sambro Road
149	139	OSR34	449725	4935399	dug					134	6.9	**0.003**	**2**	Old Sambro Road
150	138	OSR33	449713	4935379	drilled					310	5.9	**0.01**	**1281**	Old Sambro Road

Table 6.4a. Continued (iii). Rn and U in well waters, Harrietsfield ara.

MAP ID	ID	REF	EASTINGS	NORTHINGS	DUG/ DRILLED	WELL DEPTH	WELL DIAMETER	BEDROCK DEPTH	WATER DEPTH	COND	pH	U mg/L	Rn Bq/L	REGION
151	129	OSR23	449580	4935123	drilled	150				790	5.7	0.009	38	Old Sambro Road
152	128	OSR22	449562	4935103	drilled	155	0.5			400	4.9	0.2	1726	Old Sambro Road
153	127	OSR21	449553	4935066	drilled					250	5.8	0.008	491	Old Sambro Road
154	122	OSR16	449514	4934941	drilled	120	0.5	48	23	190	7.5	0.04	0	Old Sambro Road
155	121	OSR14	449496	4934883	dug					260	6.7	0.003	7	Old Sambro Road
156	115	OSR3	449277	4934400										
157	114	OSR2	449221	4934343	drilled					177	7.3	0.01	1009	Old Sambro Road
158	201	OSR101	448968	4931455	dug					129	5.9	0.003	23.5	Old Sambro Road
159	206	OSR106	448917	4931313	dug					133	6.3	0.003	2	Old Sambro Road
160	209	OSR108	448937	4931141	drilled	115	0.5	55	30	210	7.1	0.01	738.5	Old Sambro Road
161	208	OSR107A	448931	4931170	dug					150	6.9	0.01	199.5	Old Sambro Road
162	207	OSR107B	448937	4931174	drilled	180	0.5	54		48	5.9	0.003	2	Old Sambro Road
163	214	OSR113A	448930	4931052	drilled	180	0.5	50	14	220	7.4	0.05	890.5	Old Sambro Road
164	215	OSR113B	448942	4931043	dug					75	5	0.003	5.3	Old Sambro Road
165	224	OSR123	448968	4930745	drilled	120	0.5	21		560	6.1	0.09	1914	Old Sambro Road
166	225	OSR124	448968	4930676	drilled	47	0.5			1550	5	0.003	183	Old Sambro Road
167	230	OSR130	448973	4930664	drilled	75	0.5	9	29	640	5.8	0.003	143.5	Old Sambro Road
168	233	OSR134	448973	4930599	dug					310	5.8	0.003	75	Old Sambro Road
169	236	OSR137	448981	4930513	drilled	95	0.5	25	87	146	6	0.003	255.5	Old Sambro Road
170	238	OSR141	448945	4930305	drilled	55				940	5.4	0.003	102	Old Sambro Road
171	261	OSR166	448956	4929237	drilled					161	7.1	0.003	1218.5	Old Sambro Road
172	264	OSR169	448968	4929164	drilled	140	0.5	81		220	7.4	0.04	884.5	Old Sambro Road
173	266	OSR171	448966	4929152	drilled					230	7.5	0.03	1181	Old Sambro Road
174	269	OSR174A	448965	4929097	drilled					220	7.4	0.03	554	Old Sambro Road
175	270	OSR174B	448969	4929096	dug					94	6	0.003	2	Old Sambro Road
176	273	OSR177	448974	4929006	drilled					250	7.6	0.04	947.5	Old Sambro Road
177	274	OSR178	448981	4928980	drilled					180	7.2	0.01	347.5	Old Sambro Road
178	275	OSR179	448996	4928958	drilled	160	0.5	75		250	7.7	0.04	537.5	Old Sambro Road
179	277	OSR182	449019	4928840	drilled							0.09	398	Old Sambro Road
180	278	OSR183	449026	4928794	drilled	100	0.5	64	5	310	7.6	0.1	350.5	Old Sambro Road
181	282	OSR188	449076	4928604	drilled	55	0.5	30	15	145	7.6	0.003	178.5	Old Sambro Road
182	296	OSR202	449292	4927924	dug					400	4.8	0.003	65	Old Sambro Road
183	154	OSR48	449391	4936139	drilled					850	4.6	0.003	224	Old Sambro Road
184	169	OSR64	449099	4936544	drilled					800	6.4	0.003	448	Old Sambro Road
185	186	OSR85	449117	4936914	dug					320	5.8	0.003	60	Old Sambro Road
186	188	OSR87	449135	4936937	drilled	128	0.5			220	7.4	0.06	215	Old Sambro Road
187	191	OSR90	449181	4936960	drilled	190	0.5	15		240	7.7	0.05	292	Old Sambro Road
188	194	OSR93	449263	4936995	drilled	70	0.5	20	22			0.07	294	Old Sambro Road
189	200	OSR100	449613	4935035	drilled	130	0.5	8	8	720	5.7	0.02	243	Old Sambro Road
190	211	OSR110	449005	4931206	drilled	130	0.5	58	20	180	7.1	0.02	341	Old Sambro Road
191	220	OSR119	449024	4930826	drilled	115	0.5	55	30	300	4.8	0.003	81	Old Sambro Road
192	221	OSR120	449024	4930798	drilled					360	6.4	0.02	1025	Old Sambro Road
193	231	OSR131	449033	4930608	drilled					220	6.2	0.03	1252	Old Sambro Road
194	243	OSR146	448955	4930112	drilled					210	7.1	0.01	852	Old Sambro Road
195	248	OSR152	449017	4929952	drilled	150	0.5	40	24	220	6.4	0.006	1252.5	Old Sambro Road
196	245	OSR149	448984	4930050	drilled	140	0.5	60		230	6.7	0.007	1516.5	Old Sambro Road
197	250	OSR154	449020	4929887										
198	253	OSR156	449026	4929792	drilled	144	0.5	62		250	7.7	0.04	1566	Old Sambro Road
199	257	OSR162	449031	4929584	drilled					240	7.7	0.09	1433.5	Old Sambro Road
200	258	OSR163	448975	4929507	drilled					260	7.3	0.12	923	Old Sambro Road
201	259	OSR164	448969	4929456	drilled	140	0.5	33	45	260	6.8	0.04	1264.5	Old Sambro Road
202	260	OSR165	448975	4929430	drilled	150	0.5	36	32	250	7	0.03	1221.5	Old Sambro Road
203	280	OSR185	449100	4928753	drilled					250	7.7	0.07	395	Old Sambro Road
204	285	OSR191	449106	4928703	drilled	300	0.5	70		260	8	0.05	697.6	Old Sambro Road
205	286	OSR192	449147	4928694	drilled	175	0.5	50	16	250	7.8	0.006	1369.5	Old Sambro Road
206	287	OSR193	449126	4928653	drilled					240	7.8	0.06	1557	Old Sambro Road
207	288	OSR194	449135	4928620	drilled					240	7.8	0.1	1708	Old Sambro Road
208	291	OSR197	449198	4928427	drilled	80	0.5	15		166	6.5	0.007	485	Old Sambro Road
209	292	OSR198	449204	4928403	drilled					210	6.2	0.003	348.5	Old Sambro Road

Table 6.4a, continued (iv). Rn and U in well waters, Harrietsfield area.

ID	Location	U max mg/L	Rn max Bq/L	U min mg/L	Rn Bq/L	U std dev	Rn std dev	U # samples	Rn # samples
1	Acres, Big Acres, Birchwood	0.07	2596.5	0.003	6.8	0.018	797.6	22	22
2	Brunt Road	0.28	1919	0.009	245	0.11	667	5	5
3	Venus Drive	0.04	1856	0.02	338	0.01	623	4	4
4	Mercury Ave	0.05	1447	0.01	1190	0.023	130.6	3	3
5	Fraser Road	0.02	1596	0.003	2	0.005	593.6	12	12
6	Francie Drive	0.03	2594	0.003	2	0.009	902.5	8	8
7	Moody Park 1	0.23	1180.5	0.03	154.5	0.041	259.8	28	21
8	Moody Park - OSR	0.06	1866	0.003	164.5	0.017	524	15	14
9	Gordon Stewart Drive	0.23	1448.5	0.03	157.5	0.072	443.3	6	6

Table 6.4b. Rn and U well water average values for wells without specific northings and eastings readings. Harrietsfield area, near Halifax.

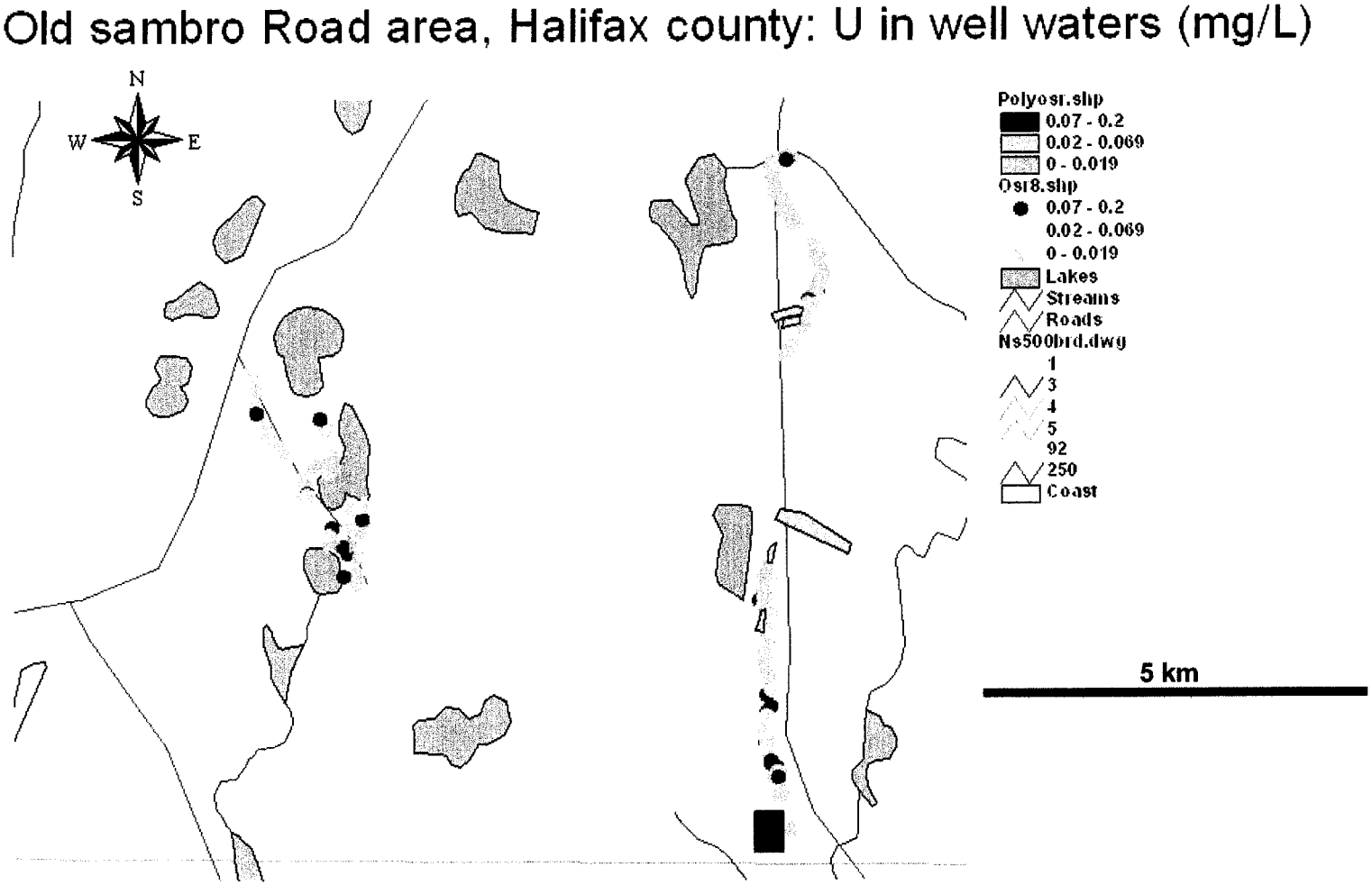

Figure 6.4a. Old sambro Road area, Halifax County: Uranium in well waters (mg/L).

Figure 6.4B. Old Sambro Road area, Halifax County: Rn in well waters (Bq/L)

6.2.3.1.2 Data Processing

All data in paper format were entered into digital format (.dbf files) (Table 6.4a). Although street addresses were available for most of the data, a number of values were only referenced to street or subdivision name and not to specific # on street. Data were entered onto a 1:50 000 digital topographic base map (11D 12) using head-up digitizing (locating the point on the computer screen, "drawing" a point, and recording the coordinates) (Fig. 6.4). Limitations and conditions of the data entry onto digital map format are discussed further below.

Street addresses were matched to data available through Housing and Municipal Affairs; however, complications arose in some instances due to recent changes in the civic address numbering system. With the introduction of the (911) response system, apparently some of the civic address numbers were changed; in the records available through Housing and Municipal Affairs (Terminal Road) some addresses were in the old system, some in the new, and it was not always possible to determine which was which. It was hoped that driving the area might further narrow down some of the addresses, however this did not give any clearer results. As a result of these changes, the following approach was taken: (1) only those numbers which could be clearly matched (those on Old Sambro Road, Brookside Road, etc) were entered to "exact" locations; (2) house numbers were filled in where possible from surrounding data - for example, if 2460 and 2490 were known, and there were 2 unlabeled buildings in between, then 2480 was deemed to be the unlabeled building beside 2490. Any error introduced in this way was considered to be in the same order as any error involved in entering the data on the map at the scale of 1:50 000. A total of 219 points were entered using one or other of these criteria.

Civic addresses which did not clearly match up with numbers and owner names, and which were not on any of the maps provided by DOE, were entered as polygons for the specific street on the digital map(Fig. 6.4). Tables for these polygons were constructed, and give maximum, minimum, range, and standard deviation (Table 6.4b). The individual datum points are also available in tabular format in the original .dbf file.

Individual datum information can be accessed by clicking on the polygon using the **"i"** button, and all values for this polygonal region appear in tabular form on the screen. As a consequence of this compilation, a total of 97 data were entered into 10 polygons for the Harrietsfield map sheet (Table 6.4b).

Houses on Old Sambro Road with numbers >2791 were not included on the digital map, as they fall beyond the boundaries of the 1:50 000 map sheet 11D 12. These data were entered into the .dbf database. A total of 22 points were omitted from the digital map in this way. The remaining 37 points were not entered into digital map format because either the address was unknown or ambiguous; these data are included in the database .dbf file, without a link to a point on the map.

6.2.3.1.3 Preliminary Analysis

The geological map of the area indicates that all data fall within the same unit of the Halifax Pluton of the South Mountain Batholith, the Harrietsfield biotite monzogranite (MacDonald et al., 1992). No well water samples are close to any known contacts with other phases or rock types. No known mineral occurrence of Uranium exists in the area (Fig. 6.2), nor do the rocks themselves have elevated U values, and all uranium values from whole rock geochemistry of the pluton lie in the range of 4 -12 ppm (Ham and MacDonald, 1991).

Digital data on geologic structures within the granitic units are not currently available; however paper map copies indicate the presence of NW-trending lineaments, joints, and dykes in the Harrietsfield-Brookside area (MacDonald and Horne, 1987).

Surficial geology data, although available in digital format, were not easily accessible in a user-friendly format and as a result, have not been analyzed in depth.

6.2.3.2 Leminster-Vaughan Data

Number of data output in .dbf format	47 samples
File names and tables	leminster.dbf (database) leminster.shp (map) (Table 6.5; Figure 6.5)
Nature of spatial data output	47 samples

6.2.3.2.1 Original Data

The original data were made available through Nova Scotia Department of the Environment. The data were in hand-written tabular format. A map of the area was also available, and aided in entering the data into a GIS (orthophoto map, scale unknown - possibly 1:10 000, with most well locations marked).

6.2.3.2.2 Data Processing

All data in paper format were entered into digital format (.dbf files) (Table 6.5). Well locations were entered onto a 1:500 000 digital geological base map using head-up digitizing (Figure 6.4). Although it may have been more accurate to enter the data at a scale of 1:10 000, or even 1:50 000, neither geological nor topographic maps on this scale were readily available, nor was it considered critical to purchase the digital topographic map, as there were less than 50 data points involved. A total of 47 points (well sites) were entered in this way.

6.2.3.2.3 Preliminary Analysis

Despite the large scale map entry, the data show a strong NE-trend of elevated

ID	Name	Eastings	Northings	Name of sample	Address	Dug/ drilled	Well Depth	Well Diameter	Depth to Bedrock	Water depth	COND	pH	U mg/L	Rn Bq/L	REGION
1	NR1	394298	4962147	NR1	RR#3 Windsor	dug	16	3			111	7.5	**0.003**	**63**	Leminster-Vaughn A
2	NR2A	394430	4962160	NR2A	RR#3 Windsor	dug	20	2			66	5.9	**0.003**	**12**	Leminster-Vaughn A
3	NR3	395700	4962517	NR3	RR#3 Windsor	dug	12	3		3.0	2200	5.7	**0.003**	**99**	Leminster-Vaughn A
4	NR4A	395806	4962570	NR4A	RR#3 Windsor	dug	4	4		0.5	83	5.9	**0.003**	**306**	Leminster-Vaughn A
5	NR5A	395581	4962702	NR5A	RR#3 Windsor	dug		3			210	6.5	**0.003**	**27**	Leminster-Vaughn A
5	NR5B	395674	4962742	NR5B	RR#3 Windsor	dug	15	3		3.0	95	6.3	**0.003**	**20**	Leminster-Vaughn A
50	NR50A	402927	4966183	NR50A	RR#3 Windsor	dug					106	6.8	**0.003**	**35**	Leminster-Vaughn A
49	NR49	402753	4966147												
48	NR48	402569	4966132												
47	NR47	402341	4966087												
46	NR46	402236	4966132												
45	NR45	401967	4966097	NR45	RR#3 Windsor	dug	22	4		7.0	290	6.5	**0.003**	**18**	Leminster-Vaughn A
44	NR44	401976	4966256	NR44	DNR Park	dug					300	7.4	**0.003**		Leminster-Vaughn A
43	NR43	401812	4965790	NR43	RR#3 Windsor	dug	14	4			99	6.7	**0.003**	**18**	Leminster-Vaughn A
35	NR35	400230	4964941	NR35	RR#3 Windsor	dug	9	4			33	5.9	**0.003**	**364**	Leminster-Vaughn A
31	NR31A	399676	4964717	NR31A	RR#3 Windsor	pond					700	5.8	**0.003**	**48**	Leminster-Vaughn A
32	NR32	399864	4964735	NR32	RR#3 Windsor	dug	12	2			270	5.6	**0.003**	**73**	Leminster-Vaughn A
33	NR33	399962	4964798	NR33	RR#3 Windsor	dug	12			6.0	33	5.9	**0.003**	**61**	Leminster Vaughn A
34	NR34	399971	4964950	NR34	RR#3 Windsor	sprin					46	6.1	**0.003**	**411**	Leminster-Vaughn A
36	NR36	400507	4965298												
37	NR37	400740	4965441												
38	NR38	400749	4965334												
39	NR39	400847	4965620	NR39	RR#3 Windsor	dug	10	3.5			45	6.3	**0.003**	**72**	Leminster-Vaughn A
40	NR40	400856	4965504	NR40	RR#3 Windsor	dug	10	3.5			35	6.1	**0.003**	**88**	Leminster-Vaughn A
41	NR41	400910	4965557	NR41	RR#3 Windsor	dug	11	3		2.0	79	6.5	**0.003**	**56**	Leminster-Vaughn A
42	NR42	401097	4965682	NR42	RR#3 Windsor	dug	7	3.5		4.0	36	6.1	**0.003**	**224**	Leminster-Vaughn A
22	NR22	398175	4963734	NR22	RR#3 Windsor	dug	9	3		5.0	130	6.7	**0.003**	**593**	Leminster-Vaughn A
23	NR23	398541	4963859	NR23	RR#3 Windsor	dug	3	4		2.0	112	5.9	**0.003**	**1384**	Leminster-Vaughn A
25	NR25	398666	4963770	NR25	RR#3 Windsor	dug	28				94	6.4	**0.003**	**11**	Leminster-Vaughn A
26	NR26	398720	4963966	NR26	RR#3 Windsor	dug	15	3			410	6.4	**0.003**	**120**	Leminster-Vaughn A
27	NR27	398666	4964100	NR27	RR#3 Windsor	dug	21	6		8.0	280	6.7	**0.003**	**22**	Leminster-Vaughn A
30	NR30	398648	4964306	NR30	RR#3 Windsor	sprin					32	5.5	**0.003**	**312**	Leminster-Vaughn A
28	NR28	398979	4964020	NR28	RR#3 Windsor	drill	145	6			160	8.2	**0.02**	**1151**	Leminster-Vaughn A
21	NR21	397817	4963788	NR21	RR#3 Windsor	dug	18				83	6.2	**0.003**	**12**	Leminster-Vaughn A
20	NR20	397728	4963966	NR20	RR#3 Windsor	dug	12	3		6.0	290	6.2	**0.003**	**17**	Leminster-Vaughn A
19	NR19	397576	4963850												
18	NR18	397478	4963904	NR18	RR#3 Windsor	dug	18	4			80	6.5	**0.003**	**38**	Leminster-Vaughn A
16	NR16	397397	4964047												

Table 6.5. Leminster Rn and U well water data. Original data from Uranium Task force (MacFarland, 1983). Blanks are missing data.

ID	Name	Eastings	Northings	Name of sample	Address	Dug/ drilled	Well Depth	Well Diameter	Depth to Bedrock	Water depth	COND	pH	U mg/L	Rn Bq/L	REGION
17	NR17	397326	4964226												
15	NR15	397283	4964018	NR15	RR#3 Windsor	dug	12	3		10.0	500	5.7	**0.003**	**26**	Leminster-Vaughn
14	NR14	397212	4963946												
12	NR12	397033	4963857	NR12	RR#3 Windsor	dug	12	7			53	6	**0.003**	**6**	Leminster-Vaughn
13	NR13	396926	4963902	NR13	RR#3 Windsor	dug	15	2		8.0	58	5.9	**0.003**	**25**	Leminster-Vaughn
11	NR11	397078	4963634	NR11	RR#3 Windsor	dug				3.0	60	6.2	**0.003**	**7**	Leminster-Vaughn
10	NR10	396783	4963535	NR10	RR#3 Windsor	dug	15	3		3.0	410	7.1	**0.003**	**53**	Leminster-Vaughn
9	NR9	396899	4963446	NR9	RR#3 Windsor	dug	15	3			78	6	**0.003**	**22**	Leminster-Vaughn
8	NR8	396720	4963294	NR8	RR#3 Windsor	dug	15	3		1.0	310	7.5	**0.003**	**16**	Leminster-Vaughn
7	NR7	396667	4963169	NR7	RR#3 Windsor	dug	17	4		8.0	280	7.9	**0.003**	**2**	Leminster-Vaughn
6	NR6	396399	4962981	NR6	RR#3 Windsor	drill	195	0.5	4	10.0	87	6.1	**0.003**	**979**	Leminster Vaughn
51	CR1	399330	4964054	CR1	RR#3 Windsor	dug	15	3			320	6.8	**0.003**	**355**	Leminster-Vaughn
52	CR2	399374	4963723	CR2	RR#3 Windsor	dug	10	5			67	6	**0.003**	**24**	Leminster-Vaughn
53	HR1	397828	4963535	HR1	RR#3 Windsor	drill					184	6.5	**0.13**	**7794**	Leminster-Vaughn
54	HR2	397891	4963267	HR2	RR#3 Windsor	drill	150	0.5			260	6.6	**0.003**	**100**	Leminster-Vaughn
55	HR3	397944	4962928												
56	HR4A	397980	4962856												
57	HR4B	398070	4962820												
62	WS2			WS2	RR#3 Windsor	dug	20	3			260	6.1	**0.003**	**32**	Leminster-Vaughn
63	WS5			WS5	RR#3 Windsor	dug	16	3			35	6	**0.003**	**7.2**	Leminster-Vaughn
64	NR4B	395786	4962590	NR4B	RR#3 Windsor	dug	18	3		5.0	65	5.8	**0.003**	**5**	Leminster-Vaughn
65	NR2B	394430	4962180	NR2B	RR#3 Windsor	sprin					109	6.8	**0.003**	**54**	Leminster-Vaughn
66	NR31B	399661	4964747	NR31B	RR#3 Windsor	dug	16	10		2.0	1320	5.6	**0.003**	**13**	Leminster-Vaughn
67	NR50B	402912	4966213	NR50B	RR#3 Windsor	dug					79	6.4	**0.003**	**189**	Leminster-Vaughn

Table 6.5. Continued..

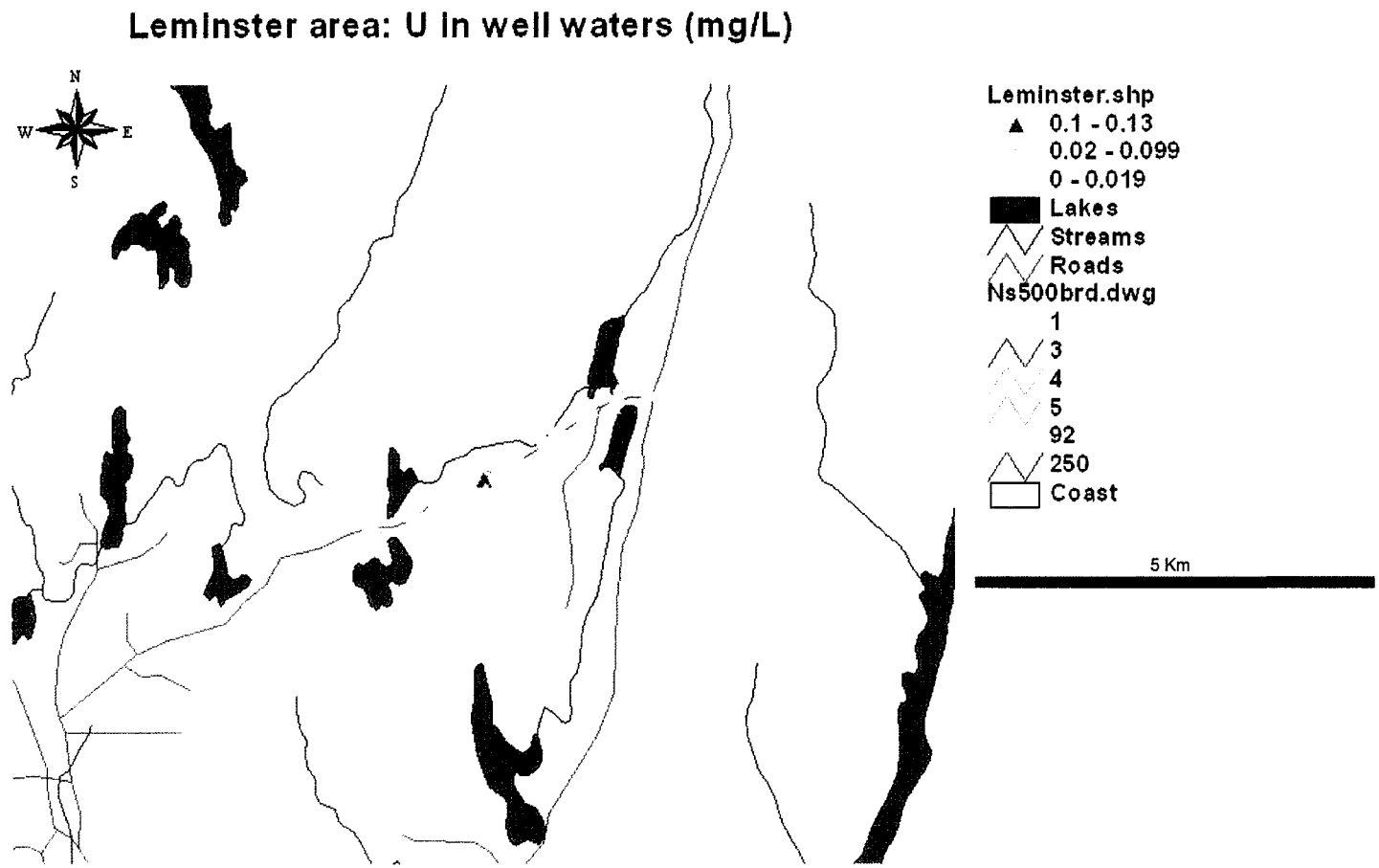

Figure 6.5A Leminster area: Uranium in well waters (mg/L)

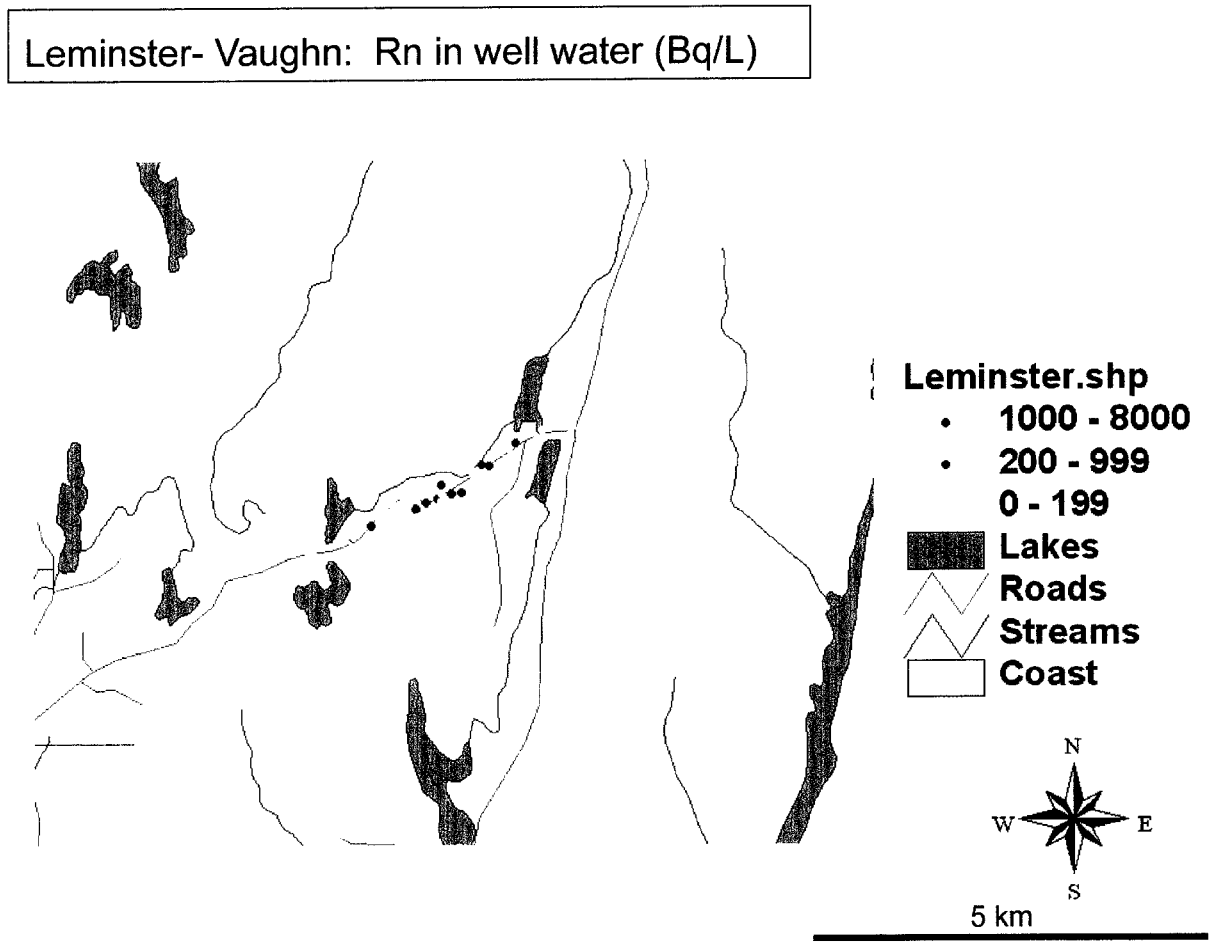

Figure 6.5B. Leminster area: Rn in well water (Bq/L)

Rn in well water values. This trend is also evident when the paper map copy is examined. Almost all wells are dug wells, and although Rn values are as high as 7794 Bq/L, U values are low in all but one well (0.13 mg/L - drilled well). The linear nature of the elevated Rn values is similar to the linear trend of fractures associated with U mineralization of the Millet Brook site which is in close geographic proximity (Chatterjee and Muecke, 1982). The Millet Brook uranium occurrence is located due north of the New Ross road on which the Leminster-Vaughan wells are located, approximately 1 km (Chatterjee and Muecke, 1982) (Fig. 6.2). This structural trend and similarity to the Millet Brook showing, suggests that the presence of Rn and possibly U in this area at least, may be strongly fracture-controlled.

Several of the wells with elevated values lie within or near the contact with Meguma Group rocks, although some lie within the rocks of the batholith itself; if fracture-controlled, the fractures clearly post-date the intrusion of the batholith, and the source of the U (and its daughter products) is not the Meguma Group.

That elevated levels of radioelements in this region may be associated with fractures, has implications for the development of any radon potential map, and in particular, for a radon potential map for the region underlain by the South Mountain Batholith in Nova Scotia. If elevated U and Rn (and Ra) are controlled in part by the presence of fractures, developing a radon potential map for the region would require detailed structural information for the entire area. Given the glacial coverage for much of this region, a detailed map of the structural features present is not possible for all areas of the batholith. In addition, fractures may be localized, making their detection and importance as channels for radioelement migration difficult to assess accurately. Thus, although all regions of the batholith clearly do not have associated elevated radioelement levels, the precautionary principle would suggest that individuals consider the possibility that their home or well may lie on a radioelement-bearing fracture if they live in an area underlain by rocks of the South Mountain Batholith.

6.2.3.3 New Ross

Number of data output in .dbf format	230 values
File names and tables	newross.dbf (database) newross.shp (map) (Table 6.6; Figure 6.6)
Nature of spatial data output	230 of these values "grouped"into 22 "points" = centroids of mining tracts

6.2.3.3.1 Original data

The original data were made available through Nova Scotia Department of the Environment. The data were in hand-written tabular format. No data were available in map format.

6.2.3.3.2 Data Processing

All data in paper format were entered into digital format (.dbf files) (Table 6.6). Addresses for these data were non site-specific (e.g. Box 24, New Ross, or RR #3 New Ross, etc). As a result, it was not possible to locate these data accurately on a map. This is particularly unfortunate, as the data show a wide range of variability (Table 6.6).

Given the non-site-specific nature of the data, it was determined that the "best" way to locate these data on a map was to index to the mining tract, if possible. In most cases the original tabular data included this information. This allowed for dividing the data into 22 "points" rather than a single point centered on New Ross (Figure 6.5). It should be clearly understood that the points indicated on the map, are head-up digitized centroids of a given mining tract and do not represent actual points where wells are located. Information on individual data points can be examined by clicking on the point with the **"i"** button, and all data belonging to that point will appear in tabular form on the screen.

#	ID	Eastings	Northings	Mining	dug/	well	well	depth to	water	COND	pH	U	Rn	Ra	Region
				Claim #	drilled	depth	diameter	bedrock	depth			m/L	Bq/L	Bq/L	
1	NR117	363739	4946378	21A 10D 35	drilled	297	0.5	30		167	7.8	0.2	6300	0.5	New Ross
2	NR118	363739	4946378	21A 10D 35	dug	17	2.5			69	6.4	0.003	0	0.05	New Ross
3	NR198	373790	4953880	21A 10D 92	dug	17	7			210	6.8	0.003	12	0.05	New Ross
4	NR199	373790	4953880	21A 10D 92	drilled	215	0.5	84	61	210	8	0.003	440	0.05	New Ross
5	NR200	373790	4953880	21A 10D 92	drilled	127	0.5			168	8	0.01	380	0.05	New Ross
6	NR201	373790	4953880	21A 10D 92	dug	13	5			174	6.8	0.003	8	0.05	New Ross
7	NR202	373790	4953880	21A 10D 92	dug	13				149	6.5	0.003	8	0.05	New Ross
8	NR203	373790	4953880	21A 10D 92	drilled	72	0.5	24	15	400	7.6	0.007	520	0.05	New Ross
9	NR204	373790	4953880	21A 10D 92	dug	12	4		6	1200	5.6	0.003	50	0.1	New Ross
10	NR205	373790	4953880	21A 10D 92	drilled	135	0.5	47		140	7.7	0.07	0	0.05	New Ross
11	NR207	373790	4953880	21A 10D 92	dug	5	2		0	117	5.5	0.003	51	0.05	New Ross
12	NR208	373790	4953880	21A 10D 92	dug			0		420	6.2	0.003	270	0.05	New Ross
13	NR209	373790	4953880	21A 10D 92	dug	20	4			510	7	0.003	7	0.05	New Ross
14	NR210	373790	4953880	21A 10D 92	dug	13	3			600	6.5	0.003	14	0.05	New Ross
15	NR211	373790	4953880	21A 10D 92	dug	19	3		3	420	7.6	0.003	6	0.05	New Ross
16	NR212	373790	4953880	21A 10D 92	dug		3			116	6.5	0.003	10	0.05	New Ross
17	NR213	373790	4953880	21A 10D 92	drilled	65	0.5			108	6.5	0.03	640	0.05	New Ross
18	NR214	373790	4953880	21A 10D 92	drilled	55	0.5			210	7.9	0.01	600	0.05	New Ross
19	NR215	373790	4953880	21A 10D 92	dug	24	4		8	67	6.9	0.003	10	0.05	New Ross
20	NR216	373790	4953880	21A 10D 92	dug	17	3		10	950	7.5	0.003	8	0.05	New Ross
21	NR217	373790	4953880	21A 10D 92	drilled	135	0.5	8	10	158	7.9	0.009	650	0.05	New Ross
22	NR218	373790	4953880	21A 10D 92	dug	20	3		2	149	6.8	0.003	18	0.05	New Ross
23	NR219	373790	4953880	21A 10D 92	dug	13	5		2	134	6.3	0.003	7	0.05	New Ross
24	NR220	373790	4953880	21A 10D 92	drilled	118	0.5			230	8	0.02	370	0.05	New Ross
25	NR221	373790	4953880	21A 10D 92	dug					200	6.6	0.003	11	0.05	New Ross
26	NR222	373790	4953880	21A 10D 92	drilled	75	0.5			167	6	0.003	600	0.05	New Ross
27	NR225	373790	4953880	21A 10D 92	drilled					220	8	0.006	760	0.05	New Ross
28	NR226	373790	4953872	21A 10D 92	dug	12	4			230	6.4	0.003		0.05	New Ross
29	NR227	373790	4953880	21A 10D 92	drilled	95	0.5	12	12	400	6.2	0.003	270	0.05	New Ross
30	NR228	373790	4953872	21A 10D 92	dug	18	3		12	750	7.6	0.003	2	0.05	New Ross
31	NR229	373790	4953872	21A 10D 92	spring				0	270	7	0.02	49	0.05	New Ross
32	NR230	373790	4953872	21A 10D 92	drilled	215	0.5	36	30	240	8.2	0.02	750	0.1	New Ross
33	NR231	373790	4953872	21A 10D 92	dug	18	3			230	8.2	0.02		0.01	New Ross
34	NR233	373790	4953872	21A 10D 92	dug	27			7	250	7.1	0.003	2	0.01	New Ross
35	NR234	373790	4953872	21A 10D 92	drilled	72	0.5	36		300	7.7	0.003	510	0.01	New Ross
36	NR235	373790	4953872	21A 10D 92	drilled	99	0.5	60	40	240	7.5	0.008	740	0.01	New Ross
37	NR236	373790	4953880	21A 10D 92	drilled	85	0.5			250	7.8	0.003	440	0.01	New Ross
38	NR237	373790	4953872	21A 10D 92	dug	16			8	240	7.2	0.003	7	0.01	New Ross
39	NR238	373790	4953872	21A 10D 92	drilled	200	0.5	70	40	127	8.3	0.02	370	0.01	New Ross
40	NR239	373790	4953872	21A 10D 92	dug	21			10	115	6.8	0.003	2	0.01	New Ross

Table 6.6. New Ross U and Rn in well water data. Original data from Uranium Task Forc (MacFarlane, 1983)

#	ID	Eastings	Northings	Mining Claim #	dug/ drilled	well depth	well diameter	depth to bedrock	water depth	COND	pH	U m/L	Rn Bq/L	Ra Bq/L	Region
41	NR240	373790	4953872	21A 10D 92	dug	20				220	7.7	0.003	33	0.01	New Ross
42	NR241	373790	4953872	21A 10D 92	dug	14	5			184	7	0.003		0.01	New Ross
43	NR242	373790	4953872	21A 10D 92	pond	9				31	6.2			0.01	New Ross
44	NR243	373790	4953872	21A 10D 92	spring	4	4.5		3	340	6.7	0.02	180	0.01	New Ross
45	NR244	373790	4953872	21A 10D 92	drilled	186	0.5			510	7.4	0.009	510	0.01	New Ross
46	NR245	373790	4953872	21A 10D 92	dug	8	8			1400	6.6	0.003	17	0.01	New Ross
47	NR246	373790	4953872	21A 10D 92	dug	14	8		3	550	6.5	0.003		0.01	New Ross
48	NR247	373790	4953872	21A 10D 92	drilled		0.5			470	7.1	0.01	580	0.01	New Ross
49	NR248	373790	4953872	21A 10D 92	drilled	53	0.5			450	8	0.02	480	0.01	New Ross
50	NR249	373790	4953872	21A 10D 92	dug	10	2		4	83	6.4	0.003		0.01	New Ross
51	NR250	373790	4953872	21A 10D 92	dug	19	2.5		10	420	7.8	0.003	17	0.01	New Ross
52	NR252	373790	4953872	21A 10D 92	drilled	65	0.5	10	9	164	7.3	0.003	40	0.05	New Ross
53	NR14	375443	4953852	21A 10D 93	drilled	220	0.5	10	5	98	6.8	0.003	0	0.3	New Ross
54	NR188	375443	4953852	21A 10D 93	dug	25	3.5		10	550	6.5	0.003	6	0.05	New Ross
55	NR189	375443	4953852	21A 10D 93	drilled	50	0.5	6		230	6.7	0.005	800	0.05	New Ross
56	NR190	375443	4953852	21A 10D 93	drilled	215	0.5	10		131	7.9	0.005	250	0.05	New Ross
57	NR191	375443	4953852	21A 10D 93	dug	20	3		18	64	6.3	0.003	7	0.05	New Ross
58	NR192	375443	4953852	21A 10D 93	dug	17	3		3	390	6.6	0.003	13	0.05	New Ross
59	NR193	375443	4953852	21A 10D 93	dug	18	3		3	220	6.9	0.003	0	0.05	New Ross
60	NR194	375443	4953852	21A 10D 93	spring		3		8	620	5.9	0.003	290	0.05	New Ross
61	NR195	375443	4953852	21A 10D 93	drilled	95	0.5	16		560	7.1	0.02	650	0.05	New Ross
62	NR196	375443	4953852	21A 10D 93	dug	18	4		10	140	7	0.003	6	0.05	New Ross
63	NR197	375443	4953852	21A 10D 93	dug	12	4		10	350	6.9	0.003	15	0.05	New Ross
64	NR1	377089	4953824	21A 10D 94	drilled	135	0.5	45	20	176	7.8	0.13	6900	0.3	New Ross
65	NR2	377089	4953824	21A 10D 94	drilled	110	0.5	20		360	7.1	0.03	0	0.1	New Ross
66	NR15	377089	4953824	21A 10D 94	dug	21	2.5		10	77	6.3	0.003	0	0.05	New Ross
67	NR224	377089	4953824	21A 10D 94	drilled	95	0.5	17	16	142	7.9	0.009	490	0.05	New Ross
68	NR232	377089	4953824	21A 10D 94	dug	14	3		3	171	8.5	0.003	6	0.01	New Ross
69	NR4	378738	4953784	21A 10D 95	drilled	195	0.5	26	20	260	7.3	0.22	195	0.6	New Ross
70	NR6	378738	4953784	21A 10D 95	drilled	195	0.5	26	20	115	7.7	0.005	0	0.05	New Ross
71	NR169	378738	4953784	21A 10D 95	drilled	95	0.5	17	16	230	7.9	0.008	500	0.05	New Ross
72	NR161	380388	4953762	21A 10D 96	dug	19	3			310	7.5	0.006	37	0.05	New Ross
73	NR162A	380388	4953762	21A 10D 96	drilled	165	0.5	3	7	34	5.6	0.003	470	0.1	New Ross
74	NR162B	380388	4953762	21A 10D 96	dug	8	3		2	42	5.9	0.003	0	0.05	New Ross
75	NR163	380388	4953762	21A 10D 96	dug	10	3		8	350	7.1	0.009	590	0.05	New Ross
76	NR164	380388	4953762	21A 10D 96	dug	5	6			94	6.6	0.003	240	0.05	New Ross
77	NR165	380388	4953762	21A 10D 96	drilled	129	0.5			220	7.7	0.04	1080	0.05	New Ross
78	NR167	380388	4953762	21A 10D 96	drilled	180	0.5			114	5.2	0.003	380	0.05	New Ross
79	NR168	380388	4953762	21A 10D 96	drilled	200	0.5			68	5.9	0.003	320	0.05	New Ross
80	NR170	380388	4953762	21A 10D 96	dug	14	3		6	1030	6.3	0.007	1790	0.3	New Ross
81	NR171	380388	4953762	21A 10D 96	dug	12	3		9	350	7.8	0.003	50	0.05	New Ross

Table 6.6, continued.

#	ID	Eastings	Northings	Mining Claim #	dug/ drilled	well depth	well diameter	depth to bedrock	water depth	COND	pH	U m/L	Rn Bq/L	Ra Bq/L	Region
82	NR172	380388	4953762	21A 10D 96	drilled	95	0.5	43	39	480	7.8	0.04	1460	0.05	New Ross
83	NR173	380388	4953762	21A 10D 96	dug		6			140	6	0.003	190	0.05	New Ross
84	NR176	380388	4953762	21A 10D 96	drilled	125	0.5	2		420	5.9	0.02	4475	0.08	New Ross
85	NR251	380388	4953762	21A 10D 96	dug	18	8			260	7.6	0.03	13	0.05	New Ross
86	NR260	380388	4953762	21A 10D 96	drilled	38	0.5			230	5.3	0.006	2880	2.2	New Ross
87	NR160A	380428	4955303	21A 10D 97	drilled	16	8			450	6.9	0.003	0	0.05	New Ross
88	NR160B	380428	4955303	21A 10D 97	dug					41	7.1	0.003	13	0.05	New Ross
89	NR146	380428	4955303	21A 10D 97	dug	12	3		3	91	5.8	0.003	210	0.05	New Ross
90	NR147	380428	4955303	21A 10D 97	dug	12	3		6	1340	5.3	0.008	1765	1.9	New Ross
91	NR149	380428	4955303	21A 10D 97	dug		3			167	5.4	0.003	1500	0.2	New Ross
92	NR159	380428	4955303	21A 10D 97	dug	15				230	6.6	0.003	79	0.05	New Ross
93	NR179	380428	4955303	21A 10D 97	dug	33			5	123	7.4	0.003	6	0.05	New Ross
94	NR104	383734	4956815	21A 16B 11	dug		3			86	6.2	0.003	5	0.05	New Ross
95	NR105	383734	4956815	21A 16B 11	dug		3		4	41	6.5	0.003	6	0.05	New Ross
96	NR115	383734	4956815	21A 16B 11	dug	12	3.5			300	6.9	0.003	64	0.05	New Ross
97	NR19	382080	4956789	21A 16B 12	dug	23	2			56	6.1	0.003	16	0.05	New Ross
98	NR101	383776	4958359	21A 16B 14	drilled	115	0.5	6	20	69	6	0.003	540	0.05	New Ross
99	NR102	383785	4958359	21A 16B 14	dug	25	3			50	6.3	0.003	17	0.05	New Ross
100	NR103	383785	4958359	21A 16B 14	dug	20	4			74	5.8	0.003	19	0.05	New Ross
101	NR148	383804	4959845	21A 16B 35	dug		3			300	7.7	0.003	9	0.05	New Ross
102	NR90	387062	4959844	21A 16B 33	drilled	43	0.5			41	6	0.003	320	0.05	New Ross
103	NR33	386990	4955186	21A 9C 105	spring	3	2.5		1	138	6.2	0.007	210	0.05	New Ross
104	NR75	386990	4955186	21A 9C 105	dug	12	3		6	162	6	0.003	0	0.05	New Ross
105	NR76	386990	4955186	21A 9C 105	dug	14	3			124	8.1	0.003	35	0.05	New Ross
106	NR77	386990	4955186	21A 9C 105	dug	21	10.5			152	7.1	0.003	18	0.05	New Ross
107	NR174	386990	4955186	21A 9C 105	dug	28	5		12	280	6.9	0.003	39	0.05	New Ross
108	NR175	386990	4955186	21A 9C 105	dug	29	3		2	45	6.7	0.003	19	0.05	New Ross
109	NR11	385291	4955202	21A 9C 106	drilled	255	0.5	122		250	8.1	0.04	660	0.2	New Ross
110	NR12	385291	4955202	21A 9C 106	drilled	78	0.5	36	21	109	7.9	0.02	0	0.05	New Ross
111	NR20	385291	4955202	21A 9C 106	drilled	180	0.5	40	8	340	7.9	0.01	530	0.05	New Ross
112	NR27	385291	4955202	21A 9C 106	dug		2.5		1	65	6.3	0.003	12	0.05	New Ross
113	NR34	385291	4955202	21A 9C 106	dug	30	4		2	600	6.1	0.003	12	0.05	New Ross
114	NR48	385291	4955202	21A 9C 106	drilled	42	0.5		5	65	6.7	0.003	99	0.05	New Ross
115	NR49	385291	4955202	21A 9C 106	drilled	110	0.5	30	20	178	5.6	0.003	680	0.05	New Ross
116	NR54	385291	4955202	21A 9C 106	drilled	160	0.5	80	27	139	7.4	0.03	923	0.05	New Ross
117	NR78	385291	4955202	21A 9C 106	drilled	250	0.5	90		125	7.4	0.24	0	0.05	New Ross
118	NR80	385291	4955202	21A 9C 106	dug					360	6.4	0.003	30	0.05	New Ross
119	NR81	385291	4955202	21A 9C 106	dug	15	2		8	370	6.3	0.003	0	0.05	New Ross
120	NR82	385291	4955202	21A 9C 106	dug	22	3		16	166	6.4	0.003	15	0.05	New Ross
121	NR83	385291	4955202	21A 9C 106	dug	18	6		8	140	7.2	0.009	1700	0.05	New Ross
122	NR84	385291	4955202	21A 9C 106	dug	23	2		10	72	7.4	0.003	11	0.05	New Ross
123	NR85	385291	4955202	21A 9C 106	drilled	295	0.5	113	80	130	7.7	0.16	2900	0.05	New Ross
124	NR100	385291	4955202	21A 9C 106	dug	18	3		12	220	7.4	0.003	11	0.05	New Ross
125	NR107	385291	4955202	21A 9C 106	drilled	52	0.5	28	3	181	7.1	0.003	210	0.05	New Ross
126	NR108	385291	4955202	21A 9C 106	dug	16	4		2	60	6.6	0.003	10	0.05	New Ross
127	NR109	385291	4955202	21A 9C 106	dug	18	4		2	144	6.7	0.003	29	0.05	New Ross

Table 6.6, continued.

#	ID	Eastings	Northings	Mining Claim #	dug/ drilled	well depth	well diameter	depth to bedrock	water depth	COND	pH	U m/L	Rn Bq/L	Ra Bq/L	Region
128	NR110	385291	4955202	21A 9C 106	dug	8	1		1	50	6.5	0.003	340	0.05	New Ross
129	NR111	385291	4955202	21A 9C 106	dug	3	3		2	26	5.6	0.003	490	0.05	New Ross
130	NR86	385291	4955202	21A 9C 106	dug f	15	3		7	330	7.7	0.003	10	0.05	New Ross
131	NR87	385291	4955202	21A 9C 106	drilled	220	0.5	108	45	130	7.6	0.17	3500	0.05	New Ross
132	NR88	385291	4955202	21A 9C 106	drilled	255	0.5	122		136	7.2	0.02	1900	0.1	New Ross
133	NR112	385291	4955202	21A 9C 106	drilled f	188	0.5			178	8	0.03	440	0.05	New Ross
134	NR43	383729	4955218	21A 9C 107	drilled	215	0.5	17		160	7.3	0.1	1620	0.2	New Ross
135	NR51	383729	4955218	21A 9C 107	drilled	195	0.5	3	3	174	6.4	0.006	1310	0.05	New Ross
136	NR79	383729	4955218	21A 9C 107	drilled	215	0.5	84	71	121	7.3	0.08	0	0.05	New Ross
137	NR106	383729	4955218	21A 9C 107	dug	10			4.5	220	7.5	0.18	29	0.05	New Ross
138	NR113	383729	4955218	21A 9C 107	drilled	190	0.5	50	30	210	7	0.009	810	0.05	New Ross
139	NR114	383729	4955218	21A 9C 107	dug	18	3.5		3	137	7.2	0.003	4	0.05	New Ross
140	NR119	383729	4955218	21A 9C 107	dug	30	2.5		15	450	7.2	0.003	32	0.05	New Ross
141	NR120	383729	4955218	21A 9C 107	dug	4				167	7.9	0.003	14	0.05	New Ross
142	NR121	383729	4955218	21A 9C 107	dug	11	2.5		4	300	6.3	0.003	28	0.05	New Ross
143	NR122	383729	4955218	21A 9C 107	dug				5	280	6.8	0.003	66	0.05	New Ross
144	NR134	383729	4955218	21A 9C 107	dug		4		4	8.4	6.8	0.003	6	0.05	New Ross
145	NR137	383729	4955218	21A 9C 107	dug	15	5		4	130	6.6	0.003	20	0.05	New Ross
146	NR116	383729	4955218	21A 9C 107	drilled	125	0.5	40	30	220	8.2	0.003	37	0.05	New Ross
147	NR7	382027	4955283	21A 9C 108	drilled	195	0.5	15	15	104	6.2	0.008	0	0.7	New Ross
148	NR123	382027	4955274	21A 9C 108	dug	20	4		4	860	6.5	0.003	31	0.05	New Ross
149	NR124	382027	4955274	21A 9C 108	dug	17	3		10	250	7	0.01	47	0.05	New Ross
150	NR125	382027	4955274	21A 9C 108	dug	20	3		15	980	6.2	0.003	27	0.05	New Ross
151	NR126	382027	4955274	21A 9C 108	dug	12	3		1	400	7.1	0.003	26	0.05	New Ross
152	NR127	382027	4955274	21A 9C 108	dug		3.5		8	350	7.4	0.003	11	0.05	New Ross
153	NR128	382027	4955274	21A 9C 108	drilled	180	0.5	58		146	7.7	0.19	1300	0.3	New Ross
154	NR129	382027	4955274	21A 9C 108	dug	16	10		4	360	6.3	0.003	9	0.05	New Ross
155	NR130	382027	4955274	21A 9C 108	dug	4	3		1	151	5.7	0.003	350	0.05	New Ross
156	NR131	382027	4955274	21A 9C 108	dug	10	4		1.5	47	5.9	0.003	13	0.05	New Ross
157	NR132	382027	4955274	21A 9C 108	dug		3			230	7.5	0.003	27	0.05	New Ross
158	NR133	382027	4955274	21A 9C 108	dug		4		3	172	7.2	0.003	0	0.05	New Ross
159	NR138	382027	4955274	21A 9C 108	dug		5		5	71	6.4	0.003	12	0.05	New Ross
160	NR139	382027	4955274	21A 9C 108	dug		3.5		2	61	6.1	0.005	1400	0.2	New Ross
161	NR140	382027	4955274	21A 9C 108	dug	12	5		3	46	5.8	0.003	200	0.05	New Ross
162	NR141	382027	4955274	21A 9C 108	dug		3		2	77	5.9	0.003	820	0.05	New Ross
163	NR143	382027	4955274	21A 9C 108	dug	19	4		2	106	5.9	0.003	200	0.05	New Ross
164	NR144	382027	4955274	21A 9C 108	dug	8	4		3	120	5.5	0.003	3000	1.1	New Ross
165	NR145	382027	4955274	21A 9C 108	dug	10	3		4	320	4.7	0.003	46	0.05	New Ross
166	NR152	382027	4955274	21A 9C 108	dug					2400	5.1	0.003	670	1.7	New Ross
167	NR155	382027	4955274	21A 9C 108	dug	22				280	7.4	0.003	9	0.05	New Ross
168	NR156	382027	4955274	21A 9C 108	dug	9	5			240	5.9	0.003	560	0.1	New Ross

Table 6.6, continued.

#	ID	Easting	Northing	Mining Claim #	dug/ drilled	well depth	well diameter	depth to bedrock	water depth	COND	pH	U m/L	Rn Bq/L	Ra Bq/L	Region
169	NR157	382027	4955274	21A 9C 108	dug	10				250	5.9	0.003	490	0.1	New Ross
170	NR158	382027	4955274	21A 9C 108	dug	12				120	6	0.003	50	0.05	New Ross
171	NR177	382027	4955274	21A 9C 108	drilled	195	0.5	10	15	360	6.3	0.01	4300	0.4	New Ross
172	NR178	382027	4955274	21A 9C 108	drilled	275	0.5	7	15	141	7.8	0.003	2000	0.4	New Ross
173	NR154	382027	4955274	21A 9C 108	drilled	135	0.5	45	20	174	7.8	0.12	7130	0.3	New Ross
174	NR153A	382027	4955274	21A 9C 108	dug	8			5	730	6.3	0.005	160	0.05	New Ross
175	NR153E	382027	4955274	21A 9C 108	dug	9	4			260	7	0.003	0	0.05	New Ross
176	NR3	382018	4955292	21A 9C 10B	drilled	340	0.5	8	50	124	6.7	0.008	0	0.3	New Ross
177	NR26	386982	4952100	21A 9C 81	dug				3	430	6.2	0.005	29	0.05	New Ross
178	NR35	386982	4952100	21A 9C 81	drilled	32	0.5			510	6.4	0.003	130	0.05	New Ross
179	NR36	386982	4952100	21A 9C 81	drilled	65	0.5	20	10	175	8.1	0.05	1880	0.05	New Ross
180	NR50	386982	4952109	21A 9C 81	drilled	180	0.5			160	7.8	0.08	560	0.05	New Ross
181	NR60	386982	4952109	21A 9C 81	drilled	93	0.5	35		310	7	0.003	1900	0.05	New Ross
182	NR63	386982	4952109	21A 9C 81	drilled	257	0.5			250	7.6	0.03	370	0.05	New Ross
183	NR65	386982	4952109	21A 9C 81	dug	25	4.5			34	6.5	0.003	0	0.05	New Ross
184	NR66	386982	4952109	21A 9C 81	drilled	110	0.5	30	20	62	5.6	0.003	510	0.05	New Ross
185	NR68	386982	4952109	21A 9C 81	drilled	100	0.5	35		230	6.6		510	0.05	New Ross
186	NR69	386982	4952109	21A 9C 81	dug	14	5		3	880	6.3	0.003	25	0.05	New Ross
187	NR70	386982	4952109	21A 9C 81	dug	15	5		3	430	6.6	0.008	49	0.05	New Ross
188	NR71	386982	4952109	21A 9C 81	dug	12	4		3	210	6.3	0.003	38	0.05	New Ross
189	NR72	386982	4952109	21A 9C 81	dug	20	4			296	6.8	0.006	69	0.05	New Ross
190	NR73	386982	4952109	21A 9C 81	dug		4		3	290	7.5	0.005	11	0.1	New Ross
191	NR30	385297	4952120	21A 9C 82	drilled	135	0.5	45	25	145	7.8	0.27	550	0.05	New Ross
192	NR53	385297	4952112	21A 9C 82	drilled	80			50	610	6.4	0.003	2	0.05	New Ross
193	NR55	385297	4952112	21A 9C 82	drilled	115	0.5			280	8	0.01	200	0.05	New Ross
194	NR56	385297	4952120	21A 9C 82	dug	15	6		4	280	6.9	0.003	59	0.05	New Ross
195	NR57	385297	4952120	21A 9C 82-I	drilled	210	0.5			300	6.7	0.01	354	0.05	New Ross
196	NR5	382016	4953749	21A 9C 85	drilled	315	0.5	9	10	145	6.4	0.006	0	0.1	New Ross
197	NR92	383666	4953693	21A 9C 86	drilled	115	0.5	90	25	260	7.5	0.06	380	0.05	New Ross
198	NR93	383666	4953693	21A 9C 86	dug	12	3			490	7.2	0.06	13	0.05	New Ross
199	NR94	383666	4953693	21A 9C 86	dug	8	3			4200	6.4	0.003	26	0.05	New Ross
200	NR95	383666	4953693	21A 9C 86	drilled	235	0.5			300	7.3	0.12	810	0.05	New Ross
201	NR96	383666	4953693	21A 9C 86	drilled	385	0.5	128	60	154	7.3	0.003	270	0.05	New Ross
202	NR97	383666	4953693	21A 9C 86	drilled	135	0.5	18		127	6.9	0.003	470	0.1	New Ross
203	NR98	383666	4953693	21A 9C 86	dug	10	4		5	178	7	0.003	49	0.05	New Ross
204	NR99	383666	4953693	21A 9C 86	dug	12	4			84	6.3	0.003	19	0.05	New Ross
205	NR150	383666	4953693	21A 9C 86	dug	28	4			250	7.8	0.003	31	0.05	New Ross
206	NR151	383666	4953693	21A 9C 86	dug	12	5			400	6.9	0.003	39	0.05	New Ross
207	NR9	385333	4953681	21A 9C 87	drilled	108	0.5	4	10	120	6	0.005	0	0.05	New Ross
208	NR38	385333	4953681	21A 9C 87	dug	22	6			94	6.9	0.003	9.7	0.05	New Ross
209	NR39	385333	4953681	21A 9C 87	drilled	80	0.5			130	5.8	0.005	2850	0.3	New Ross

Table 6.6, continued.

#	ID	Easting	Northing	Mining Claim #	dug/ drilled	well depth	well diameter	depth to bedrock	water depth	COND	pH	U m/L	Rn Bq/L	Ra Bq/L	Region
210	NR40	385333	4953681	21A 9C 87	drilled	160	0.5	20	10	123	7.7	0.08	300	0.05	New Ross
211	NR41	385333	4953681	21A 9C 87	dug		6		4	124	7.5	0.003	18	0.05	New Ross
212	NR42	385333	4953681	21A 9C 87	dug	18			10	630	6.4	0.003	14	0.05	New Ross
213	NR44	385333	4953681	21A 9C 87	drilled	100	0.5		90	300	7.5	0.7	3000		New Ross
214	NR58	385333	4953681	21A 9C 87	spring		0			450	6.1	0.003	500	0.05	New Ross
215	NR61	385333	4953681	21A 9C 87	drilled	70	0.5			500	7	0.003	43	0.05	New Ross
216	NR62	385333	4953681	21A 9C 87	drilled	140	0.5	3	6	260	6.2	0.03	2200	0.05	New Ross
217	NR37	385324	4953690	21A 9C 87 Ne	drilled					270	7	0.11	484	0.05	New Ross
218	NR46	385324	4953681	21A 9C 87(NI	drilled	70	0.5		14	250	6.8	0.003	51	0.05	New Ross
219	NR47	385324	4953690	21A 9C 87 (N	drilled	460	0.5	18	15	400	6.8	0.08	361	0.05	New Ross
220	NR22	386966	4953652	21A 9C 88	dug		2.5		2	149	7.7	0.003	20	0.05	New Ross
221	NR23	386966	4953652	21A 9C 88	dug		6		1.5	173	7.5	0.003	90	0.05	New Ross
222	NR24	386966	4953652	21A 9C 88	dug	16	4			540	5.6	0.003	59	0.05	New Ross
223	NR25	386966	4953652	21A 9C 88	drilled	255	0.5			300	8	0.01	560	0.05	New Ross
224	NR29	386966	4953652	21A 9C 88	dug	4	3			75	5.8	0.003	150	0.05	New Ross
225	NR31	386966	4953652	21A 9C 88	dug	15	3			156	7.3	0.003	13	0.05	New Ross
226	NR32	386966	4953652	21A 9C 88	drilled	135	0.5	6		210	5.5	0.003	160	0.05	New Ross
227	NR45	386966	4953652	21A 9C 88	dug	10	3			156	7.5	0.003	130	0.05	New Ross
228	NR74	386966	4953652	21A 9C 88	dug		3		3	116	6	0.003	36	0.05	New Ross
229	NR89	386966	4953652	21A 9C 88	dug		3			470	6	0.003	62	0.05	New Ross
230	NR206	386966	4953652	21A 9C 88	dug	13	3		3	28	5.8	0.003	250	0.05	New Ross
231	NR17	385316	4953690	High School	drilled					300	6.9	0.09	0	0.1	New Ross

Table 6.6, continued.

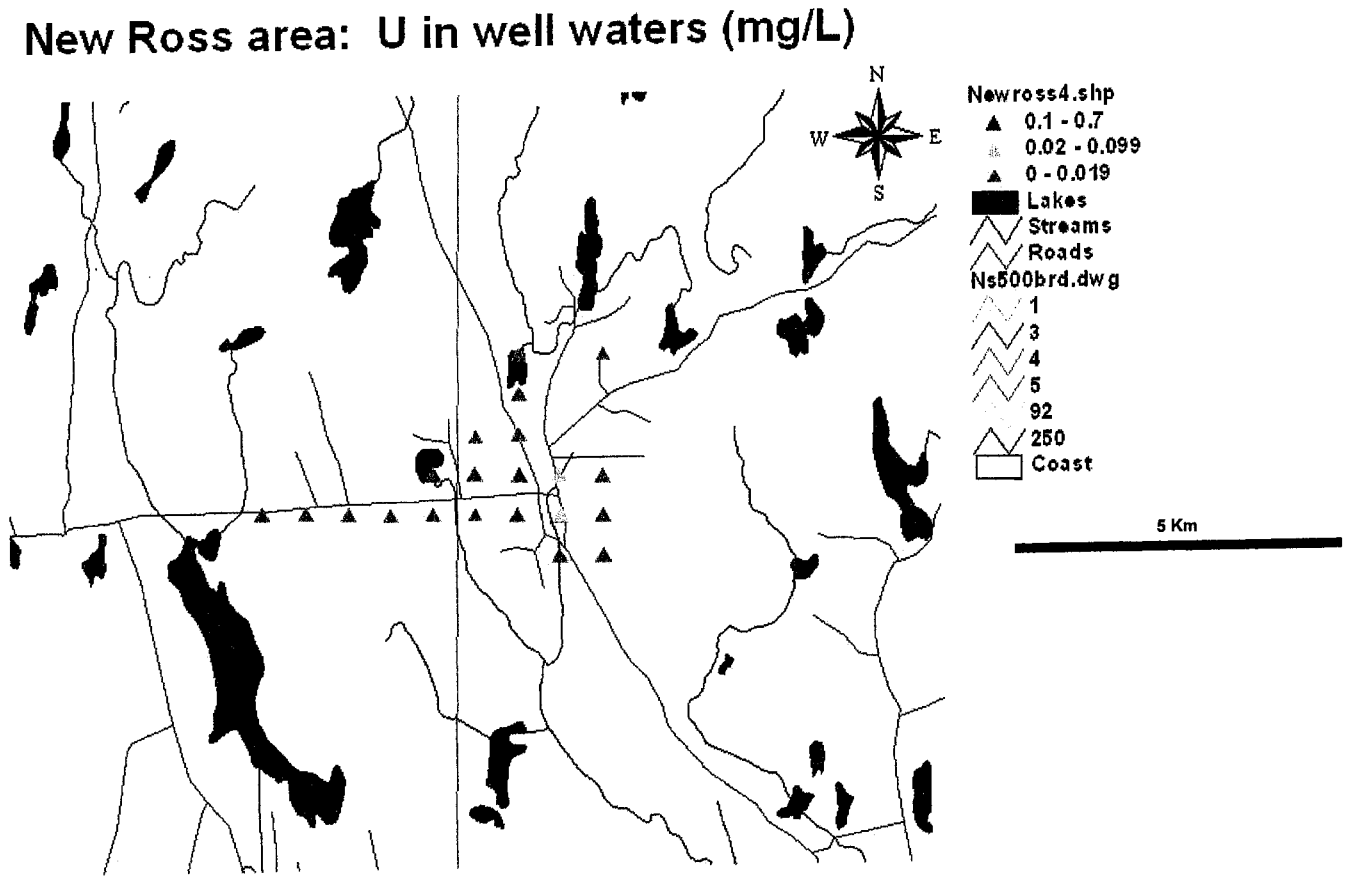

Figure 6.6A. New Ross area: Uranium in well waters (mg/L)

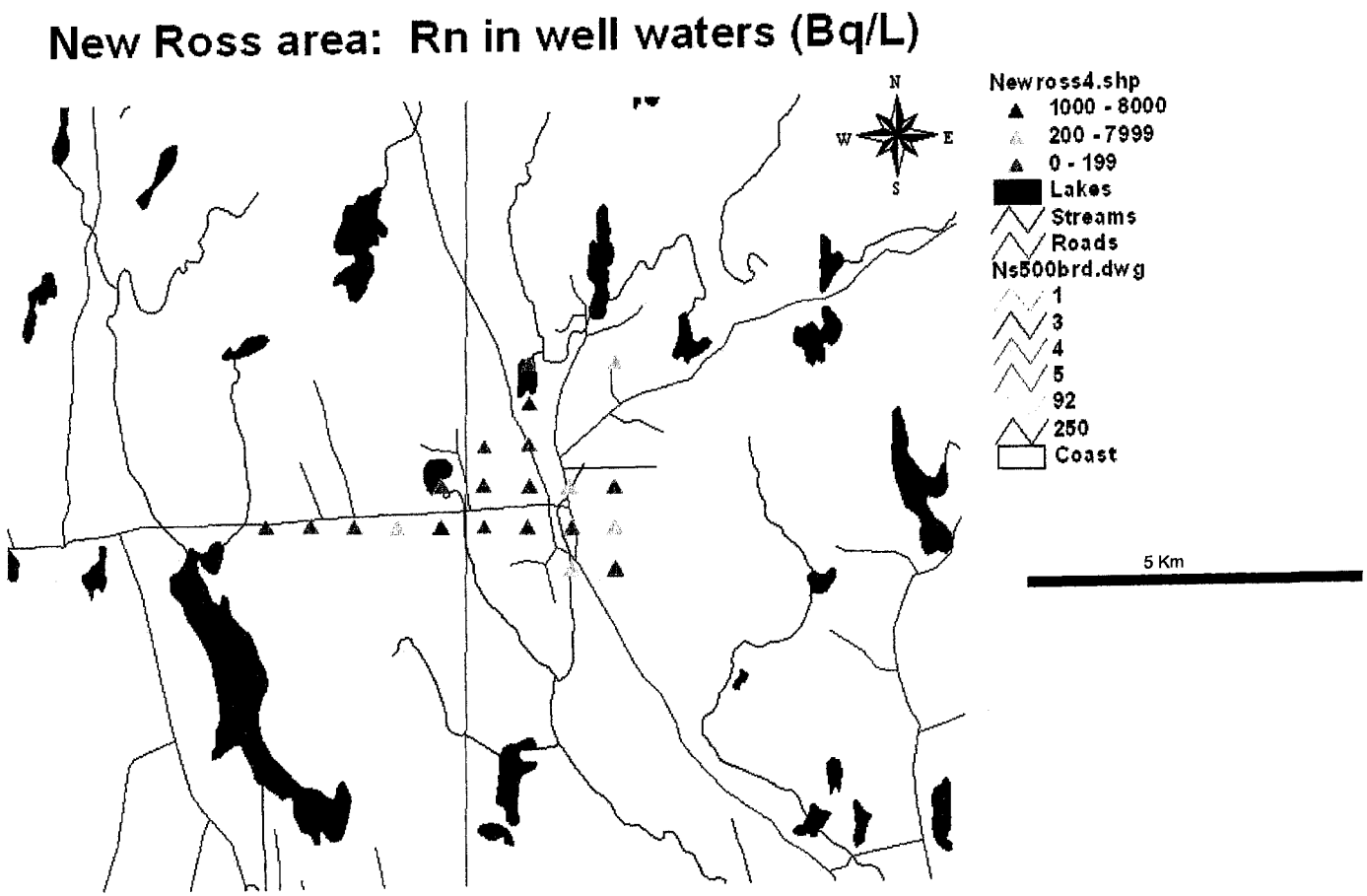

Figure 6.6B. New Ross area Radon in well waters (Bq/L).

6.2.3.3.3 Preliminary Analysis

Given that the sites of the individual wells are not clearly delimited, an interpretation based on the geology was not undertaken, as the region is underlain by a complex of several different types of granitic rocks. If, at some point, original maps for the original data for the New Ross area are relocated, it would be interesting and potentially very useful to determine more accurately the distribution of elevated U, Rn, and Ra in the New Ross area. This information may also serve to offer clues to understanding the nature of U, Rn, and Ra distribution in other areas of the batholith.

6.2.3.4 Northern Nova Scotia

Number of data output in .dbf format	130 values
Name of file and spatial output	north.dbf (tabular data) - Table 6.7 north.shp (map data) - Fig. 6.7
Nature of spatial data output	130 data grouped to 5 sites (towns)

6.2.3.4.1 Original data

The original data were made available through Nova Scotia Department of the Environment. The data were in hand-written tabular format. No data were available in map format.

6.2.3.4.2 Data Processing

All data in paper format were entered into digital format (.dbf files) (Table 6.7). Addresses for these data were non site-specific (e.g. RR#4 Tatamagouche), and unlike

Town	Eastings	Northings	Dug / Drilled	Well depth	Well diameter	Depth Bedrock	Casing length	Water depth	Conductivity	pH	U mg/L	Rn Bq/L	Data source
River John	495200	5066200	drilled	35.0	0.33				750	7.2	**0.005**	**86.0**	Task force
River John	495200	5066200	dug						260	6.6	**0.003**	**23.0**	Task force
River John	495200	5066200	drilled	27.0	0.25	8.0	16.0	10.0	650	6.8	**0.003**	**75.0**	Task force
River John	495200	5066200	drilled	135.0	0.45				970	8.9	**0.040**	**35.0**	Task force
River John	495200	5066200	drilled	180.0	0.50	12.0	21.0	15.0	2300	7.7	**0.030**	**132.0**	Task force
River John	495200	5066200	drilled	105.0	0.33	26.0	26.0	16.0	700	7.6	**0.020**	**162.0**	Task force
River John	495200	5066200	drilled	112.0	0.33		18.0		370	7.8	**0.010**	**224.0**	Task force
River John	495200	5066200	spring						141	6.9	**0.003**	**41.0**	Task force
River John	495200	5066200	drilled						1350	7.7	**0.020**	**141.0**	Task force
River John	495200	5066200	drilled	86.0	0.33	22.0	32.0	32.0	440	7.1	**0.003**	**96.0**	Task force
River John	495200	5066200	drilled	108.0	0.50	40.0	44.5	16.0	1460	7.5	**0.030**	**92.0**	Task force
River John	495200	5066200	drilled	75.0	0.33	22.0	25.0	17.0	1310	7.3	**0.009**	**246.0**	Task force
River John	495200	5066200	drilled	51.0	0.33	21.0	31.0	11.0	520	7.6	**0.006**	**95.0**	Task force
River John	495200	5066200	drilled	100.0	0.50		20.0		890	6.6	**0.003**	**52.0**	Task force
River John	495200	5066200	drilled	60.0					480	7.5	**0.008**	**89.0**	Task force
River John	495200	5066200	dug	20.0					560	7.5	**0.030**	**152.0**	Task force
River John	495200	5066200	drilled	83.0	0.33	20.0	24.0		1610	7.4	**0.030**	**140.0**	Task force
River John	495200	5066200	drilled	90.0	0.33	25.0	31.0	70.0	350	8.5	**0.009**	**122.0**	Task force
River John	495200	5066200	drilled	28.0	0.10				480	7.6	**0.010**	**183.0**	Task force
River John	495200	5066200	drilled						950	7.3	**0.030**	**161.0**	Task force
River John	495200	5066200	drilled	50.0	0.10		20.0		500	7.5	**0.110**	**1529.0**	Task force
River John	495200	5066200	drilled	100.0	0.45	35.0	43.0	35.0	560	7.5	**0.050**	**392.0**	Task force
River John	495200	5066200	drilled	55.0	0.33	30.0	35.0	8.0	330	7.8	**0.020**	**48.0**	Task force
River John	495200	5066200	drilled	94.0	0.33		26.0	10.0	320	6.8	**0.003**	**71.0**	Task force
River John	495200	5066200	drilled						360	7.5	**0.020**	**79.0**	Task force
Louisville, Pictou Co	490600	5064275	drilled						650	7.1	**0.006**	**70.0**	Task force
Louisville, Pictou Co	490600	5064275	drilled	94.0	0.33	29.0	33.0	15.0	480	7.5	**0.020**	**263.0**	Task force
Louisville, Pictou Co	490600	5064275	drilled	90.0	0.33	34.0	34.0	30.0	360	7.8	**0.010**	**207.0**	Task force
Louisville, Pictou Co	490600	5064275	drilled	80.0	0.33				360	8.2	**0.003**	**75.0**	Task force
Louisville, Pictou Co	490600	5064275	drilled	73.0	0.33		42.0		390	7.6	**0.008**	**150.0**	Task force
Louisville, Pictou Co	490600	5064275	drilled	65.0					410	7.4	**0.010**	**363.0**	Task force
Louisville, Pictou Co	490600	5064275	drilled	80.0					350	7.5	**0.003**	**126.0**	Task force

Table 6.7. U and Rn in well water data, Northern Nova Scotia. Original data from Uranium Task Force (MacFarlane, 1983)

Town	Eastings	Northings	Dug / Drilled	Well depth	Well diameter	Depth Bedrock	Casing length	Water depth	Conductivity	pH	U mg/L	Rn Bq/L	Data source
Louisville, Pictou Co	490600	5064275	drilled	176.0	0.33	40.0	43.0	26.0	310	7.5	**0.003**	**112.0**	Task force
Louisville, Pictou Co	490600	5064275	drilled	70.0	0.33		21.0		340	7.6	**0.010**	**144.0**	Task force
Louisville Pictou Co	490600	5064275	drilled						690	8.7	**0.007**	**115.0**	Task force
Louisville, Pictou Co	490600	5064275	drilled	80.0					350	6.5	**0.003**	**98.0**	Task force
Louisville, Pictou Co	490600	5064275	drilled	72.0	0.33		37.0	18.0	340	6.7	**0.003**	**89.0**	Task force
Louisville, Pictou Co	490600	5064275	drilled	37.0	0.33	22.0	24.0	8.0	330	7.8	**0.050**	**168.0**	Task force
Louisville, Pictou Co	490600	5064275	drilled						640	7.6	**0.003**	**53.0**	Task force
Louisville Pictou Co	490600	5064275	drilled	60.0	0.10		24.0		500	7.6	**0.006**	**49.0**	Task force
Louisville, Pictou Co	490600	5064275	dug						450	6.8	**0.003**	**162.0**	Task force
Louisville, Pictou Co	490600	5064275	drilled	100.0	0.33	25.0	27.0	25.0	700	7.2	**0.040**	**114.0**	Task force
Louisville, Pictou Co	490600	5064275	drilled	83.0	0.33	30.0	35.0	20.0	630	7.4	**0.080**	**113.0**	Task force
Middleton, Pictou Co			dug	15.0	3.00				191	5.9	**0.003**	**9.0**	Task force
Middleton, Pictou Co			drilled	123.0	0.15		62.0		240	7.8	**0.020**	**25.0**	Task force
Middleton, Pictou Co			drilled	120.0	0.15				1110	6.4	**0.003**	**52.0**	Task force
Pugwash	448900	5077525	drilled						600	7.7	**0.090**	**75.0**	Task force
Pugwash	448900	5077525	drilled						600	9.1	**0.060**	**95.0**	Task force
Pugwash	448900	5077525	drilled	65.0	0.10				380	6.9	**0.020**	**89.0**	Task force
Pugwash	448900	5077525	drilled	100.0					280	7.8	**0.020**	**133.0**	Task force
Pugwash	448900	5077525									**0.020**	**84.0**	Task force
Pugwash	448900	5077525							600	7.7	**0.010**	**156.0**	Task force
Pugwash	448900	5077525	drilled	90.0	0.10		40.0		410	7.6	**0.010**	**133.0**	Task force
Pugwash	448900	5077525	drilled	230.0	0.45		70.0		1210	7.9	**0.020**	**112.0**	Task force
Pugwash	448900	5077525	drilled	221.0					1530	7.8	**0.020**	**122.0**	Task force
Pugwash	448900	5077525	drilled						550	7.6	**0.020**	**26.0**	Task force
Pugwash	448900	5077525							600	7.6	**0.020**	**54.0**	Task force
Pugwash	448900	5077525	drilled						470	7.6	**0.010**	**103.0**	Task force
Pugwash	448900	5077525							710	7.6	**0.040**	**79.0**	Task force
Pugwash	448900	5077525	drilled	49.0	0.33	25.0	26.0	5.0	750	7.3	**0.003**	**41.0**	Task force
Pugwash	448900	5077525	drilled						500	7.5	**0.020**	**136.0**	Task force
Pugwash	448900	5077525	drilled						460	7.7	**0.020**	**88.0**	Task force
Pugwash	448900	5077525	drilled						820	6.9	**0.020**	**85.0**	Task force
Pugwash	448900	5077525	drilled						400	8.2	**0.010**	**72.0**	Task force
Pugwash	448900	5077525	drilled						500	7.6	**0.020**	**80.0**	Task force
Pugwash	448900	5077525	drilled						550	7.6	**0.020**	**209.0**	Task force

Table 6.7, continued.

Town	Eastings	Northings	Dug / Drilled	Well depth	Well diameter	Depth Bedrock	Casing length	Water depth	Conductivity	pH	U mg/L	Rn Bq/L	Data source
Pugwash	448900	5077525	dug						470	7.8	**0.003**	**19.0**	Task force
Pugwash	448900	5077525							450	7.8	**0.020**	**79.0**	Task force
Pugwash	448900	5077525	drilled	116.0					580	8.0	**0.020**	**146.0**	Task froce
Pugwash	448900	5077525	drilled	83.0	0.33	28.0	31.0	28.0	550	7.6	**0.040**	**51.0**	Task force
Pugwash	448900	5077525	drilled	108.0					400	7.8	**0.020**	**36.0**	Task force
Pugwash	448900	5077525	drilled						610	8.8	**0.020**	**76.0**	Task force
Pugwash	448900	5077525	drilled	112.0	0.33		57.0		550	8.6	**0.020**	**77.0**	Task force
Pugwash	448900	5077525	drilled	92.0	0.10		48.0		360	7.6	**0.010**	**192.0**	Task force
Pugwash	448900	5077525	dug						850	7.1	**0.020**	**53.0**	Task force
Pugwash	448900	5077525	drilled	200.0	0.33		36.0		880	7.3	**0.020**	**87.0**	Task force
Pugwash	448900	5077525	drilled						420	7.5	**0.010**	**24.0**	Task force
Pugwash	448900	5077525	drilled	100.0					360	7.8	**0.020**	**56.0**	Task force
Pugwash	448900	5077525	drilled	200.0	0.33		80.0		1790	8.5	**0.030**	**79.0**	Task force
Pugwash	448900	5077525	drilled	128.0	0.50		34.0		970	8.5	**0.030**	**81.0**	Task force
Pugwash	448900	5077525	drilled	180.0					940	8.8	**0.030**	**116.0**	Task force
Pugwash	448900	5077525	drilled	325.0	0.50	40.0	60.0		460	7.9	**0.030**	**103.0**	Task force
Pugwash	448900	5077525	drilled	29.0	0.10		12.0		690	9.0	**0.040**	**56.0**	Task force
Pugwash	448900	5077525	drilled						570	9.2	**0.020**	**75.0**	Task force
Pugwash	448900	5077525	drilled	200.0	0.33		60.0		600	9.2	**0.020**	**87.0**	Task force
Pugwash	448900	5077525	drilled	100.0	0.50				450	7.5	**0.030**	**61.0**	Task force
Pugwash	448900	5077525	drilled	104.0	0.33				550	7.4	**0.030**	**157.0**	Task force
Pugwash	448900	5077525	drilled		0.10				430	7.6	**0.030**	**219.0**	Task force
Pugwash	448900	5077525	drilled	#####	0.33				310	7.5	**0.003**	**51.0**	Task force
Wentworth	457325	5055900	drilled	100.0	0.33		60.0		500	7.5	**0.020**	**68.0**	Task force
Wentworth	457325	5055900	drilled	170.0	0.33		95.0		540	8.0	**0.030**	**76.0**	Task force
Wentworth	457325	5055900	drilled						620	7.9	**0.030**	**53.0**	Task force
Wentworth	457325	5055900	drilled						550	7.9	**0.050**	**78.0**	Task force
Wentworth	457325	5055900	drilled		0.33				460	7.6	**0.020**	**52.0**	Task force
Wentworth	457325	5055900	dug	20.0	6.00				171	6.9	**0.003**	**2.0**	Task force
Wentworth	457325	5055900	drilled	155.0	0.33		95.0	62.0	1140	9.1	**0.090**	**95.0**	Task force
Wentworth	457325	5055900	dug						550	7.2	**0.010**	**10.0**	Task force
Wentworth	457325	5055900	drilled		0.10				650	7.5	**0.050**	**169.0**	Task force
Wentworth	457325	5055900	drilled	61.0	0.33				420	8.3	**0.030**	**57.0**	Task force
Wentworth	457325	5055900	drilled	76.0	0.33	46.0	50.0	50.0	440	7.6	**0.020**	**35.0**	Task force

Table 6.7, continued.

Town	Eastings	Northings	Dug / Drilled	Well depth	Well diameter	Depth Bedrock	Casing length	Water depth	Conductivity	pH	U mg/L	Rn Bq/L	Data source
Wentworth	457325	5055900	drilled	104.0	0.33		34.0		510	7.8	**0.010**	**107.0**	Task force
Wentworth	457325	5055900	drilled	114.0	0.33				440	7.7	**0.010**	**41.0**	Task force
Wentworth	457325	5055900	drilled	56.0					500	7.5	**0.060**	**78.0**	Task force
Wentworth	457325	5055900	drilled	67.0	0.33	28.0	32.0	14.0	460	7.5	**0.050**	**66.0**	Task force
Wentworth	457325	5055900	drilled	57.0	0.33				370	7.3	**0.010**	**138.0**	Task force
Wentworth	457325	5055900	drilled	40.0					490	7.4	**0.008**	**59.0**	Task force
Wentworth	457325	5055900	drilled		0.33				900	6.3	**0.003**	**54.0**	Task force
Wentworth	457325	5055900	drilled	120.0	0.33	25.0	27.0	18.0	2700	7.5	**0.030**	**99.0**	Task force
Wentworth	457325	5055900	drilled	80.0	0.25				1420	6.8	**0.020**	**56.0**	Task force
Wentworth	457325	5055900	drilled	128.0	0.50				310	7.6	**0.020**	**52.0**	Task force
Wentworth	457325	5055900	drilled	125.0	0.33		80.0		350	7.7	**0.030**	**137.0**	Task force
Wentworth	457325	5055900	drilled	139.0	0.33				400	7.9	**0.020**	**71.0**	Task force
Tatamagouche	477050	5061700	drilled	60.0					600	8.6	**0.030**	**122.0**	Task force
Tatamagouche	477050	5061700	drilled						770	7.7	**0.040**	**88.0**	Task force
Tatamagouche	477050	5061700	drilled						330	8.1	**0.020**	**146.0**	Task force
Tatamagouche	477050	5061700	drilled						1000	7.9	**0.010**	**146.0**	Task force
Tatamagouche	477050	5061700	drilled	190.0					600	7.9	**0.010**	**132.0**	Task force
Tatamagouche	477050	5061700	drilled						420	7.7	**0.010**	**161.0**	Task force
Tatamagouche	477050	5061700	drilled	60.0					730	6.8	**0.003**	**93.0**	Task force
Tatamagouche	477050	5061700	drilled	119.0	0.45	45.0	47.0	15.0	540	7.4	**0.020**	**47.0**	Task force
Tatamagouche	477050	5061700	drilled						440	7.4	**0.020**	**42.0**	Task force
Tatamagouche	477050	5061700	drilled						440	7.5	**0.010**	**31.0**	Task force
Tatamagouche	477050	5061700	drilled						590	8.5	**0.003**	**144.0**	Task force
Tatamagouche	477050	5061700	drilled						310	6.8	**0.003**	**31.0**	Task force
Tatamagouche	477050	5061700	drilled						590	7.5	**0.020**	**170.0**	Task force
Tatamagouche	477050	5061700	drilled						400	8.7	**0.020**	**122.0**	Task force
Tatamagouche	477050	5061700	drilled	183.0	0.50				8600	7.3	**0.020**	**54.0**	Task force
Tatamagouche	477050	5061700	drilled						710	8.5	**0.060**	**66.0**	Task force
Tatamagouche	477050	5061700	drilled						760	8.5	**0.050**	**75.0**	Task force
Tatamagouche	477050	5061700	drilled	90.0	0.33				480	7.4	**0.040**	**55.0**	Task force

Table 6.7, continued.

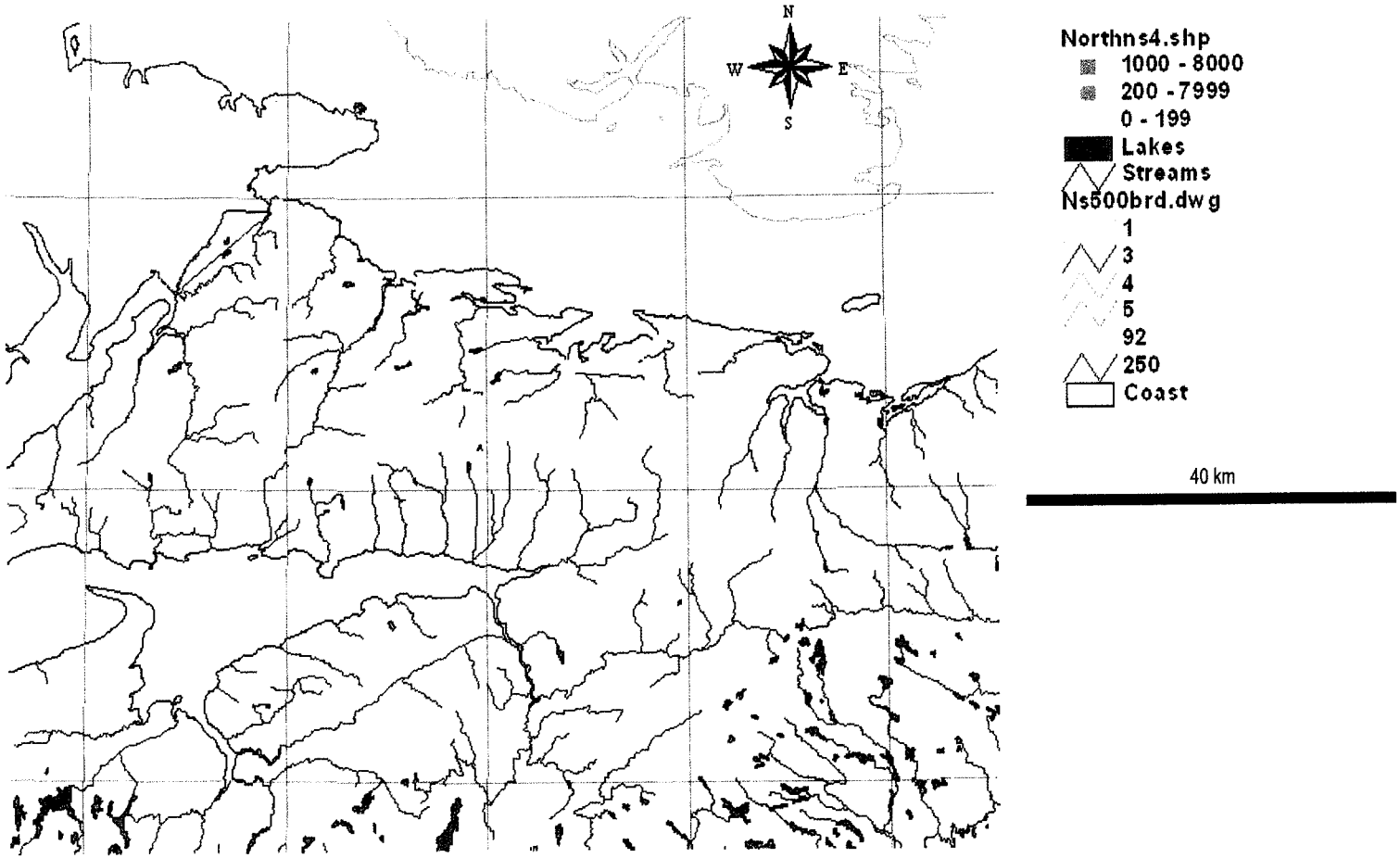

Figure 6.7 Northern Nova Scotia: Radon in well waters (Bq/L)

the New Ross data, the mining tracts for individual wells were not recorded. As a result, it was determined that the only way to handle the data was to group all points from a given town (e.g. River John) together and plot as a single point on the map (Fig. 6.7). It should be clearly understood that the points indicated on the map DO NOT represent actual points where wells are located. Information on individual data points can be examined by clicking on the point with the **"i"** button, and all data belonging to that particular point will appear in tabular form on the screen.

6.2.3.4.3 Preliminary Analysis

Given that the sites of the individual wells are not clearly delimited, only a very rudimentary comparison with the geology can be undertaken. Each of the towns represented lies within, or along contacts with the Late Carboniferous Pictou Group (red and grey sandstones and shales). However, as only one well in River John has a U value > 0.1 mg/L (well value = 0.11 mg/l), there are few homes with the potential for elevated radioelement values in waters, based on the information from this dataset.

Dyck et al. (1976) undertook a well water survey for Northern Nova Scotia, P.E.I., and part of New Brunswick. Their analyses included data for U and Rn in well waters. These data are available in map format, although difficult to read, and also (?) in tabular format. However, efforts to locate the tabular data have not been successful to date, although attempts to do so are continuing.

Based on preliminary study of the map data, U values are indeed within "acceptable limits" for most wells, although there are several wells in which Rn values are greater than 1000 Bq/L (it is recognized in this report that there are no defined "acceptable" limits for Rn levels in well waters).

It should be noted that there are several documented uranium occurrences in the area (see for example, mining assessment reports available through DNR), and although the Task Force data do not suggest elevated levels of U (or Rn), the presence

of local occurrences of U at surface (Chatterjee, 1983) suggests that there is potential for local areas to have elevated uranium and radon in well waters.

6.2.3.5 Rn indoor air data

In 1990, a study of indoor air Rn levels involved analysis of over 700 indoor air samples from various localities throughout Nova Scotia (Jackson, 1992). The purpose of the study by Jackson was to compare indoor radon with areas of radiometric highs, as indicated by airborne radiometric readings (Ford et al., 1989). These data were included in this report, as they provide an additional source of information on radioelements in the environment. The original data were not available in digital format, or indeed, in any map.

Number of data output in .dbf format	723 values
Name	radonair.dbf (database) - Table 6.8 radonair.shp (map) - Fig. 6.8
Nature or spatial data output	648 of these values grouped into 64 towns; each town entered as a single point

6.2.3.5.1 Original Data

The data were made available through Nova Scotia department of the Environment. Originally the data were available as max/min and number of points only, for each town region. However, within a short time of starting work on this project, a more complete dataset with actual individual values of indoor Rn became available. This latter dataset had postal codes, towns, and phone numbers, however civic addresses were not available. These data were entered into .dbf format (Table 6.8).

Postal Code	Town	Room sampled	Rn Bq/L	GAZ_ID	Eastings	Northings	Rn max/town
B0W 1B0	Arcadia	first floor living	299.7	11	253525	4857250	299.70
B0W 1B0	Arcadia	first floor living	81.4	11	253525	4857250	299.70
B0W 1B0	Arcadia	kitchen	188.7	11	253525	4857250	299.70
B0W 1B0	Arcadia	first floor	118.4	11	253525	4857250	299.70
B0W 1B0	Arcadia	first floor living	14.8	11	253525	4857250	299.70
B3L 4J1	Armdale	first floor	14.8				703.00
B3L 4J2	Armdale	living room	51.8				703.00
B3L 4J1	Armdale	basement	14.8				703.00
B3L 4J2	Armdale	basement	14.8				703.00
B3L 4J3	Armdale	n.r.	366.3				703.00
B3L 4J2	Armdale	living room	14.8				703.00
B3L 4J3	Armdale	basement	629.0				703.00
B3L 4J1	Armdale	first floor	33.3				703.00
B3L 4J4	Armdale	living room	14.8				703.00
B3L 4J1	Armdale	basement	14.8				703.00
B3L 4J1	Armdale	n.r.	14.8				703.00
B3L 4J1	Armdale	first floor	14.8				703.00
B3L 4J1	Armdale	basement	703.0				703.00
B3L 4J4	Armdale	basement	25.9				703.00
B3L 4J3	Armdale	living room	344.1				703.00
B3L 4R7	Armdale	kitchen	55.5				703.00
B3L 4R7	Armdale	living room	14.8				703.00
B3L 4J2	Armdale	living room	14.8				703.00
B3L 4R7	Armdale	basement	14.8				703.00
B3L 4J1	Armdale	living room	14.8				703.00
B3L 4J3	Armdale	first floor	14.8				703.00
B3L 4J3	Armdale	basement	81.4				703.00
B3L 4J4	Armdale	basement	14.8				703.00
B3L 4J3	Armdale	living room	14.8				703.00
B3L 4J1	Armdale	basement	592.0				703.00
B3L 4J3	Armdale	basement	340.4				703.00
B3L 4J3	Armdale	front room	136.9				703.00
B3L 4R7	Armdale	basement	14.8				703.00
B3L 4J4	Armdale	dinging room	22.2				703.00
B3L 2R7	Armdale	living room	37.0				703.00
B3L 4J1	Armdale	basement	14.8				703.00
B3L 4J9	Armdale	basement	14.8				703.00
B3L 4J3	Armdale	first floor	14.8				703.00
B3L 4J3	Armdale	first floor	14.8				703.00
B3L 4J4	Armdale	first floor	14.8				703.00
B3L 4J3	Armdale	basement	14.8				703.00
B3L 4J1	Armdale	basement	22.2				703.00
B3L 4J1	Armdale	first floor	33.3				703.00
B3L 4J1	Armdale	first floor	196.1				703.00
B3L 4J3	Armdale	first floor	99.9				703.00
B3L 4J3	Armdale	basement	366.3				703.00
B3L 4J4	Armdale	basement	14.8				703.00
B3L 4J3	Armdale	first floor	277.5				703.00

Table 6.8. Rn in indoor air (Data from Jackson, 1992).

Postal Code	Town	Room sampled	Rn Bq/L	GAZ_ID	Eastings	Northings	Rn max/town
B3L 4J3	Armdale	master bedroo	29.6				703.00
B3L 4J1	Armdale	basement	14.8				703.00
B0J 1T0	Bayswater	first floor	62.9	42	414525	4927950	111.00
B0J 1T0	Bayswater	basement	14.8	42	414525	4927950	111.00
B0J 1T0	Bayswater	first floor	29.6	42	414525	4927950	111.00
B0J 1C0	Bayswater	basement	99.9	42	414525	4927950	111.00
B0J 1T0	Bayswater	basement	111.0	42	414525	4927950	111.00
B0S 1B0	Bear River	living room	122.1	31	290075	4938850	144.30
B0S 1B0	Bear River	living room	14.8	31	290075	4938850	144.30
B0S 1B0	Bear River	basement	125.8	31	290075	4938850	144.30
B0S 1B0	Bear River	living room	14.8	31	290075	4938850	144.30
B0S 1B0	Bear River	living room	14.8	31	290075	4938850	144.30
B0S 1B0	Bear River	living room	14.8	31	290075	4938850	144.30
B0S 1B0	Bear River	kitchen	14.8	31	290075	4938850	144.30
B0S 1B0	Bear River	living room	14.8	31	290075	4938850	144.30
B0S 1B0	Bear River	hallway	14.8	31	290075	4938850	144.30
B0S 1B0	Bear River	basement	59.2	31	290075	4938850	144.30
B0S 1B0	Bear River	basement	118.4	31	290075	4938850	144.30
B0S 1B0	Bear River	basement	14.8	31	290075	4938850	144.30
B0S 1B0	Bear River	living room	144.3	31	290075	4938850	144.30
B0S 1B0	Bear River	kitchen	14.8	31	290075	4938850	144.30
B0S 1B0	Bear River	living room	14.8	31	290075	4938850	144.30
B0S 1B0	Bear River	living room	14.8	31	290075	4938850	144.30
B0S 1B0	Bear River	living room	59.2	31	290075	4938850	144.30
B0S 1B0	Bear River	living room	14.8	31	290075	4938850	144.30
B0S 1B0	Bear River	living room	14.8	31	290075	4938850	144.30
B3L 4J1	Beechville	first floor	125.8	54	445475	4942850	125.80
B0J 1B0	Black Point	basement	14.8	71	422275	4945050	14.80
B0J 1B0	Black Point	living room	14.8	71	422275	4945050	14.80
B0J 1T0	Blandford	first floor	14.8	73	412200	4927150	1073.00
B0J 1T0	Blandford	first floor	14.8	73	412200	4927150	1073.00
B0J 1T0	Blandford	basement	14.8	73	412200	4927150	1073.00
B0J 1T0	Blandford	first floor	14.8	73	412200	4927150	1073.00
B0J 1T0	Blandford	basement	1073.0	73	412200	4927150	1073.00
B0J 1T0	Blandford	first floor	74.0	73	412200	4927150	1073.00
B0J 1G0	Boutiliers Point	living room	14.8	80	424625	4945750	240.50
B0J 1G0	Boutiliers Point	living room	14.8	80	424625	4945750	240.50
B0J 1G0	Boutiliers Point	basement	14.8	80	424625	4945750	240.50
B0J 1G0	Boutiliers Point	basement	14.8	80	424625	4945750	240.50
B0J 1G0	Boutiliers Point	basement	14.8	80	424625	4945750	240.50
B0J 1G0	Boutiliers Point	basement	240.5		424625	4945750	240.50
B0C 1B0	Bras d'Or	basement	59.2		709150	5125175	99.99
B0C 1B0	Bras d'Or	basement	55.5		709150	5125275	99.99
B0C 1B0	Bras d'Or	basement	14.8		709150	5125175	99.99
B0C 1B0	Bras d'Or	basement	14.8		709150	5125175	99.99
B0C 1B0	Bras d'Or	basement	99.9		709150	5125175	99.99
B0S 1C0	Bridgetown	cellar stairway	177.6	50	319200	4968000	177.60
B0S 1C0	Bridgetown	basement	14.8	50	319200	4968000	177.60

Table 6.8, continued.

Postal Code	Town	Room sampled	Rn Bq/L	GAZ_ID	Eastings	Northings	Rn max/town
B0S 1C0	Bridgetown	basement	14.8	50	319200	4968000	177.60
B4V 2W6	Bridgewater	first floor	103.6	83	378925	4915350	103.60
B0J 1H0	Brooklyn	basement	14.8	55	333175	4978850	14.80
B0J 1H0	Brooklyn	first floor	14.8	55	333175	4978850	14.80
B0J 1H0	Brooklyn	first floor	14.8	55	333175	4978850	14.80
B0J 1H0	Brooklyn	basement	14.8	55	333175	4978850	14.80
B0J 1H0	Brooklyn	first floor	14.8	55	333175	4978850	14.80
B0T 1K0	Brooklyn	basement	14.8	55	333175	4978850	14.80
B0J 1H0	Brooklyn	basement	14.8	55	333175	4978850	14.80
B0J 1H0	Brooklyn	basement	14.8	55	333175	4978850	14.80
B0J 1H0	Brooklyn	first floor	14.8	55	333175	4978850	14.80
B0W 1L0	Carleton	basement	14.8	60	264950	4877050	14.80
B0W 1L0	Carleton	living room	14.8	60	264950	4877050	14.80
B0W 1L0	Carleton	living room	14.8	60	264950	4877050	14.80
B0J 1J0	Chester	basement	55.5	126	401225	4933500	888.00
B0J 1J0	Chester	basement	14.8	126	401225	4933500	888.00
B0J 1J0	Chester	first floor	14.8	126	401225	4933500	888.00
B0J 1J0	Chester	first floor	114.7	126	401225	4933500	888.00
B0J 1J0	Chester	basement	14.8	126	401225	4933500	888.00
B0J 1J0	Chester	n.r.	48.1	126	401225	4933500	888.00
B0J 1J0	Chester	basement	14.8	126	401225	4933500	888.00
B0J 1J0	Chester	first floor	14.8	126	401225	4933500	888.00
B0J 1J0	Chester	basement	88.8	126	401225	4933500	888.00
B0J 1J0	Chester	basement	185.0	126	401225	4933500	888.00
B0J 1J0	Chester	basement	14.8	126	401225	4933500	888.00
B0J 1J0	Chester	basement	203.5	126	401225	4933500	888.00
B0J 1J0	Chester	basement	18.5	126	401225	4933500	888.00
B0J 1J0	Chester	basement	122.1	126	401225	4933500	888.00
B0J 1J0	Chester	basement	240.5	126	401225	4933500	888.00
B0J 1J0	Chester	first floor	55.5	126	401225	4933500	888.00
B0J 1J0	Chester	basement	255.3	126	401225	4933500	888.00
B0J 1J0	Chester	first floor	888.0	126	401225	4933500	888.00
B0J 1J0	Chester	basement	125.8	126	401225	4933500	888.00
B0J 1J0	Chester	basement	14.8	126	401225	4933500	888.00
B0J 1J0	Chester	first floor	14.8	126	401225	4933500	888.00
B0J 1J0	Chester	first floor	14.8	126	401225	4933500	888.00
B0J 1J0	Chester	first floor	14.8	126	401225	4933500	888.00
B0J 1J0	Chester	basement	18.5	126	401225	4933500	888.00
B0J 1K0	Chester Basin	n.r.	18.5	127	395975	4935475	229.40
B0J 1K0	Chester Basin	basement	18.5	127	395975	4935475	229.40
B0J 1K0	Chester Basin	basement	51.8	127	395975	4935475	229.40
B0J 1K0	Chester Basin	basement	151.7	127	395975	4935475	229.40
B0J 1K0	Chester Basin	basement	88.8	127	395975	4935475	229.40
B0J 1K0	Chester Basin	basement	233.1	127	395975	4935475	229.40
B0J 1K0	Chester Basin	basement	14.8	127	395975	4935475	229.40
B0J 1K0	Chester Basin	basement	44.4	127	395975	4935475	229.40
B0J 1K0	Chester Basin	basement	14.8	127	395975	4935475	229.40
B0J 1K0	Chester Basin	basement	66.6	127	395975	4935475	229.40

Table 6.8, continued.

Postal Code	Town	Room sampled	Rn Bq/L	GAZ_ID	Eastings	Northings	Rn max/town
B0S 1G0	Clementsvale	living room	14.8	84	296675	4943700	25.90
B0S 1J0	Deep Brook	living room	125.8	96	290100	4946300	125.80
B0S 1J0	Deep Brook	living room	14.8	96	290100	4946300	125.80
B0S 1J0	Deep Brook	living room	14.8	96	290100	4946300	125.80
B0S 1J0	Deep Brook	living room	14.8	96	290100	4946300	125.80
B0S 1J0	Deep Brook	living room	14.8	96	290100	4946300	125.80
B0S 1J0	Deep Brook	living room	14.8	96	290100	4946300	125.80
B0V 1A0	Digby	kitchen	14.8	99	280375	4943750	14.80
B0V 1A0	Digby	living room	14.8	99	280375	4943750	14.80
B0J 1J0	East Chester	basement	92.5	186	402875	4935100	314.50
B0J 1J0	East Chester	basement	14.8	186	402875	4935100	314.50
B0J 1J0	East Chester	first floor	14.8	186	402875	4935100	314.50
B0J 1J0	East Chester	basement	314.5	186	402875	4935100	314.50
B0J 1T0	East River	first floor	355.2	208	407650	4938050	355.20
B0J 1T0	East River	basement	14.8	208	407650	4938050	355.20
B0J 1T0	East River	first floor	62.9	208	407650	4938050	355.20
B0J 1T0	East River	first floor	18.5	208	407650	4938050	355.20
B0J 1T0	East River	first floor	14.8	208	407650	4938050	355.20
B0J 1T0	East River	basement	125.8	208	407650	4938050	355.20
B0J 1T0	East River	first floor	14.8	208	407650	4938050	355.20
B0C 1H0	Englishtown	basement offic	14.8	133	689825	5128050	18.50
B0C 1H0	Englishtown	basement	14.8	133	689825	5128050	18.50
B0C 1H0	Englishtown	basement	18.5	133	689825	5128050	18.50
B0P 1L0	Falmouth	basement	14.8	233	407850	4983350	103.60
B0P 1L0	Falmouth	first floor	14.8	233	407850	4983350	103.60
B0P 1L0	Falmouth	basement	103.6	233	407850	4983350	103.60
B0P 1L0	Falmouth	basement	14.8	233	407850	4983350	103.60
B0P 1L0	Falmouth	basement	14.8	233	407850	4983350	103.60
B0P 1L0	Falmouth	first floor	14.8	233	407850	4983350	103.60
B0P 1L0	Falmouth	first floor	14.8	233	407850	4983350	103.60
B0P 1L0	Falmouth	first floor	59.2	233	407850	4983350	103.60
B0P 1L0	Falmouth	basement	14.8	233	407850	4983350	103.60
B0P 1L0	Falmouth	first floor	14.8	233	407850	4983350	103.60
B0P 1L0	Falmouth	first floor	14.8	233	407850	4983350	103.60
B0L 1L0	Falmouth	first floor	14.8	233	407850	4983350	103.60
B0P 1L0	Falmouth	first floor	14.8	233	407850	4983350	103.60
B0P 1L0	Falmouth	first floor	14.8	233	407850	4983350	103.60
B0P 1L0	Falmouth	first floor	14.8	233	407850	4983350	103.60
B0E 1L0	Grand Etang	basement	14.8	178	649800	5156425	114.70
B0E 1L0	Grand Etang	basement	14.8	178	649800	5156425	114.70
B0E 1L0	Grand Etang	basement	14.8	178	649800	5156425	114.70
B0E 1L0	Grand Etang	basement	14.8	178	649800	5156425	114.70
B0E 1L0	Grand Etang	basement	55.5	178	649800	5156425	114.70
B0E 1L0	Grand Etang	basement	14.8	178	649800	5156425	114.70
B0E 1L0	Grand Etang	basement	14.8	178	649800	5156425	114.70
B0E 1L0	Grand Etang	basement	14.8	178	649800	5156425	114.70
B0E 1L0	Grand Etang	basement	114.7	178	649800	5156425	114.70
B0P 1N0	Greenwood	basement	37.0	202	348175	4982275	37.00

Table 6.8, continued.

Postal Code	Town	Room sampled	Rn Bq/L	GAZ_ID	Eastings	Northings	Rn max/town
B3H 3V2	Halifax	basement	14.8	321	453125	4945000	814.00
B2V 1W3	Halifax	basement	814.0	321	453125	4945000	814.00
B3L 4J3	Halifax Co	basement	370.0				0.00
B3L 4J3	Halifax Co	living room	555.0				0.00
B0J 1G0	Halifax Co	basement	14.8				0.00
B0J 1Z0	Halifax Co	first floor	14.8				0.00
B3L 4J3	Halifax Co	first floor	181.3				0.00
B0J 1J0	Halifax Co	basement	14.8				0.00
B3L 2S3	Halifax Co	basement	14.8				0.00
B3L 4J3	Halifax Co	basement	74.0				0.00
B3L 4R7	Halifax Co	living room	44.4				0.00
B3L 4J3	Halifax Co	dining room	14.8				0.00
B0J 3J0	Halifax Co	first floor	14.8				0.00
B0J 1R0	Halifax Co	living room	14.8				0.00
B3L 4J3	Halifax Co	basement	14.8				0.00
B0J 3J0	Halifax Co	dining room	14.8				0.00
B0J 3J0	Halifax Co	first floor	22.2				0.00
B3L 4J2	Halifax Co	basement	14.8				0.00
B0J 1G0	Halifax Co	living room	14.8				0.00
B0J 1G0	Halifax Co	first floor	14.8				0.00
B0J 1G0	Halifax Co	living room	14.8				0.00
B0J 3J0	Halifax Co	first floor	14.8				0.00
B3L 4J2	Hatchet Lake	bedroom	14.8	339	443125	4935925	48.10
B3L 4J2	Hatchet Lake	first floor	14.8	339	443125	4935925	48.10
B3L 4J2	Hatchet Lake	living room	14.8	339	443125	4935925	48.10
B3L 4J2	Hatchet Lake	living room	14.8	339	443125	4935925	48.10
B3L 4J2	Hatchet Lake	basement	48.1	339	443125	4935925	48.10
B0J 1T0	Hubbards	first floor	14.8	360	415550	4943475	1517.00
B0J 1T0	Hubbards	basement	140.6	360	415550	4943475	1517.00
B0J 1T0	Hubbards	basement	347.8	360	415550	4943475	1517.00
B0J 1T0	Hubbards	first floor	111.0	360	415550	4943475	1517.00
B0J 1T0	Hubbards	basement	229.4	360	415550	4943475	1517.00
B0J 1T0	Hubbards	basement	14.8	360	415550	4943475	1517.00
B0J 1T0	Hubbards	first floor	14.8	360	415550	4943475	1517.00
B0J 1T0	Hubbards	main floor	14.8	360	415550	4943475	1517.00
B0J 1T0	Hubbards	basement	740.0	360	415550	4943475	1517.00
B0J 1T0	Hubbards	basement	51.8	360	415550	4943475	1517.00
B0J 1T0	Hubbards	basement	14.8	360	415550	4943475	1517.00
B0J 1T0	Hubbards	basement	18.5	360	415550	4943475	1517.00
B0J 1T0	Hubbards	living room	14.8	360	415550	4943475	1517.00
B0J 1T0	Hubbards	basement	555.0	360	415550	4943475	1517.00
B0J 1T0	Hubbards	basement	1369.0	360	415550	4943475	1517.00
B0J 1T0	Hubbards	first floor	14.8	360	415550	4943475	1517.00
B0J 1T0	Hubbards	basement	151.7	360	415550	4943475	1517.00
B0J 1T0	Hubbards	first floor	14.8	360	415550	4943475	1517.00
B0J 1T0	Hubbards	basement	62.9	360	415550	4943475	1517.00
B0J 1T0	Hubbards	basement	114.7	360	415550	4943475	1517.00
B0J 1T0	Hubbards	dining room	14.8	360	415550	4943475	1517.00
B0J 1T0	Hubbards	first floor	22.2	360	415550	4943475	1517.00
B0J 1T0	Hubbards	basement	103.6	360	415550	4943475	1517.00

Postal Code	Town	Room sampled	Rn Bq/L	GAZ_ID	Eastings	Northings	Rn max/town
B0J 1T0	Hubbards	basement	362.6	360	415550	4943475	1517.00
B0J 1T0	Hubbards	basement	144.3	360	415550	4943475	1517.00
B0J 1T0	Hubbards	basement	518.0	360	415550	4943475	1517.00
B0J 1T0	Hubbards	basement	14.8	360	415550	4943475	1517.00
B0J 1T0	Hubbards	first floor	55.5	360	415550	4943475	1517.00
B0J 1T0	Hubbards	first floor	14.8	360	415550	4943475	1517.00
B0J 1T0	Hubbards	basement	210.9	360	415550	4943475	1517.00
B0J 1T0	Hubbards	basement	170.2	360	415550	4943475	1517.00
B0J 1T0	Hubbards	basement	185.0	360	415550	4943475	1517.00
B0J 1T0	Hubbards	basement	114.7	360	415550	4943475	1517.00
B0J 1T0	Hubbards	n.r.	14.8	360	415550	4943475	1517.00
B0J 1T0	Hubbards	first floor	14.8	360	415550	4943475	1517.00
B0J 1T0	Hubbards	basement	70.3	360	415550	4943475	1517.00
B0J 1T0	Hubbards	basement	1517.0	360	415550	4943475	1517.00
B0J 1T0	Hubbards	first floor	25.9	360	415550	4943475	1517.00
B0J 1T0	Hubbards	first floor	81.4	360	415550	4943475	1517.00
B0J 1T0	Hubbards	first floor	14.8	360	415550	4943475	1517.00
B0J 1T0	Hubbards	first floor	14.8	360	415550	4943475	1517.00
B0J 1T0	Hubbards	basement	92.5	360	415550	4943475	1517.00
B0J 1T0	Hubbards	basement	14.8	360	415550	4943475	1517.00
B0J 1T0	Hubbards	basement	81.4	360	415550	4943475	1517.00
B0J 1T0	Hubbards	living room	14.8	360	415550	4943475	1517.00
B0J 1T0	Hubbards	first floor	1110.0	360	415550	4943475	1517.00
B0J 1T0	Hubbards	basement	1443.0	360	415550	4943475	1517.00
B0J 1T0	Hubbards	basement	318.2	360	415550	4943475	1517.00
B0J 1T0	Hubbards	first floor	14.8	360	415550	4943475	1517.00
B0J 1T0	Hubbards	first floor	1369.0	360	415550	4943475	1517.00
B0J 1T0	Hubbards	basement	318.2	360	415550	4943475	1517.00
B0T 1G0	Hunts Point	basement	14.8	365	357300	4869200	14.80
B0T 1G0	Hunts Point	basement	14.8	365	357300	4869200	14.80
B0C 1K0	Ingonish	basement	14.8	213	701650	5174450	3626.00
B0C 1K0	Ingonish	pantry	14.8	213	701650	5174450	3626.00
B0C 1L0	Ingonish	basement	14.8	213	701650	5174450	3626.00
B0C 1L0	Ingonish	basement	14.8	213	701650	5174450	3626.00
B0C 1K0	Ingonish	basement	188.7	213	701650	5174450	3626.00
B0C 1L0	Ingonish	basement	14.8	213	701650	5174450	3626.00
B0C 1L0	Ingonish	basement	14.8	213	701650	5174450	3626.00
B0C 1K0	Ingonish	basement	14.8	213	701650	5174450	3626.00
B0C 1L0	Ingonish	basement	14.8	213	701650	5174450	3626.00
B0C 1K0	Ingonish	basement	481.0	213	701650	5174450	3626.00
B0C 1K0	Ingonish	basement	1332.0	213	701650	5174450	3626.00
B0C 1K0	Ingonish	basement	14.8	213	701650	5174450	3626.00
B0C 1K0	Ingonish	basement	74.0	213	701650	5174450	3626.00
B0C 1L0	Ingonish	basement	14.8	213	701650	5174450	3626.00
B0C 1L0	Ingonish	basement	14.8	213	701650	5174450	3626.00
B0C 1K0	Ingonish	basement	3626.0	213	701650	5174450	3626.00
B0C 1L0	Ingonish	basement	14.8	213	701650	5174450	3626.00
B0C 1K0	Ingonish	basement	362.6	213	701650	5174450	3626.00

Table 6.8, continued.

		sampled	Bq/L				max/town
B0C 1L0	Ingonish	basement	14.8	213	701650	5174450	3626.00
B0C 1K0	Ingonish	wood box hole	1887.0	213	701650	5174450	3626.00
B0C 1K0	Ingonish	basement	14.8	213	701650	5174450	3626.00
B0C 1L0	Ingonish	basement	14.8	213	701650	5174450	3626.00
B0C 1K0	Ingonish	basement	3626.0	213	701650	5174450	3626.00
B0C 1L0	Ingonish	basement	14.8	213	701650	5174450	3626.00
B0C 1L0	Ingonish	basement	170.2	213	701650	5174450	3626.00
B0C 1K0	Ingonish	basement	14.8	213	701650	5174450	3626.00
B0C 1L0	Ingonish	stairway upstai	14.8	213	701650	5174450	3626.00
B0C 1K0	Ingonish	basement	14.8	213	701650	5174450	3626.00
B0W 1Y0	Kemptville	basement	14.8	163	273000	4881100	14.80
B0W 1Y0	Kemptville	basement	14.8	163	273000	4881100	14.80
B0W 1Y0	Kemptville	living room	14.8	163	273000	4881100	14.80
B0W 1Y0	Kemptville	living room	14.8	163	273000	4881100	14.80
B0W 1Y0	Kemptville	first floor	14.8	163	273000	4881100	14.80
B0W 1Y0	Kemptville	living room	14.8	163	273000	4881100	14.80
B0W 1Y0	Kemptville	basement	14.8	163	273000	4881100	14.80
B0W 1Y0	Kemptville	first floor	14.8	163	273000	4881100	14.80
B0W 1Y0	Kemptville	basement	14.8	163	273000	4881100	14.80
B0W 1Y0	Kemptville	living room	14.8	163	273000	4881100	14.80
B0W 1Y0	Kemptville	living room	14.8	163	273000	4881100	14.80
B0P 1R0	Kingston	basement	14.8	391	346325	4983325	14.80
B0J 1Z0	Lakeside	basement	814.0	169	444475	4942700	1406.00
B0J 1Z0	Lakeside	basement	740.0	169	444475	4942700	1406.00
B0J 1Z0	Lakeside	first floor	125.8	169	444475	4942700	1406.00
B0J 1Z0	Lakeside	first floor	129.5	169	444475	4942700	1406.00
B0J 1Z0	Lakeside	basement	1406.0	169	444475	4942700	1406.00
B0J 1Z0	Lakeside	basement	962.0	169	444475	4942700	1406.00
B0J 1Z0	Lakeside	basement	14.8	169	444475	4942700	1406.00
B0S 1M0	Lawrencetown	basement	14.8	423	329425	4972350	25.90
B0S 1M0	Lawrencetown	basement	14.8	423	329425	4972350	25.90
B0S 1M0	Lawrencetown	basement	14.8	423	329425	4972350	25.90
B0S 1M0	Lawrencetown	basement	14.8	423	329425	4972350	25.90
B0S 1M0	Lawrencetown	basement	14.8	423	329425	4972350	25.90
B0S 1M0	Lawrencetown	basement	14.8	423	329425	4972350	25.90
B0S 1M0	Lawrencetown	basement	25.9	423	329425	4972350	25.90
B0S 1M0	Lawrencetown	basement	14.8	423	329425	4972350	25.90
B0T 1K0	Liverpool	basement	14.8	436	362225	4877025	214.60
B0T 1K0	Liverpool	basement	14.8	436	362225	4877025	214.60
B0T 1K0	Liverpool	basement	214.6	436	362225	4877025	214.60
B0T 1K0	Liverpool	basement	74.0	436	362225	4877025	214.60
B0T 1K0	Liverpool	basement	14.8	436	362225	4877025	214.60
B0T 1K0	Liverpool	basement	14.8	436	362225	4877025	214.60
B0T 1K0	Liverpool	basement	14.8	436	362225	4877025	214.60
B0T 1G0	Liverpool	basement	14.8	436	362225	4877025	214.60
B0T 1K0	Liverpool	basement	14.8	436	362225	4877025	214.60
B0T 1K0	Liverpool	basement	85.1	436	362225	4877025	214.60
B0T 1K0	Liverpool	first floor	14.8	436	362225	4877025	214.60

Table 6.8 , continued.

Postal Code	Town	Room sampled	Rn Bq/L	GAZ_ID	Eastings	Northings	Rn max/town
B0T 1K0	Liverpool	first floor	14.8	436	362225	4877025	214.60
B0T 1K0	Liverpool	basement	14.8	436	362225	4877025	214.60
B0T 1G0	Liverpool	basement	14.8	436	362225	4877025	214.60
B0T 1K0	Liverpool	first floor	14.8	436	362225	4877025	214.60
B0T 1K0	Liverpool	first floor	14.8	436	362225	4877025	214.60
B0T 1K0	Liverpool	first floor	14.8	436	362225	4877025	214.60
B0T 1K0	Liverpool	basement	14.8	436	362225	4877025	214.60
B0J 2C0	Lunenburg	living room	14.8	474	394450	4914700	55.50
B0J 2C0	Lunenburg	basement	14.8	474	394450	4914700	55.50
B0J 2C0	Lunenburg	basement	14.8	474	394450	4914700	55.50
B0J 2C0	Lunenburg	basement	14.8	474	394450	4914700	55.50
B0J 2C0	Lunenburg	basement	14.8	474	394450	4914700	55.50
B0J 2C0	Lunenburg	first floor	14.8	474	394450	4914700	55.50
B0J 2C0	Lunenburg	basement	14.8	474	394450	4914700	55.50
B0J 2C0	Lunenburg	basement	55.5	474	394450	4914700	55.50
B0J 2C0	Lunenburg	basement	14.8	474	394450	4914700	55.50
B0J 2C0	Lunenburg	basement	14.8	474	394450	4914700	55.50
B0J 2C0	Lunenburg	living room	14.8	474	394450	4914700	55.50
B0J 2C0	Lunenburg	basement	14.8	474	394450	4914700	55.50
B0J 2C0	Lunenburg	basement	33.3	474	394450	4914700	55.50
B0J 2C0	Lunenburg	living room	14.8	474	394450	4914700	55.50
B0J 2C0	Lunenburg	basement	14.8	474	394450	4914700	55.50
B0J 2C0	Lunenburg	living room	14.8	474	394450	4914700	55.50
B0J 2C0	Lunenburg	basement	14.8	474	394450	4914700	55.50
B0J 2C0	Lunenburg	n.r.	14.8	474	394450	4914700	55.50
B0J 2C0	Lunenburg	basement	14.8	474	394450	4914700	55.50
B0J 2C0	Lunenburg	living room	14.8	474	394450	4914700	55.50
B0J 2C0	Lunenburg	living room	14.8	474	394450	4914700	55.50
B0J 2C0	Lunenburg	living room	14.8	474	394450	4914700	55.50
B0J 2C0	Lunenburg	basement	14.8	474	394450	4914700	55.50
B0J 2C0	Lunenburg	living room	14.8	474	394450	4914700	55.50
B0J 2C0	Lunenburg	basement	14.8	474	394450	4914700	55.50
B0J 2C0	Lunenburg	basement	14.8	474	394450	4914700	55.50
B0J 2C0	Lunenburg	basement	14.8	474	394450	4914700	55.50
B0J 2C0	Lunenburg	living room	14.8	474	394450	4914700	55.50
B0J 2C0	Lunenburg	living room	14.8	474	394450	4914700	55.50
B0J 2C0	Lunenburg	first floor	14.8	474	394450	4914700	55.50
B0A 1P0	Marion Bridge	basement	103.6	317	715900	5095825	118.40
B0A 1P0	Marion Bridge	living room	14.8	317	715900	5095825	118.40
B0A 1P0	Marion Bridge	kitchen	14.8	317	715900	5095825	118.40
B0A 1P0	Marion Bridge	basement	118.4	317	715900	5095825	118.40
B0A 1P0	Marion Bridge	basement	14.8	317	715900	5095825	118.40
B0S 1P0	Middleton	basement	14.8	340	336625	4978625	777.00
B0S 1P0	Middleton	basement	55.5	340	336625	4978625	777.00
B0S 1P0	Middleton	basement	14.8	340	336625	4978625	777.00
B0S 1P0	Middleton	basement	18.5	340	336625	4978625	777.00
B0S 1P0	Middleton	basement	777.0	340	336625	4978625	777.00
B0S 1P0	Middleton	basement	370.0	340	336625	4978625	777.00

Table 6.8, continued.

Postal Code	Town	Room sampled	Rn Bq/L	GAZ_ID	Eastings	Northings	Rn max/town
B0S 1P0	Middleton	basement	29.6	340	336625	4978625	777.00
B0S 1P0	Middleton	basement	14.8	340	336625	4978625	777.00
B0S 1P0	Middleton	basement	81.4	340	336625	4978625	777.00
B0S 1P0	Middleton	basement	44.4	340	336625	4978625	777.00
B0S 1P0	Middleton	basement	51.8	340	336625	4978625	777.00
B0S 1P0	Middleton	basement	14.8	340	336625	4978625	777.00
B0S 1P0	Middleton	basement	66.6	340	336625	4978625	777.00
B0T 1P0	Milton	basement	14.8	541	359675	4880325	96.20
B0T 1P0	Milton	basement	96.2	541	359675	4880325	96.20
B0T 1K0	Milton	first floor	14.8	541	359675	4880325	96.20
B0T 1P0	Milton	basement	14.8	541	359675	4880325	96.20
B0T 1P0	Milton	basement	14.8	541	359675	4880325	96.20
B0T 1P0	Milton	basement	92.5	541	359675	4880325	96.20
B0R 1E0	New Germany	basement	210.9	567	363050	4934050	210.90
B0J 2M0	New Ross	basement	14.8	574	384475	4954575	0.00
B0J 2M0	New Ross	basement	14.8	574	384475	4954575	214.60
B0J 2M0	New Ross	basement	14.8	574	384475	4954575	214.60
B0J 2M0	New Ross	basement	14.8	574	384475	4954575	214.60
B0J 2M0	New Ross	basement	40.7	574	384475	4954575	214.60
B0J 2M0	New Ross	basement	14.8	574	384475	4954575	214.60
B0J 2M0	New Ross	basement	22.2	574	384475	4954575	214.60
B0J 1M0	New Ross	basement	14.8	574	384475	4954575	214.60
B0J 2M0	New Ross	basement	14.8	574	384475	4954575	214.60
B0J 2M0	New Ross	basement	14.8	574	384475	4954575	214.60
B0J 2M0	New Ross	basement	140.6	574	384475	4954575	214.60
B0J 2M0	New Ross	basement	214.6	574	384475	4954575	214.60
B0J 2M0	New Ross	basement	14.8	574	384475	4954575	214.60
B0J 2N0	New Ross	basement	14.8	574	384475	4954575	214.60
B0J 2M0	New Ross	basement	14.8	574	384475	4954575	214.60
B0J 2M0	New Ross	basement	14.8	574	384475	4954575	214.60
B0J 2M0	New Ross	basement	14.8	574	384475	4954575	214.60
B0J 2M0	New Ross	basement	14.8	574	384475	4954575	214.60
B0J 2M0	New Ross	basement	14.8	574	384475	4954575	214.60
B0J 2M0	New Ross	basement	14.8	574	384475	4954575	214.60
B0J 2M0	New Ross	basement	14.8	574	384475	4954575	214.60
B0J 2M0	New Ross	basement	14.8	574	384475	4954575	214.60
B0J 2M0	New Ross	basement	14.8	574	384475	4954575	214.60
B0J 2M0	New Ross	basement	107.3	574	384475	4954575	214.60
B0J 2M0	New Ross	basement	14.8	574	384475	4954575	214.60
B0J 2M0	New Ross	basement	14.8	574	384475	4954575	214.60
B0J 2M0	New Ross	basement	14.8	574	384475	4954575	214.60
B0S 1N0	Nictaux West	basement	14.8	237	336975	4975450	85.10
B0S 1P0	Nictaux West	basement	85.1	237	336975	4975450	85.10
B2A 3M5	North Sydney	basement	14.8	597	711575	5120525	555.00
B2A 1W3	North Sydney	basement	555.0	597	711575	5120525	555.00
B2A 2N4	North Sydney	basement	14.8	597	711575	5120525	555.00
B2A 1A6	North Sydney	basement	14.8	597	711575	5120525	555.00
B2A 2B5	North Sydney	lr. level bedroo	196.1	597	711575	5120525	555.00

Postal Code	Town	Room sampled	Rn Bq/L	GAZ_ID	Eastings	Northings	Rn max/town
B2A 3P3	North Sydney	basement	14.8	597	711575	5120525	555.00
B2A 3M5	North Sydney	basement	59.2	597	711575	5120525	555.00
B2A 3A1	North Sydney	basement	29.6	597	711575	5120525	555.00
B0S 1R0	Paradise	basement	14.8	252	325175	4970850	14.80
B0S 1R0	Paradise	basement	14.8	252	325175	4970850	14.80
B0E 2L0	Petit Etang	basement	366.3	383	654400	5167275	366.30
B0R 1G0	Pleasantville	basement	207.2	624	385200	4909400	207.20
B3L 4J2	Prospect	living room	14.8	645	436475	4924875	14.80
B3L 4J4	Prospect	dining area	14.8	645	436475	4924875	14.80
B3L 4J2	Prospect	living room	14.8	645	436475	4924875	14.80
B0K 1N0	River John	first floor	14.8	426	495200	5066200	29.60
B0K 1N0	River John	first floor	14.8	426	495200	5066200	29.60
B0K 1N0	River John	first floor	14.8	426	495200	5066200	29.60
B0K 1N0	River John	first floor	14.8	426	495200	5066200	29.60
B0K 1N0	River John	basement	14.8	426	495200	5066200	29.60
B0K 1N0	River John	first floor	14.8	426	495200	5066200	29.60
B0K 1N0	River John	first floor	14.8	426	495200	5066200	29.60
B0K 1N0	River John	basement	29.6	426	495200	5066200	29.60
B0K 1N0	River John	basement	14.8	426	495200	5066200	29.60
B0K 1N0	River John	first floor	14.8	426	495200	5066200	29.60
B0K 1N0	River John	first floor	14.8	426	495200	5066200	29.60
B0K 1N0	River John	n.r.	14.8	426	495200	5066200	29.60
B0K 1N0	River John	basement	14.8	426	495200	5066200	29.60
B0K 1N0	River John	living room	14.8	426	495200	5066200	29.60
B0K 1N0	River John	first floor	14.8	426	495200	5066200	29.60
B0K 1N0	River John	first floor	14.8	426	495200	5066200	29.60
B0K 1N0	River John	first floor	14.8	426	495200	5066200	29.60
B0K 1N0	River John	basement	14.8	426	495200	5066200	29.60
B0K 1N0	River John	first floor	14.8	426	495200	5066200	29.60
B0K 1N0	River John	n.r.	14.8	426	495200	5066200	29.60
B0S 1S0	Smiths Cove	living room	14.8	311	283775	4942975	85.10
B0S 1S0	Smiths Cove	basement	14.8	311	283775	4942975	85.10
B0S 1S0	Smith's Cove	basement	85.1				85.10
B0S 1S0	Smith's Cove	living room	14.8				85.10
B0S 1S0	Smith's Cove	basement	48.1				85.10
B0S 1S0	Smith's Cove	basement	14.8				85.10
B0J 1R0	St Margaret's Bay	living room	14.8				14.80
B0J 1R0	St Margaret's Bay	living room	14.8				14.80
B0N 2E0	Ste. Croix	first floor	159.1				159.10
B1N 1H2	Sydney	basement	14.8	520	717000	5112125	166.50
B1P 2V6	Sydney	basement	14.8	520	717000	5112125	166.50
B1S 1Y1	Sydney	basement	14.8	520	717000	5112125	166.50
B1P 1Y1	Sydney	basement	166.5	520	717000	5112125	166.50
B1P 1A6	Sydney	living room	14.8	520	717000	5112125	166.50
B1P 5W5	Sydney	first floor	14.8	520	717000	5112125	166.50
B1P 3A8	Sydney	basement	14.8	520	717000	5112125	166.50
B1P 3L6	Sydney	basement	14.8	520	717000	5112125	166.50
B1S 2L9	Sydney	downstairs	14.8	520	717000	5112125	166.50

Table 6.8, continued.

Postal Code	Town	Room sampled	Rn Bq/L	GAZ_ID	Eastings	Northings	Rn max/town
B1N 2P8	Sydney	first floor	14.8	520	717000	5112125	166.50
B1S 2B4	Sydney	basement	14.8	520	717000	5112125	166.50
B1N 1Y6	Sydney	basement	14.8	520	717000	5112125	166.50
B1S 2R4	Sydney	basement	133.2	520	717000	5112125	166.50
B1P 3K1	Sydney	basement	14.8	520	717000	5112125	166.50
B1R 2E3	Sydney	basement	14.8	520	717000	5112125	166.50
B1P 5C2	Sydney	basement	14.8	520	717000	5112125	166.50
B1P 3L6	Sydney	basement	14.8	520	717000	5112125	166.50
B1S 2Z2	Sydney	basement	14.8	520	717000	5112125	166.50
B1P 3K3	Sydney	basement	14.8	520	717000	5112125	166.50
B1P 6E3	Sydney	first floor	14.8	520	717000	5112125	166.50
B1N 2P8	Sydney	first floor	14.8	520	717000	5112125	166.50
B1N 2P8	Sydney	first floor	14.8	520	717000	5112125	166.50
B1P 5V3	Sydney	basement	14.8	520	717000	5112125	166.50
B1R 1P5	Sydney River	basement	14.8	523	714625	5109125	129.50
B1S 3A7	Sydney River	basement	129.5	523	714625	5109125	129.50
B1S 1H8	Sydney River	basement	81.4	523	714625	5109125	129.50
B1P 3K2	Sydney River	basement	14.8	523	714625	5109125	129.50
B1S 1S6	Sydney River	living room	14.8	523	714625	5109125	129.50
B0J 3J0	Tantallon	living room	14.8	776	429000	4945875	148.00
B0J 3J0	Tantallon	living room	22.2	776	429000	4945875	148.00
B0J 3J0	Tantallon	living room	14.8	776	429000	4945875	148.00
B0J 3J0	Tantallon	living room	14.8	776	429000	4945875	148.00
B0J 3J0	Tantallon	first floor	140.6	776	429000	4945875	148.00
B0J 3J0	Tantallon	living room	14.8	776	429000	4945875	148.00
B0J 3J0	Tantallon	downstairs stu	99.9	776	429000	4945875	148.00
B0J 3J0	Tantallon	basement	14.8	776	429000	4945875	148.00
B0J 3N0	Tantallon	living room	14.8	776	429000	4945875	148.00
B0J 3J0	Tantallon	basement	148.0	776	429000	4945875	148.00
B0J 3J0	Tantallon	living room	14.8	776	429000	4945875	148.00
B0J 3J0	Tantallon	first floor	14.8	776	429000	4945875	148.00
B0J 3J0	Tantallon	basement	55.5	776	429000	4945875	148.00
B0J 3J0	Tantallon	basement	66.6	776	429000	4945875	148.00
B0J 3J0	Tantallon	basement	14.8	776	429000	4945875	148.00
B0J 3J0	Tantallon	living room	14.8	776	429000	4945875	148.00
B0J 3J0	Tantallon	dining room	14.8	776	429000	4945875	148.00
B0J 3J0	Tantallon	living room	99.9	776	429000	4945875	148.00
B0J 3J0	Tantallon	basement	14.8	776	429000	4945875	148.00
B0J 3J0	Tantallon	living room	14.8	776	429000	4945875	148.00
B0J 3J0	Tantallon	living room	51.8	776	429000	4945875	148.00
B0J 3J0	Tantallon	basement	14.8	776	429000	4945875	148.00
B0J 3J0	Tantallon	first floor	14.8	776	429000	4945875	148.00
B0K 1V0	Tatamagouche	basement	14.8	493	477050	5061700	70.30
B0K 1V0	Tatamagouche	basement	14.8	493	477050	5061700	70.30
B0K 1V0	Tatamagouche	first floor	14.8	493	477050	5061700	70.30
B0K 1V0	Tatamagouche	basement	14.8	493	477050	5061700	70.30
B0K 1V0	Tatamagouche	basement	70.3	493	477050	5061700	70.30
B0K 1V0	Tatamagouche	first floor	14.8	493	477050	5061700	70.30

Table 6.8, continued.

Postal Code	Town	Room sampled	Rn Bq/L	GAZ_ID	Eastings	Northings	Rn max/town
B0K 1V0	Tatamagouche	first floor	14.8	493	477050	5061700	70.30
B0K 1V0	Tatamagouche	first floor	14.8	493	477050	5061700	70.30
B0K 1V0	Tatamagouche	basement	14.8	493	477050	5061700	70.30
B0K 1V0	Tatamagouche	basement	14.8	493	477050	5061700	70.30
B0K 1V0	Tatamagouche	basement	14.8	493	477050	5061700	70.30
B0K 1V0	Tatamagouche	basement	14.8	493	477050	5061700	70.30
B0K 1V0	Tatamagouche	first floor	14.8	493	477050	5061700	70.30
B0K 1V0	Tatamagouche	first floor	14.8	493	477050	5061700	70.30
B0K 1V0	Tatamagouche	basement	14.8	493	477050	5061700	70.30
B0K 1V0	Tatamagouche	basement	14.8	493	477050	5061700	70.30
B0K 1V0	Tatamagouche	first floor	14.8	493	477050	5061700	70.30
B0K 1V0	Tatamagouche	first floor	33.3	493	477050	5061700	70.30
B0K 1V0	Tatamagouche	basement	14.8	493	477050	5061700	70.30
B0K 1V0	Tatamagouche	basement	14.8	493	477050	5061700	70.30
B0K 1V0	Tatamagouche	basement	59.2	493	477050	5061700	70.30
B0K 1V0	Tatamagouche	first floor	14.8	493	477050	5061700	70.30
B0K 1V0	Tatamagouche	first floor	14.8	493	477050	5061700	70.30
B0J 3K0	Terence Bay	first floor	14.8	778	442150	4925300	14.80
B3L 4J3	Timberlea	first floor	173.9	789	440575	4945800	666.00
B3L 4J1	Timberlea	first floor	14.8	789	440575	4945800	666.00
B3L 4J1	Timberlea	basement	40.7	789	440575	4945800	666.00
B3L 4J1	Timberlea	basement	170.2	789	440575	4945800	666.00
B3L 4J3	Timberlea	basement	122.1	789	440575	4945800	666.00
B3L 4J3	Timberlea	basement	284.9	789	440575	4945800	666.00
B3L 4J1	Timberlea	basement	247.9	789	440575	4945800	666.00
B3L 4J1	Timberlea	basement	162.8	789	440575	4945800	666.00
B3L 4J3	Timberlea	basement	14.8	789	440575	4945800	666.00
B3L 4J1	Timberlea	basement	14.8	789	440575	4945800	666.00
B3L 4J3	Timberlea	kitchen	14.8	789	440575	4945800	666.00
B3L 4J3	Timberlea	kitchen	22.2	789	440575	4945800	666.00
B3L 4J3	Timberlea	basement	14.8	789	440575	4945800	666.00
B3L 4J1	Timberlea	front room	14.8	789	440575	4945800	666.00
B3L 4J3	Timberlea	basement	122.1	789	440575	4945800	666.00
B3L 4J1	Timberlea	first floor	325.6	789	440575	4945800	666.00
B3L 4J1	Timberlea	basement	666.0	789	440575	4945800	666.00
B3L 4J1	Timberlea	basement	14.8	789	440575	4945800	666.00
B0J 1Z0	Timberlea	first floor	92.5	789	440575	4945800	666.00
B3L 4J3	Timberlea	basement	518.0	789	440575	4945800	666.00
B3L 4J3	Timberlea	rec room	55.5	789	440575	4945800	666.00
B0J 1Z0	Timberlea	basement	14.8	789	440575	4945800	666.00
B3L 4J3	Timberlea	living room	59.2	789	440575	4945800	666.00
B3L 4J1	Timberlea	basement	14.8	789	440575	4945800	666.00
B3L 4J3	Timberlea	rec room	592.0	789	440575	4945800	666.00
B2N 5A9	Truro	basement	14.8	510	478125	5023275	14.80
B2N 5B6	Truro	basement	14.8	510	478125	5023275	14.80
B2N 5A9	Truro	living room	14.8	510	478125	5023275	14.80
B2N 5A9	Truro	basement	14.8	510	478125	5023275	14.80
B2N 5A9	Truro	basement	14.8	510	478125	5023275	14.80

Table 6.8, continued.

Postal Code	Town	Room sampled	Rn Bq/L	GAZ_ID	Eastings	Northings	Rn max/town
B2N 5A9	Truro	basement	14.8	510	478125	5023275	14.80
B2N 5A9	Truro	basement	14.8	510	478125	5023275	14.80
B2N 5A9	Truro	living room	14.8	510	478125	5023275	14.80
B2N 5A9	Truro	basement	18.5	510	478125	5023275	14.80
B2N 5C1	Truro	basement	14.8	510	478125	5023275	14.80
B2N 5A9	Truro	living room	14.8	510	478125	5023275	14.80
B2N 5A9	Truro	basement	14.8	510	478125	5023275	14.80
B0N 2S0	Waverley	living room	14.8	849	452325	4958625	14.80
B0N 2S0	Waverley	first floor	14.8	849	452325	4958625	15.80
B0N 2S0	Waverley	sewing room	14.8	849	452325	4958625	14.80
B0N 2S0	Waverley	first floor bedro	14.8	849	452325	4958625	14.80
B0N 2S0	Waverley	basement	14.8	849	452325	4958625	14.80
B0N 2S0	Waverley	living room	14.8	849	452325	4958625	14.80
B0N 2S0	Waverley	first floor	14.8	849	452325	4958625	14.80
B0N 2S0	Waverley	living room	14.8	849	452325	4958625	14.80
B0N 2S0	Waverley	basement	14.8	849	452325	4958625	14.80
B0N 2S0	Waverley	basement	14.8	849	452325	4958625	14.80
B0W 3P0	Wedgeport	living room	14.8	362	259650	4847400	66.60
B0W 3P0	Wedgeport	living room	14.8	362	259650	4847400	66.60
B0W 3P0	Wedgeport	basement	66.6	362	259650	4847400	66.60
B0W 3P0	Wedgeport	living room	14.8	362	259650	4847400	66.60
B0J 3L0	West Dover	basement	14.8	876	429475	4927350	74.00
B0J 3L0	West Dover	basement	14.8	876	429475	4927350	74.00
B0J 3L0	West Dover	basement	74.0	876	429475	4927350	74.00
B0J 3M0	Western Shore	basement	77.7	879	395625	4930750	77.70
B1R 2B3	Westmount	basement	14.8	608	715375	5112800	14.80
B1R 1G2	Westmount	basement	14.8	608	715375	5112800	14.80
B3L 4J4	White's Lake	living room	14.8				0.00
B0P 1W0	Wilmot	basement	173.9	387	341950	4980425	173.90
B0P 1W0	Wilmot	basement	14.8	387	341950	4980425	173.90
B0P 1W0	Wilmot	basement	14.8	387	341950	4980425	173.90
B0N 2T0	Windsor	first floor	37.0	913	410975	4982050	2183.00
B0N 2T0	Windsor	first floor	133.2	913	410975	4982050	2183.00
B0N 2T0	Windsor	first floor	14.8	913	410975	4982050	2183.00
B0N 2T0	Windsor	first floor	14.8	913	410975	4982050	2183.00
B0N 2T0	Windsor	basement	14.8	913	410975	4982050	2183.00
B0N 2T0	Windsor	first floor	44.4	913	410975	4982050	2183.00
B0N 2T0	Windsor	first floor	177.6	913	410975	4982050	2183.00
B0N 2T0	Windsor	first floor	14.8	913	410975	4982050	2183.00
B0N 2T0	Windsor	basement	111.0	913	410975	4982050	2183.00
B0N 2T0	Windsor	first floor	14.8	913	410975	4982050	2183.00
B0N 2T0	Windsor	first floor	888.0	913	410975	4982050	2183.00
B0N 2T0	Windsor	first floor	14.8	913	410975	4982050	2183.00
B0N 2T0	Windsor	basement	2183.0	913	410975	4982050	2183.00
B0N 2T0	Windsor	first floor	40.7	913	410975	4982050	2183.00
B0N 2T0	Windsor	first floor	14.8	913	410975	4982050	2183.00
B0N 2T0	Windsor	first floor	14.8	913	410975	4982050	2183.00
B0N 2T0	Windsor	first floor	14.8	913	410975	4982050	2183.00

Table 6.8, continued.

Postal Code	Town	Room sampled	Rn Bq/L	GAZ_ID	Eastings	Northings	Rn max/town
B0N 2T0	Windsor	basement	14.8	913	410975	4982050	2183.00
B0N 2T0	Windsor	basement	14.8	913	410975	4982050	2183.00
B0N 2T0	Windsor	basement	33.3	913	410975	4982050	2183.00
B0N 2T0	Windsor	first floor	14.8	913	410975	4982050	2183.00
B0N 2T0	Windsor	living room	14.8	913	410975	4982050	2183.00
B0N 2T0	Windsor	first floor	14.8	913	410975	4982050	2183.00
B0N 2T0	Windsor	first floor	14.8	913	410975	4982050	2183.00
B0N 2T0	Windsor	basement	14.8	913	410975	4982050	2183.00
B0N 2T0	Windsor	first floor	14.8	913	410975	4982050	2183.00
B0N 2T0	Windsor	first floor	14.8	913	410975	4982050	2183.00
B0N 2T0	Windsor	first floor	14.8	913	410975	4982050	2183.00
B0N 2T0	Windsor	first floor	14.8	913	410975	4982050	2183.00
B0N 2T0	Windsor	first floor	14.8	913	410975	4982050	2183.00
B0N 2T0	Windsor	first floor	14.8	913	410975	4982050	2183.00
B0N 2T0	Windsor	first floor	14.8	913	410975	4982050	2183.00
B0N 2T0	Windsor	first floor	14.8	913	410975	4982050	2183.00
B0N 2T0	Windsor	basement	14.8	913	410975	4982050	2183.00
B0N 2T0	Windsor	basement	14.8	913	410975	4982050	2183.00
B0N 2T0	Windsor	basement	14.8	913	410975	4982050	2183.00
B0N 2V0	Windsor	basement bedr	173.9	913	410975	4982050	2183.00
B5A 4B3	Yarmouth	living room	14.8	388	249450	4859225	14.80

Table 6.8, continued.

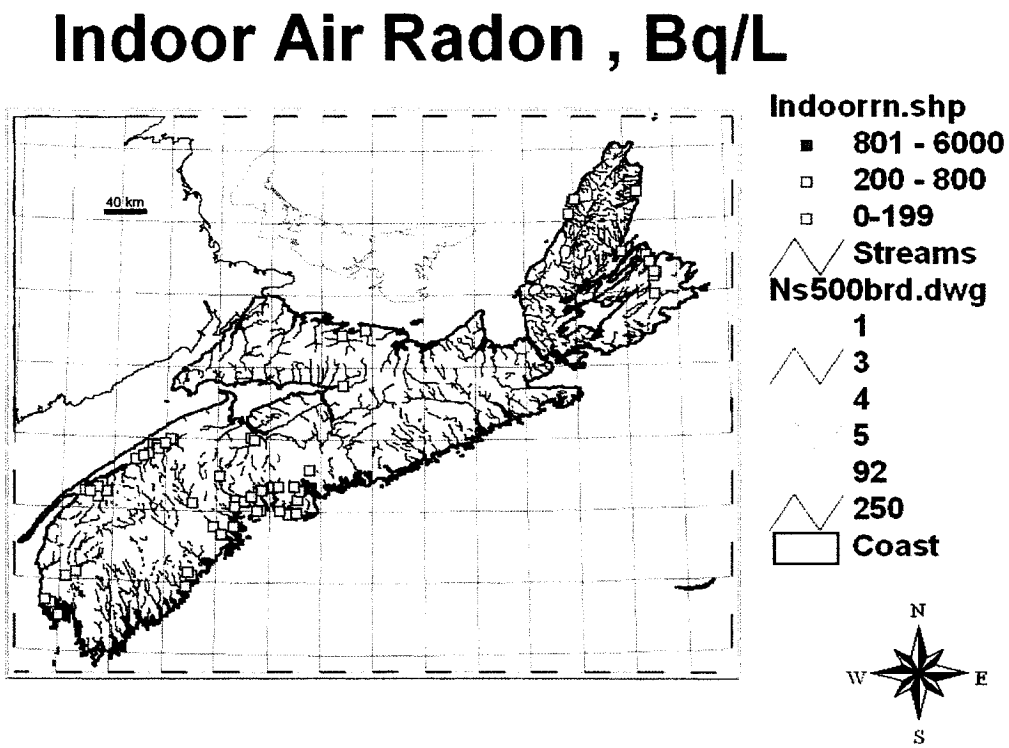

Figure 6.8. Summary data, indoor air radon for the province of Nova Scotia (Bq/L).

It should be noted that there were sometimes several samples from the same town, with the same owner initials, but the samples were taken from different locations in the house. Sometimes the same phone number was recorded; sometimes no phone number was recorded. While it might be assumed that these samples are from different locations in the same house, this assumption was not made in recording the number of points or the values, as the same owner and phone number can belong to more than one property. These "ambiguous" data are indicated as such in the "Notes" section of the data file. No data were available in map format.

6.2.3.5.2 Data Processing

Seven hundred and twenty-three data points in paper format were entered into digital format (.dbf files) (Table 6.8). The data were georeferenced from the Nova Scotia gazetteer, and the UTM (NAD 27) coordinates for each town were then entered onto the digital map at the scale of 1:500 000.

Duplicate town names exist in different regions of Nova Scotia, so it was necessary to try and establish from phone numbers or postal codes where these analyses were taken. However, postal codes for some areas have changed since these data were collected so it was not always possible to establish the location of a given datum. As well, Armdale and Halifax Co. data are entered in the .dbf file (Table 6.8), but they are not located in the map produced from these data (Fig. 6.8), as neither can be georeferenced. The towns of Milton and Brooklyn require further location confirmation as there are more than one town with these names, and it was not possible to determine from which of the towns the data came. As well, postal code records are available through the internet; however, as mentioned above, they have changed in some cases since these data were originally collected.

6.2.3.5.3 Preliminary Analysis

Although the data can only be located to nearest-town, there are several points that merit comment:

Twenty-three of the 723 data indicate Rn values above 800 Bq/m^3, the level at which Canada recommends remedial action be taken (Health Canada, as of April 1999). These towns include: Blandford, Cheticamp, Halifax, Lakeside, Hubbards, Ingonish, Chester, and Windsor, with the highest values being recorded in Cheticamp and Ingonish. Most of these high values are restricted to a limited number of geologic units: (1) Lower Carboniferous rocks (Cheticamp, Ingonish, Windsor); (2) granitic rocks of the South Mountain Batholith (Lakeside, Hubbards); and (3) the Meguma Group rocks (Halifax, Blandford, Chester). It should be noted that it is also possible that some of the sample locations lie on contacts between units. Geologic contact may serve as conduits for higher than background U levels, and consequently elevated Rn levels. Without more detailed information, such as exact location of the higher than background levels, it is not possible to analyze these data further.

6.2.4 Conclusions and Recommendations

6.2.4.1 Conclusions

The original intent of this project was to develop a preliminary Rn-risk potential map for the province of Nova Scotia. However, the results of the analyses undertaken suggest that a better way to represent the data from a scientific viewpoint, is to provide the data in the attached format, that is, as database files and corresponding shapefiles. In this way, all data, either individual or grouped, are linked to a data table which can be accessed to show the exact nature of the information available. In addition, gaps in information or non site-specific information is evident under these localized representations. The decision to present the data in this way arose because there are large areas of the Province for which there are no data, and although some of these

areas are not populated, many are well-populated.

Providing this information in this form is done for several reasons, as outlined in the following list: (1) Not all regions of the Province have been the target of U, Rn, or Ra measurements, so any map produced from these data would of necessity have large areas for which there is no information. (2) The data available represent a mix of individual sample locations, as well as grouped analyses, with grouping based either on the centroid of a mining tract or on the location of the nearest town (based on postal addresses?). As well, the number of samples for each point/town/mining tract is variable, so is not statistically meaningful. Under these conditions the data cannot be consistently represented on a map. (3) The possibility for misinterpretation is high, particularly in relation to the conclusions that may be drawn based on the site locations data, as the variability even within a short distance, can be great. (4) It is not always possible to determine the original accuracy or reliability of the data from the various sources, and therefore the data may not always be easily reproducible. (5) The geological and other digital databases are constantly being upgraded and updated, and some layers are not yet ideally suited to detailed interpretation based on the data available. (6) The nature of the original data and the available base maps required that the data be entered at various scales; whereas this does not introduce large errors on the scale of 1:500 000, the errors are more pronounced at scales of 1:50 000, for example.

Despite these limitations, general conclusions can be made: (1) There are regions within the Province which have higher than currently acceptable levels of U in well waters (> 0.1 mg/L) and indoor air Rn (> 800 Bq/m^3). These regions tend to be concentrated in areas underlain by granitic rocks of the South Mountain Batholith, shales and sandstones of Lower Carboniferous age, in Cambro-Ordovician metasediments, or in contact zones between these rock types. However, not all areas within these rock types display "anomalous" levels of U or Rn. (2) Within the Leminster-Vaughan area of the South Mountain Batholith (near the Millet Brook uranium occurrence), the pattern of elevated Rn in well-waters suggest that it is structurally-controlled; this has ramifications for the nature of distribution of Rn and U in well waters and Rn in indoor air throughout rocks of the South Mountain Batholith, and indeed, in

any area underlain by fracture systems which might have served as conduits for U mobilization. (3) The nature of the uranium distribution in the Panuke Road area (south of Windsor, N.S.) (Rikeit, 1979) suggests that houses in this vicinity be checked for indoor air Rn. (4) Areas within the Province for which there are currently no data available, should be tested for U in well waters and/or Rn in indoor air, as the variability in the data to date do not allow for narrowing down the potential for elevated U or Rn levels based on location. (5) In the event that Health Canada lowers the acceptable limit for U in well waters from the current 0.1 mg/L (as of 1999), many more wells in Nova Scotia will have values above the action limit.

6.2.4.2 Recommendations

In addition to (4) and (5) in the conclusions above (6.3.4.1), it is recommended that any analyses undertaken in the future be added to this database and georeferenced clearly. The time involved in preparing the data to this point was enormous because accurate records of geographic locations had not been kept. Furthermore, the number of data which are not useable, or not as useful as they might otherwise be, is unacceptably high. This is particularly significant, given that the elements involved have possible negative health effects. This recommendation should apply whether the analysis is undertaken through the Department of Health, the Department of Environment, or through the Department of Natural Resources.

It is assumed that all individuals whose well water or wells were tested, or indoor air values, and found to have above acceptable levels of U in well waters or Rn in indoor air, have been notified to this effect; if this is not so, then it is recommended that they be notified at this time (1999). Furthermore, if the acceptable level of U in well water is lowered, then individuals whose well waters have U values less than the current level of 0.1 mg/L and higher than the "new" level, should be notified of the levels of U in their well waters.

6.2.4.3 Addendum (June 2006)

Since this report was produced, the guideline for Uranium in drinking water has been re-evaluated, and is currently set at 0.02 mg/l (Health Canada, 1999). (http://www.hc-sc.gc.ca/ewh-semt/alt_formats/hecs-sesc/pdf/pubs/water-eau/doc-sup-appui/sum_guide-res_recom/summary-sommaire_e.pdf). This lowered value of 0.02 mg/l means that a number of wells within the acceptable limits in 1999, are now above the acceptable limit. A guideline limit of < 0.2 mg/L of U, means that for the data analyzed, 83 of the 204 wells in the Harrietsfield area (approx 41%) are at or above the limit; 45 of the 231 wells in the New Ross area (approx 20%) are at or above the limit; 77 of 130 wells in Northern Nova Scotia (approx 59%) are at or above the limit. At time of writing this chapter of the thesis, new guidelines for Rn in indoor air are under consideration (2006). The proposed new limit for Rn in indoor air is 200 Bq/m^3 (Health Canada, 2006). (http://www.hc-sc.gc.ca/ahc-asc/alt_formats/ccs-scm/pdf/public-consult/col/radon/WG_Report_2006-03-10_en.pdf). A limit of 200 Bq/m^3 in indoor air, would mean that 70 of the 695 analyses (10%) would be at or above the acceptable limit for Rn in indoor air.

6.3 U and Rn in weathered horizons

6.3.1 Uranium in the South Mountain Batholith

In addition to establishing the nature of the weathering process under different conditions and at different times on the granitoids of the South Mountain Batholith, this study examines the nature and distribution of uranium in the saprolites of the SMB. The SMB is known to have U-mineralization at numerous localities, and can be considered a uraniferous granite (Chatterjee et al., 1985). In addition to a number of localities where known U mineralization occurs (Chatterjee and Muecke, 1982) (Fig. 6.2), there are also regions removed from known mineralization, where U (and / or Rn) in groundwaters is elevated (NSDOE, 1981). The NSDOE (1981) report also concludes that where no obvious mineralization is present, these anomalies have been variably attributed to the

presence of uranium in sub-till fractures, accumulation of uranium at reducing boundaries along till contacts, and even from the till itself. In all cases, the uranium is initially moblized as a result of ongoing weathering processes of some kind. However, these studies did not consider the possibility of the underlying presence of partially weathered granitoids and their potential to release uranium and its radioactive decay daughter products. A detailed study of well waters and their uranium, radium, radon contents was undertaken in the early 1980s in a region southwest of Halifax, underlain by SMB, and mostly blanketed by a thick till sequence (NSDOE, 1981). In addition, in this same area there are a number of sites where weathered granite has been intercepted during water well drilling (unpublished NSDOE data, 1981), and examining the possibility of uranium release during weathering is prudent. Given that U is obviously being liberated into groundwaters in some localities, this study examines the impact of weathering on the amount and distribution of U in fresh and weathered samples of the saprolite horizons, in order to determine whether there is a possible connection between the presence of underlying saprolites and elevated U (and / or Rn) in groundwater.

Uranium mineralization in Lower Carboniferous arkoses sourced from granitic rocks of the SMB (O'Reilly et al., 1982; Rikeit, 1979), confirms that U may be mobilized from these granitoid rocks under favourable conditions. Uranium mobility is further supported by fission track evidence of U-distribution along cleavages and secondary oxides in the biotites of the arkoses (O'Beirne-Ryan et al., 2001) (Fig. 6.9), as discussed further below.

Uranium commonly exists as U^{IV} if Eh conditions are low, and as U^{VI} in higher Eh conditions (Langmuir, 1978) (Fig. 6.10). Uranium is soluble in the U^{VI} form, and under oxidising conditions, particularly if also acidic, uranium may form aqueous uranium complexes (Langmuir, 1978). Given that the weathering process is one in which oxidation dominates, it is possible that uranium from the granitoids of the SMB may have been mobilized during formation of the saprolites. Geochemical data suggest that this does not seem to have been the case, with the exception of one of the Pre-Carboniferous sample suites (Fig. 5.6 and 5.7). Michel (1984) discusses a similar non-decreasing distribution of uranium in granite saprolite in South Carolina, and concludes

that U may have been released, but immediately fixed on newly-formed minerals and / or as a result of re-redistribution of U within the saprolite under fluctuating groundwater levels. Van der Weidjen and van der Weidjen (1995), Cramer and Nesbitt (1983) and Guthrie (1989) conclude that U^{VI} is readily adsorbed onto secondary Fe minerals. Ruhlmann (1980) indicates that precipitation of U onto secondary Ti oxides and hydroxides as well as Fe oxides and hydroxides is possible, as also suggested by Guthrie (1989). Guthrie (1989) and Guthrie and Kleeman (1986) discuss the distribution of U within a granitic rock, and conclude that U can be concentrated in resistate minerals (such as zircon) where it is not available for mobilization, in rock-forming minerals (such as biotite), where it may be mobilized if the biotite is altered or weathered, and in interstitial, altered or secondary phases, from which it may migrate, if geochemical conditions change (Fig. 6.10 and 6.11). For example, uranium forms soluble uranyl carbonate complexes if HCO_3^- is present, soluble fluoride complexes if fluorine is present, and soluble phosphate complexes if phosphorous is present (Langmuir, 1978).

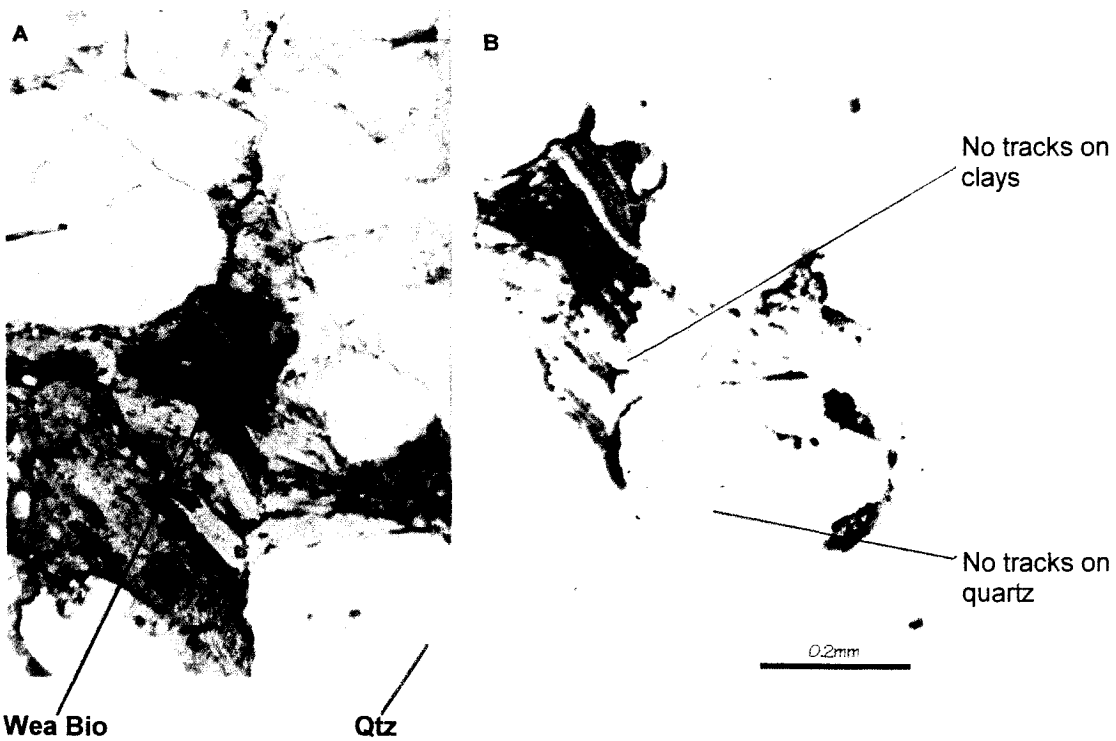

Figure 6.9. Left diagram: arkose matrix, with partially weathered biotite and clays. Right diagram: fission tracks produced by U in biotite grains and in matrix oxides/hydroxides, show as black against the mica sheet (in white). Note the absence of tracks in the clays and quartz grains.

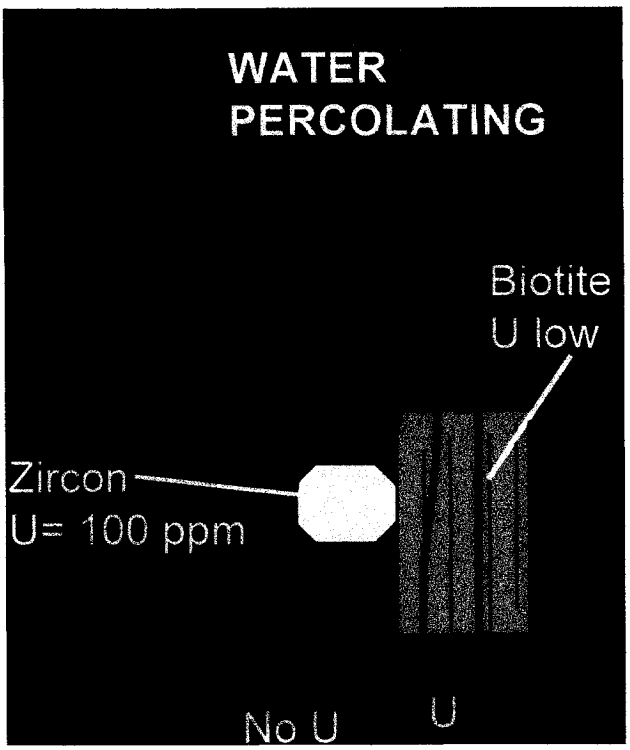

Figure 6.10. Cartoon demonstrating the selective scavenging of water on uranium loosely-held along cleavage traces in biotite, in contrast to the lact of mobility of uranium from resistate minerals such as zircon.

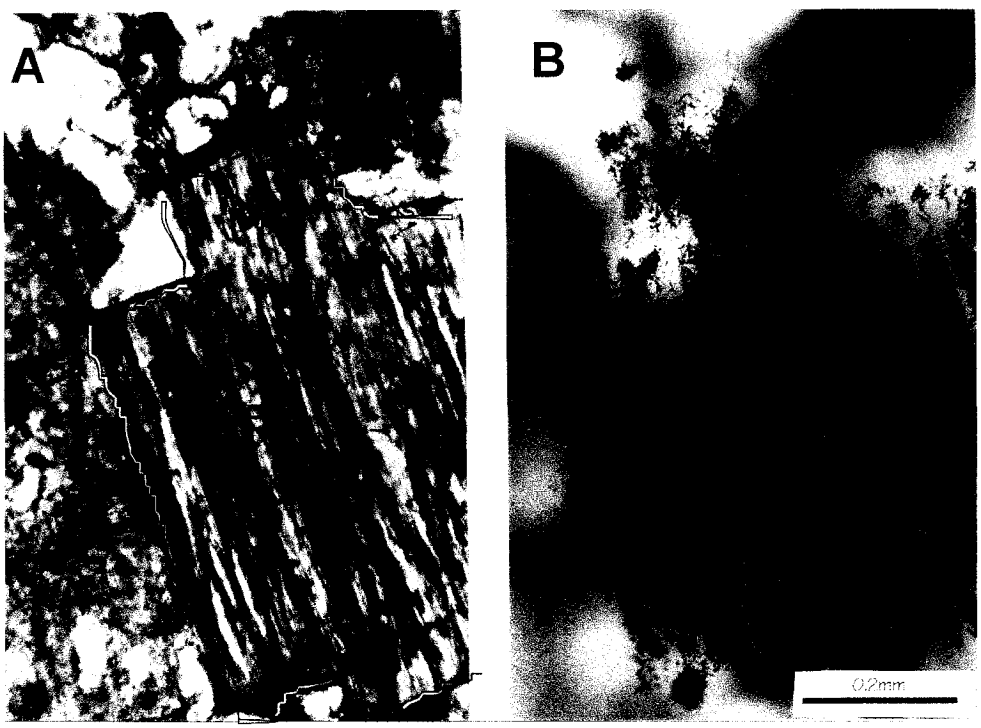

Figure 6.11. (A) Weathered biotite, with oxides / hydroxides developing along the cleavage. (B) Fission tracks from weathered biotite, developed along the cleavages, and on the oxides / hydroxides. The fission tracks have been superimposed on an out-of-focus photo of the biotite grain from (A).

Guthrie (1989) concludes that typically up to 60% of U is bound in resistate minerals, and is therefore not available for liberation under weathering conditions. Leaching experiments on granite by Kovalev and Malyasova (1971) indicate that 20-80% of uranium is leachable, however Szalay and Samsoni (1966) indicate that following leaching, much of the uranium is subsequently readsorbed onto other minerals, and is consequently not liberated from the rock. However, the gaseous Rn that forms as this U decays is most likely to be released.

6.3.2 Fission tracks as indicators of uranium distribution in rocks

Fission track mapping affords the opportunity to examine the distribution of uranium in a rock, and in the weathered horizon. Fission track mapping of fresh and weathered samples from all three ages of horizons was undertaken in order to determine the fate of uranium under weathering conditions. Fission track analysis is commonly used for dating rocks: fission tracks from the decay of ^{238}U contained in minerals in trace amounts are counted and measured. Fission track mapping makes use of a common step in the external detector method of fission track dating (e.g. Wagner and Van der haute, 1992): (1) a thin slab of the rock is cut and polished; (2) a sheet of (uranium-free) mica is affixed as a "detector" to the surface; (3) this combination is irradiated with thermal neutrons in a nuclear reactor, which induces the fission of any ^{235}U contained (in nature, the proportion of ^{235}U occurs in a fixed ratio with ^{238}U), expelling high energy nuclear particles in all directions; some of these particles impact the mica detector and disrupt its lattice (metamictization), forming latent fission tracks; (4) the mica detector is etched with hydrofluoric acid to enable the latent tracks to be visible; (5) the areas in the detector with the largest numbers of tracks per unit area correspond with the greatest concentration of uranium on the surface of the rock slab studied, thus forming a microscopic "distribution map" of uranium. The irradiation is calibrated with the use of standards of known U content. In this way, induced fission tracks record the distribution of uranium in a rock.

6.3.3 Uranium distribution and potential for uranium liberation during weathering in the South Mountain Batholith

In order to determine the potentiial for uranium release during weathering of granitoids of the SMB, an examination of the distribution of uranium in the fresh and in the weathered samples of these rocks is necessary. Using fission track mapping of uranium distribution, Guthrie and Kleeman (1986) determined that uranium was indeed mobilized during weathering of three different granite types in New South Wales, Australia. Examination of fission track distribution of granitoids of the SMB, may help determine whether there is the potential for uranium release during the weathering process.

6.3.3.1 U-distribution in the Pre-Carboniferous saprolite

In a thin section from the freshest sample of monzogranite from the base of the drill core (1186) which had been irradiated and the tracks "captured" on a mica detector, the fission tracks are dominantly associated with zircon and apatite, as in Figure 6.12A, and are evenly distributed throughout these grains: rarely are tracks observed elsewhere in the slide. In the thin sectio of the weathered sample from higher up in the profile, fission tracks similarly are observed in the accessory phases, zircon and apatite. In addition to uranium in these resistate grains, lower numbers of fission tracks (lower quantities of uranium) are observed associated with individual grains of secondary Ti (or Fe) minerals (Fig. 6.12B), and occasionally with fractures where secondary opaque minerals are found (Fig. 6.12C). In the case of fracture-associated opaque minerals, it should be noted that not all fractures have associated fission tracks. Microprobe analyses of these secondary opaques indicate that they are dominated by Ti and not by Fe (Fig. 4.5).

6.3.3.2 U-distribution in Pre-Triassic saprolite

There is some variation in the distribution of uranium from the base to the top of the weathering horizon, as expressed in fission track maps. In the lowermost level, where the rock is only incipiently weathered, uranium is dominantly found in resistate minerals (including apatite), as trace amounts on cleavages and grain boundaries of biotites, as well as rarely along grain boundaries or cracks with secondary Fe (or Ti) oxyhydoxides (Fig. 6.13). There is little evidence of uranium scattered throughout biotites. However, closer to the top of the horizon, some of the weathered biotites have low quantities of scattered uranium throughout the grains as well as the higher quantities within resistate minerals. Some, though not all secondary oxides have notable quantities of uranium, some within crack infillings, others as individual, ragged, secondary opaque grains following the breakdown of biotite (Fig. 6.13). In summary, the distribution of fission tracks with increased weathering changes from resistate mineral-dominant to a combination of resistate minerals, tracks scattered within weathered biotite, and tracks within some secondary oxides.

6.3.3.3 U-distribution in Pre-Pleistocene saprolites

Uranium distribution maps from the fresh and the weathered monzogranite from Hardwood Lake suggest that in this rock, uranium is concentrated in the accessory phases (mainly zircon and apatite) and also along the grain boundaries, particularly between grains of biotite. As this rock weathers, the uranium is localized in alteration patches associated with secondary minerals after the biotite. In the more felsic Smith's Corner horizon, the biotite content is much lower (<5%), however unlike the uranium found in the monzogranite of Hardwood Lake, uranium in this felsic phase is found in accessories and is also scattered throughout the biotite itself, as well as along thin fractures within biotite or plagioclase grains. This is the case in both the fresh and the slightly weathered samples from this horizon.

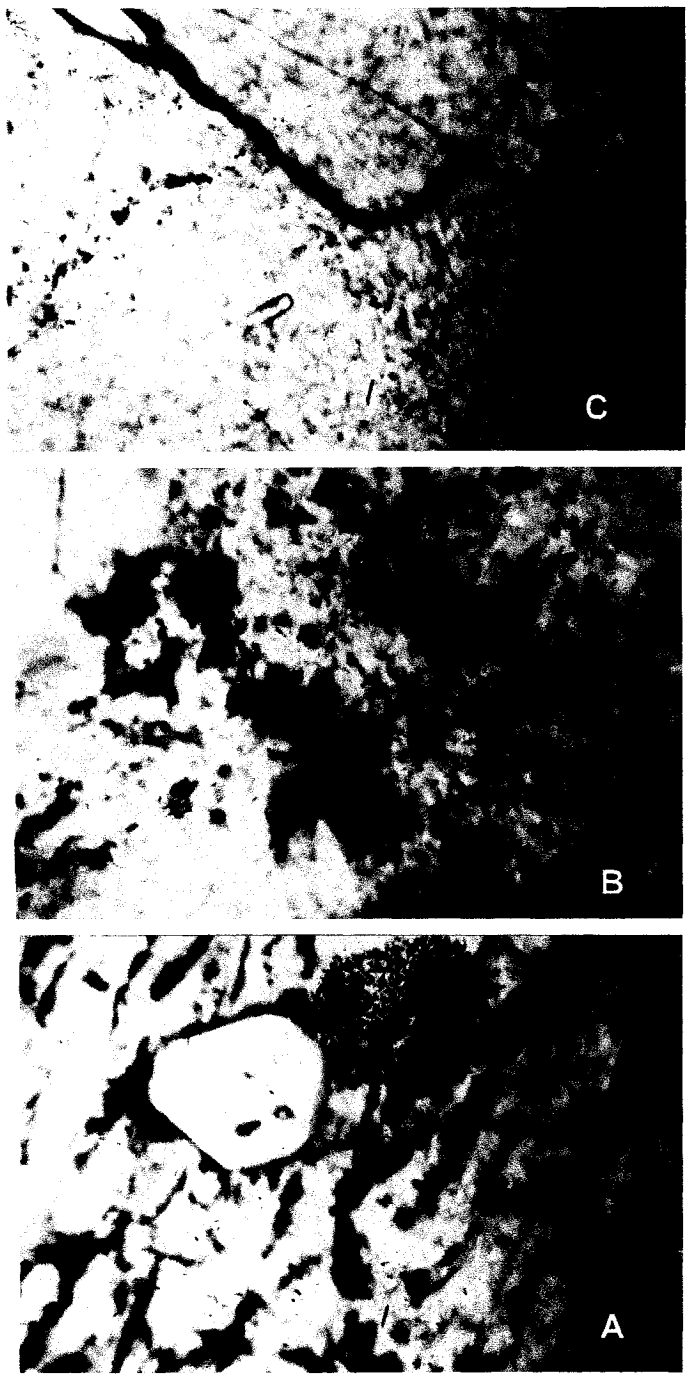

Figure 6.12. Fission tracks superimposed and slightly offset, for Pre-Carboniferous suite.

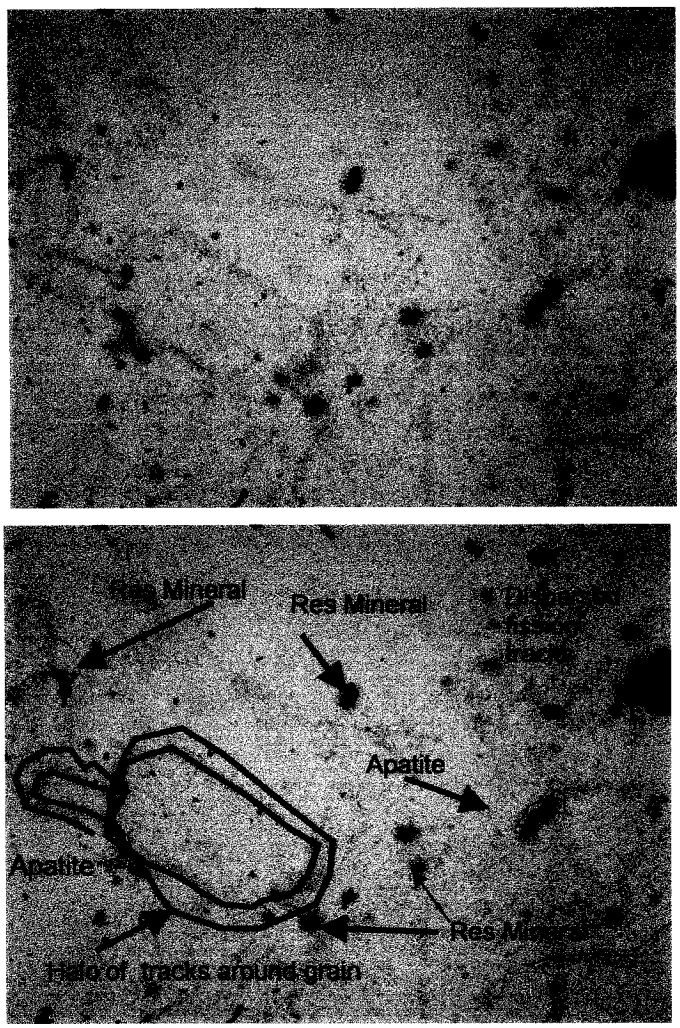

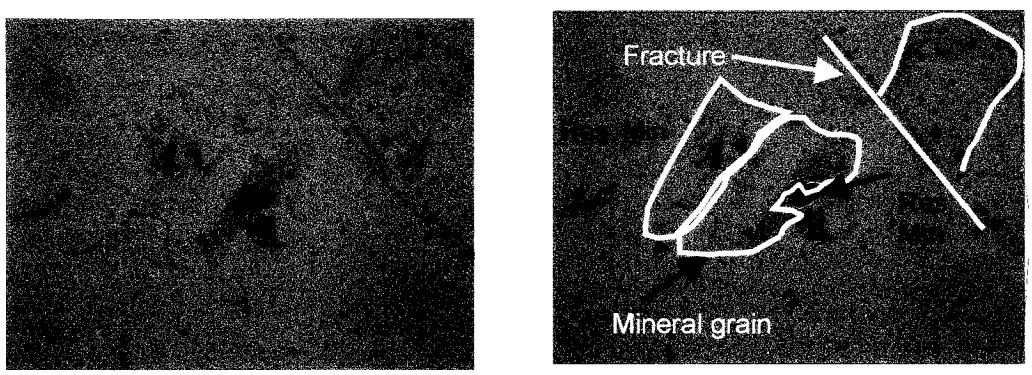

Figure 6.14. Weathered versus fresh fission track distribution, note the dispersion in the weathered sample at top of the diagram in comparison to the fresher lower photos.

6.4 Discussion of U-distribution in SMB saprolites of different ages

Fission track data indicate that much of the U in the SMB and in the saprolites developed from the granitoids, is concentrated in resistate minerals, and does not notably decrease in quantity during saprolite formation, in agreement with the geochemical data (Fig. 5.6 and 5.7). However, with the increase in fractures and secondary phases during weathering to saprolite, there is an increase in the proportion of U found in fractures and in association with secondary oxides and hydroxides. If these saprolites of the SMB are exposed at surface (as happens when these sites are quarried, blasted for road construction, or otherwise disturbed), changes in pH and Eh may be expected, and in particular, an increase in oxidizing conditions is likely. Such conditions are more favourable to the release of leachable uranium from a rock (Langmuir, 1978) (Fig. 6.10). Given that the more weathered samples of SMB saprolite show some increase in fractures and in secondary phases, re-exposure of these weathered horizons may result in re-liberation of uranium, and potential for increase in groundwater U and / or Rn. Indeed, Rn levels are most likely to increase in saprolites, even when U levels do not, as the open fracture system is conducive to the migration of the gaseous Rn into the voids during decay of radium, its immediate parent. Further work on radon in air above unweathered and weathered, fractured granitoid is necessary in order to determine what, if any, variability in radon release occurs under an increased fracture density.

Chapter 7

Discussion

7.1 Introduction

Weathered horizons record important information about the processes and conditions that impacted a rock following its exposure at surface, and prior to its partial erosion or reburial. Weathered horizons provide a window into the past, and enable us to view interactions between the lithosphere, atmosphere, hydrosphere and possibly the biosphere throughout geologic history. This study assumed an interdisciplinary approach to weathering within the granitoids of the SMB for two reasons: (1) although identification of weathered features had been reported prior to this work, no studies of this weathering had been undertaken in relation to timing, mineralogical or geochemical evolution, and possible environmental or engineering impacts; and (2) a multi-discipline study is consistent with a systems approach, in that it attempts to develop a broader understanding of the nature of the SMB weathered horizons, by bringing together a number of different aspects in order to understand a feature of the natural world.

In order to synthesize the various aspects of this study it is advantageous to revisit the questions raised prior to and during the research, and reflect on the few questions that remain unanswered. Questions of particular pertinence include: (1) what was the timing of weathering events on the South Mountain Batholith? (2) whereas the base of each weathered horizon is the SMB, do the weathered horizons trapped beneath strata of different ages actually represent different weathering episodes, or do they represent the same episode, buried at different times? (3) what are the mineralogical signatures of weathering? (4) what are the chemical signatures of weathering? (5) under what condition(s) did the weathering episode(s) happen? (6) is it possible to distinguish between hydrothermal alteration and weathering? (7) what environmental, economic, and engineering impacts do these weathered horizons pose?

(8) what, if any, specific implications are there for the cycling of U in the environment of southwestern Nova Scotia? (9) what contribution does this study make to our understanding of the geology and geologic history of Nova Scotia? (10) what are the broader implications of this study? (11) what educational needs of geologists, engineers, and planners are implicit from this study? (12) what further work is recommended?

What follows is an integration of the data from various aspects of the study, as each of these questions is addressed in turn.

7.2 Timing of weathering and evidence for multiple episodes

(1) What was the timing of weathering episodes on the South Mountain Batholith? (2) As the base of each weathered horizon is the SMB, do the weathered horizons trapped beneath strata of different ages actually represent different weathering episodes, or do they represent the same episode, buried at different times?

7.2.1 Conclusion

Based on stratigraphy and mineralogy, there are three weathered horizons of distinctly different ages: Pre-Carboniferous; Pre-Triassic; and Pre-Pleistocene.

7.2.2 Explanation

Many of the weathered horizons of the SMB have been buried beneath younger sedimentary rocks or tills. Localities include: core from Castlefrederick Bridge near Windsor (Fig. 1.1), where a weathered horizon on granitoid is preserved beneath Carboniferous sedimentary strata; core from Bridgetown (Fig. 1.1), in which a weathered granitoid succession is buried beneath Triassic strata; and near-surface outcrops at Hardwood Lake and New Ross (Fig. 1.1), where Pleistocene till clearly overlies a weathered horizon. The age of the strata (or intrusion) below and above the saprolite

impose certain restrictions on the timing of these weathering episodes, although precise dates are not known. The oldest episode occurred between intrusion of the batholith *circa* 372 Ma (MacDonald, 2001) and the deposition of the overlying strata during Early Carboniferous times. It should be noted that recent U/Pb data on the early, granodiorite phase, molybdenite Re/Os data on the age of mineralization, and laser Ar/Ar data on various phases of the batholith indicate that emplacement of the batholith may be as old as c. 380 Ma (Carruzzo et al., 2003; Carruzzo, pers.comm., 2006). A second period of weathering occurred prior to deposition of the Triassic sediments, and the most recent event occurred sometime post-Early Jurassic and prior to deposition of glacial till.

Each of these 3 horizons is *in situ*, and has as its base fresh or relatively fresh granitoid. It could be argued that these overlying strata represent burial of a single weathering episode at different times in the geologic past. However, evidence from field and analytical work indicates that the weathered horizon beneath the Carboniferous strata underwent intense weathering during which all biotites and feldspars were altered within 4-5 metres of the fresh granitoid. This weathered horizon was subsequently buried and diagenetically modified. Despite relithification, granitic textures were retained, and kaolinite pseudomorphs after biotite show little if any evidence of compaction (Fig. 4.3).

In the case of the sub-Triassic horizon, the alteration (weathering) involved similar intense clay development which created an argillaceous horizon, however even 30 metres above the weathering front, at the top of the preserved portion of the weathered horizon, biotite remains present in a variably altered form, and although reduced significantly in proportion, K-feldspar is also present. In this saprolite, the dominant clay mineralogy is montmorillonite together with kaolinite. The thickness over which these minerals have been retained together with the differing nature of the clay mineralogy when compared to the clays of the Pre-Carboniferous horizon, indicate different conditions during the formation of these saprolites.

The weathered horizon beneath glacial till is significantly different from either of the older 2 horizons in that clay development is minimal, resulting in the development of an arenaceous horizon, with only weakly weathered biotites and feldspars, even 2-3

metres above the weathering front.

Given that these three sequences have geochemically similar, biotite-bearing monzogranite as parent, differences in geochemistry between these weathered horizons cannot be attributed to differences in original parent geochemistry.

It could be argued that these textural and mineralogical differences simply represent different environments of formation of a single event, such as might be associated with different topographic environments. However, even if it were possible that weathering during pre-Carboniferous times resulted in a weathered horizon that was not homogeneous over space, relithification of the sub-Triassic and the sub-Pleistocene horizons has not occurred, indicating that reburial of these weathered horizons did not happen. We can therefore conclude that the evidence available indicates that there were at least 3 different weathering episodes since Devonian times, each with its own textural and mineralogical signature.

7.3 Mineralogical signatures of weathering

(3) What are the mineralogical signatures of weathering?

7.3.1 Conclusion

The mineralogical characteristics that are shared by the three episodes are hydration, breakdown of biotite, retention of apatite, creation of secondary Ti-oxides. However, the three episodes are mineralogically distinct.

7.3.2 Explanation

All horizons show a number of mineralogical and textural modifications as a result of weathering, including the following: (1) feldspars are variably altered to clay minerals (smectite / montmorillonite to kaolinite); (2) biotites are variably weathered to

kaolinite through intermediate phases, although the intermediate phases are chemically different for each of the 3 horizons; (3) development of secondary iron and / or titanium oxides/hydroxides as weathering products of biotite; (4) preservation of apatite throughout all horizons; (5) decrease in textural integrity of the horizon from base to top; (6) relithification of the oldest horizon, resulting in a suite of diagenetic minerals in addition to the secondary suite of weathered minerals.

Key distinct features of each saprolite define different weathering episodes. Diagnostic characteristics of the Pre-Carboniferous horizon include near-complete breakdown of all primary feldspars and biotite to clay minerals producing an argillaceous saprolite, dominance of kaolinite as the clay mineral throughout the sequence, a distinctly different biotite weathering trend when compared to the younger horizons, and relithification of the horizon.

In comparison to the other horizons, the Pre-Triassic saprolite is characterized by its argillaceous nature, combined with the thickness over which the profile exists, the persistence of biotite throughout the horizon, the biotite breakdown signature distinctly different to either that of the Pre-Carboniferous or the Pre-Pleistocene horizon, and the dominance of the combined clay mineral pair, montmorillonite and kaolinite.

In contrast to the argillaceous nature of the older horizons, the Pre-Pleistocene saprolite is arenaceous in character, clay mineral development is minimal and dominated by vermiculite with some kaolinite, the biotite breakdown signature is different from either of the older horizons, and physical disaggregation of the rock dominates over chemical breakdown.

The intermediate phases of biotite weathering to kaolinite, referred to above as the biotite breakdown signature, record different stories for the 3 horizons. Given that the parent biotite composition for all horizons is similar (Fig. 3.11), it is most likely that variations in paleoenvironmental conditions have contributed significantly to the differences observed. In addition to recording changes in paleoenvironment and post-weathering effects, the mineralogy also reflects changes in the geochemistry, particularly in relation to oxidation (development of secondary oxides and

oxyhydroxides), hydration (development of clay minerals and oxyhydroxides), and pH conditions during development (biotite retention in the Pre-Triassic horizon).

7.4 Chemical signatures of weathering

(4) What are the chemical signatures of weathering?

7.4.1 Conclusion

Oxidation and hydration dominate the weathering process in all 3 horizons. The behaviour of other elements within each of the episodes differs, reflecting the differing environmental conditions during development.

7.4.2 Explanation

Even in the early stages of weathering, oxidation and hydration reactions dominate in all 3 suites particularly in the monzogranites, as indicated by the increases in LOI and Fe_2O_3 (where measured), and a decrease in CaO and Na_2O. In the Pre-Carboniferous suite, most trace elements are significantly depleted (Fig. 4.5), which is not the case in the Pre-Triassic or the Pre-Pleistocene suites (Fig. 4.5). Whereas the intensity of chemical weathering within the Pre-Pleistocene horizon is relatively low, this is not the case in the Pre-Triassic horizon. The retention of elevated levels of trace elements within the Pre-Triassic horizon may reflect element-liberation followed by immediate adsorption onto newly-formed smectite or Fe (Ti) oxides. Alternatively, the retention of many of the trace elements within the system may be the result of the existence of relatively low-acidity conditions during weathering, as also might be suggested by the incomplete weathering of biotite in this horizon (Chapter 4). Further evidence for a possible low-acidity environment is the retention of Pb (Siegel, 2002). Data from aqua regia digestion (Appendix) indicate that Pb is not liberated under this acid digestion, indicating that it is held in relatively insoluble phases, and not simply adsorbed onto clay minerals or oxides. Therefore, while oxidation and hydration

increase and CaO and Na_2O decrease in all cases within the SMB monzogranites, the behaviour of other elements is variable, and as in the case of the mineralogical changes, reflects different conditions during weathering.

7.5 Paleoenvironmental interpretation

(5) Under what condition(s) did the weathering episode(s) happen?

7.5.1 Conclusion

Pre-Carboniferous weathering was most intense; Pre-Pleistocene weathering intensity was the least. The most likely paleoenvironmental condition for the Pre-Carboniferous were warm and humid; for the Pre-Triassic a warm, semi-arid environment with seasonal rainfall, combined with fluctuating groundwater levels, dominated; for the Pre-Pleistocene, warm temperate conditions dominated.

7.5.2 Explanation

Weathering during the Pre-Carboniferous resulted in the near-complete transformation of primary minerals to secondary minerals, dominantly kaolinite and Ti-oxides, and the depletion of many of the alkali and trace elements within 5 metres of the weathering front. This relatively intense weathering suggests a warm, humid climate, or at least, topographic conditions at the sample sites dominated by warm, humid conditions, such as a south-facing, well-drained flat or gently sloping region.

In the case of the Pre-Triassic weathering episode, the persistence of K-minerals and the incomplete leaching of trace elements, indicates a less intense leaching environment, such as a warm, semi-arid environment with seasonal rainfall. Such an environment has been suggested for Permian through Triassic times by Parrish (1993), who refers to this time in the central regions of Pangea as possibly similar to a

megamonsoon. However, preservation rather than erosion of a thick saprolite under such conditions would not be expected unless the site of formation of the saprolite was somewhat protected from erosion. Alternatively, Ollier (1988) suggests that deep weathering does not necessarily require warmer temperatures (surface temperatures do not impact below depths of between 5-10 metres), and contends that prolonged exposure to groundwater can result in the development of a deep weathering profile. In such cases, the zone of saturation is dominated by reducing somewhat alkaline conditions, and the unsaturated zone is dominated by oxidizing, acidic conditions (Ollier, 1988). In the case of the Pre-Triassic horizon, the persistence of biotite and the ubiquitous and dominant occurrence of montmorillonite throughout most of the sequence is consistent with less intense leaching, as might be expected under high watertable conditions. However, in order for the groundwater to access the granitoid in the first place, presumably weathering at surface had progressed to a significant degree, and fracture and pore systems were well-developed so groundwater flow through the system was possible. In other words, a combination of weathering, perhaps under semi-arid, seasonal monsoon conditions, coupled with subsequent fluctuating groundwater infiltration and saturation, produced the rather unique saprolite developed during Pre-Triassic times. The preservation of a horizon since Pre-Triassic times in which montmorillonite dominates, is unusual and is likely a characteristic signature of the environment under which it formed (Singer, 1980).

Weathering during the Pre-Triassic was more intense than is found developing at surface today, or indeed at any time since the ice retreated *circa* 10, 000 years ago, as evidenced by well-preserved glacial striations commonly occurring on surface outcrops of the SMB. More intense weathering during Pre-Pleistocene times is suggestive of a warmer and perhaps wetter climate than the present. Elsewhere, an arenaceous saprolite development in Europe has been assigned an Eocene age (Migon and Lidmar-Bergstrom, 2002), a time when the climate was warmer and more humid than today. However, in comparison to the weathering intensity in a similar 3-4 metres from the weathering front in the older 2 horizons, weathering during Pre-Pleistocene times did not involve extensive leaching of elements, indicating warm temperate, rather than tropical conditions.

7.6 Weathering versus hydrothermal alteration

(6) Is it possible to distinguish between hydrothermal alteration and weathering?

7.6.1 Conclusion

The decrease in intensity of "alteration" downwards, distinguishes these as weathering episodes rather than hydrothermal events.

7.6.2 Explanation

The secondary mineralogy developed could be consistent with either weathering or a hydrothermal event, however the gradational nature of the change from fresh to increasingly "altered" rock in all cases is unidirectional upwards. This is consistent with weathering from the top down, with the more intense alteration being closest to the earth's surface. In cases where weathering progresses along fractures and pre-existing shear zones as a result of water and air infiltration along a weakened horizon extending downwards from the surface, such a distinction is perhaps more tenuous, in the absence of weathering features such as corestones. Oxygen isotopic studies should serve to distinguish meteoric from hydrothermal fluid conditions in such cases.

7.7 Possible environmental, economic, and engineering impacts

(7) What environmental, economic, and engineering impacts do these weathered horizons pose?

7.7.1 Conclusion

Saprolites are structural material used in roads. As highly permeable media, saprolites

are groundwater reservoirs in the SMB. Because of their chemically compromised state, they likely contribute to metal migration into the groundwater and soil systems.

7.7.2 Explanation

Amoozegar et al. (1993) contend that saprolites are important with regard to groundwater recharge and pollution attenuation in the unsaturated zone, as well as being significant factors in terms of waste disposal. Recognizing the existence of these horizons is not only interesting in terms of unraveling geological history, but also in terms of the implications for a number of environmental and engineering factors. Saprolites provide a highly porous and chemically compromised medium, and as such, awareness of their extent and their textural, mineralogical and geochemical nature are significant factors in: (1) identification of possible gravel resources; (2) hydrologic conditions generally considered atypical in granitoid terrains, which directly impacts on the siting of landfills, wells, septic fields, and underground storage facilities, as well as pollution plume migration and groundwater-surface water interaction; (3) their potential in contamination attenuation, particularly if they are smectite-rich and cation exchange capacity is high; (4) the weakened horizons may pose hazards to construction or excavation; and (5) particularly if incompletely weathered or under changing Eh-pH conditions, their potential as elemental sieves, a factor of even greater concern when such weathered horizons coincide with mineralized zones associated with uranium or other environmentally sensitive elements. Further work on the geochemical signatures of the aqueous environment surrounding these saprolite outcrops is required, in order to better establish actual parameters involved.

7.8 Uranium and radon cycling in the SMB

(8) What, if any, specific implications are there for the cycling of U in the environment of southwestern Nova Scotia?

7.8.1 Conclusion

There is strong evidence of uranium migration under weathering conditions in the SMB. Uranium associated with the subsequent Horton Group unit is most likely derived from the weathering of uranium-bearing granitoid of the SMB. Exposure of these paleosaprolites at surface can, in the presence of acidic precipitation, result in the liberation of uranium from loosely-held sites into the groundwater.

7.8.2 Explanation

Chatterjee and Strong (1985) concluded that the uranium mineralization at Millet Brook formed as a result of migration in waters with meteoric as well as hydrothermal isotopic signatures. The migration of uranium under meteoric conditions is related to weathering of uranium-bearing minerals. Sedimentary rocks of the Horton have elevated levels of uranium (Ryan and O'Beirne-Ryan, 2006), again related to weathering of uraniferous mineral in the underlying granitoids (Chapter 6). Therefore, we can conclude that uranium has been mobilized from the granitoids during weathering, in the geologic past. Uranium loosely-bound to secondary minerals or easily weathered primary minerals, may be mobilized under oxidizing conditions, particularly if these conditions are also acidic. This uranium will migrate through circulating waters until it intersects a reducing barrier, where it will revert to insoluble U^{4+}, and precipitate out of the system. Paleosaprolites in which uranium is finely distributed in weatherable minerals, or loosely-held on oxides, may be re-exposed at surface today as a result of quarrying, construction, or other development. Under surface conditions where acidic precipitation is common today, such uranium can be mobilized. Indeed, Kronfeld et al. (2004) concluded that elevated levels of uranium in groundwaters today, are attributable to the present-day weathering of uranium-mineralized zones.

7.9 Contributions of this study to Nova Scotia geologic history

(9) What contribution does this study make to our understanding of the geology and geologic history of Nova Scotia?

7.9.1 Conclusion

In addition to confirming exhumation and weathering episodes at three different times in the geologic past, the identification of weathering episodes accounts for the nature of stratigraphic idiosyncracies such as the glass sand unit of the Lower Carboniferous, and the gravelly granitic Pleistocene till with rounded corestones.

7.9.2 Explanation

Nova Scotia has a complex geologic history, and documenting the existence and nature of these saprolites as records of incompletely-eroded weathering episodes, contributes to developing a more complete picture of the geologic history of Nova Scotia. The saprolites record exhumation and weathering episodes at three different times in the geologic history of Nova Scotia. As these saprolites are not everywhere throughout the SMB, their eroded remnants source the sediments of subsequent horizons. Recognition of the differing mineralogical and geochemical nature of granite and granite saprolite, and that these episodes have occurred at three different times in the past, contributes to our understanding of the overlying sedimentary sequences, and can offer explanations for such anomalous units as the glass sand unit of the Lower Carboniferous, or the gravelly, granitic Pleistocene till, with reworked corestones of granitic material.

7.10 Implications of this study for interpretation of weathering horizons in general

(10) What are the broader implications of this study?

7.10.1 Conclusion

The behaviour of a given element is a function of conditions during weathering as well as composition of the parent, but most importantly, where the element is sited in relation to the mineralogy of the rock.

7.10.2 Explanation

Geochemically similar granitoid of the SMB has been variably weathered at three different times in the geologic past. In all sites where saprolite is present, the uppermost part of the sequence has been eroded and so only the more "primitive" portion of the weathered horizon is preserved. Different environmental conditions have resulted in different mineralogical and geochemical signatures at different times in the past. Consistent features of all three horizons most likely to be "diagnostic" of some kind of weathering episode include: (1) structural weakening of the rock; (2) increased oxidation and hydration with degree of weathering; (3) mineralogical and geochemical changes that intensify vertically upwards in the sequence; and (4) removal of CaO and Na_2O, and the resulting increase in the chemical index of weathering (CIW). Other changes reflect different conditions of weathering, and care should be taken when interpreting such information, as it may not be universally applicable.

Given that mineralogical and geochemical signatures of each of the horizons differ as a result of differences in environmental conditions during weathering, when incompletely weathered saprolites are exposed at surface, changing conditions, particularly in relation to Eh, pH and hydration, can result in significant liberation of elements, depending on their mobility under such changed conditions, and their siting

mobilized under changed conditions if it is suitably positioned within a mineral structure, adsorbed onto a clay or oxide, or in proximity to newly-developing cracks and fractures within the rock. In the case of the SMB saprolites, further studies are needed to determine the potential of specific metal mobility under present-day acid precipitation conditions, discussed further in 7.12 below. Data from this study conclude that differing weathering conditions result in differing behaviour of elements, even from rocks of similar geochemical protolith. Similarly, data from this study indicate that similar weathering conditions do not always result in similar behaviour of elements in different protoliths, and assuming that a given element, such as barium, will behave in a given way as a result of weathering, is not a valid assumption. For example, Ba decreases during weathering of the Pre-Carboniferous horizon, but increases during weathering of the monzogranite in both the Pre-Triassic and the Pre-Pleistocene horizons. This indicates that Ba responds differently to different environmental conditions of weathering. However, in the youngest weathering episode, Ba in leucogranite is decreased whereas Ba in the monzogranite is increased, indicating that siting of the Ba is an important consideration in determining the likelihood of Ba being liberated during a given set of weathering conditions. Therefore, it is reasonable to conclude that the behaviour of Ba depends neither on the weathering conditions nor on the rock type alone, and so understanding the system as a whole is critical in any interpretation of the behaviour of many of the trace elements during weathering.

7.11 Educational implications

(11) What educational needs of geologists, engineers, and planners are implicit from this study?

7.11.1 Explanation

Saprolite eureka, or... a cautionary tale of 2 myopic geologists

Two geologists, a sedimentologist-economic geologist and an environmental geochemist-igneous petrologist (the author) examined a sequence of drill core a number of years ago. To the sedimentologist, much of the core represented granitic rock, and hence beyond their immediate interest; to the igneous petrologist, the rock was decidedly sedimentary, and similarly, not worth regarding with more than a passing interest. This core was set aside and revisited periodically, only for the same difference of opinion to resurface. What both of us missed, was that while neither was completely correct, neither was completely incorrect. Perfect hindsight now allows us to look at this core and see a saprolitic horizon on a granitic rock, which had been relithified during diagenesis.

The generally-held assumption amongst geologists and engineers, and indeed amongst the general public, is that granitic rocks are stable and impermeable when not compromised by tectonic or mineralizing events. Drilling in granitic terrain is difficult, and accessing groundwater unlikely, unless the granite is highly fractured. Furthermore, the acidic nature of granitic rocks suggests they are poor buffers of acidic precipitation, and create acid soils, in which vegetation type and growth is restricted. In the case where granitic rocks have been weathered, and the weathered material has remained *in situ* to form saprolite horizons, such assumptions are ill-founded, and it is important that we begin to recognize that such horizons can and do exist, and that their character is distinctly different to their parent, unweathered granitoid.

Paleoweathered horizons are important markers in the stratigraphic and in the paleoenvironmental record, and their presence and nature contributes to greater understanding of the geologic past. However, it is not uncommon to relegate their presence to that of a nuisance, as we endeavour to collect "pristine" samples for data analysis.

The general public commonly expresses grave concerns in relation to the possibility of contamination of the environment as a result of mining activities, however

the potential for contamination (or containment) by metals released during weathering processes is not considered, as typically the processes involved are relatively slow in human terms. It is reasonable to assume that changing Eh-pH conditions of these weakened and chemically modified rocks will effect element solubility. These newly dissolved elements will enter and move through the hydrologic environment, and can result in higher than acceptable levels of metals in water or soil. For example, decrease in pH and increase in Eh will increase uranium solubility (Langmuir, 1978); uranium mobilized in this way will flow until it reaches a reducing barrier, such as an organic-rich soil, where it will precipitate.

While those who study weathering commonly recognize its significance from a number of different perspectives, perhaps it is most critical that we bring attention to these horizons in more general forums, where their significance to other branches of geology and societal concerns can be addressed. As is the case whenever there is a poor general understanding of the potential issues, we need to avoid the temptation to speak only to the converted, and to more widely publish our findings, so those not normally exposed to terms such as "saprolite" or "paleoweathering", can begin to make connections across apparently disparate fields of study, and push the boundaries of our understandings of the implications, as well as the need for greater understanding of the processes and interactions even further.

7.12 Recommendations for further study

(12) What further work is recommended?

(1) Determination of the effects of weathering on mineralized zones, as these zones commonly have associated toxic metals. Does weathering impact on these mineralized zones in similar ways to that observed in regions that are unmineralized?

(2) Sequential leaching analyses of these horizons would provide information regarding the nature of metal distribution in the material, and help develop a greater

understanding of the potential for elemental migration or retention under changing Eh-pH conditions.

(3) Further work on the impact of changing pH conditions on these horizons, in order to understand the impact of acidic precipitation on these materials; initial solutions tend to be alkaline, as Ca and Na dissolve from these horizons, but what is the longer term impact, and how does naturally increased acidity impact on the rate of dissolution of these and other elements such as uranium?

(4) Recording sites where these horizons occur within the SMB during general mapping projects, would elucidate further their extent and their nature. This is linked to education of the geologic community within the Province, as road construction, logging, quarrying, and development cut through previously-hidden outcrops, result in new sources of geologic information. This may best be undertaken initially by those working in close proximity to such disturbances documenting such structurally weakened rock.

(5) Given that these horizons do record paleoenvironmental conditions, it would be ideal to bracket the ages of these horizons more clearly. With the advent of new technologies in K-Ar dating techniques, it will soon be possible to analyze a specific "spot" on the order of microns (P. Reynolds, pers.comm., 2006); this obviously would be a potentially useful technique to apply to K-bearing minerals such as weathered biotite and illite, in the hope of determining a more refined age for the Pre-Pleistocene horizon.

REFERENCES

Acker, J.G. and Bricker, O.P., 1992. The influence of pH on biotite dissolution and alteration kinetics at low temperature. Geochimica et Cosmochimica Acta, 56: 3073-3092.

Amoozegar, A., Hoover, M.T., Kleiss, H.J., Guertal, W.R. and Surbrugg, J.E., 1993. Evaluation of saprolite for on-site wastewater disposal. Available from National Technical Information Service, Springfield, VA 22161 as PB93-190635. North Carolina Water Resource Research Institute, Raleigh, UNC-WRRI Unpublished Report, March 1993. 183p, 51 fig, 83 tab, 83 ref. USGS Contract No. 14-08-0001-G1633.

Bakker, J.P., 1967. Weathering of granites in different climates, particularly in Europe. Congres et Colloques de l'Universite de Liege, 40: 51-68.

Banfield, J.F. and Eggleton, R.A., 1988. Transmission electron microscope study of biotite weathering. Clays and clay minerals, 36: 47-60.

Barshad, I., 1948. Vermiculite and its relation to biotite as revealed by base exchange reactions, x-ray analyses, differential thermal curves, and water content. American Mineralogist, 33: 655-678.

Bell, W.A. 1929. Horton-Windsor district, Nova Scotia. Geological Survey of Canada Memoir: 155.

Bisdom, E.B.A., Stoops, G., Delvigne, J., Curmi, P. and Altermuller, 1982. Micromorphology of weathering biotite and its secondary products. Pedalogie 32: 225-252.

Blank, H.R. 1978. Fossil laterite in bedrock in Brooklyn, New York; Geology, 6: 21-24.

Bouchard, M. and Jolicoeur, S., 2000. Chemical weathering studies in relation to geomorphological research in southeastern Canada. Geomorphology, 32: 213-238.

Bouchard, M., Jolicoeur, S., and Pierre, G. 1995. Characteristics and significance of two pre-late-Wisconsinan weathering profiles (Adirondacks, USA and Miramichi Highlands, Canada). Geomorphology , 12: 75-89.

Burgess, N.M., d'Entremont, A.A., Drysdale, C., Vaidya, O., and Brun, G.L., 1998. Mercury in yellow perch in Kejimkujik National Park; Mercury in Atlantic Canada: A Progress Report. Mercury Team, Regional Science Coordinating Committee, Minister of Public Works and Government Services Canada. Environmental Canada Atlantic Region and collaborators. September 1998. p.72-76.

Calder J. H. 1998. The Carboniferous evolution of Nova Scotia. *In* Lyell: the past is the key to the present. *Edited by* D.J. Blundell and A.C. Scott. Geological Society of London Special Publication, 143: 261-302.

Calder J.H., Boehner, R.C., Brown, D.E., Gibling, M.R., Mukhopadhyay, P.K., Ryan, R.J., and Skilliter, D.M. 1998. Classic Carboniferous Sections of the Minas and Cumberland Basins in Nova Scotia, with special reference to Organic Deposits. Nova Scotia Department of Natural Resources Open File Report ME1998-5.

Calvo, R.M., Garcia-Rodeja, E., and Macias, F. 1983. Mineralogical variability in weathering microsystems of a granitic outcrop of Galicia (Spain). Catena, 10: 225-236. Chalmers, R. 1898. Preglacial decay of rocks in Eastern Canada. American Journal of Science, 5: 273-282.

Carruzzo, S., Kontak, D.J., Reynolds, P.H., Clarke, D.B., Dunning, G.R., Selby, D., and Creaser, R.A., 2003. U/Pb, Re/Os, and Ar/Ar dating of the South Mountain Batholith and its mineral deposits. Geochimica et Cosmochimica Act, 67: 1.

Chalmers, R., 1898. The pre-glacial decay of rocks in eastern Canada. American Journal of Science, 4: 273-282.

Chatterjee, A.K. 1983. Mineral deposit studies: contrasting granophile (Sn, W, Mo, Cu, U) deposits of Nova Scotia. Nova Scotia Department of Mines and Energy, Mines and Minerals Branch, Report 83-1: 49-51.

Chatterjee A.K. and Muecke, G.K., 1982. Geochemistry and the distribution of uranium and thorium in the granitoid rocks of the South Mountain Batholith, Nova Scotia: some genetic and exploration implications. Geological Survey of Canada, Paper 81-23: 11-17.

Chatterjee, A.K. and Strong, D.F. 1985. Review of some chemical and mineralogical characteristics of granitoid rocks josting Sn, W, U, and Mo deposits in Newfoundland and Nova Scotia. In: High heat production granites, hydrothermal circulation and ore genesis. Inst. Mining and Metallurgy, Strong, D.F.and Taylor, R., eds. 593p: 489-516.

Clarke, D.B. MacDonald, M.A. Reynolds, R.H. and Longstaffe, F.J. 1993. Leucogranites from the Eastern Part of the South Mountain Batholith, Nova Scotia. Journal of Petrology, 34: 653-679.

Coleman, N.T., Leroux, F.H, and Cady, J.G., 1963. Biotite-hydrobiotite-vermiculite in soils. Nature, 198: 409-410.

Condie, K.C., Dengate, J. And Cullers, R.L., 1995. Behaviour of rare earth elements in a paleoweathering profile on granodiorite in the Front Range, Colorado, USA. Geochim et Cosmochim Acta, 59: 279-294.

Cramer, J.J. and Nesbitt, H.W., 1983. Mass-balance relations and trace-element mobility during continental weathering of various igneous rocks. Sci. Geol., Mem., 73: 63-73.

Cumming, L.M.,1979. The geology of the Kejimkujik National Park. Nova Scotia Department of Mines and Energy, Open File Rep. ME-467. 67p.

Cumming, L.M. 1979. Bedrock geology of Kejimujik National Park. Nova Scotia

Department of Mines and Energy. Open File Report ME-467.

Dall'Aglio, M., 1971. A study of the circulation of uranium in the supergene environment in the Italian Alpine range. Geochim. et Cosmochim. Acta, 35: 47-59.

Davies, E.H., Akande, S.O., and Zentilli,M. 1984. Early Cretaceous deposits in the Gays River lead-zinc mine, Nova Scotia. *In* Current Research Part A, Geological Survey of Canada. Paper 84-1A: 353-358.

de la Calle, C. and Suquet, H., 1988. Vermiculite. Reviews in mineralogy and geochemistry, 19: 455-496.

Delvigne, J. E., 1998. Atlas of micromorphology of mineral alteration and weathering. Canadian Mineralogist Special Publication 3, Mineralogical Assoc. Canada, 509p.

Duddy, I.R., 1980. Redistribution and fractionation of rare-earth and other elements in a weathering profile. Chemical Geology, 30: 363-381.

Duzgoren-Aydin, N.S., Aydin, A., and Malpas, J. 2002. Re-assessment of chemical weathering indices: case study on pyroclastic rocks of Hong Kong. Engineering Geology, 63: 99-119.

Dyck, W., Chatterjee, A.K., Gemmell, D.E. and Murricane, K., 1976. Well water trace element reconnaissance, eastern maritime Canada. Journal of Geochemical Exploration, 6: 139-162.

Emerson, B.K.,1917. Geology of Massachusetts and Rhode Island. *U. S. Geol. Surv. Bull.* 597. 289p.

Eserwaran, H. and Heng, Y.Y., 1976. The weathering of biotite in a profile on gneiss in Malaysia. Geoderma, 16: 9-20.

Farmer, V.C., Russell, J.D., McHardy, W.J., Newman, A.C.D., Ahlrichs, J.L., Rimsaite, J.Y.H., 1971. Evidence for loss of protons and octahedral iron from oxidised biotites and vermiculites. Mineralogical Magazine 38: 121-137.

Fedo, C.M., Nesbitt, H.W. and Young, G.M., 1995. Unraveling the effects of potassium metasomatism in sedimentary rocks and Paleosols, with implications for paleoweathering conditions and provenance. Geology, 23: 921-924.

Feininger, T. ,1971. Chemical weathering and glacial erosion of crystalline rocks and the origin of till. *U. S. Geol. Surv. Prof. Pap.* 750-C: C65-C81.

Ferrell, R.E. Jr. and Carpenter, P.K., 1990. Application of electron microprobe and image analysis in the study of clays. In: Electron-optical methods in clay science, CMS Workshop Lectures, vol. 2, 108-132. Publ: The Clay Minerals Society, Evergreen, CO, USA.

Finck, P.W., Graves, R.M., and Boner, F.J. 1993: Glacial and till clast geology of New

Germany (NTS 21A/10), Nova Scotia. Nova Scotia Department of Natural Resources, Mines and Energy Branches Map 93-02, scale 1:50 000.

Finck, P.W., Graves, R.M., Boner, F.J., and Bent, H.B. 1994. Glacial and till clast geology of Gaspereau Lake, Nova Scotia. Nova Scotia Department of Natural Resources, Mines and Energy Branches Map 94-14, scale 1:50 000.

Finck, P.W. and Stea R.R ,1995. The compositional development of tills overlying the South Mountain Batholith, Nova Scotia. *Nova Scotia Department of Natural Resources, Mines and Energy Branches, Pap.* 95-1. 52p.

Ford, K.L., Nova Scotia Summary, Airborne Gamma Ray Spectrometric - Magnetic - VLF-EM Surveys. In: Applications of Gamma ray spectrometric/magnetic/VLF-EM surveys. Geological Survey of Canada, Workshop Manual. Eds. Shives, R.B.K., Ford, K.L., and Charbonneau, B.W.. ps. 26-31.

Flint, R.F., 1957. *Glacial and Pleistocene Geology*. New York John Wiley and Sons, 553p.

Fritz, S.J., 1988. A comparative study of gabbro and granite weathering. Chem. Geol. 68: 275-290.

Gardner, L.R., Kheoruenromne, I., and Chen, H.S., 1978. Isovolumetric geochemical investigation of a buried granite saprolite near Columbia, U.S.A. Geochimica et Cosmochimica Acta, 42: 417-424.

Garrels, R.M. and Christ, C.L., 1965. Solutions, minerals, and equilibria. Harper and Row, New York, 450p.

Gauthier, C. 1980. Decomposed granite, Big Balk Mountain area, New Brunswick. *In* Current Research, Part B. Geological Survey of Canada, Paper 80-1B: 277-282.

Gerrard, A.J., 1994. Weathering of granitic rocks: Environment and clay mineral formation. In: Rock Weathering and Landform Evolution, Robinson, D.A. and Williams, R.B.G., eds. Wiley publ. 519p: 3-20.

Giles, P.S. 1981. The Windsor Group of the Mahone Bay Area, Nova Scotia. Nova Scotia Department of Mines and Energy, Paper 81-3.

Gilkes, R.J., Young, R.C., and Quirk, J.P., 1972. The oxidation of octachedral iron in biotite. Clays and clay minerals, 20: 303-315.

Gilkes, R.J., 1973. The alteration products of potassium depleted oxybiotite. Clays and clay minerals 21: 303-313.

Gold, C.M., Cavell, P.A., and Smith, D.G.W., 1983. Clay minerals in mixtures: sample preparation, analysis, and statistical interpretation. Clays and clay minerals, 31: 191-199.

Goldich, S.S., 1938. A study in rock weathering. Journal of Geology, 46: 17-58.

Gouveia, M.A., Prudencio, M.I., Figueiredo, M.O., Pereira, L.C.J., Waerenborgh, J.C., Morgado, I., Pena, T., and opes, A., 1993. Behavior of REE and other trace and major elements duing weathering of granitic rocks, Evora, Portugal. Chemical Geology, 107: 293-296.

Goyer, R.A., 1991. Toxic effects of Metals. In: Casarett and Doull's Toxicology, 4th ed., Amdur, M.O. and Klaassen, C.D., eds. Pergamon Press, N.Y., p.623-680.

Grant, D.R. 1989. Quaternary geology of the Atlantic Appalachian region of Canada, Ch. 5. *In* Quaternary Geology of Canada and Greenland. Geology of Canada, No. 1. *Edited by* R.J. Fulton. Geological Survey of Canada, p.391-440.

Grant, D.R. 1997. Report on the glacial features and geological history of Kejimkujik National Park, Nova Scotia. Nova Scotia Department of Natural Resources Open File Report ME 1997-9: 117p.

Grantham, D., 1986. The Occurrence and Significance of Uranium, Radium and Radon in Water Supplies in Nova Scotia: A report of the investigation carried out by the provincial uranium task force. Nova Scotia Department of Natural Resources Open File Report 86-070. Nova Scotia Department of Natural Resources, 256p.

Grist, A.M. and Zentilli, M. 1999. Apatite fission track constraints on the late Cretaceous heating of the Atlantic Margin: possible effects of anomalously high paleo-mean surface temperatures. Atlantic Geology 35: 93.

Gross, G.A. 1968. Geology of iron deposits in Canada: Volume III, Iron Ranges of the Labrador Geosyncline. Geological Survey of Canada Economic Geology Report 22.

Guthrie, V.A., 1989. Fission-track analysis of uranium distribution in granitic rocks. Chemical Geology 77: 87-103.

Guthrie, V.A. and Kleeman, J.D., 1986. Changing uranium distributions during weathering of granite. Chemical Geology, 54: 113-126.

Ham, L. and MacDonald, M., 1991. Preliminary Geological Map of Wentworth Lake, 21A/04. Open file map ME 1991-020. Nova Scotia Department of Natural Resources.

Harbin, R.W., 2003. The industrial Minerals Handybook - A Guide to Markets, Specifications, and Rpices, Fourth Edition. Industrial Minerals Information Services, UK. 412p.

Harnois, L., 1988. The CIW index: a new chemical index of weathering. Sedimentary Geology, 55: 319-322.

Horbe, A.M.C. and da Costa, M.L.,1999. Geochemical evolution of a lateritic Sn-Zr-Th-Nb-Y-REE-bearing ore body derived from apogranite: the case of Pitinga, Amazonas–Brazil. Journal of Geochemical Exploration, 66: 339-351.

Islam, M.R., Peuraniemi, V., Aario, R., and Rojstaczer, S., 2002. Geochemistry and mineralogy of saprolite in Finnish Lapland. Applied Geochemistry, 17: 885-902.

Ismail, F.T. 1970. Biotite weathering and clay formation in arid and humid regions, California. Soil Science, 109: 257-261.

Ismail, F.T, 1969. Role of ferrous iron oxidation in the alteration of biotite and its effect on the type of clay minerals formed in soils of arid and humid regions. American Mineralogist, 54: 1460-1466.

Jackson, S.A., 1992. Estimating radon potential from aerial radiometric survey. Health Physics, 62: 450-452.

Jenne, E.A., 1968. Controls on Mn, Fe, Co, Ni, Cu and Zn concentrations in soils and water: the significant role of hydrous Mn and Fe oxides. Advances in Chem. Ser. 73: 337-387.

Jenne, E.A., 1977. Trace element sorption by sediments and soils-sites and processes. In: Symposium on molybdenum in the environment; Chappel, W. And Peterson, K., eds. M.Dekker Inc., New York, p.425-552.

Jeong, G.Y., 2002. Biotite oxidation in the weathering profiles of granitic rocks; chemistry, mineralogy, and implications for elemental behavior. Geochimica et Cosmochimica Acta, 66: 366.

Jeong, G.Y., and Kim, H.B., 2003. Mineralogy, chemistry, and formation of oxidized biotite in the weathering profile of granitic rocks. American Mineralogist, 88: 352-364.

Jiao, J.J. 2000. A confined groundwater zone in weathered igneous rocks and its impact on slope stability. International Symposion on Hydrogeology and the Environment, Wuhan, China, October 2000, p.1-8.

Jolicoeur, S., Ildefonse, P., and Bouchard, M., 2000. Kaolinite and gibbsite weathering of biotite within saprolites and soils of Central Virginia. Soil Sci. Soc. Am. J., 64: 1118-1129.

Koons, Robert Dey, 1978. Behavior of trace and major elements and minerals during early stages of weathering of diabase and granite in Central Wisconsin. PhD thesis, University of Wisconsin-Madison.

Kovalev V. P. and Malyasova Z. V., 1971. The content of mobile uranium in extrusive and intrusive rocks of the eastern margins of the South Minusinsk Basin. Geokkimiya 7: 855-865.

Kretzschmar, R., Robarge, W.P., Amoozegar, A., and Vepraskas, M.J., 1997. Biotite alteration to halloysite and kaolinite in soil-saprolite profiles developed from mica schist and granite gneiss. Geoderma, 75: 155-170.

Kronfeld, J., Godfrey-Smith, D.I., Johannessen, D., and Zentilli, M., 2004.

Uranium series isotopes in the Avon Valley, Nova Scotia. Journal of Environmental Radioactivity, 73: 335-352.

Langmuir, D., 1978. Uranium solution-mineral equilibria at low temperatures with applications to sedimentary ore deposits. Geochim. Et Cosmochim. Acta, 42: 547-569.

Levinson, A.A., 1980. Introduction to exploration geochemistry. 2nd ed., The 1080 supplement, Applied Publishing, Illinois.

Leybourne, M.I., Boyle, D.R., Goodfellow, W.D., and Wright, D.F. 2000. Distribution and speciation of Hg and Au in surface waters and stream sediments; anthropogenic and geogenic sources. Geological Society of America Abstracts with Programs, 32- 3: 33.

Lidmar-Bergstrom, K., Olsson, S., and Olvmo, M. 1997. Paleosurfaces and associated saprolites in southern Sweden. *In* Paleosurfaces: Recognition, Reconstruction and Paleoenvironmental Interpretation. Geological Society Special Publication No. 120. *Edited by* M. Widdowson. Published by Geological Society, London, p. 95-124.

Lidmar-Bergstrom, K., Olsson, S., and Roaldset, E. 1999. Relief features and paleoweathering remnants in formerly glaciated Scandinavian basement areas. *In* Paleoweathering, Paleosurfaces and Related Continental Deposits. International Association of Sedimentologists, Special Publication Number 27. *Edited by* M. Thiry and R. Simon-Coincon. Blackwell Science, New York. p. 275-302.

Ma, Y., (Huo, R.,) and Liu, C., 2002. Speciation and fractionation of rare earth elements in a lateritic profile from southern China; identification of the carriers of Ce anomalies. Geochim. Et Cosmochim. Acta, 66, 15A: 471.

MacDonald, M. 2001. Geology of the South Mountain Batholith, Southwestern Nova Scotia. Nova Scotia Department of Natural Resources Open File Report ME 2001-2.

MacDonald, M.A. and Horne, R.J., 1987. Bedrock Geological Map of Halifax and Sambro (11D/12 and 11D/05), 1:50:5000. Nova Scotia Department of Natural Resources, Map 1987-6

MacDonald, M.A., Horne, R.J. and Ham, L.J., 1992. An overview of recent bedrock mappand and follow up studies of the SMB, southwesthern Nova Scotia. Atlantic Geology, 28: 7-28.

MacFarlane, 1983. Uranium Task Force Report: The hydrogeology and distribution of naturally-occurring uranium in well water in Nova Scotia.

Mahaney, W.C. ,1995. Glacial crushing, weathering and diagenetic histories of quartz grains inferred by scanning electron microscopy. In: *Modern Glacial Environments, Processes, Dynamics and Sediments.* (Editor J. Menzies),

Butterworth-Heinemann Ltd., Oxford, p.487-506.

McKeague, J.A., Grant, D.R., Kodama, H., Beke, G.J., and Wang, C., 1983. Properties and genesis of a soil and underlying gibbsite-bearing saprolite, Cape Breton Island, Nova Scotia, Canada. Canadian Journal of Earth Sciences, 20: 37-48.

McKinney, J. and Rogers, R., 1992. Metal bioavailability, EPA workshop, Identified Research Needs. Environmental Science and Technology.

McNeil, R.H., 1954. Deeply weathered granite in Nova Scotia. Nova Scotia Research Foundation Report, 1954-1: 42p.

Melfi, A.J., Cerri, C.C., Kronberg, B.I., Fyfe, W.S., McKinnon, B., 1983. Granitic weathering: a Brazilian study. Journal of Soil Science, 34: 841-851.

Meunier, A. And Velde, B., 1978. Biotite weathering in granites of western France. In: Mortland, M.M. and Farmer, V.C., eds., International Clay Conference, 1978; Developments in Sedimentology 27. p. 405-414. Elsevier Scientific Publ. Co., Amsterdam.

Michel, J., 1984. Redistribution of uranium and thorium series isotopes during isovolumetric weathering of granite. Geochim. Et Cosmochim. Acta, 48: 1249-1255.

Middleburg J.J., van der Weijden, C.H. and Woittiez, J.R.W., 1988. Chemical processes affecting the mobility of major, minor and trace elements during weathering of granitic rocks. Chemical Geology, 68: 253-273.

Migon, P. And Lidmar-Bergstrom, K., 2001. Weathering mantles and their significance for geomorphological evolution of central and northern Europe since the Mesozoic. Earth Science Reviews, 56: 285-324.

Migon, P., and Lidmar-Bergstrom, K., 2002. Deep weathering through time in central and northwestern Europe: problems of dating and interpretation of geological record. Catena, 49: 25-40.

Migon, P and Thomas, M.F., 2002. Grus weathering mantles - problems of interpretation. Catena, 49: 5-24.

Mongelli, G., 1993. REE and other trace elements in a granitic weathering profile form Serre, southern Italy. Chemical Geology, 103: 17-25.

Mongelli, G., Culler, R.L., Dinelli, E. and Rottura, A., 1998. Elemental mobility during the weathering of exposed lower crust: the kinzigitic paragneisses from the Serre, Calabria, southern Italy. Terra Nova, 10: 190-195.

Moon, H., Song, Y., and Lee, S.Y., 1994. Supergene vermiculitization of phlogopite and biotite in ultramafic and mafic rocks, Central Korea. Clays and clay

minerals, 42: 259-268.

Moore, R.G., Ferguson, S.A., Boehner, R.C., and Kennedy, C.M. 2000. Preliminary map of the Wolfville/Windsor Area, Kings and Hants Counties, Nova Scotia [21H/01 and Parts of 21A/16C and D]. Scale 1:50,000.

Mortimer, N. and Little, T., 1998. Altered biotites in the Marlborough Schist, New Zealand? New Zealand Journal of Geology and Geophysics, 41: 105-109.

Nahon, D., 1991. Introduction to the petrology of soils and chemical weathering. Wiley, New York Publ. 312p.

Nedachi, Y., Bennett, G. and Ohmoto, H., 2005. Geochemistry and mineralogy of the 2.45 Ga Pronto paleosols, Ontario, Canada. Chemical Geology, 214: 21-44.

Nesbitt, H.W., 1979. Mobility and fractionation of rare earth elements during weathering of a granodiorite. Nature, 27: 206-210.

Nesbitt, H.W., Markovics, G. and Price, R.C., 1980. Chemical processes affecting alkalis and alkaline earths during continental weathering. Geochimica et Cosmochimica Acta, 44: 1659-1666.

Nesbitt, H.W., and Markovics, G. 1997. Weathering of granodioritic crust, long-term storage of elements in weathering profiles, and petrogenesis of siliciclastic sediments. Geochimica et Cosmochimica Acta, 61: 1653-1670.

Nesbitt, H.W. and Young, G.M., 1982. Early Proterozoic climates and plate motions inferred from major element chemistry of lutites. Nature, 299: 715-717.

Nesbitt, H.W. and Young, G.M., 1984. Prediction of some weathering trends of plutonic and volcanic rocks based on thermodynamic and kinetic considerations. Geochim. et Cosmochim. Acta, 48: 1523-1534.

Nesbitt, H.W., and Young, G.M. 1989. Formation and diagenesis of weathering profiles. Journal of Geology, 97: 129-147.

Nesbitt, H.W., and Young, G.M., 1996. Petrogenesis of sediments in the absence of chemical weathering: effects of abrasion and sorting on bulk composition and mineralogy. Sedimentology, 43: 351-358.

Nesbitt, H.W., Young, G.M., McLennan, S.M., Keays, R.R., 1996. Effects of chemical weathering and sorting on the petrogenesis of siliciclastic sediments, with implications for provenance studies. Journal of Geology, 104: 525-542.

Nova Scotia Department of the Environment, 1981. Preliminary Report on the occurrence of uranium in groundwater in the Harrietsfield-Williamswood area. Water Resources Planning Section, Water Planning and Management Division, Nova Scotia Department of Environment. 70p.

O'Beirne-Ryan, A.M., Ryan, R.J., and Zentilli, M., 2001. When has a rounded cobble not traveled far? Recycling of corestones from weathered granitoids: examples from the South Mountain Batholith in Nova Scotia, Canada. Atlantic Geology, 37: 113.

O'Beirne-Ryan, A.M. and Zentilli, M., 1999. Distribution of uranium in selected rock types in central mainland Nova Scotia: implications for the occurrence of high levels of radon in domestic well waters and indoor air. Atlantic Geology, 35: 99-100.

O'Beirne-Ryan, A.M., and Zentilli, M., 2002. Paleoweathered granitoid surfaces of southern Nova Scotia: Environmental implications of saprolite.

O'Beirne-Ryan, A.M. and Zentilli, M., 2003. Paleoweathered surfaces on granitoids of southern Nova Scotia: Paleoenvironmental implications of saprolites. Canadian Journal of Earth Sciences, 40: 805-817.

O'Beirne-Ryan, A.M. and Zentilli, M. 2003(a). Geochemistry of weathered horizons within the South Mountain Batholith, Nova Scotia, Canada: A window into the early stages of metal migration into the environment. *Geol. Soc. Am., Northeastern Section* 38th Annual Meeting, Program and Abstracts, 35:3

O'Beirne-Ryan, A.M. and Zentilli, M., 2006. Weathered granites as potential chemical sieves: impacts of ancient pre-glaciation on the granitoids of south-western Nova Scotia and the environment. AGS 32nd Colloquium and Annual Meeting, Abstract with programs, Feb 2006. p.54-55.

O'Driscoll, N.J., Rencz, A.N. and Lean, R.S. eds., 2005. Mercury cycling in a Wetland-Dominated Ecosystem: A Multidisciplinary Study. Published by Society of Environmental Toxicology and Chemistry, SETAC Press, 392p.

O'Reilly, G.A. 1982. Uranium in Nova Scotia: a background summary for the unraium inquiry. Nova Scotia Department of Natural Resources Report 82-7.

Ollier, C.D. 1965. Some features of granite weathering in Australia. Zeitschrift fur Geomorphology 9: 285-304.

Ollier, C.D., 1988. Deep weathering, groundwater and climate. Geografiska Annaler. Series A: Physical Geography, 70: 285-290.

Page, K.D., 1999. Uranium, radium, and radon in streams, domestic well waters, and soils: a GIS analysis of geological, geochemical, and geophysical relationships. Unpublished B.Sc. Honours thesis, Dalhousie University. 298p.

Parker, A., 1970. An index of weathering for silicate rocks. Geological Magazine, 107: 501-504.

Parrish, J.T., 1993. Climate of the Supercontinent Pangea. Jounral of Geology, 101: 215-233.

Pereira, L.C.J., Waerenborgh, J.C., Figueiredo, M.O., Prudencio, M.I., Gouveia, M.A., Silva, T.P., Morgado, I. and Lopes, A., 1993. A comparative study of biotite weathering from two different granitic rocks. Chemical geology 107: 301-306.

Perel'man, Al., 1986. Geochemical barriers: theory and practical applications. Applied geochemistry, 1: 669-680.

Pettijohn, F. J.,1975. *Sedimentary Rocks.* Third Edition, Harper and Row Publishers, New York. 628p.

Plumlee, G.S., 1999. The environmental geology of mineral deposits. In: Review on Economic Geology, Review Volume 6: The Environmental Geochemistry of Mineral Deposits; Part A: Processes, Techniques, and Health Issues; Part B: Case Studies and Research Topics. Eds. Part A: Plumlee, G.S., Logson, M.J.; Part B: Filipek, L.F., and Plumles, G.S. 583p.

Powell, R.E., Matti, J.C. and Cossette, P.M., 2000. Geological Map and digital database of Cougar Buttes, San Bernardino County, California. *USGS OF* 00-175: 35p.

Power, E.T., and Smith, B.J., 1994. A Comparative Study of Deep Weathering and Weathering Products: Case Studies from Ireland, Corsica, and Southeast Brazil. *In* Rock Weathering and Landform Evolution. *Edited by* D.A. Robinson and R.G.B. Williams. Wiley Publications, New York, p.21-40.

Price, J.R., and Velbel, M.A., 2000. Weathering of the Eaton Sandstone (Pennsylvanian), Grand Ledge, Michigan: Geochemical mass-balance and implications for reservoir properties beneath unconformities. Journal of Sedimentary Research, 70: 1118-1128.

Price, J.R., and Velbel, M.A., 2003. Chemical weathering indices applied to weathering profiles developed on heterogeneous felsic metamorphic parent rocks. Chemical Geology, 202: 397-416.

Prime, G. 2001. Overview of bedrock aggregate potential in the Halifax-Dartmouth metropolitan area, Nova Scotia. Nova Scotia Department of Natural Resources, Minerals and Energy Branch, Economic Geology Series ME 2001-1.

Quarch, H., Rikeit, K. , Ryan, R.J. and Adams, G.C. 1981. Report on drilling, Hants and Kings Counties, Nova Scotia; Saarberg Interplan Canada Limited. Nova Scotia Department of Mines and Energy Assessment Report 81-019.

Rainbird, R.H., Nesbitt, H.W. and Donaldson, J.A., 1990. Formation and diagenesis of a sub-Huronian saprolith; Comparison to a modern weathering profile. *J. Geol.,* 89: 801-823.

Ravenhurst, C. and Zentilli, M., 1987. A model for the evolution of hot (>200°C) overpressured brines under an evaporite seal: The Fundy/Magdalen Carboniferous Basin of Atlantic Canada and its Pb-Zn-Ba deposits. In: T Tankard

and C Beaumont (Editors) Sedimentary Basins and Basin Forming Mechanisms, Canadian Society of Petroleum Geologists, Memoir 12, 335-350.

Ravenhurst, C.E., Reynolds, P.H. and Zentilli, M., 1986. Strontium isotopic studies of rock and mineral samples in the Shubenacadie Basin, Nova Scotia. In: Current research, Part B, Geological Survey of Canada, Paper 86-1B: 547-555.

Reider, M., Cavazzini, G., D'Yakonov, Y., Frank-Kamenetskii, V.A., Gottardi, G., Guggenheim, S., Koval, P.V., Muller, G., Beiva, A.M.R., Radoslovich, E.W., Robert, J-L., Sassi, F.P., Takeda, H., Weiss, Z. and Wones, D.R., 1998. Nomenclature of the micas. Canadian Mineralogist 36: 905-912.

Rikeit, K., 1979. Information on the natural occurrence of uranium, radium and radon in well waters, stream waters, stream sediments and soil Caboniferous environments south and north-west of Wondsor, Hants County, Nova Scotia. Nove Scotia Dept. Mines and Energy, Report Ar-79-008: 41p., 5 maps.

Rose, A.W., Hawkes, H.E., Webb, J.S., 1979. Geochemistry in mineral exploration. Academic Press, 639p.

Rose, A.W. and Keith, 1976. Reconnaissance geochemical techniques for detecting uranium deposits in sandstones of northeastern Pennsylvania. Journal of Geochemical Exploration, 6: 119-137.

Ruhlmann, F., 1980. Quelques exemples de relation uranium-titane. Bull. Mineral., 103: 240-244.

Rutherford, G.K., and Thacker, D.J., 1988. Characteristics of two mafic saprolites and their associated soil profiles in Canada. Canadian Journal of Soil Science, 68: 223-231.

Ruxton, B.P., 1968. Measures of the degree of chemical weathering of rocks. Journal of Geology, 76: 518-527.

Ryan, R.J. , 1998. The Falls Brook Quarry near Three Mile Plains, Windsor, Nova Scotia. In: *Classic Carboniferous Sections of the Minas and Cumberland Basins in Nova Scotia,* Calder, J.H., Boehner, R.C., Brown, D.E., Gibling, M., Mukhopadhyay, P.K., Ryan, R.J. and Skilliter, D.M.. Nova Scotia Open File Report ME 1998-5: 86p.

Ryan, R.J. and O'Beirne-Ryan, A.M., 2006. Radioactive elements in the Horton Group: possible connection to paleosaprolites developed under the Carboniferous unconformity in the Martimes Basin of Eastern Canada. 32nd Colloquium and Annual Meeting, Abstracts with Programs, p.64.

Ryan, R.J., O'Beirne-Ryan, A.M. and Zentilli, M., 2005. Rounded cobbles that have not travelled far; incorporation of corestones from saprolites in the South Mountain area of southern Nova Scotia, Canada. Sedimentology 52: 1109-1121.

Ryan, R.J. and Skilliter, D.M., 1998. *Nova Scotia Department of Natural Resources Open File Rep. ME* 1998-5: 16-24.

Ryan, R.J. and Zentilli, M., 1993. Allocyclic and thermochronological constraints on the evolution of the Maritimes Basin, Atlantic Geology, 29: 187-197.

Schenk P., 1995. Meguma Zone. *In* Geology of the Appalachian-Caledonian Orogen in Canada and Greenland. *Edited by* H. Williams. Geological Survey of Canada, Geology of Canada, 6: 261-277.

Schroeder, P.A., Kim, J.G. and Melear, N.D., 1997. Mineralogical and textural criteria for remnant recognizing Cenozoic deposits on the Piedmont; evidence from Sparta and Green County, Georgia, USA. *Sed. Geol.,* 108: 195-206.

Selby, M.J., 1985. Earth's Changing Surface: an introduction to geomorphology. Oxford: Clarendon Press.

Sequiera Braga, M.A., Paquet, H. and Begonha, A., 2002. Weathering of franites in a temperate climate (NW Portugal): granitic saprolites and arenization. Catena, 49: 41-56.

Setterholm, D.R., Morey, G.B., Boerboom, T.J., and Lamons, R.C., 1989. Minnesota
Kaolin Deposits: A subsurface study in selected areas of southwestern and east-central Minnesota. Minnesota Geological Survey, Information Circular 27.

Sidle, W.C., 1993. Naturally occurring mercury contamination in a pristine environment? Environmental Geology, 21: 42-50.

Siegel, F.R., 2002. Environmental Geochemistry of Potentially Toxic Metals. Springer-Verlag, Germany. 218p.

Simon-Coinçon, R., Thiry, M., and Schmitt, J.M.,1997. Variety and relationships of weathering features along the early Tertiary palaeosurface in the southwestern French Massif Central and the nearby Aquitaine Basin. Palaeogeogr., Palaeoclimatol., Palaeoecol., 44: 71-92.

Singer, A., 1980. The paleoclimatic interpretation of clay minerals in soils and weathering profiles. Earth Science Reviews, 15: 303-326.

Smith D.G.W., and Cavell, P.A., 1978. An energy dispersive technique for quantitative analysis of clay minerals by the electron microprobe. Proceedings, Annual Conference - Microbeam Analysis Society, 13: 45A-45F.

Smith, K.S. and Huyck, H.L.O.,1999. An overview of the abundance, relative mobility, bioavailability, and human toxicity of metals. In: Plumlee, G.S. and Logsdon, M.J., eds..
The environmental Geochemistry of Mineral Deposits, Part A: Society of Economic Geologists, Reviews in Economic Geology, 6A: 29-70

Smith, P.K., Sangster, Al L. and O'Beirne-Ryan, A.M., 2005. Bedrock mercury at Kejimkujik National Park, Nova Scotia. In: Mercury cycling in a Wetland-Dominated Ecosystem: A Multidisciplinary Study. O'Driscoll, N.J., Rencz, A.N. and Lean, R.S., eds. Published by Society of Environmental Toxicology and Chemistry, SETAC Press. Ch 7: 131-237.

Stanton, M.R., Wanty, R.B., Lawrence, E.P., Briggs, P.H., 1996. Dissolved radon and uranium, and ground-water geochemistry in an area near Hylas, Virginia. U.S. Geological Survey Bulletin, Report: B 2070, 23p.

Stea, R.R., 1982. Pleistocene geology and till geochemistry of south central Nova Scotia. *Nova Scotia Department of Mines and Energy*, Map 82-1, scale 1:100 000.

Stea, R.R., Finck, P.W., Pullan, S.E., and Corey, M.C., 1995. Cretaceous Deposits of Kaolin Clay and Silica Sand in the Shubenacadie and Musquodoboit Valleys, Nova Scotia, Canada. Nova Scotia Department of Natural Resources, Open File Report 96-003.

Stea, R.R., Finck, P.W., Pullman, S.E. and Corey, M.C., 1996. Cretaceous deposits of kaolin and silica sand in the Shubenacadie and Musquodoboit Valleys, Nova Scotia, Canada.. *Nova Scotia Department of Natural Resources, Minerals and Energy Branch, Open File Rep.* 96-003, 58 pp.

Sueoka, T., Lee, I.K., Muramatsu, M. and Imamura, S., 1985. Geomechanical properties and engineering classification for decomposed granite soils in Kaduna district, Nigeria. First Int. Conf. Geomech. Trop. Lateritic Saprolitic soils. Brasilia, 1: 175-186.

Sutton, S.J. and Maynard, J.B., 1992. Multiple alteration events in the history of a sub-Huronian regolith at Lauzon Bay, Ontario. Canadian Journal of Earth Science, 29: 432-445.

Szalay, S., and Samsoni, Z., 1966. Investigation of the leaching of uranium fromcrushed magmatic rocks. Geochemistry, 14: 613-623.

Tardy, Y., Bocquier, G., Paquest, H., and Millot, G., 1973. Formation of clay from granite and its distribution in relation to climate and topography. Geoderma, 10: 271-284.

Thomas, M.F. 1994. Age and Geomorphic Relationships of Saprolite Mantles. *In* Rock Weathering and Landform Evolution. *Edited by* D.A. Robinson and R.G.B. Williams. Wiley Publications, p. 287-302.

Tieh, T.T., Ledger, E.B., Rowe, M.W., 1980. Release of uranium from granitic rocks during in situ weathering and initial erosion (Central Texas). Chemical Geology, 29: 227-248.

Turekian, K.K., 1978. Co, Ni, Cu, Zn. In: Wedepohl, K.M. ed., Handbook of Geochemistry, II: 3.

Van der Weijden, C.H. and Reith, M., 1982. Chromium (III) - Chromium (VI) interconversions in seawater. Marine Chemistry, 11: 565-572.

Van der Weijden, C.H. and van der Weijden, R.D., 1995. Mobility of major, minor and some redox-sensitive trace elements and rare-earth elements during weathering of four granitoids in central Portugal. Chemical Geology, 125: 149-167.

Velbel, M.A., 1985. Geochemical mass balances and weathering rates in forested watersheds of the southern Blue Ridge. American Journal of Science, 285: 904-930.

Velde, B., 1995. Origin and mineralogy of Clays: Clays and the Environment. Springer publ., 356p.

Vogel, D.E., 1975. Precambrian weathering in acid metavolcanic rocks from the superior Province, Villebon township, south-central Quebec. Canadian Journal Earth Science, 12: 2080-2085.

Vogt, T., 1927. Sulitjelmafeltets geologi og petrografi. Norges geologiske Undersokelse, 121.1-560 (In: Norwegian, with English Abstract).

Wagner, G., and Van den haute, P., 1992. Fission-Track Dating. Geological Institute, Gent University, Belgium. Sold Earth Sciences Library, 6, 296p.

Wang, C., Ross, G.J., Gray, J.T., and Lafreniere, L.B., 1982. Mineralogy and genesis of saprolite and strongly weathered soils in the Appalachian region of Canada. Maritime Sediments and Atlantic Geology, 18: 130-138.

Wang, C., Ross, G.J., and Rees, H.W., 1981. Characteristics of residual and colluvial soils developed on granite and of the associated pre-Wisconsin landforms in north-central New Brunswick. Canadian Journal of Earth Sciences, 18: 487-494.

White, A.F., Bullen, T.D., Schulz, M.S., Blum, A.E., Huntington, T.G., and Peters, N.E., 2001. Differential rates of feldspar weathering in granitic regoliths. Geochim Cosmochim Acta, 65: 847-869.

Wightman, J.F., 1999. Report on Drilling, Bridgetown Area, Annapolis County, Nova Scotia. Nova Scotia Department of Natural Resources, Assessment Report ME 1999-74.

Williams, H., 1995. Introduction, Chapter 1. *In* Geology of the Appalachian-Caledonian Orogen in Canada and Greenland. *Edited by* H. Williams; Geological Survey of Canada, Geology of Canada, 6: 1-19.

Wilson, J., 2004. Weathering of the primary rock-forming minerals; processes, products and rates. Clay Minerals, 39: 233-266.

Wilson, M.J., 1970. A study of weathering in a soil derived from a biotite-hornblende rock. I. Weathering of biotite. Clay mineralogy 8: 291-303.

Wronkiewicz, D.J. and Condie, K.C., 1987. Geochemistry of Archean shales from the Witwatersrand Supergroup, South Africa: Source-area weathering and provenance. Geochim. et Cosmochim. Acta, 51: 2401-2416.

APPENDICES

APPENDIX A1

X-Ray Diffraction (XRD) Analytical Techniques

Sample Separation

Clay (light coloured material) and biotite separates were hand-picked by A.M. O'Beirne-Ryan from weathered rock samples (no crushing required), using a binocular microscope to facilitate separation. Every attempt was made to remove the quartz and any stained grains from the sample sent for analysis. Samples selected for analysis from Pre-Triassic saprolite included clay separates from (AMR-) 2-110, (AMR-) 2-139, (AMR-) 2-168, and (AMR-) 2-200. Samples selected for biotite analysis included (AMR-) 2-110Bi, (AMR-) 2-139Bi, (AMR-) 2-168. Sample number 2-110 is from the top of the preserved portion of the profile, and sample 2-200 is from the base of the saprolite, next to the fresh monzogranite; samples 2-139 and 2-168 are from intermediate depths.

Sample Analysis (taken from report prepared by Dr. Beatrice Levi)

Sample analyses were undertaken by Dr. Beatrice Levi, in Sweden, in 2001. XRD analysis was performed on 4 clay samples and 3 biotite/clay samples from the Pre-Triassic core, using Cu-radiation; 2θ = 3-65°. Clay analyses were performed on non-oriented samples, with scans at half degree per minute. Each sample was then re-run three times from 3° to 16° at the same velocity: (1) dry, (2) saturated with ethylene glycol, and (3) after heating to 500°C for one hour, to check the swelling characteristics of the clays, and whether Fe-rich chlorite was present with the kaolinite. Biotite/clay separates were analyzed as oriented samples with scans at one degree per minute. Further details regarding the analyses is available from the author.

APPENDIX A2

Microprobe Analysis

Sample Preparation

Samples for microprobe analysis were impregnated in order to reduce the amount of plucking of the clays from the samples, then cut and polished to a thickness of approximately 30 μm. The slides were then carbon coated prior to analysis. The samples were prepared for analysis at the thin section laboratory at Dalhousie University, by Gordon Brown.

Sample Analysis

Samples were analyzed using a JEOL JXA-8200 microprobe, at an acceleration voltage of 15.0 kV, with probe diameter focused, and a current of 20 μA. The individual samples were calibrated against lab samples of known chemistry, and as appropriate to the mineral being analyzed. The analyses were undertaken by A.M. O'Beirne-Ryan, with the assistance of Bob MacKay and Particia Stoffyn. X-ray maps were produced using varying conditions (sample-dependant), and details for individual samples are available from the author.

Summary Diagram of Mineralogical and Textural Changes in Saprolite at Varying Depths

Fractures ubiquitous and numerous / plagioclase increasingly destroyed/ K-feldspar increasingly weathered to kaolinite / physical breakup of minerals dominates / increased degree of complex weathering in biotite / bending of biotite grains / kaolinite-dominant

⇑

Fractures small and rare/ plagioclase only incipiently altered / K-feldspar unchanged / fractures around grains, rarely through grains / minimal complex weathering of biotite / biotite grains not bent / clays rare or smectite-dominant

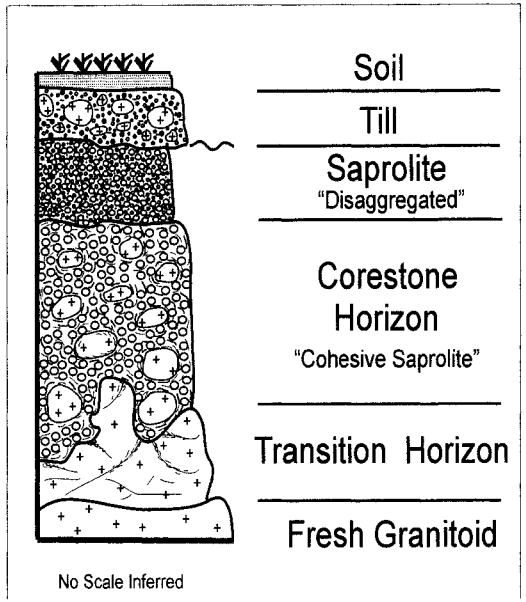

APPENDIX A3

Original XRF Data

Appendix A-3 presents the original XRF data, Saint Mary's University.

NOTES:

1. The following samples are duplicates:

   SMB #1 and SMB #2

   AMR-W00-131 and AMR-W00-150

   AMR-W00-144 and AMR-W00-151

2. Samples AGV-1, BE-N, and HFL-1 are internal standards.

SAMPLE	L.O.I. %	SiO2 %	TiO2 %	Al2O3 %	Fe2O3 %	MnO %	MgO %	CaO %
SMB #1	0.67	71.57	0.368	14.27	3.24	0.078	0.73	1.31
SMB #2	0.70	71.22	0.365	14.22	3.23	0.077	0.74	1.28
AMR-WOO-100	0.83	68.93	0.653	14.43	4.51	0.084	1.22	1.82
AMR-WOO-106	1.47	67.31	0.616	15.22	4.54	0.076	0.99	1.58
AMR-WOO-107	1.32	67.50	0.497	15.58	4.50	0.142	0.86	0.86
AMR-WOO-111	0.80	67.19	0.667	15.03	4.78	0.076	1.17	1.90
AMR-WOO-112	0.80	67.04	0.756	15.26	5.38	0.091	1.30	1.96
AMR-WOO-113A	1.38	67.83	0.663	15.23	4.65	0.080	1.09	1.37
AMR-WOO-126	1.11	74.47	0.073	13.69	1.35	0.015	0.07	0.38
AMR-WOO-127	0.90	75.05	0.062	13.78	1.11	0.011	0.07	0.32
AMR-WOO-128	0.99	72.10	0.282	14.55	2.33	0.024	0.37	0.72
AMR-WOO-129	1.03	72.95	0.240	13.76	2.26	0.026	0.33	0.47
AMR-WOO-131	0.77	73.41	0.175	14.14	1.79	0.040	0.26	0.58
AMR-WOO-132	0.98	73.52	0.205	14.50	1.60	0.036	0.25	0.49
AMR-WOO-134	1.17	71.19	0.467	13.93	3.56	0.134	0.71	1.43
AMR-WOO-135	2.77	71.14	0.450	14.41	3.54	0.168	0.59	0.40
AMR-WOO-138	1.51	73.97	0.062	14.59	1.19	0.024	0.05	0.60
AMR-WOO-139	1.50	74.35	0.060	14.74	1.15	0.024	0.02	0.66
AMR-WOO-140	1.84	72.48	0.251	14.26	2.44	0.033	0.36	0.46
AMR-WOO-141	0.78	68.68	0.530	15.09	3.69	0.073	1.23	2.02
AMR-WOO-142	0.74	75.12	0.186	13.46	1.90	0.031	0.24	0.51
AMR-WOO-143	1.14	74.50	0.182	12.83	1.87	0.030	0.26	0.46
AMR-WOO-144	1.88	67.48	0.680	15.06	4.86	0.092	1.11	1.13
AMR-WOO-145	0.80	73.74	0.089	13.81	1.43	0.019	0.11	0.44
AMR-WOO-150	0.92	73.65	0.179	14.17	1.65	0.040	0.27	0.58
AMR-WOO-151	1.88	67.95	0.683	15.03	4.96	0.093	1.12	1.14
AMR-2-110	5.13	66.87	0.680	16.44	4.77	0.074	1.11	0.32
AMR-2-139	4.29	69.46	0.586	14.41	4.10	0.063	1.02	0.71
AMR-2-168	4.94	67.73	0.587	14.99	4.15	0.090	1.25	0.80
AMR-2-193	2.06	67.88	0.609	14.41	4.27	0.065	1.28	1.60
AMR-2-200	5.09	64.03	0.617	14.18	4.64	0.070	1.49	1.84
AMR-2-201	0.98	68.03	0.653	15.10	4.58	0.072	1.13	2.09
AGV-1	1.20	58.91	1.047	17.06	6.73	0.096	1.55	4.91
BE-N	2.45	38.39	2.622	9.98	12.79	0.202	13.15	13.83
HFL-1	2.20	60.20	0.960	22.03	7.12	0.074	1.77	0.29
SAMPLE	**L.O.I.**	**SiO2**	**TiO2**	**Al2O3**	**Fe2O3**	**MnO**	**MgO**	**CaO**

SAMPLE	Na2O %	K2O %	P2O5 %	V ppm	Cr ppm	Co ppm	Zr ppm	Ba ppm
SMB #1	3.23	4.43	0.192	50	27	6	140	541
SMB #2	3.21	4.40	0.185	50	32	6	134	574
AMR-WOO-100	2.90	3.95	0.173	87	23	10	205	716
AMR-WOO-106	3.06	4.03	0.224	77	22	11	219	695
AMR-WOO-107	2.83	5.66	0.104	66	18	11	175	995
AMR-WOO-111	3.19	3.74	0.216	85	25	11	216	674
AMR-WOO-112	3.11	4.01	0.304	94	26	13	228	704
AMR-WOO-113A	2.81	4.47	0.272	85	23	10	194	806
AMR-WOO-126	3.06	5.00	0.321	16	6	<5	31	164
AMR-WOO-127	2.99	5.22	0.294	16	<4	<5	22	191
AMR-WOO-128	2.87	5.56	0.213	38	12	<5	110	688
AMR-WOO-129	2.48	5.57	0.166	34	8	<5	107	446
AMR-WOO-131	3.35	4.71	0.256	26	16	<5	65	374
AMR-WOO-132	3.06	5.20	0.224	27	11	<5	76	445
AMR-WOO-134	2.86	4.13	0.215	62	18	9	155	512
AMR-WOO-135	1.03	5.06	0.238	62	14	7	148	666
AMR-WOO-138	3.02	4.01	0.564	15	3	<5	19	168
AMR-WOO-139	3.13	4.03	0.597	15	<4	<5	21	121
AMR-WOO-140	2.37	4.98	0.141	37	11	5	105	369
AMR-WOO-141	3.22	4.22	0.204	72	24	7	159	912
AMR-WOO-142	2.65	5.62	0.145	31	10	<5	87	405
AMR-WOO-143	2.47	4.99	0.135	27	8	<5	88	323
AMR-WOO-144	2.76	4.33	0.262	86	26	13	208	785
AMR-WOO-145	3.29	4.74	0.283	19	6	<5	33	211
AMR-WOO-150	3.38	4.73	0.258	27	16	<5	63	360
AMR-WOO-151	2.76	4.35	0.260	86	27	13	214	810
AMR-2-110	0.20	4.82	0.132	83	31	17	251	664
AMR-2-139	0.25	5.78	0.197	70	22	11	206	921
AMR-2-168	1.07	5.25	0.201	68	12	11	224	956
AMR-2-193	2.52	4.25	0.206	78	18	11	204	847
AMR-2-200	1.53	5.17	0.208	76	22	14	214	799
AMR-2-201	3.06	4.19	0.224	83	25	11	237	773
AGV-1	4.26	2.91	0.501	149	9	18	241	1133
BE-N	3.17	1.39	1.045	319	342	53	318	832
HFL-1	1.65	4.37	0.128	129	88	33	178	821
SAMPLE	Na2O	K2O	P2O5	V	Cr	Co	Zr	Ba

SAMPLE	La	Nd	Ni	Cu	Zn	Ga	Rb	Sr
	ppm	ppm	ppm	ppm	ppm	ppm	ppm	ppm
SMB #1	25	24	12	4	64	19	222	106
SMB #2	18	20	15	4	63	19	224	102
AMR-WOO-100	32	33	8	<4	62	20	159	141
AMR-WOO-106	42	48	11	7	77	22	157	134
AMR-WOO-107	35	33	4	6	64	20	177	140
AMR-WOO-111	44	43	10	11	74	21	146	145
AMR-WOO-112	45	50	10	14	84	23	192	149
AMR-WOO-113A	18	12	8	8	86	21	206	143
AMR-WOO-126	7	7	<3	4	28	22	512	7
AMR-WOO-127	8	<5	<3	5	28	23	512	<5
AMR-WOO-128	20	21	3	6	73	19	232	73
AMR-WOO-129	17	22	<3	5	74	19	248	43
AMR-WOO-131	15	15	3	4	69	22	355	47
AMR-WOO-132	18	16	5	<4	64	23	373	42
AMR-WOO-134	23	22	8	6	54	19	176	83
AMR-WOO-135	19	17	7	<4	47	19	188	35
AMR-WOO-138	12	<5	<3	<4	88	35	927	<5
AMR-WOO-139	7	<5	<3	7	92	35	916	<5
AMR-WOO-140	15	25	3	4	80	21	248	33
AMR-WOO-141	32	30	9	6	53	21	141	178
AMR-WOO-142	12	7	3	<4	59	17	254	46
AMR-WOO-143	11	9	3	6	63	17	245	32
AMR-WOO-144	42	37	9	11	111	22	220	139
AMR-WOO-145	<5	5	3	7	40	23	466	11
AMR-WOO-150	23	20	<3	6	71	23	354	48
AMR-WOO-151	42	47	9	13	110	21	220	140
AMR-2-110	63	63	8	19	75	23	202	43
AMR-2-139	41	20	7	11	85	19	200	64
AMR-2-168	44	33	<3	14	107	20	218	99
AMR-2-193	44	50	9	7	70	19	157	130
AMR-2-200	39	32	9	8	91	22	207	141
AMR-2-201	44	42	9	7	71	21	149	141
AGV-1	44	42	17	70	92	20	62	665
BE-N	87	76	261	61	111	16	36	1377
HFL-1	53	54	41	35	107	29	180	212
SAMPLE	**La**	**Nd**	**Ni**	**Cu**	**Zn**	**Ga**	**Rb**	**Sr**

SAMPLE	Y	Nb	Pb	Th	U	Totals
	ppm	ppm	ppm	ppm	ppm	
SMB #1	25	7	14	7	4	100.09
SMB #2	25	9	16	7	4	99.63
AMR-WOO-100	29	12	14	10	3	99.50
AMR-WOO-106	40	15	23	9	3	99.12
AMR-WOO-107	41	12	25	8	3	99.85
AMR-WOO-111	35	14	21	11	4	98.76
AMR-WOO-112	27	14	17	8	3	100.01
AMR-WOO-113A	26	13	23	6	4	99.85
AMR-WOO-126	12	10	7	<2	3	99.54
AMR-WOO-127	8	9	13	<2	3	99.81
AMR-WOO-128	22	10	17	5	5	100.01
AMR-WOO-129	29	10	18	3	4	99.28
AMR-WOO-131	13	16	64	4	5	99.48
AMR-WOO-132	13	17	24	8	6	100.07
AMR-WOO-134	30	10	17	6	5	99.80
AMR-WOO-135	31	11	15	3	5	99.80
AMR-WOO-138	5	32	2	<2	3	99.59
AMR-WOO-139	6	28	2	<2	4	100.26
AMR-WOO-140	32	12	22	6	5	99.62
AMR-WOO-141	28	10	16	9	3	99.74
AMR-WOO-142	24	6	17	3	5	100.60
AMR-WOO-143	24	9	15	3	4	98.87
AMR-WOO-144	26	13	36	9	5	99.64
AMR-WOO-145	14	12	13	<2	4	98.75
AMR-WOO-150	12	15	67	4	5	99.83
AMR-WOO-151	26	13	31	7	4	100.23
AMR-2-110	32	14	98	8	5	100.55
AMR-2-139	27	9	46	7	4	100.87
AMR-2-168	25	11	38	5	4	101.06
AMR-2-193	28	13	20	9	3	99.15
AMR-2-200	28	14	155	7	4	98.87
AMR-2-201	34	14	20	7	4	100.11
AGV-1	21	12	17	5	1	99.17
BE-N	23	105	5	10	<1	99.02
HFL-1	32	20	38	14	2	100.79
SAMPLE	Y	Nb	Pb	Th	U	Totals

APPENDIX A4

Original REE data

APPENDIX A4: Original REE and Zr, Nb, Th, U analysis; samples 131 &150 are duplicates.

Sample ID	Client ID	units	Ce (Det Limit = 0_07)	Cs (Det Limit = 0_007)	Dy (Det Limit = 0_008)
02-0463-0001	AMR-W00-112	ppm	80.85	11.931	5.883
02-0463-0002	AMR-W00-131	ppm	40.89	24.925	2.136
02-0463-0003	AMR-W00-128	ppm	41.52	8.172	4.054
02-0463-0004	AMR-W00-141	ppm	62.66	6.121	5.090
02-0463-0005	AMR-W00-111	ppm	79.17	8.562	7.644
02-0463-0006	AMR-W00-134	ppm	N.M.	N.M.	N.M.
02-0463-0007	AMR-W00-145	ppm	14.12	16.546	2.421
02-0463-0008	AMR-W00-113A	ppm	62.90	12.071	5.288
02-0463-0009	AMR-W00-144	ppm	70.77	15.359	5.737
02-0463-0010	AMR-W00-132	ppm	48.27	23.152	2.243
02-0463-0011	AMR-W00-129	ppm	33.66	10.322	4.517
02-0463-0012	AMR-W00-140	ppm	44.06	13.229	5.799
02-0463-0013	AMR-W00-106	ppm	74.63	6.334	7.694
02-0463-0014	AMR-W00-107	ppm	72.96	9.269	8.049
02-0463-0015	AMR-W00-126	ppm	11.48	16.651	2.658
02-0463-0016	AMR-W00-127	ppm	6.26	16.983	1.108
02-0463-0017	AMR-W00-135	ppm	48.84	9.424	5.738
02-0463-0018	AMR-W00-150	ppm	40.61	24.215	2.081
02-0463-0019	AMR-W00-153	ppm	60.48	1.114	8.758
02-0463-0020	AMR-2-201	ppm	79.70	8.882	7.695
02-0463-0021	AMR-2-200	ppm	63.67	36.143	6.050
02-0463-0022	AMR-2-193	ppm	60.05	13.992	5.684
02-0463-0023	AMR-2-168	ppm	84.40	28.577	5.243
02-0463-0024	AMR-2-139	ppm	94.30	23.694	5.753
02-0463-0025	AMR-2-110	ppm	50.18	22.280	3.947
02-0463-0026	CFB6-1119-20	ppm	19.12	0.286	2.729
02-0463-0027	CFB6-1125-26	ppm	49.82	7.131	5.075
02-0463-0028	CFB6-1134-35	ppm	69.38	9.940	5.931
02-0463-0029	CFB7-1168-69	ppm	63.47	1.107	8.278
02-0463-0030	CFB7-1176-77	ppm	68.54	1.140	4.533
02-0463-0031	CFB7-1184-86	ppm	68.66	6.556	6.401
02-0463-0032	SMB-1 (SMB std)	ppm	55.02	18.164	4.172

Er (Det Limit = 0_008)	Eu (Det Limit = 0_005)	Gd (Det Limit = 0_009)	Hf (Det Limit = 0_10)	Ho (Det Limit = 0_003)	La (Det Limit = 0_02)
2.992	1.486	8.065	6.2	1.143	38.35
0.809	0.392	3.865	2.4	0.351	17.78
1.845	0.787	4.377	3.2	0.714	18.51
2.745	1.206	5.988	4.3	1.019	29.29
3.664	1.402	8.745	6.2	1.437	38.38
N.M.	N.M.	N.M.	N.M.	N.M.	N.M.
0.636	0.160	2.324	1.7	0.343	6.21
2.630	1.473	6.079	5.1	0.990	22.79
2.749	1.407	7.579	5.5	1.054	34.97
0.882	0.463	4.393	2.7	0.372	20.93
2.488	0.544	4.269	2.9	0.924	15.03
3.170	0.680	5.757	3.5	1.211	20.21
3.640	1.231	8.869	5.5	1.455	35.85
5.535	1.324	7.490	5.0	1.853	33.90
0.798	0.118	2.270	1.7	0.404	4.95
0.304	0.077	1.009	1.2	0.156	2.79
3.050	0.900	6.273	4.2	1.095	21.63
0.816	0.392	3.704	2.4	0.327	17.66
4.285	1.023	9.400	4.9	1.673	27.58
4.198	1.511	8.611	6.3	1.591	36.74
2.974	1.183	7.361	5.4	1.187	29.73
2.643	1.425	6.975	5.6	1.058	30.33
2.457	1.203	7.039	4.8	0.969	32.27
2.584	1.300	7.423	5.4	1.032	33.46
1.913	0.626	5.520	6.6	0.738	23.79
1.368	0.337	2.973	1.9	0.533	8.60
2.684	1.032	5.587	4.2	1.007	22.76
2.916	1.282	7.423	5.6	1.162	32.57
4.010	0.966	9.106	5.2	1.581	28.72
2.138	1.490	6.193	4.6	0.845	32.70
3.207	1.255	7.165	5.0	1.221	31.24
2.459	0.838	5.059	4.1	0.836	25.45

Lu (Det Limit = 0_003)	Nb (Det Limit = 0_20)	Nd (Det Limit = 0_03)	Pr (Det Limit = 0_006)	Rb (Det Limit = 0_05)	Sm (Det Limit = 0_01)
0.427	14.3	41.52	10.636	>150.00	9.11
0.097	17.2	20.38	5.291	>150.00	4.77
0.222	11.2	19.49	5.105	>150.00	4.82
0.396	10.0	31.17	8.006	>150.00	6.69
0.427	14.5	40.31	10.385	>150.00	8.97
N.M.	N.M.	N.M.	N.M.	N.M.	N.M.
0.045	13.8	7.03	1.864	>150.00	2.24
0.383	12.8	27.92	6.956	>150.00	6.52
0.390	13.1	37.71	9.694	>150.00	8.35
0.106	18.9	24.29	6.373	>150.00	5.76
0.316	10.7	17.12	4.497	>150.00	4.19
0.397	12.2	22.75	5.862	>150.00	5.78
0.372	14.7	39.51	10.126	>150.00	8.94
0.882	11.4	36.53	9.436	>150.00	7.68
0.059	12.2	5.82	1.545	>150.00	1.90
0.023	9.8	2.91	0.790	>150.00	0.91
0.375	11.1	25.88	6.426	>150.00	6.13
0.095	16.8	20.40	5.341	>150.00	4.96
0.461	13.2	32.90	8.057	18.34	8.23
0.549	13.9	40.02	10.305	>150.00	9.45
0.374	13.6	33.54	8.425	>150.00	7.80
0.336	13.5	33.77	8.529	>150.00	7.49
0.302	12.8	35.94	9.331	>150.00	7.83
0.341	12.2	38.16	9.554	>150.00	8.43
0.265	14.7	28.09	7.185	70.68	6.28
0.159	4.6	10.34	2.478	3.92	2.62
0.337	10.0	24.46	6.271	>150.00	5.74
0.362	13.2	34.86	8.943	>150.00	8.00
0.465	12.5	34.23	8.455	15.47	8.28
0.281	11.0	33.94	8.705	7.60	7.44
0.396	12.8	33.99	8.786	>150.00	7.85
0.338	9.7	26.64	6.942	>150.00	5.92

Sr (Det Limit = 0_50)	Ta (Det Limit = 0_17)	Tb (Det Limit = 0_003)	Th (Det Limit = 0_06)
162.7	1.64	1.173	12.41
59.9	2.26	0.516	11.28
86.8	0.91	0.753	8.88
198.8	0.83	0.915	10.48
166.3	1.23	1.390	12.73
N.M.	N.M.	N.M.	N.M.
22.6	2.07	0.496	4.79
157.8	1.40	0.977	9.99
159.7	1.46	1.109	11.30
55.9	2.32	0.567	13.97
55.8	1.04	0.783	9.41
44.6	1.20	1.012	10.44
154.4	1.23	1.456	12.68
152.9	1.00	1.260	14.22
16.5	2.60	0.510	3.68
14.1	2.13	0.218	2.13
46.7	1.14	1.028	9.00
58.8	2.20	0.494	11.65
53.8	1.18	1.571	11.02
153.0	1.06	1.394	13.23
155.5	1.03	1.158	12.16
144.9	1.03	1.068	11.34
105.1	1.04	1.038	12.30
74.9	0.97	1.094	12.50
25.2	1.16	0.794	10.38
13.7	0.40	0.518	3.10
105.0	0.91	0.899	8.22
137.5	1.14	1.111	11.62
50.7	1.14	1.526	11.04
177.5	0.95	0.859	8.71
123.5	1.10	1.170	11.10
119.0	1.10	0.773	10.96

Tm (Det Limit = 0_003)	U (Det Limit = 0_007)	Y (Det Limit = 0_02)	Yb (Det Limit = 0_01)	Zr (Det Limit = 4_00)
0.426	3.465	28.87	2.72	225.0
0.117	4.342	9.96	0.63	75.6
0.272	3.426	20.44	1.52	113.0
0.408	1.736	27.38	2.64	158.4
0.504	3.589	39.91	2.83	227.7
N.M.	N.M.	N.M.	N.M.	N.M.
0.068	2.884	10.96	0.40	40.4
0.392	4.872	25.28	2.38	186.6
0.403	5.554	28.16	2.53	201.0
0.120	5.908	11.21	0.68	86.7
0.362	2.666	26.51	2.18	97.3
0.474	3.287	34.22	2.88	117.2
0.479	2.971	41.87	2.66	208.0
0.872	3.446	48.42	5.75	173.0
0.088	1.336	12.85	0.47	38.1
0.034	1.475	5.25	0.20	24.8
0.429	3.835	32.59	2.52	152.4
0.106	4.372	9.39	0.67	76.9
0.611	4.847	49.39	3.64	175.8
0.604	4.304	41.59	3.58	230.4
0.427	3.507	31.58	2.49	192.7
0.384	2.642	28.44	2.33	206.4
0.333	3.581	25.36	2.11	174.0
0.355	3.797	27.15	2.17	200.6
0.284	5.017	19.84	1.75	247.6
0.188	1.382	14.62	1.16	65.0
0.374	3.637	27.92	2.21	151.5
0.419	3.165	31.50	2.55	201.7
0.552	3.887	44.34	3.20	184.9
0.314	3.028	24.43	1.84	166.6
0.457	3.978	33.54	2.60	183.7
0.359	2.485	23.93	2.25	147.2

APPENDIX A5

Trace element data

XRF refers to analysis using XRF; AR refers to analysis using ICP-MS, following dissolution using aqua regia.

		XRF	Ar	XRF	AR	XRF	AR	XRF	AR	XRF	AR	XRF	AR	XRF	AR	XRF	AR	XRF		XRF	AR	XRF	AR
	SAMPLE	**Cu**		**Pb**		**Zn**		**Ni**		**Co**		**Fe**		**Mn**		**Ba**		**Cr**		**V**		**La**	
Waterloo Lake	**111F**	11	7	21	-2	74	72	10	10	11	8	3.35	3.19	0.060	518	674	199	25	27	85	44	38.38	22
	106W	7	6	23	3	77	76	11	12	11	7	3.18	3.3	0.060	506	695	137	22	27	77	41	35.85	21
	107WW	6	5	25	3	64	60	4	8	11	7	3.15	2.76	0.112	667	995	115	18	22	66	32	33.90	22
Hardwood Lake	**112F**	14	10	17	2	84	78	10	10	13	10	3.77	3.46	0.072	531	704	130	26	27	94	49	38.35	18
	113AW	8	5	23	3	86	82	8	9	10	8	3.26	3.08	0.063	468	806	117	23	24	85	43	22.79	13
	144WW	11	14	36	13	111	110	9	16	13	9	3.4	3.18	0.073	511	785	116	26	31	86	43	34.97	19
Forest Home	**145F**	7	3	13	2	40	26	3	1	1	-1	1	0.8	0.015	120	211	6	6	6	19	2	6.21	6
	126W	4	1	7	-2	28	12	1	1	1	1	0.95	0.61	0.012	70	164	3	6	8	16	1	4.95	5
	127WW	5	1	13	-2	28	10	1	-1	1	-1	0.78	0.45	0.009	57	191	3	1	9	16	1	2.79	2
Smith's Corner	**128F**	6	3	17	3	73	67	3	4	1	3	1.63	1.52	0.019	163	688	31	12	12	38	13	18.51	13
	129W	5	2	18	4	74	68	1	3	1	3	1.58	1.44	0.021	182	446	28	8	10	34	11	15.03	12
	140WW	4	2	22	3	80	69	3	3	5	3	1.71	1.57	0.026	231	369	29	11	13	37	11	20.21	15
Pre-Triassic	**2-201**	7	4	20	-2	71	70	9	11	11	8	3.21	3.34	0.057	506	773	221	25	26	83	49	36.74	22
	2-193	7	5	20	3	70	68	9	9	11	7	2.99	2.99	0.051	465	847	217	18	26	78	42	30.33	20
	2-168	14	10	38	11	107	99	1	9	11	8	2.91	2.72	0.071	604	956	196	12	21	68	27	32.27	20
	2-139	11	7	46	8	85	79	7	8	11	8	2.87	2.62	0.050	438	921	154	22	26	70	28	33.46	15
	2-110	19	13	98	4	75	79	8	12	17	11	3.34	3.1	0.058	558	664	104	31	35	83	41	23.79	17
Pre-Carboniferous	**1134**	3		53		121		11		10		3.07		0.079		643		22		76		32.57	
	1125	5		23		51		4		8		2.36		0.063		489		34		59		22.76	
	1119	3		2		6		3		7		2.67		0.521		37		27		68		8.60	
Pre-Carboniferous	**1184**	7		21		63		10		11		2.71		0.079		479		28		74		31.24	
	1176	4		6		16		2		5		1.38		0.245		26		25		71		32.70	
	1168	4		2		7		12		4		1.47		0.292		36		29		76		28.72	

		XRF	AR	XRF	AR	XRF	AR	XRF	AR	XRF	AR	XRF	AR	XRF	AR	XRF	AR	XRF	AR	XRF	AR	XRF	AR
	SAMPLE	**Al**		**Mg**		**Ca**		**Na**		**K**		**Sr**		**Y**		**Ga**		**Nb**		**Ti**		**Zr**	
Waterloo Lake	**111F**	7.97	1.97	0.7	0.61	1.349	0.19	2.361	0.03	3.104	1.15	145	1	39.91	14	21	9	14.5	4	0.4	0.304	227.7	-1
	106W	8.07	2.07	0.59	0.51	1.122	0.22	2.264	0.02	3.345	0.91	134	8	41.87	18	22	10	14.7	3	0.37	0.277	208	-1
	107WW	8.26	1.56	0.52	0.4	0.611	0.08	2.094	0.02	4.698	0.76	140	5	48.42	15	20	7	11.4	2	0.298	0.221	173	-1
Hardwood Lake	**112F**	8.09	2.12	0.78	0.64	1.392	0.25	2.301	0.04	3.328	1.3	149	3	28.87	15	23	11	14.3	3	0.454	0.311	225	-1
	113AW	8.07	2.03	0.65	0.55	0.973	0.2	2.079	0.03	3.71	1.14	143	3	25.28	14	21	11	12.8	3	0.398	0.257	186.6	-1
	144WW	7.98	2.08	0.67	0.55	0.802	0.19	2.042	0.03	3.594	1.08	139	4	28.16	15	22	10	13.1	2	0.408	0.242	201	-1
Forest Home	**145F**	7.32	0.45	0.07	0.03	0.312	0.2	2.435	0.02	3.934	0.15	11	6	10.96	5	23	3	13.8	-1	0.053	-0.01	40.4	8
	126W	7.26	0.32	0.04	0.01	0.27	0.21	2.264	0.02	4.15	0.16	7	5	12.85	4	22	2	12.2	-1	0.044	-0.01	38.1	5
	127WW	7.3	0.29	0.04	0.01	0.227	0.13	2.213	0.02	4.333	0.12	1	4	5.25	2	23	-2	9.8	-1	0.037	-0.01	24.8	3
Smith's Corner	**128F**	7.71	1.04	0.22	0.18	0.511	0.09	2.124	0.02	4.615	0.49	73	2	20.44	8	19	6	11.2	2	0.169	0.092	113	4
	129W	7.29	1	0.2	0.16	0.334	0.03	1.835	0.02	4.623	0.5	43	2	26.51	7	19	6	10.7	1	0.144	0.085	97.3	3
	140WW	7.56	1.27	0.22	0.16	0.327	0.02	1.754	0.02	4.133	0.51	33	2	34.22	10	21	6	12.2	-1	0.151	0.086	117.2	4
Pre-Triassic	**2-201**	8	1.85	0.68	0.58	1.484	0.3	2.264	0.04	3.478	1.3	141	6	41.59	14	21	10	13.9	3	0.392	0.305	230.4	-1
	2-193	7.64	1.91	0.77	0.59	1.136	0.3	1.865	0.04	3.528	1.16	130	22	28.44	12	19	10	13.5	2	0.365	0.25	206.4	-1
	2-168	7.94	2	0.75	0.47	0.568	0.43	0.792	0.03	4.358	1.08	99	48	25.36	11	20	10	12.8	-1	0.352	0.178	174	-1
	2-139	7.64	1.77	0.61	0.42	0.504	0.43	0.185	0.02	4.797	1.04	64	26	27.15	12	19	10	12.2	1	0.352	0.207	200.6	-1
	2-110	8.71	2.22	0.67	0.54	0.227	0.22	0.148	0.02	4.001	1.2	43	15	19.84	15	23	13	14.7	2	0.408	0.263	247.6	1
Pre-Carboniferous	**1134**	8.14		0.66		1.512		2.213		3.619		129		31.5		22		13.2		0.331		201.7	
	1125	7.47		0.43		1.2		2.013		3.71		97		27.92		18		10		0.238		151	
	1119	8.11		0.64		2.18		0.007		0.166		34		14.62		21		4.6		0.269		65	
Pre-Carboniferous	**1184**	9.17		0.53		1.626		2.139		3.486		115		33.54		22		12.8		0.312		183.7	
	1176	9.12		0.42		1.448		0.022		0.274		178		24.43		24		11		0.255		166.6	
	1168	8.54		0.5		1.953		0.007		0.315		48		44.34		22		12.5		0.317		184.9	

APPENDIX A6

Duplicate Samples from XRF Data

APPENDIX A6: Duplicate samples from XRF data, with approx % deviation

SAMPLE	L.O.I. %	SiO2 %	TiO2 %	Al2O3 %	Fe2O3 %	MnO %
SMB #1	0.67	71.57	0.368	14.27	3.24	0.078
SMB #2	0.70	71.22	0.365	14.22	3.23	0.077
AMR-WOO-100	0.83	68.93	0.653	14.43	4.51	0.084
AMR-WOO-106	1.47	67.31	0.616	15.22	4.54	0.076
AMR-WOO-107	1.32	67.50	0.497	15.58	4.50	0.142
AMR-WOO-111	0.80	67.19	0.667	15.03	4.78	0.076
AMR-WOO-112	0.80	67.04	0.756	15.26	5.38	0.091
AMR-WOO-113A	1.38	67.83	0.663	15.23	4.65	0.080
AMR-WOO-126	1.11	74.47	0.073	13.69	1.35	0.015
AMR-WOO-127	0.90	75.05	0.062	13.78	1.11	0.011
AMR-WOO-128	0.99	72.10	0.282	14.55	2.33	0.024
AMR-WOO-129	1.03	72.95	0.240	13.76	2.26	0.026
AMR-WOO-131	0.77	73.41	0.175	14.14	1.79	0.040
AMR-WOO-132	0.98	73.52	0.205	14.50	1.60	0.036
AMR-WOO-134	1.17	71.19	0.467	13.93	3.56	0.134
AMR-WOO-135	2.77	71.14	0.450	14.41	3.54	0.168
AMR-WOO-138	1.51	73.97	0.062	14.59	1.19	0.024
AMR-WOO-139	1.50	74.35	0.060	14.74	1.15	0.024
AMR-WOO-140	1.84	72.48	0.251	14.26	2.44	0.033
AMR-WOO-141	0.78	68.68	0.530	15.09	3.69	0.073
AMR-WOO-142	0.74	75.12	0.186	13.46	1.90	0.031
AMR-WOO-143	1.14	74.50	0.182	12.83	1.87	0.030
AMR-WOO-144	1.88	67.48	0.680	15.06	4.86	0.092
AMR-WOO-145	0.80	73.74	0.089	13.81	1.43	0.019
AMR-WOO-150	0.92	73.65	0.179	14.17	1.65	0.040
AMR-WOO-151	1.88	67.95	0.683	15.03	4.96	0.093
AMR-2-110	5.13	66.87	0.680	16.44	4.77	0.074
AMR-2-139	4.29	69.46	0.586	14.41	4.10	0.063
AMR-2-168	4.94	67.73	0.587	14.99	4.15	0.090
AMR-2-193	2.06	67.88	0.609	14.41	4.27	0.065
AMR-2-200	5.09	64.03	0.617	14.18	4.64	0.070
AMR-2-201	0.98	68.03	0.653	15.10	4.58	0.072
AGV-1	1.20	58.91	1.047	17.06	6.73	0.096
BE-N	2.45	38.39	2.622	9.98	12.79	0.202
HFL-1	2.20	60.20	0.960	22.03	7.12	0.074
SAMPLE	**L.O.I.**	**SiO2**	**TiO2**	**Al2O3**	**Fe2O3**	**MnO**
sum (150+131)/2	0.845	73.53	0.177	14.155	1.72	0.04
approx % deviation from average	10%	1%	1%	1%	4%	0
(SMB1+SMB2)/2	0.685	71.395	0.367	14.25	3.24	0.078
approx % deviation from average	2%	1%	1%	1%	0%	1%

MgO %	CaO %	Na2O %	K2O %	P2O5 %	V ppm	Cr ppm	Co ppm
0.73	1.31	3.23	4.43	0.192	50	27	6
0.74	1.28	3.21	4.40	0.185	50	32	6
1.22	1.82	2.90	3.95	0.173	87	23	10
0.99	1.58	3.06	4.03	0.224	77	22	11
0.86	0.86	2.83	5.66	0.104	66	18	11
1.17	1.90	3.19	3.74	0.216	85	25	11
1.30	1.96	3.11	4.01	0.304	94	26	13
1.09	1.37	2.81	4.47	0.272	85	23	10
0.07	0.38	3.06	5.00	0.321	16	6	<5
0.07	0.32	2.99	5.22	0.294	16	<4	<5
0.37	0.72	2.87	5.56	0.213	38	12	<5
0.33	0.47	2.48	5.57	0.166	34	8	<5
0.26	0.58	3.35	4.71	0.256	26	16	<5
0.25	0.49	3.06	5.20	0.224	27	11	<5
0.71	1.43	2.86	4.13	0.215	62	18	9
0.59	0.40	1.03	5.06	0.238	62	14	7
0.05	0.60	3.02	4.01	0.564	15	3	<5
0.02	0.66	3.13	4.03	0.597	15	<4	<5
0.36	0.46	2.37	4.98	0.141	37	11	5
1.23	2.02	3.22	4.22	0.204	72	24	7
0.24	0.51	2.65	5.62	0.145	31	10	<5
0.26	0.46	2.47	4.99	0.135	27	8	<5
1.11	1.13	2.76	4.33	0.262	86	26	13
0.11	0.44	3.29	4.74	0.283	19	6	<5
0.27	0.58	3.38	4.73	0.258	27	16	<5
1.12	1.14	2.76	4.35	0.260	86	27	13
1.11	0.32	0.20	4.82	0.132	83	31	17
1.02	0.71	0.25	5.78	0.197	70	22	11
1.25	0.80	1.07	5.25	0.201	68	12	11
1.28	1.60	2.52	4.25	0.206	78	18	11
1.49	1.84	1.53	5.17	0.208	76	22	14
1.13	2.09	3.06	4.19	0.224	83	25	11
1.55	4.91	4.26	2.91	0.501	149	9	18
13.15	13.83	3.17	1.39	1.045	319	342	53
1.77	0.29	1.65	4.37	0.128	129	88	33
MgO	**CaO**	**Na2O**	**K2O**	**P2O5**	**V**	**Cr**	**Co**
0.265	0.58	3.365	4.72	0.257	26.5	16	#VALUE!
2%	0	4%	1%	1%	2%	0	n.a.
0.074	1.3	3.22	4.42	0.189	50	30	6
1%	2%	1%	1%	2%	0%	8%	0%

Zr ppm	Ba ppm	La ppm	Nd ppm	Ni ppm	Cu ppm	Zn ppm	Ga ppm	Rb ppm
140	541	25	24	12	4	64	19	222
134	574	18	20	15	4	63	19	224
205	716	32	33	8	<4	62	20	159
219	695	42	48	11	7	77	22	157
175	995	35	33	4	6	64	20	177
216	674	44	43	10	11	74	21	146
228	704	45	50	10	14	84	23	192
194	806	18	12	8	8	86	21	206
31	164	7	7	<3	4	28	22	512
22	191	8	<5	<3	5	28	23	512
110	688	20	21	3	6	73	19	232
107	446	17	22	<3	5	74	19	248
65	374	15	15	3	4	69	22	355
76	445	18	16	5	<4	64	23	373
155	512	23	22	8	6	54	19	176
148	666	19	17	7	<4	47	19	188
19	168	12	<5	<3	<4	88	35	927
21	121	7	<5	<3	7	92	35	916
105	369	15	25	3	4	80	21	248
159	912	32	30	9	6	53	21	141
87	405	12	7	3	<4	59	17	254
88	323	11	9	3	6	63	17	245
208	785	42	37	9	11	111	22	220
33	211	<5	5	3	7	40	23	466
63	360	23	20	<3	6	71	23	354
214	810	42	47	9	13	110	21	220
251	664	63	63	8	19	75	23	202
206	921	41	20	7	11	85	19	200
224	956	44	33	<3	14	107	20	218
204	847	44	50	9	7	70	19	157
214	799	39	32	9	8	91	22	207
237	773	44	42	9	7	71	21	149
241	1133	44	42	17	70	92	20	62
318	832	87	76	261	61	111	16	36
178	821	53	54	41	35	107	29	180
Zr	**Ba**	**La**	**Nd**	**Ni**	**Cu**	**Zn**	**Ga**	**Rb**
64	367	19	17.5	#VALUE!	5	70	22.5	354.5
2%	2%	21%	14%	n.a.	25%	1%	2%	0
137	557.5	21.5	22	13.5	4	63.5	19	223
2%	3%	14%	9%	10%	0%	1%	0%	1%

Sr ppm	Y ppm	Nb ppm	Pb ppm	Th ppm	U ppm	Totals
106	25	7	14	7	4	100.09
102	25	9	16	7	4	99.63
141	29	12	14	10	3	99.50
134	40	15	23	9	3	99.12
140	41	12	25	8	3	99.85
145	35	14	21	11	4	98.76
149	27	14	17	8	3	100.01
143	26	13	23	6	4	99.85
7	12	10	7	<2	3	99.54
<5	8	9	13	<2	3	99.81
73	22	10	17	5	5	100.01
43	29	10	18	3	4	99.28
47	13	16	64	4	5	99.48
42	13	17	24	8	6	100.07
83	30	10	17	6	5	99.80
35	31	11	15	3	5	99.80
<5	5	32	2	<2	3	99.59
<5	6	28	2	<2	4	100.26
33	32	12	22	6	5	99.62
178	28	10	16	9	3	99.74
46	24	6	17	3	5	100.60
32	24	9	15	3	4	98.87
139	26	13	36	9	5	99.64
11	14	12	13	<2	4	98.75
48	12	15	67	4	5	99.83
140	26	13	31	7	4	100.23
43	32	14	98	8	5	100.55
64	27	9	46	7	4	100.87
99	25	11	38	5	4	101.06
130	28	13	20	9	3	99.15
141	28	14	155	7	4	98.87
141	34	14	20	7	4	100.11
665	21	12	17	5	1	99.17
1377	23	105	5	10	<1	99.02
212	32	20	38	14	2	100.79
Sr	**Y**	**Nb**	**Pb**	**Th**	**U**	**Totals**
47.5	12.5	15.5	65.5	4	5	99.654
1%	4%	3%	2%	0	0	
104	25	8	15	7	4	
2%	0	11%	6%	0	0	

APPENDIX A7

Geochemistry Paper, Atlantic Geology, 2006

WEATHERING OF DEVONIAN MONZOGRANITES AS RECORDED IN THE GEOCHEMISTRY OF SAPROLITES FROM THE SOUTH MOUNTAIN BATHOLITH, NOVA SCOTIA, CANADA

Anne Marie O'Beirne-Ryan, Department of Earth Sciences, Dalhousie University, Halifax, Nova Scotia, B3H 3J5 Canada
Marcos Zentilli, Department of Earth Sciences, Dalhousie University, Halifax, Nova Scotia, B3H 3J5 Canada
Corresponding author email: amryan@dal.ca

KEYWORDS

Weathering Saprolite Nova Scotia Monzogranite Geochemistry

ABSTRACT

Parent mineralogy, paleoenvironment, and subsequent diagenetic and erosional history, contribute to the nature of the paleoweathering profiles (saprolites) developed on the South Mountain Batholith. Saprolites of three different ages (pre-Carboniferous, pre-Triassic, and pre-Pleistocene), which developed on Devonian monzogranite, exhibit increases in oxidation and hydration, and decreases in rare earth elements with increasing weathering. In addition, changes in Ca, Ba, Rb, Zn, Pb, and Co, and other elements in the oldest saprolite, indicate element mobility during weathering. Re-exposure of these partially-weathered profiles at surface in today's acidic and oxygen-rich environment may result in further migration of elements from these saprolites.

Introduction

Weathering profiles of three distinctly different ages have been identified on the monzogranite of the South Mountain Batholith (O''Beirne-Ryan and Zentilli 2003), (Fig. 1): (I) A pre-Carboniferous weathering profile 4 - 6 m thick and characterized by a relithified clay-rich saprolite beneath a Carboniferous sedimentary sequence; (II) A pre-Triassic profile approximately 30 metres thick, characterized by unlithified saprolite beneath Triassic sandstones and shales; and (3) A pre-Pleistocene weathering profile with up to 3 metres preserved, and

characterizedby an arenaceous saprolite beneath Pleistocene till. The first two paleo-profiles are found in drill cores whereas the youngest profile is observed in outcrops of monzogranite and other felsic phases of the South Mountain Batholith.

The preserved portions of the weathering profiles developed on the South Mountain Batholith and in particular, the sections of pre-Pleistocene age, represent either (I) the lowest least weathering part of a thicker, more complete weathering profile, the bulk of which has now been removed by erosion, or (II) an arrested stage in the development of a weathering profile, representing an early, incipient weathering event (O'Beirne-Ryan and Zentilli 2003). As a result of this incomplete weathering, there is a considerable amount of readily available soluble material remaining within the younger saprolites, and they are "primed" for further chemical alteration. In combination with the intensity of microfractures developed within the saprolites with a resulting increase in surface area for reaction, and the acidic precipitation currently prevailing throughout Nova Scotia, these saprolites are potential elemental sieves if disturbed or exposed at surface. The purpose of this study was to establish the nature of the chemical changes which occurred on chemically similar rocks at different times in the geologic past, in order to access the potential for further changes when these partially-eroded and incompletely weathered saprolites are re-exposed at surface today. In recent years, a number of locations of these saprolites have been subjected to quarrying for use as road bed material, and the friable and permeable nature of

these saprolites means that water and air flow-through is high. In re-exposing these profiles, it is possible that loosely-bound elements may be mobilised under conditions of increased Eh and decreased pH, as might be expected at surface today. Consequently the term "elemental sieve" is used to denote the possibility of further leaching of elements from these saprolites under present-day changing conditions.

This paper summarises the geochemical changes that occur within saprolites developed on monzogranites of the South Mountain Batholith, and discusses the implications of these changes in relation to mobilization or retention of elements when these profiles are re-exposed at surface today.

Sampling procedures and analytical methods

Monzogranites of the the South Mountain Batholith (SMB), Nova Scotia, Canada, consist of subequal quartz, plagioclase, and alkali feldspar, and 8 - 15% biotite. Dominant accessory minerals include apatite, zircon, and titanite. Suites from the pre-Pleistocene, the pre-Triassic, and the pre-Carboniferous saprolites were analyzed for majors elements, trace elements, the rare earths (REEs), and LOI (Table 1, Fig. 2), and details of analytical methods are outlined in O'Beirne-Ryan (2006). The pre-Pleistocene suite includes three samples of increasing

weathering intensity based on field evidence (O'Beirne-Ryan and Zentilli 2003). The pre-Triassic monzogranite saprolite of similar whole rock chemistry to the monzogranite of the pre-Pleistocene profile, provides the most complete, undisturbed record of weathering. Five samples of increasing weathering intensity were analysed from this profile. The original monzogranite of the Pre-Carboniferous saprolite also has similar whole rock geochemistry, and three samples of increasing weathering intensity from one of the pre-Carboniferous profiles are included in this study (Fig. 1). Major elements and trace elements, with the exception of Zr, Y, Nb, Th, and U, were analysed by XRF; Zr, Y, Nb, Th, U, and REEs, were analysed using ICP-MS; Fe^{3+} was analysed by titration; and LOI was determined by heating to 250°C for 1.5 hours, then at 1050°C for 2.5 hours (David Slaunwhite, Saint Mary's Geochemical Centre, Nova Scotia, pers.comm. 2005). Details of sample preparation, analysis and precision are given in O'Beirne-Ryan (2006). Because chemical weathering is not necessarily an isovolumetric process (Nesbitt 1979; Cramer and Nesbitt 1983), the geochemical data were normalized against Ti (Fig. 2) using the formula of Nesbitt (1979):

$$\% \text{ change of element X} = [(X/Ti)_{sample} / (X/Ti)_{parent} - 1].100$$

Results

Major Element changes during weathering

Relative to the least altered parent rock, the pre-Triassic and pre-Pleistocene saprolite suites show notable increases of 20% or more in Fe^{3+}, LOI, and K. The pre-Triassic suite shows decreases of more than 20% in Fe^{2+}, Ca, and Na. In the older Pre-Carboniferous suite, LOI, Ca and Mn content increases, whereas Na and K decrease with increased degree of weathering. Among the three saprolite suites the total iron content does not change significantly throughout the weathering process. Other major element changes are inconsistent between samples, although in the Pre-Triassic suite there is a tendency for P to decrease with increasing degree of weathering.

Trace Element changes during weathering

Within the Pre-Triassic and the Pre-Pleistocene saprolites (Fig.2) there are some broadly similar trends: Rb, Ba, Pb, Zn, and Co tend to increase on weathering relative to Ti in both suites. Cu increases dramatically in the Pre-Triassic suite. No trace element is notably depleted in the Pre-Pleistocene suite; however, in the Pre-Triassic suite Sr and Y exhibit notable decreases. The pre-Carboniferous suite is significantly depleted in most trace elements as weathering intensity

increases.

Rare Earth changes during weathering

Rare earth element data are presented normalized to chondrite (Fig. 2). For all suites, there is a general tendency for decrease, or little change, in rare earth elements (REEs) with increasing degree of weathering. In the Pre-Triassic suite there is a tendency towards fractionation of the REEs, with greater decreases recorded in the heavy REEs than in the light REEs; the opposite trend is observed in the younger Pre-Pleistocene suite. However, sub-parallel trend lines exist for the Pre-Carboniferous suite, suggesting minimal fractionation during this weathering event.

Discussion

The dominant and most pervasive features of weathering in the various profiles from the South Mountain Batholith are the processes of oxidation as recorded in the changing ratio of Fe^{3+} : Fe^{2+}, and hydration, as recorded in the increased water content of the more weathered samples, a reflection of the development of clay mineralogy at the expense of the feldspars and biotite. Calcium also shows significant depletion in the younger suites, similar to observations elsewhere (Islam et al. 2002; Nesbitt et al.1980). The retention of alkali elements throughout

the sequence in the younger suites confirms either arrested or less intense weathering events or erosion of the more weathered upper profiles, leaving the profiles incompletely preserved. Although Nova Scotia's cool temperate climate is not likely to induce intense weathering of the exposed Pre-Pleistocene profiles today, the impact of acid rain on changing the chemistry of these profiles is possible. For example, U that was mobilized from weathering of biotites during the initial stage of weathering was adsorbed or relocated on iron and titanium oxides. Under conditions of reduced pH such as is typical of acid rain, particularly where Eh is high, this adsorbed uranium can be mobilized and migrate into ground or surface waters.

The weathering geochemistry of the pre-Carboniferous suite is different than the younger two except that the behaviour in terms of LOI is very similar (Fe^{2+} was not measured for this suite). The less systematic behaviour of most other elements in this suite suggests a more complex origin of the geochemical signature. The magnitude of the geochemical changes from the lower to upper portion of the saprolite suggests that the initial weathering process was more intense than in the younger Pre-Triassic and Pre-Pleistocene suites. The geochemical signature of this weathering event is more typical of a tropical weathering environment, and is consistent with the sub-equatorial location of Nova Scotia during the Devono-Carboniferous (e.g. Calder, 1998). The increased complexity of the elemental behaviour compared to that of the 2 younger suites also reflects the superimposed relithification process on this

saprolite. Ryan and Zentilli (1993) established burial temperatures of upwards of 150°C during the Permian for strata overlying the Pre-Carboniferous paleosaprolite. The increase in Ca and Mn in the weathered samples is not typical of the behaviour of these elements in the younger suites, or in weathering profiles elsewhere (Middleburg et al. 1988; van der Weijden and van der Weijden 1995). This increase in Ca and Mn in this Pre-Carboniferous saprolite can be attributed to the addition, post-weathering, of Ca and Mn; thin section textural and mineralogical evidence further supports the later addition of Ca, Mn and other elements to the system (O'Beirne-Ryan and Zentilli 2006). The increase in Mn levels is interesting, and is consistent with Mn mineralization found in granitoids in the surrounding region (Chatterjee 1983).

In the younger saprolites (Pre-Triassic and Pre-Pleistocene) the chemical changes reflect the mineralogy of the monzogranite and its response to the weathering conditions. Even in the Pre-Triassic profile, where there is over 30 metres of saprolite preserved, it is only in the uppermost levels that the alkali elements show relative depletion, suggesting that more temperate conditions prevailed during the development of both the Pre-Triassic and Pre-Pleistocene profiles, rather than the more intense conditions prevailing during the Pre-Carboniferous event. Middleburg et al. (1988) discuss the behaviour of the redox elements during weathering. In the younger saprolites of the SMB, Fe^{3+} increases of >100% confirm the significance of oxygen, even in the lowermost levels of the weathering profile. The variable behaviour of U, V, Th, and other redox-sensitive

elements, may be explained by retention of these elements in insoluble or weakly-soluble phases (zircon, for example) or by partial adsorption of these elements on the newly-formed Fe-Ti oxides and oxyhydroxides, and clays. Further studies on the actual distribution of uranium in these weathered profiles is ongoing, as unlike uranium found in resistate minerals such as zircon, uranium adsorbed onto secondary minerals or concentrated in apatite may be liberated and mobilized under changing Eh-pH conditions. U-mineralization in Lower Carboniferous arkoses formed from granitic rocks of the SMB (O'Reilly et al. 1982), confirms that U may be mobilized from these granitic rocks under favourable conditions; it is possible that the impact of acid precipitation on recently-exposed saprolites may provide the impetus for mobilization of U, or other redox-sensitive elements. Furthermore, Kronfeld et al. (2004) concluded that present-day localized elevated levels of uranium in groundwaters was attributable to weathering of zones of uranium mineralization.

The REEs in all suites are increasingly depleted on weathering. This depletion is counter to the trends observed by Nesbitt (1979) and Middleburg et al. (1988), but similar to that documented by Koons (1978). However, Nesbitt (1979) indicated that the behaviour of the REEs is dependant on pH conditions, and on which minerals host the REEs. If the REEs of the SMB are concentrated in apatite or some other mineral which weathers more readily than zircon, then the REEs may be mobilized more readily (Nesbitt, 1979). Aqua regia dissolution of saprolite samples causes the release of La and Y but not of Zr, suggesting that at

least some of the REEs are located in phases more soluble than zircon. Nesbitt (1979) concluded that increasing pH may result in the mobilized REEs becoming concentrated in the secondary minerals. The consistent depletion of REEs in all of the monzogranite saprolites of the SMB included in this study, suggests that the behaviour of the REES is related to weathering of their host minerals, rather than changing conditions during weathering.

Conclusions

1. There are three weathering profiles developed on the same rocks, at different times in the geologic past.

2. These profiles show different chemical patterns according to the prevailing weathering conditions during their formation.

3. Although no overall dramatic depletion of trace elements occurs (except in the Pre-Carboniferous), a redistribution of elements has occurred, and it is possible that these elements can be more readily mobilized under changing conditions at the earth's surface today.

4. Whereas similar parent mineralogies and chemistry occur at the sampled

profiles regardless of age of weathering, and geochemical analyses of the weathered products of these saprolites indicates different weathering conditions at different times in the past; the shared distribution characteristics of the REEs for all ages of weathering suggests that mineralogy rather than weathering conditions controls the REE patterns in each of the 3 suites studied.

Acknowledgments

The authors would like to thank John Wightman and Larry Riteman for providing analytical samples from drill core. Thanks is also extended to Jarda Dostal for helpful comments on early drafts of this paper, and to Steve McCutcheon and Allen Seaman, for review and suggestions on the final manuscript.

References

Calder, J.H. 1998. The Carboniferous evolution of Nova Scotia. *In* Lyell: the past is the key to the present. *Edited by* D. Blundell and A.C. Scott (eds.). Geological Society of London Special Publication, pp. 296-331.

Chatterjee, A.K. 1983. Metallogenic map of Nova Scotia. Map ME-1983-5, Nova Scotia Department of Natural Resources.

Cramer, J.J. & Nesbitt, H.W. 1983. Mass-balance relations and trace-element mobility during continental weathering of various igneous rocks. Sciences Geologiques. Memoire, 73, pp. 63-73.

Islam, M.R., Peuraniemi, V., Aario, R. & Rojstaczer, S. 2002. Geochemistry and mineralogy of saprolite in Finnish Lapland. Applied Geochemistry 17, pp. 885-902.

Koons, R.D. 1978. Behavior of trace and major elements and minerals during early stages of weathering of diabase and granite in Central Wisconsin. PhD Thesis,University of Wisconsin-Madison. 243 p.

Kronfeld, J., Godfrey-Smith, D.I., Johannessen, D. and Zentilli, M., 2004. Uranium series isotopes in the Avon Valley, Nova Scotia. Journal of Environmental Radioactivity, 73, 335-352.

Middelburg, J.J., van der Weijden, C.H., & Woittiez, J.R.W. 1988. Chemical processes affecting the mobility of major, minor and trace elements during weathering of granitic rocks. Chemical Geology, 68, pp. 253-273.

Nesbitt, H.W. 1979. Mobility and fractionation of rare earth elements during weathering of a granodiorite. Nature, 279, pp. 206-210.

Nesbitt, H.W., Markovics, G., & Price, R.C. 1980. Chemical processes affecting alkalis and alkaline earths during continental weathering. Geochimica et Cosmochimica Acta, 44, pp. 1659-1666.

O'Beirne-Ryan, A.M., 2006. Weathering history of granitoids of the South Mountain Batholith, N.S., Canada: Mineralogy, geochemistry, and environmental implications of saprolite. Unpublished PhD thesis, Dalhousie University.

O'Beirne-Ryan, A.M., & Zentilli, M. 2006. Weathered granites as potential chemical sieves: impacts of ancient pre-glaciation weathering on the granitoids of south-western Nova Scotia and the environment. 32nd Colloquium and Annual Meeting, Atlantic Geoscience Society, Abstract with programs, pp.54-55.

O'Beirne-Ryan, A.M. & Zentilli, M. 2003. Paleoweathered surfaces on granitoids of Southern Nova Scotia: Paleoenvironmental implications of saprolites. Canadian Journal of Earth Sciences, 40, pp.805-817.

O'Reilly, G.A., Farley, E.J., & Charest, M.H. 1982. Metasomatic and hydrothermal deposits of the New Ross - Mahone Bay area, Nova Scotia. Paper ME 1982-2, Nova Scotia Department of Natural Resources. 96 p.

Ryan, R. J. & Zentilli, M. 1993: Allocyclic and thermochronological constraints on the evolution of the Maritimes Basin, Atlantic Geology, 29, pp.187-197.

van der Weijden, C.H. and van der Weijden,R.D., 1995. Mobility of major, minor, and some redox-sensitive trace elements and rare-earth elements during weathering of four granitoids in central Portugal. Chemical Geology 125, pp.149-167.

Williams, H. 1995. Introduction, Chapter 1. *In* Geology of the Appalachian-

Caledonian Orogen in Canada and Greenland. *Edited by* H. Williams; Geological Survey of Canada, Geology of Canada, 6, pp. 1-9.

Figure and Table Captions

Fig. 1: A. Location of the study area and general geological setting of the northern Appalachians, after Williams (1995). B. Generalized map of South Mountain Batholith, Nova Scotia, showing localities and ages of saprolites: 1(Castlefrederick, pre-Carboniferous) , 2 (pre-Triassic), and 3 (Hardwood Lake, pre-Pleistocene) are sites for geochemical data presented in this study.

Fig. 2: Geochemical data normalized to fresh parent monzogranite; parent analyses are represented by the x-axis. Data have been normalized to Ti for majors and traces, and to chondrite for REEs for pre-Pleistocene (Hardwood Lake), pre-Triassic, and pre-Carboniferous (Castlefrederick) saprolites. Mild weathering refers to solid rock which is easily broken with a hammer, and moderate weathering refers to crumbly, *in situ* material. Fe^{2+}, Fe^{3+}, and H_2O^+ were not measured for the pre-Carboniferous saprolite.

Table 1: Major, trace and REEs geochemical data for the Pre-Carboniferous (1: Castlefrederick 1), Pre-Triassic, and Pre-Pleistocene (Hardwood Lake) saprolites. Major oxides in weight percent; Traces and REEs in ppm. Fe_2O_3t is total Fe measured as Fe_2O_3; Fe_2O_3* and FeO* refer to Fe^{3+} and Fe^{2+} oxides measured by titration. In the Pre-Pleistocene and Pre-Carboniferous suites, f = fresh monzogranite; w = moderately weathered; ww = most weathered (top of preserved portion of the profile). In the Pre- Triassic suite, the numbers are depths below surface (e.g. 2-193 refers sample from drill core #2, 193 feet below surface).

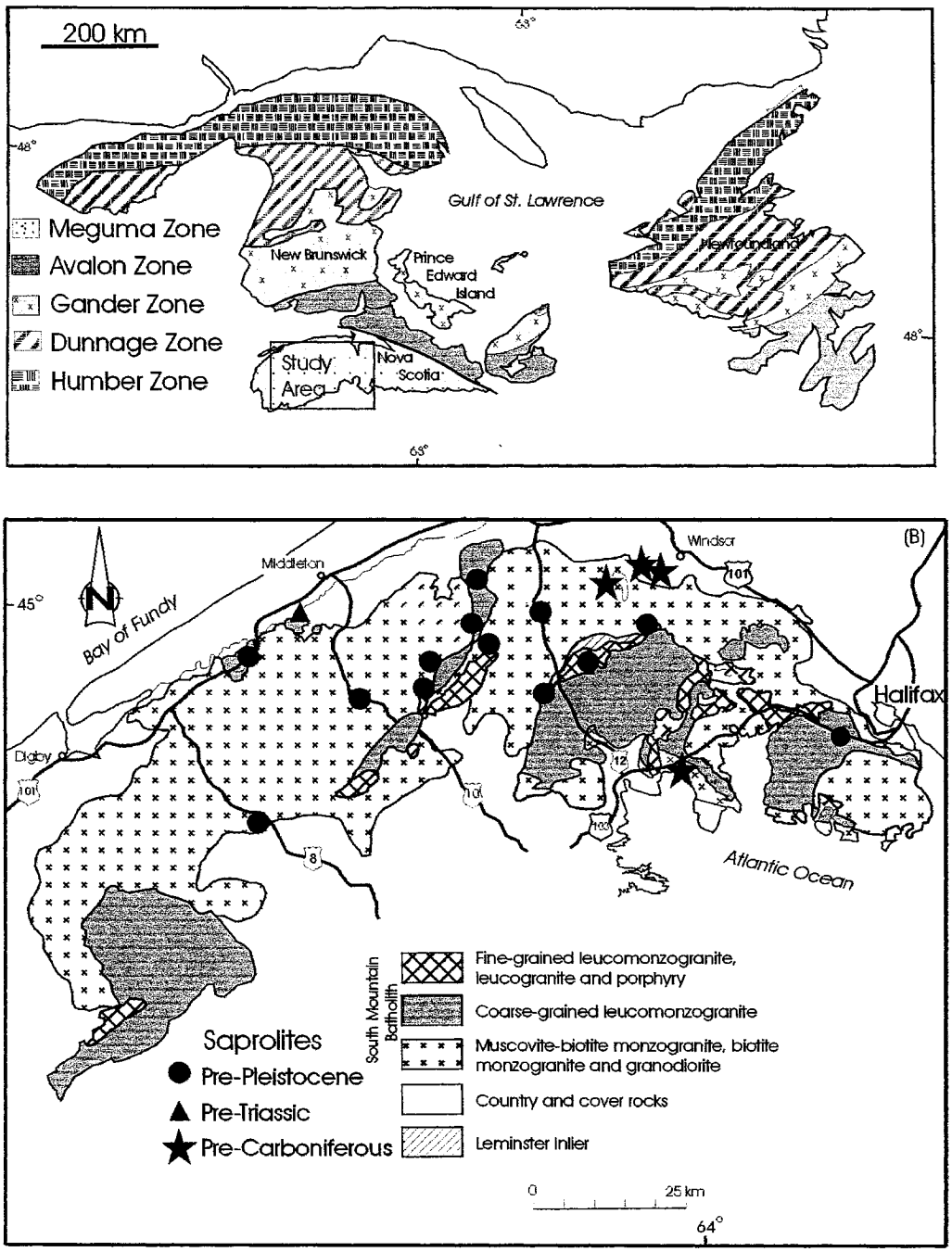

Figure 1: O'Beirne-Ryan and Zentilli

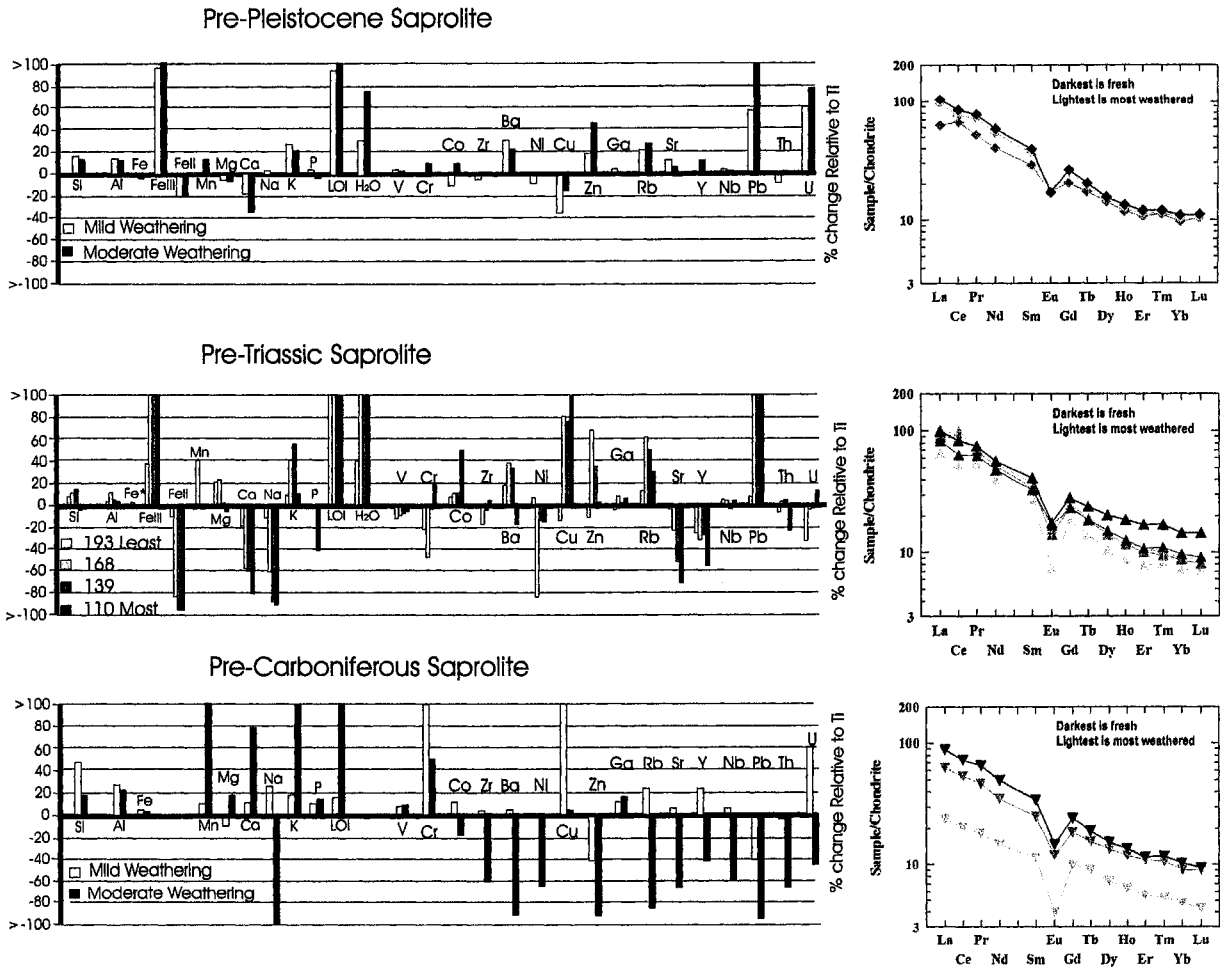

FIGURE 2: (O'Beirne-Ryan & Zentilli)

	Pre-Pleistocene			Pre-Triassic					Pre-Carboniferous		
	Hardwood Lake								Castlefrederick 1		
SAMPLE	112f	113Aw	144ww	2-201	2-193	2-168	2-139	2-110	1134f	1126w	1119ww
SiO2	67.04	67.83	67.48	68.03	67.88	67.73	69.46	66.87	67.45	70.95	65.15
TiO2	0.756	0.663	0.68	0.653	0.609	0.587	0.586	0.68	0.551	0.396	0.449
Al2O3	15.26	15.23	15.06	15.1	14.41	14.99	14.41	16.44	15.35	14.09	15.31
Fe2O3t	5.38	4.65	4.86	4.58	4.27	4.15	4.1	4.77	4.38	3.37	3.82
Fe2O3*	1.03	1.77	1.83	1.00	1.28	3.85	3.92	4.55	n.a.	n.a.	n.a.
FeO*	3.91	2.59	2.72	3.22	2.69	0.27	0.16	0.2	n.a.	n.a.	n.a.
MnO	0.091	0.08	0.092	0.072	0.065	0.09	0.063	0.074	0.1	0.08	0.66
MgO	1.3	1.09	1.11	1.13	1.28	1.25	1.02	1.11	1.1	0.72	1.06
CaO	1.96	1.37	1.13	2.09	1.6	0.8	0.71	0.32	2.13	1.69	3.07
Na2O	3.11	2.81	2.76	3.06	2.52	1.07	0.25	0.2	2.99	2.72	0.01
K2O	4.01	4.47	4.33	4.19	4.25	5.25	5.78	4.82	4.36	4.47	0.2
P2O5	0.304	0.272	0.262	0.224	0.206	0.201	0.197	0.132	0.228	0.175	0.209
LOI**	0.8	1.38	1.68	0.98	2.06	4.94	4.29	5.13	1.05	0.85	10.22
H2Op	0.89	1	1.42	0.83	1.08	2.17	2.51	3.8	n.m.	n.m.	n.m.
V	94	85	86	83	78	68	70	83	76	59	68
Cr	26	23	26	25	18	12	22	31	22	34	27
Co	13	10	13	11	11	11	11	17	10	8	7
Zr	225	186.6	201	230.4	206.4	174	200.6	247.6	201.7	151	65
Ba	704	806	785	773	847	956	921	664	643	489	37
Ni	10	8	9	9	9	1	7	8	11	4	3
Cu	14	8	11	7	7	14	11	19	<4	5	<4
Zn	84	86	111	71	70	107	85	75	121	51	6
Ga	23	21	22	21	19	20	19	23	22	18	21
Rb	192	206	220	149	157	218	200	202	173	156	15
Sr	149	143	139	141	130	99	64	43	129	97	34
Y	28.67	25.28	28.16	41.59	28.44	25.36	27.15	19.84	31.5	27.92	14.62
Nb	14.3	12.8	13.1	13.9	13.5	12.8	12.2	14.7	13.2	10	4.6
Pb	17	23	36	20	20	38	46	98	53	23	<3
Th	12.41	9.99	11.3	13.23	11.34	12.3	12.5	10.38	11.62	8.22	3.1
U	3.47	4.87	5.55	4.3	2.64	3.58	3.8	5.02	3.17	3.64	1.38
Cs	11.93	12.07	15.35	8.88	13.99	28.58	23.69	22.28	9.94	7.13	0.29
Hf	6.2	5.1	5.5	6.3	5.6	4.8	5.4	6.6	5.6	4.2	1.9
Ta	1.64	1.40	1.46	1.06	1.03	1.04	0.97	1.16	1.14	0.91	0.40
La	38.35	22.79	34.97	36.74	30.33	32.27	33.46	23.79	32.57	22.76	8.60
Ce	80.85	62.90	70.77	79.70	60.05	84.40	94.30	50.18	69.38	49.82	19.12
Pr	10.64	6.96	9.69	10.31	8.53	9.33	9.55	7.19	8.94	6.27	2.47
Nd	41.52	27.92	37.71	40.02	33.77	35.94	38.16	28.09	34.86	24.46	10.34
Sm	9.11	6.52	8.35	9.45	7.49	7.83	8.43	6.28	8.00	5.74	2.62
Eu	1.486	1.473	1.407	1.511	1.425	1.203	1.300	0.626	1.282	1.032	0.337
Gd	8.065	6.079	7.579	8.611	6.975	7.039	7.423	5.520	7.423	5.587	2.973
Tb	1.173	0.977	1.109	1.394	1.068	1.038	1.094	0.794	1.111	0.899	0.518

Table 1 (O'Beirne-Ryan, A.M. & Zentilli, M.)

APPENDIX A8

Permission to include manuscripts of published papers